Synthesis and characterisation of some novel low-coordinate phosphorus compounds containing bulky electron-withdrawing substituents

M. D. Roden

Synthesis and Characterisation of some Novel Low-Coordinate Phosphorus Compounds containing Bulky Electron-Withdrawing Substituents

by

M. D. Roden B.Sc., M. Sc., (Dunelm)
Hatfield College

A thesis submitted for the degree of Doctor of Philosophy
at the University of Durham

September 1998

Statement of Copyright

Declaration

The work described in this thesis was carried out in the Department of Chemistry at the University of Durham between October 1994 and October 1997. All the work is my own unless stated to the contrary, and it has not been submitted previously for at this or any other University.

Abbreviations

Ar, Fluoromes,	1,3,5-tris(trifluoromethyl)phenyl
Ar', Fluoroxyl	1,3-bis(trifluoromethyl)phenyl
Ar''	1,3-bis(trifluoromethyl)phenyl
CCD	Charge Couple Device (Area Detector)
DBU	1,8-diazabicyclo[5,4,0]undec-2-ene
dppe	diphenylphosphinoethane
ESD	Estimated Standard Deviations
IR	Infra Red
LUMO	Lowest Unoccupied Molecular Orbital
NQR	Nuclear Quadropole Resonance
PMDETA	Pentamethyldiethylenediamine
Supermes	1,3,5-tris(tertiarybuty)phenyl
THF	Tetrahydrofuran
UV	Ultra Violet

Acknowledgements

I would like to thank Dr K. B. Dillon for his patience, understanding and encouragement through my time in Durham. Over the past five years, Dr Dillon has been a great influence on me; working with him has been great fun.

I would also like to thank Professor J. A. K. Howard for allowing me access to the X-ray facilities at Durham University and to the rest of her team for explaining time and time again the fundamentals of crystallography, which just never seemed to stick, particularly Janet Moloney.

Thanks also go to Mr D. Hunter, without whom the synthesis of Fluoromes would have been impossible. His experience with the high-pressure facilities was invaluable.

I would like to thank all the Ph.D. students in the Inorganic Section with whom I worked. Their encouragement over the odd jar or two was equally invaluable.

I would like to say a special thank you to my wife Kayo. Her encouragement, love and patience have been invaluable.

Abstract

The synthesis of several new phosphorus derivatives including new monophosphanes of the type RPX_2 (X = F, Cl and H), containing either the Fluoromes [2,4,6-$(CF_3)_3C_6H_2$] or Fluoroxyl [2,6-$(CF_3)_2C_6H_3$] group has been carried out successfully.

The synthesis of a number of *Cis*-Platin analogous has been facilitated by the reaction of these new monophosphanes with a platinum dimer $[(PCl_2(PEt_3)_2]_2$. These compounds are of the type $PtCl_2(PEt_3)RPX_2$ (X = Cl, H and F, R = 2,6-bis(trifluoromethyl)phenyl). These compounds have shown an interesting correlation between bond length and $^1J_{P\text{-}Pt}$ NMR coupling.

Disubstituted phosphanes (RPX_2, X = Cl, H) have also been synthesised and subsequent reaction has facilitated the formation, characterisation and structure solution of a new phosphorus (I) species $(RP_2^{(-)})(Ph_3PCH_3)$[1] (R = Fluoromes).

Attempts have been made to synthesise the first phosphaalkyne containing a bulky electron withdrawing ligand. This involved the reaction of $RP{=}CCl_2$ (R = 2,6-bis(trifluoromethyl)phenyl) with a number of Pt(0) and Pd(0) species.

^{31}P NMR studies have been used extensively throughout the project to help characterise and identify the products. The single crystal, solid state structures of many of the new species were elucidated by X-ray diffraction using a Siemens Smart CCD.

Mark Roden (November 1998)

---

[1] M. G. Davidson., K. B. Dillon., J. A. K., Howard., M. D. Roden., S. Lamb., J. Organometallic Chemistry, 1998, **550** 481

To Laura and my Parents

My 2nd Book

Contents for Chapter 1

List of Figures

List of Equations

List of Tables

Contents for Chapter 2

List of Figures

List of Equations

List of Tables

Contents for Chapter 3

List of Equations

List of Figures

List of Tables

Contents for Chapter 4

List of Figures

List of Equations

List of Tables

Contents for Chapter 5

List of Figures

List of Equations

List of Tables

Contents for Appendix 1

Contents for Appendix 2

List of Figures

List of Tables

Contents for Appendix 3

Chapter 1

Introduction

1.1 1,3,5-tris(trifluoromethyl)benzene [Fluoromes (ArH)]

"Fluoromesitylene" (Fluoromes, ArH) was first prepared in 1947 by McBee and Leech[1]. This involved the fluorination of 1,3,5-tris(trichloromethyl)benzene and the extensive preparation yielded 49% product.

The modern synthesis for ArH was first described by Chambers *et al.*[2] involving the reaction of SF_4 and the commercially available trimesic acid [$C_6H_3(COOH)_3$] (yield 33%). This method was then subsequently improved dramatically by Edelmann *et al.*[3], increasing the yield of the reaction to 95%.

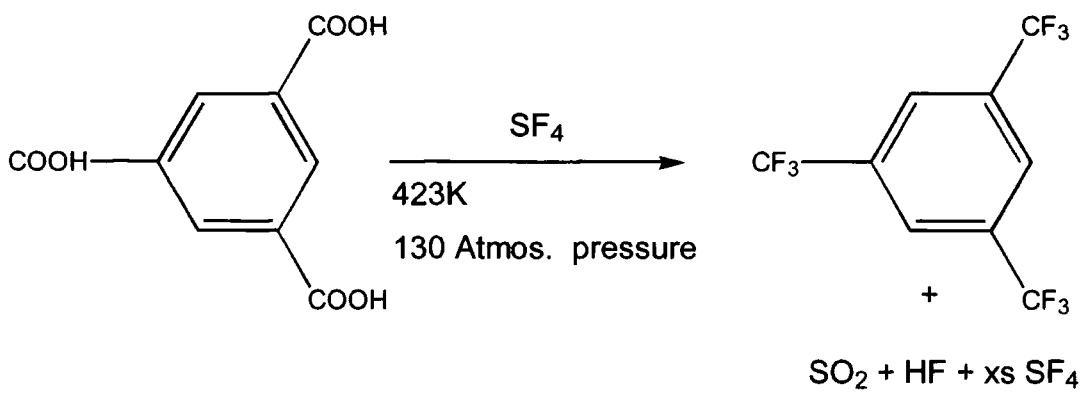

Equation 1.1 – Synthesis of 1,3,5-tris(trifluoromethyl)benzene

The chemistry of Fluoromes has since been extensively studied. The reaction of Fluoromes with ^{n}BuLi to form the lithiated species 1-lithio-2,4,6-tris(trifluoromethyl)benzene [2] (ArLi) has proved to be a very versatile reagent.

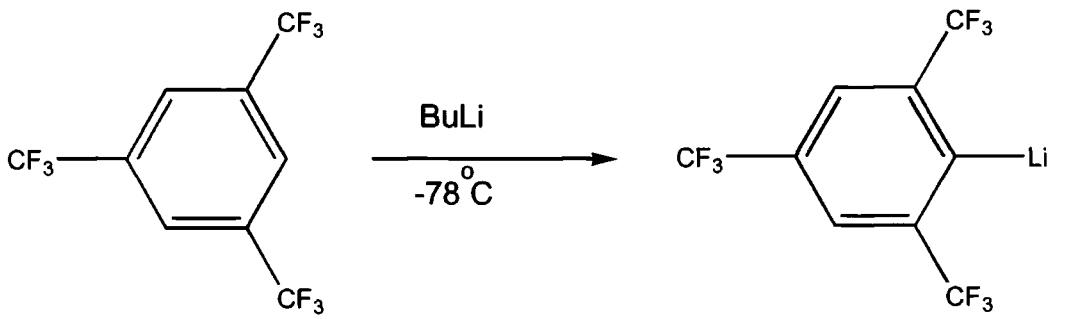

Equation 1.2 – Formation of lithiated 1,3,5-tris(trifluoromethyl)benzene

1.1.1 Reasons and advantages for using Fluoromes rather than other aryl species

Fluoromes itself is a colourless liquid which boils at 119°C at 1 atmosphere pressure. It is prepared on an approximately 100g scale in the department using the high pressure facilities available.

The Fluoromes group has a number of advantages over other aryl and alkyl groups in its inclusion in phosphorus (and other main groups element) compounds. The compounds involving phosphorus, are comparatively more oxygen- and moisture-stable than equivalent aryl and alkyl bonded P(III or V) species. In the case of phosphorus multiply bonded to other elements (e.g. RP=PR, $RP=CCl_2$), these species are more resistant to polymerisation and formation of dimer and trimer products (see Section 1.5). This is a great advantage to preparation in bulk. These properties are due to two main factors regarding the Fluoromes group itself :

1) The CF_3 groups bonded to the *ortho* and *para* carbons in the aryl group cause an overall withdrawal of electrons from the element to which the group is bonded. In this case it makes the phosphorus atom to which it is attached less electron rich and less susceptible to electrophilic attack.
2) The steric bulk of the CF_3 groups also restricts attack on the phosphorus, particularly in the case of a di-substituted species, i.e. compounds of the type Ar_2PX (X= Cl or H). In the cases where Fluoromes is bonded to main group elements there is a distinct interaction between the fluorine atoms on the *ortho*-CF_3 groups and the element itself through space (visible in the ^{31}P NMR as a $^4J_{P\text{-}F}$ coupling constant through space of approximately 25-70 Hz).

These two effects in tandem cause a greater overall stability of the phosphorus species in question.

1.1.2 Compounds containing Fluoromes

1.1.2.1 Fluoromes bonded to metals

The reaction of ArLi, like other lithiated aryl species, with metal and non-metal halides has led to the synthesis of a wide variety of compounds. There are examples of compounds formed with main group metals, (e.g. In, Ga, Sn) [4,5,6,7] and transition metals including the type $M(Fluoromes)_2$[8,9]. Some reactions of $Sn(Fluoromes)_2$ producing higher oxidation state tin compounds have also been shown by Edelmann[10].

1.1.2.2 Fluoromes bonded to phosphorus

By the same method of reacting ArLi with metal chlorides, Fluoromes-phosphorus bonds can be formed by the reaction of ArLi with P-Cl bonds, the typical starting material being PCl_3 itself. This has led to a number of low-coordinate Fluoromes-phosphorus compounds such as ($ArPX_2$ - X = Cl, H, F)[11], ArP=PAr[12] and $ArP=CCl_2$[13] and their derivatives. High-coordinate compounds such as $Ar\text{-}PCl_4$[14] have been also prepared.

1.2 1,5-bis(trifluoromethyl)benzene [Fluoroxyl (Ar'H)]

Fluoroxyl has rarely been used as a ligand in main group chemistry, with only two examples in the Cambridge structural database[15]. The first is a chromacene analogue containing two Ar' species in a sandwich complex with chromium[16]. The second is the only substituted example, the diphosphene Ar'P=PAr',[17] although it is interesting to note that there has been some chemistry achieved involving the side substituted product[18].

Ar'H was the main aryl group used at the start of the project because of the unavailability of the starting material SF_4, used for producing Fluoromes. The properties of the two ligands are similar in the respect that they are electron withdrawing and the *ortho* positions are sterically hindering. The deciding factor in using Fluoroxyl initially was the cost. The cost of Fluoroxyl from the chemical suppliers was approximately 1/20th of that of the price of Fluoromes.

1.3 Comparisons between Fluoromes and Fluoroxyl

1.3.1 One substitution site or three?

If we consider the case shown below in Figure 1.1, there are three different carbon atoms on the Fluoroxy group not bonded to CF_3 (A, B and C). In the case of Fluoromes there are three carbon atoms not bonded to CF_3, however these are all equivalent (D).

In the case of Fluoroxyl, (1), there are three possible reaction sites, (A, B and C). The *para* carbon (C) in the Fluoroxyl group does not have a substituted CF_3 group and this leads to a number of potential reactions. Reaction site C (which is *meta* to both A and B) is the most unlikely substitution site in the reaction with BuLi. Sites A and B are influenced by both groups, thus making these sites more susceptible to reaction.

For Fluoromes, (2), there is only one possible reaction site (D). The D position has two CF_3 groups *ortho* and one CF_3 group *para*. This means that this site is activated equally by all the CF_3 groups in the molecule and substitution has an equal chance at each.

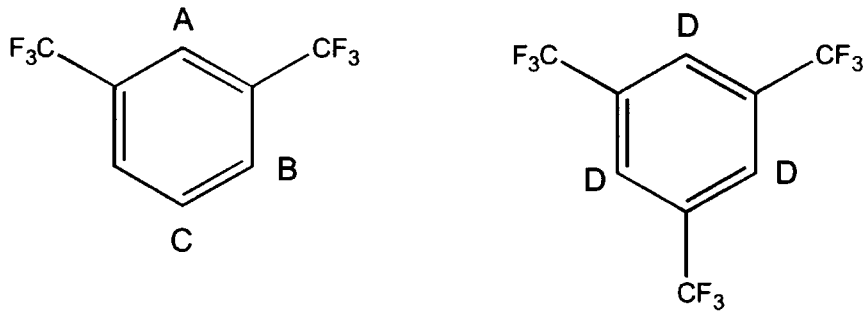

(1) (2)

Figure 1.1 – Substitution sites in Fluoroxyl and Fluoromes

	A	B	C	D
Ortho CF_3	2	1		2
Para CF_3		1		1

Table 1.1 – Number of CF_3 groups in the *ortho* and *meta* positions, relative to sites A, B, C, and D

Because the aryl ring is not symmetrical in the case of Fluoroxyl, there is more than one potential lithiation site upon reaction with BuLi (see Figure 1.2). The CF_3 groups have a directional functionality, which causes the positions *ortho* and *para* to them to become comparatively electron deficient. This in turn makes the hydrogen atom associated with these sites more acidic and susceptible to nucleophilic attack by the butyl group. This preference for nucleophilic attack leads to a number of differences in the species formed.

1) There are two possible substitution sites, the first of which is where the lithiation site is *ortho* to both CF_3 groups (i), and the second where the lithiated site is *ortho* to one CF_3 group and *para* to the other (ii). This second lithiation site is similarly activated by the CF_3 groups, as compared to the first case.

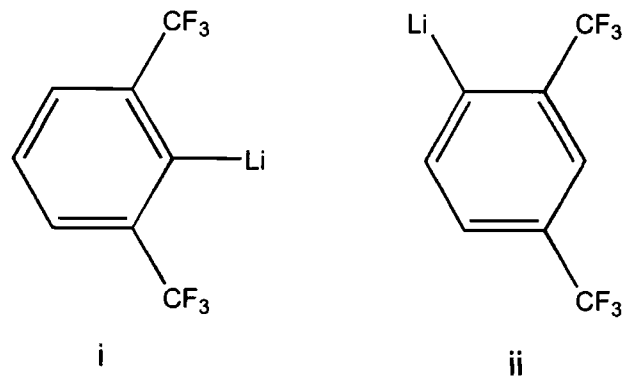

Figure 1.2 – Probable lithiation sites for Fluoroxyl

2) The desired product (i) which has the lithiated site *ortho* to both CF_3 groups retains its symmetry and the lithiated site is sterically hindered by both CF_3 groups. There is also the greatest interaction between the lithium atom and the electron rich fluorine atoms. For the compound ArLi, Helen Goodwin attempted to characterise any interaction between the lithium and the fluorine atoms using ^{7}Li NMR, but was unable to observe any.
3) The undesired product (ii) is only sterically hindered to one side and the reactivity of the compound is therefore likely to differ markedly.

^{19}F NMR studies of the reaction mixture formed in the reaction of BuLi and Ar'H have shown that the ratio of species (i) to species (ii) is approximately 50:50; however, once this mixture has been reacted with PCl_3 the ratio of products is approximately 2:1 (see Section 2.2.1.1). This implies that the side substituted Ar''Li (ii), is somehow comparatively more unstable with respect to Ar'Li. Because Ar''Li has only one CF_3 group in the *ortho* position, it has a more exposed lithium atom. This may well lead to side reactions involving the possible formation of LiF (see Section 1.4).

1.3.2 Formation of mono and di-substituted product upon further reaction

The reaction described above involving Ar'Li and PCl_3 yields a number of different products (see Figure 1.3) including the di-substituted mixed aryl species Ar'Ar''PCl which is formed by reaction of the two different lithiated species with PCl_3. There is however, no evidence for the formation of either of the potential di-substituted compounds Ar'_2PCl and Ar''_2PCl (2 and 3 below).

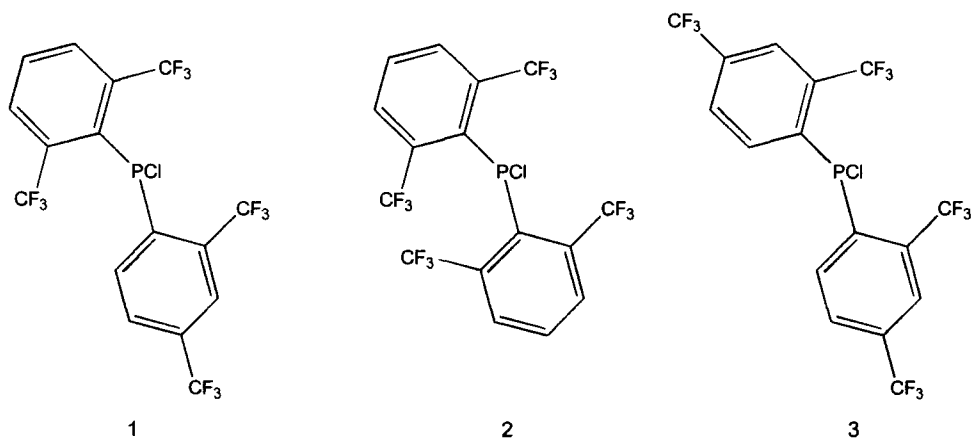

Figure 1.3 – Possible disubstituted products, in the reaction between Fluoroxyl, BuLi and PCl_3

1.3.3 NQR studies on electronegativity

A study had previously been undertaken of P(V) species of the type PCl_4R where R was a number of different electronegative withdrawing aryl groups[14]. Using NQR it is possible to show whether the aryl group is in an equatorial or axial position. If the aryl group is more electron withdrawing that chlorine, the group will be axial, otherwise equatorial.

Aryl group (R)	Structure as shown by NQR
$C_6H_4CH_3$ (tolyl)	Equatorial
$C_6H_4CF_3$	Axial
$C_6H_3(CF_3)_2$ (Fluoroxyl)	Axial
$C_6H_2(CF_3)_3$ (Fluoromes)	Axial

Table 1.2 – Structures of various substituted P(V) species, ascertained using NQR

This study shows that Fluoroxyl and Fluoromes are more electron withdrawing than chlorine and thus the relative electronegativity of the group is high.

1.4 Precautions necessary when working with fluorinated aryl groups

Addition of an excess of BuLi to a solution containing fluorinated aryl groups can cause the formation of LiF over time. LiF is insoluble in ether and precipitates out of the solution rapidly, causing localised heating in the solution, which in turn causes the ether to boil. This is believed to be the cause of explosions in previous projects.

To avoid this, all reactions of this manner are performed with an excess of the Fluoromes or Fluoroxyl and at all times with the system open to the mercury bubbler. In this way there is always a pressure release mechanism.

1.5 Steric bulk in low coordinate phosphorus species

It is interesting to compare the steric properties of the Fluoromes and Fluoroxyl groups with other comparable bulky aryl ligands of the type $C_6H_2R_3$ (R = ^{t}Bu, CH_3 and ^{i}Pr). In the formation of diphosphenes using transition metal catalysed metathesis[19], the steric bulk of the aryl ligand determines the rate at which the diphosphene trimerises to form the trimer species R_3P_3.

$$RPCl_2 \xrightarrow[\text{toluene}]{W(PMe_3)_6} RP{=}PR + WCl_4(PMe)_2$$

Equation 1.3 – Formation of diphosphenes using transition metal catalysed metathesis

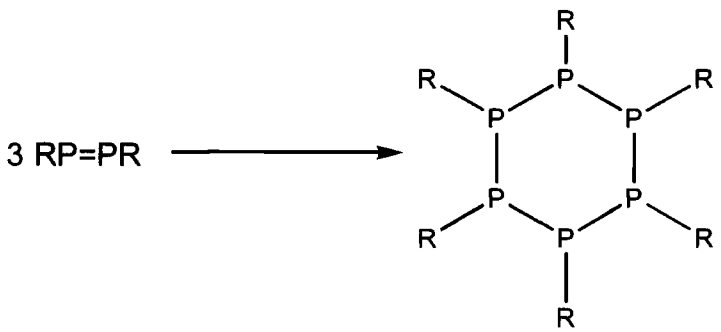

Equation 1.4 – Trimerisation of a diphosphene

Substituent used in $C_6H_2R_3$	Rate of decomposition of diphosphene
CH_3	No formation of RP=PR observed
^{i}Pr	8 Hours
^{t}Bu	RP=PR stable
CF_3	RP=PR stable

Table 1.3 – Stability of diphosphenes

The steric bulk of CF_3 is much closer to that of CH_3 than to that of the ^tBu group. Table 1.3 illustrates nicely the fact that the steric bulk itself is not the only factor affecting the stability of the compounds formed with Fluoromes and Fluoroxyl.

1.6 Low coordinate phosphorus species

Phosphorus has three common oxidation states (I, III, V) and is known to have coordination numbers from one (RCP) to six ($[PCl_6]^{(-)}$). Low coordinate phosphorus species are considered to be those with coordination number three or lower.

1.6.1 Three coordinate phosphorus species

There is a vast amount of P(III) chemistry, much of which is based around the derivatisation of PX_3 (X = Cl, Br, I) and the formation of P-F and P-H derivatives.

A very common reaction is that between an organolithium species and PCl_3 to form lithium chloride and the desired product $RPCl_2$. This is the reaction which forms the basis for the synthesis of most of the work described in this thesis.

$$RLi \xrightarrow[ether]{PCl_3} RPCl_2 + LiCl$$

Equation 1.5 – Formation of mono substituted phosphanes

Phosphorus can be derivatised to form RPX_2, R_2PX and R_3X depending on the steric bulk of the R group (e.g. PPh_3 can be synthesised, however PAr_3 cannot). The formation of di- and tri-substituted phosphanes has become more common over the last few years with the increase of research into organometallic chemistry.

PR_3 groups bond to metal centres through the lone pair on the phosphorus forming a single σ bond.

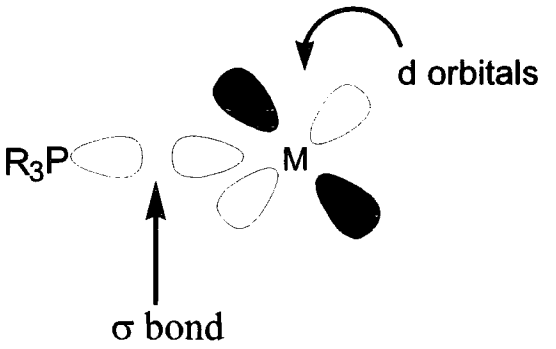

Figure 1.4 – Orbitals involved in bonding between phosphines and metal centres

The donation of the lone pair to a vacant metal orbital is not, however, the only factor that influences the bonding. Back bonding occurs from d-orbitals on the metal to the LUMO on the phosphorus (either a σ^* or π^* orbital) and this is a very important factor in transition metal chemistry. This back donation facilitates the stabilisation of 14 and 16 electron metal centres [e.g. "Wilkinson's catalyst" – $RhCl(PPh_3)_3$].

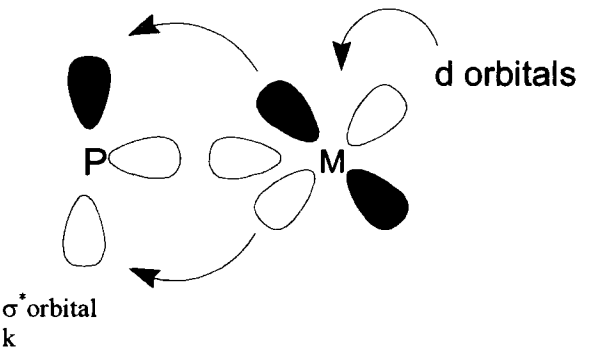

Figure 1.5 – Back donation of electron density into unoccupied orbitals on the phosphorus atom

1.6.2 Two coordinate phosphorus species

1.6.2.1 Diphosphenes

The formation of double bonds between elements outside the first long period of the periodic table was thought for many years to be impossible due to the "classical double bond rule" [20], rationalised by long bond distances and inefficient π-bonding in the second and third row elements.

The first diphosphene was synthesised by Yoshifuji[21] by the reduction of $SupermesPCl_2$ with elemental magnesium.

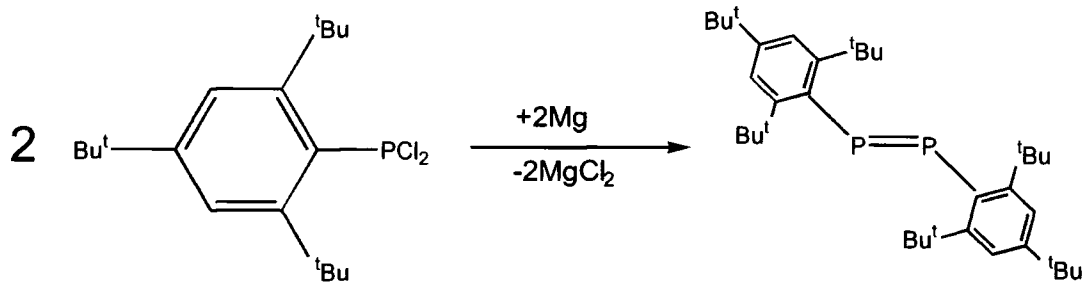

Equation 1.6 – Synthesis of the first symmetrical diphosphene

1.6.2.2 Phosphaalkenes

Phosphaalkenes are normally stabilised by bulky substituents on either the phosphorus, the carbon, or both atoms[22]. The type of phosphaalkene synthesised here was first prepared using the 2,4,6-tris(tritertiarybutyl)phenyl (Supermes) ligand[23].

One method of preparation is the reaction of RPH_2 with chloroform and alkali.

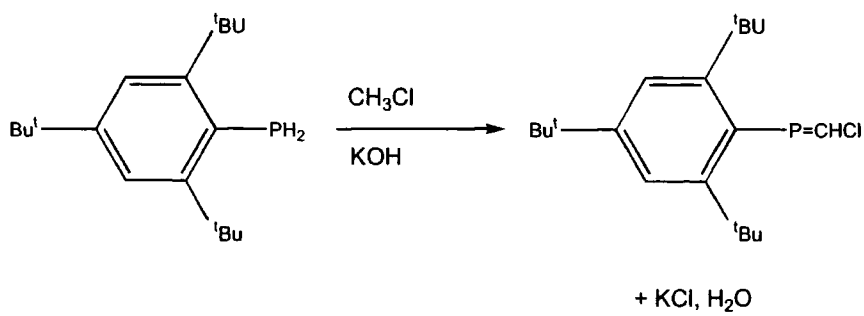

Equation 1.7 – Synthesis of a phosphaalkene (RP=CHCl)

This reaction was not successful for R= Ar' or Ar. Possible reasons for this are given in a later chapter (see Section 2.3). Goodwin did, however, synthesise a Fluoromes containing phosphaalkene, by the removal of HCl from $ArP(Cl)CHCl_2$ (see Section 2.2.15)

Since this first discovery there have been a number of 2-coordinate phosphorus compounds synthesised including species with P=As, P=C, P=Si, P=Ge, and P=Sn.[24]

1.6.2.3 P(I) species

A good example of a phosphorus species in oxidation state (I) was reported by Schmidtpeter *et al*[25] with synthesis and X-ray characterisation of $[P(CN)_2]^{(-)}$ in a sodium crown-ether salt. The standard P(I) reagent used in organometallic chemistry is $PPh_2^{(-)}Li^{(+)}$ which is synthesised as a pure yellow solid from the reaction between PPh_2H and BuLi.

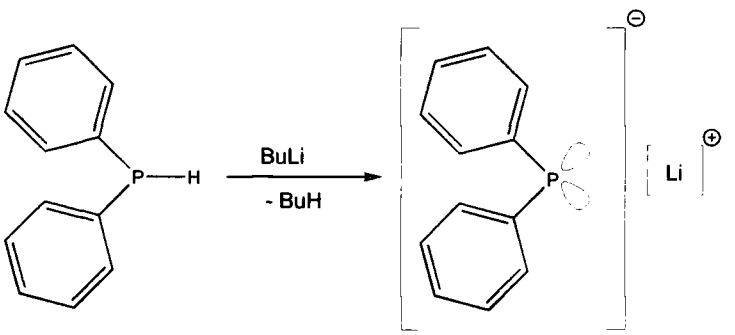

Equation 1.8 –Formation of $Li(PPh_3)_2^{(-)}$

1.6.2.4 Metal phosphides

The discovery of the $PPh_2^{[-]}$ ligand has led to the formation of metal phosphides of the type $M{=}PR_2$[26]. These compounds are analogous to the metal amides formed by the reaction of $LiNR_2$ and $M(Cp)_2Cl_2$.

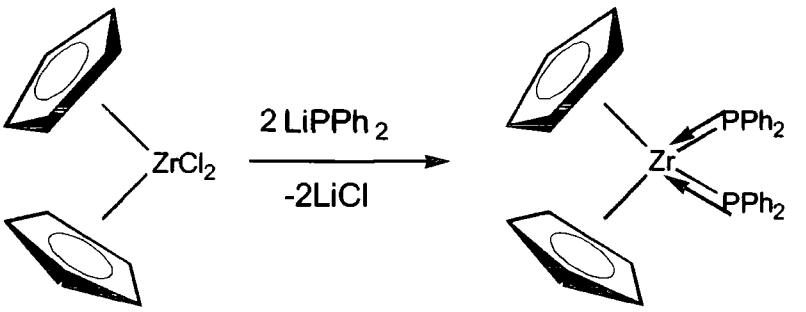

Equation 1.9 – Formation of a metal diphosphide

1.6.3 One coordinate phosphorus species

1.6.3.1 Phosphaalkynes

HCP, the most fundamental of all phosphaalkynes, has been known since 1961 when it was synthesised by the arcing of PH_3 between two graphite electrodes by Gier[27]. The compound is unstable at room temperature and was characterised by IR spectroscopy.

The synthesis of the first kinetically stable phosphaalkyne was published by Becker *et al* in 1981[28] and was slightly modified and the current synthetic method published by Regitz[29].

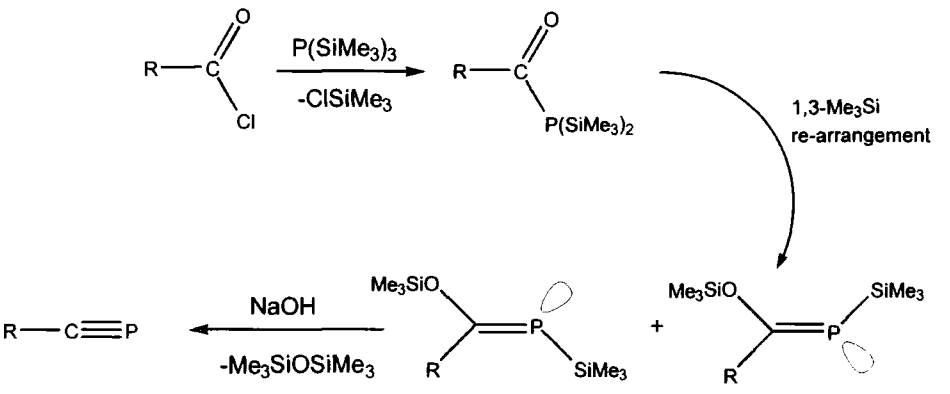

Equation 1.10 – Formation of a phosphaalkyne (R= ^{t}Bu, Adamantyl, Supermes)

1.7 Experimental

1.7.1 Preparation of 1,3,5-tris(trifluoromethyl)benzene

The vacuum line used for this reaction was specifically designed for the use and manipulation of SF_4. The inside of the line was coated with Teflon to prevent corrosion of the steel from the highly reactive gas. The vacuum system is outlined below (see Figure 1.6). An upper reservoir of known volume (425cm^3) was filled over a period of 15 minutes with SF_4 from a cylinder. The volume of this gas was equal to approximately 150g. This was subsequently transferred to a small sample bottle (teflon lined steel) using vacuum transfer methods. From the initial tare of the bottle the quantity of SF_4 transferred could be determined. This process was then repeated until the desired quantity of SF_4 (550g, 3.9moles) had been obtained. The bottle was then allowed to warm to room temperature.

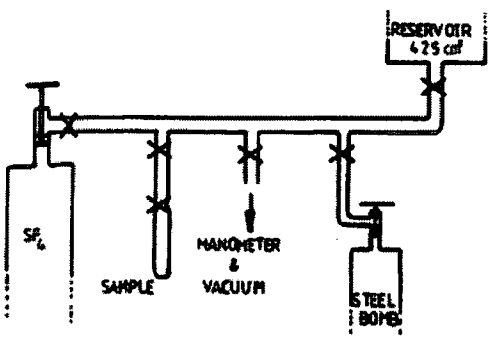

Figure 1.6 – Teflon lined steel vacuum line

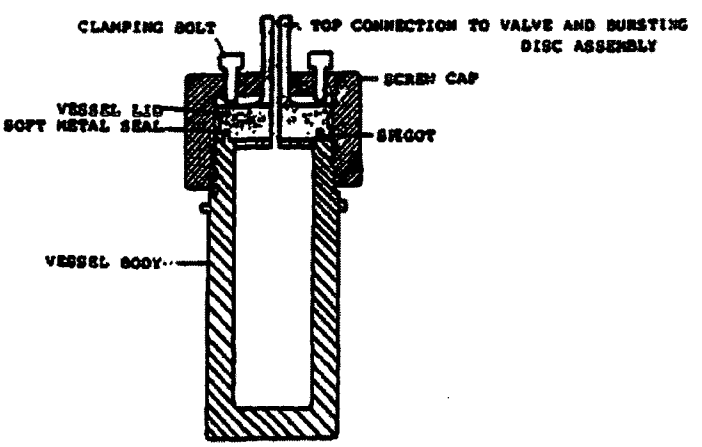

Figure 1.7 – Teflon lined steel bomb

Trimesic acid (benzene-1,3,5-tricarboxylic acid) (150g, 0.71moles) was introduced into a $1000cm^3$ bomb. It was then evacuated and cooled to 76K in liquid nitrogen.

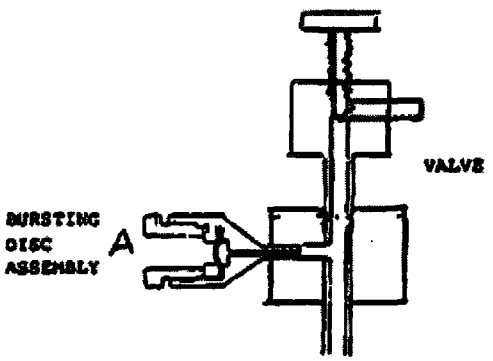

Figure 1.8 – Safety, Bursting disc assembly.

The contents of the steel bottle were then carefully condensed into the bomb and the tare of the bottle checked to ensure that all the SF_4 had been transferred. The bomb was then transferred to the high pressure facilities in a Dewar of liquid N_2 and allowed to warm up to room temperature safely under controlled conditions.

The bomb was then placed in a furnace, with the help of thermocouples heated to a temperature of 150°C which was maintained for the duration of the reaction (12 hours). The reaction was then allowed to cool to room temperature and the bomb was transferred to a fume cupboard.

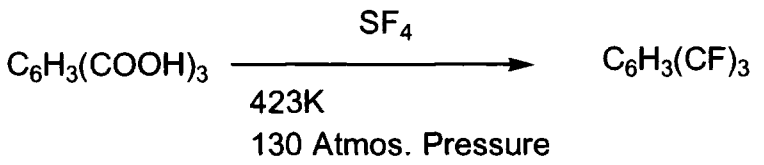

Equation 1.11 – Synthesis of Fluoromes

The by-products of the reaction are SO_2, HF, and any unreacted SF_4. These gases need to be scrubbed, neutralised, and not allowed into the atmosphere. The apparatus used for scrubbing is shown below (Figure 1.9). The gases are slowly passed over a vessel containing a saturated solution of potassium hydroxide. Sodium hydroxide is not used because the solubility of potassium fluoride is three times that of sodium fluoride. The second vessel containing KOH is there for safety should all the KOH in the first vessel is consumed during the scrubbing process.

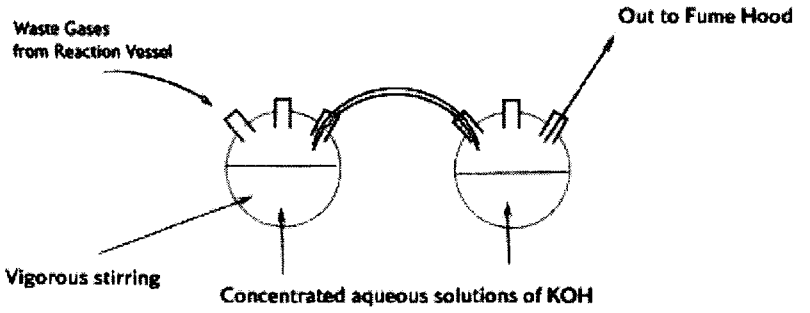

Figure 1.9 – Scrubbing system used to neutralise acidic waste gases

After scrubbing the gases, the contents of the bomb were then tipped onto crushed ice (to remove any unreacted trimesic acid and HF). The mixture was then filtered, treated with NaOH, and left to stir overnight to remove any last acidic impurities. The oily product was then separated and dried over anhydrous magnesium sulphate.

The product was then purified by distillation using a fractionating column to yield a colourless oil Bp 119°C (760mm Hg).

[1] E. T. McBee., R. E. Leech., *Ind. Eng. Chem.*, 1947, **39**, 393.
[2] G. E. Carr., R. D. Chambers., T. F. Holmes., D. G. Parker., *J. Organometallic Chem.*,1987, **325**, 13.
[3] M. Scholtz., H. W. Roesky., D. Stalke., K. Keller., F. T. Edelmann., *J Organometallic Chem.*, 1989, **366**, 73.
[4] R. D. Schulter., A. H. Atwood., R. A. Jones., M. R. Bond., C. J. Carrano., *J. Am. Chem. Soc.*,1993, **115**, 2070; R. D. Shulter., H. S. Isom., A. H. Cowley., D. A. Atwood., R. A. Jones., F. Olbright., S. Corbelin., R. J. Lagow., *Organometallics*, 1994, **13**, 4058.
[5] H. Grutzmacher., H. Prizkow., F. T. Edlemann., *Organometallics*, 1991, **10**, 23.
[6] S. Brooker., J-K. Buijink., F. T. Edlemann., *Organometallics*, 1991, **10**, 25.
[7] K. H. Whitmire., D. Labahn., H. W. Roesky., M. Noltemeyer., G. M. Sheldrick., *J. Organomet. Chem.*, 1991, **402**, 55.
[8] S. Brooker., N. Bertel., D. Stalke., M. Noltemeyer., R. W. Roesky., G. M. Sheldrick. F. T. Edelmann., *Organometallics*, 1992, **11**, 192.
[9] M. Belay., F. T. Edelmann., *J. Organomet. Chem.*, 1994, **479**, C21.
[10] F. T. Edelmann., W. Bruser., P. Poremba., *J. Fluorine. Chem.*, 1997, **82**, 43
[11] K. B. Dillon., H. P. Goodwin., *J. Organomet. Chem.*, 1992, **429**, 169.
[12] D. Stalke., K. Keller., F. T. Edlemann., M. Scholtz., H. W. Roesky., *J. Organomet. Chem.*, 1989, **366**,73
[13] K. B. Dillon., H. P. Goodwin., *J. Organomet. Chem.*, 1994, **469**, 125.
[14] T. A. Straw., *Ph. D Thesis*, Durham, **1991**.
[15] F. H. Allen., O. Kennard., *Chemical Design Automation News*, 1993, **8(1)1**, 31-37
[16] M. Y. Eyring., E. C. Zuerner., L. J. Radonovich., *Inorg. Chem.*, 1981, **20**, 3405.
[17] A. Dubourg., J. P., Declercq., H. Ranaivonjatovo., J. Escudié., C. Couret., M. Lazraq., *Acta Crystallographica., Sect. C.*, 1988, **44**, 2004.
[18] L. Heuer., P. G. Jones., R. Schmutzler., *J. Fluorine Chem.*, 1990, **46**, 243.
[19] K. B. Dillon., V. C. Gibson., L. J. Sequeira., *J. Chem. Soc. Chem. Comm.*, 1995, 2429.
[20] L. E. Gusel'nikov., N. S. Nametkin., *Chem. Rev.*, 1979, 529 and references therein.
[21] M. Yoshifuji., I. Shima., N., Inamoto., K. Hirotsu., T. Higuchi., *J. Am. Chem. Soc.*, 1981, **103**, 4587.
[22] J. F. Nixon., *Chem. Rev.*, 1988, **88**, 1327
[23] R. Appel., C. Casser., M. Immenkeppel., F. Knoch., *Angew. Chem. Ed. Int. Ed. Engl.*, 1984, **23**, 895
[24] O. J. Scherer., *Angew. Chem. Int. Ed. Engl.*, 1985, **24**, 924-943.
[25] W. S. Sheldick., J. Kroner., F. Zwaschka., A. Schmidtpeter., *Angew. Chem. Int. Ed. Engl.*, 1979, **1979**, 934.
[26] S. R. Wade., M. G. H. Wallbridge., G. R. Willey., *J. Chem. Soc. Dalton. Trans.*, 1983, 2555.
[27] T. E. Gier., *J. Am. Chem. Soc.*, 1961, **83**, 1769.
[28] G. Becker., W. Becker., R. Knebl., H. Schmidt., U. Weeber., M. Westerhausen., *Nova Acta Leopold.*, 1985, **59**, 55.
[29] M. Regitz., W. Rosch., T. Allspach., U. Annen., K. Blatter., J. Fink., M. Hermesdorf., H. Heydt., U. Vogelbacher., O. Wagner., *Phosphorus Sulfur.*, 1987, **30**, 479.

Chapter 2

Novel low-coordinate phosphane synthesis

2.1 Introduction

Dichlorophosphanes have been known since the 19th century[1], and form the starting material for the synthesis of other species of the type RPX_2 (where X = H, F) and other phosphanes described in this chapter.

2.1.1 Synthesis of P(III) species of the type RPX_2

A common and convenient method for the preparation of this type of compound is the reaction of a lithiated aryl or alkyl species with PCl_3, forming the desired alkyl/aryl phosphane. During the reaction LiCl precipitates out of solution (ether). The solvent is then removed *in vacuo* and the product is purified by distillation.

$$RLi \xrightarrow{PCl_3} RPCl_2 + LiCl$$

Equation 2.1 – Synthesis of a mono substituted phosphane

2.2 Novel phosphanes with bulky electron-withdrawing substituents

All the synthetic methods used in this chapter (unless otherwise stated) were similar to those first used by Helen Goodwin during her Ph.D[2].

2.2.1 Ar'PCl_2

The Ar'PCl_2 compound formed the basic starting material for a number of other phosphanes described later in this chapter. The product was obtained as an impure colourless oil (see Equation 2.2).

The ^{31}P NMR spectrum of the compound shows a septet at δ = 148.0ppm ($^4J_{P-F}$ = 65.2 Hz). This splitting is caused by the proximity of the fluorines on the CF_3 groups to the phosphorus atom (i.e. an interaction through space rather than through the connecting bonds). The ^{19}F NMR spectrum for this compound shows a single doublet with a chemical shift δ = -53.0 ppm ($^4J_{P-F}$ = 65.2 Hz).

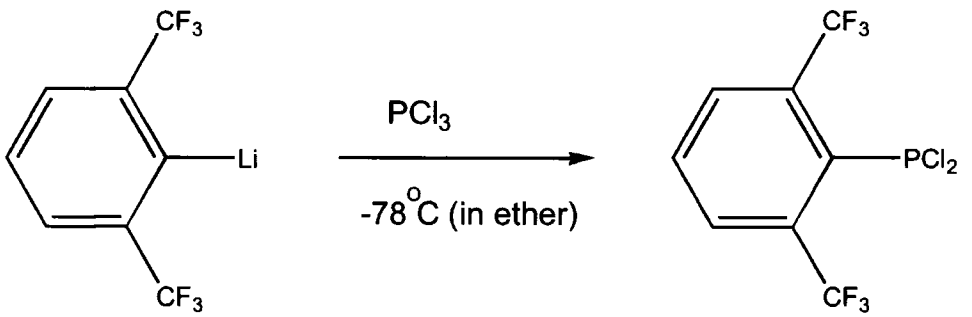

Equation 2.2 – Synthesis of Ar'PCl_2

2.2.1.1 ^{19}F Spectroscopic study on the reaction intermediates in the reaction of BuLi and Ar'H

In the reaction between Ar'H and BuLi there are a number of different possible lithiation sites shown in Figure 2.1. The most probable product, Ar'Li, will only show one resonance in the ^{19}F NMR because both CF_3 groups are equivalent. This is also true if the lithiation site is on the site *meta* to both CF_3 groups; this is the least likely site of substitution, as discussed earlier. If the *meta* site was lithiated, the resulting species would be very reactive and would then be likely to react in a coupling reaction with another aryl group.

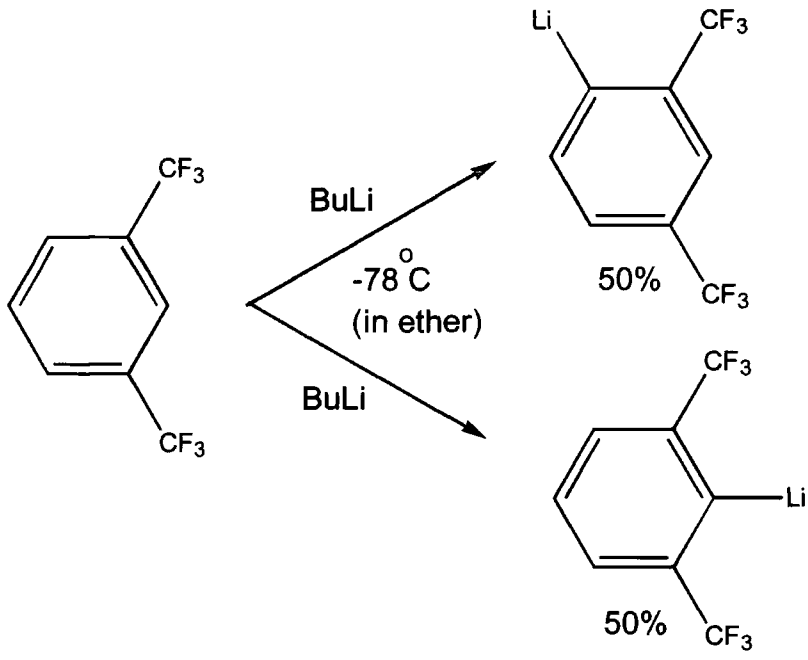

Figure 2.1 – Two products formed in the reaction between BuLi and Ar'H

If the lithiation site is *ortho* to one CF_3 group and *para* to the other, then the two CF_3 groups will be inequivalent, and two singlets should be apparent in the ^{19}F NMR spectrum.

By following the ^{19}F spectrum over the course of the reaction it is also possible to recognise when the maximum quantity of the lithiated species is present and thus maximise the yield of phosphane products.

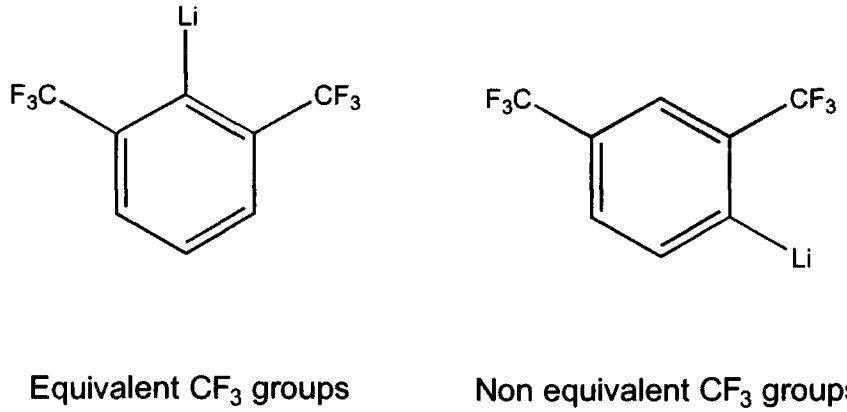

Figure 2.2 – Inequivalence of CF_3 groups in the products caused by lithiation of different sites

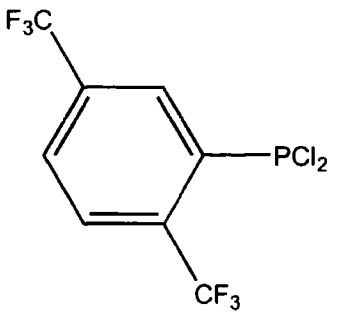

Undesired product [Ar''PCl_2]

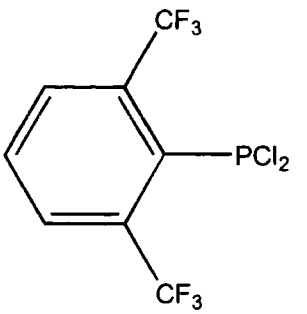

Desired product [Ar'PCl_2]

Figure 2.3 – Differences in products upon reaction of the lithiated products with PCl_3

2.2.2 Ar''PCl_2

The reaction of Ar'H with BuLi causes the formation of two distinct lithiated species. Upon further reaction with PCl_3, this in turn leads to the formation of two distinct $RPCl_2$ species. The two species (Ar'PCl_2 and Ar''PCl_2) have the same molecular mass and were therefore very difficult to separate. Fractional distillation of the resulting mixture did not separate the two compounds, although it would appear that Ar''PCl_2 boils at a slightly lower temperature than Ar'PCl_2 (the first few fractions contained a much greater percentage of Ar''PCl_2, but were impossible to obtain pure).

The ^{31}P NMR spectrum of the resulting mixed oil shows the resonance of Ar''PCl_2 to be a quartet δ = 151.1 ppm ($^4J_{P\text{-}F}$ = 84.5 Hz). The splitting is different to that of Ar'PCl_2 because there is only one CF_3 group in close proximity to the phosphorus atom. The size of the coupling constant is greater than that in the case of Ar'PCl_2, implying that the CF_3 groups are interacting more with the P atom. Knowing this, it is possible to concur that the average distance between the phosphorus atom and the fluorine atoms of the *ortho* CF_3 groups is shorter in Ar''PCl_2 than in Ar'PCl_2. The coupling constant is 29% larger than in the species containing Ar'.

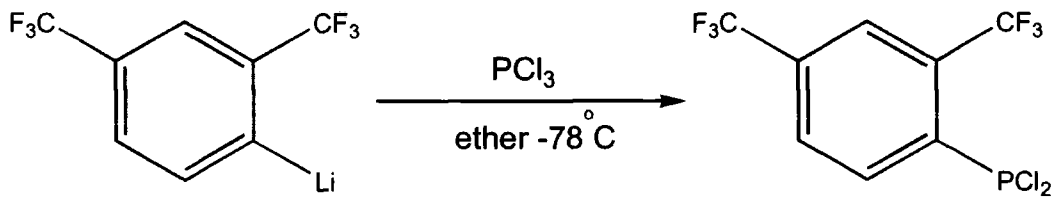

Equation 2.3 – Synthesis of Ar''PCl_2

2.2.3 Ar'PH_2

This phosphane was prepared by the reaction of the mixture of Ar'PCl_2/Ar''PCl_2 and Bu_3SnH. The product was purified by distillation and isolated as a clear colourless oil. The product obtained was Ar'PH_2 only, and showed no signs in its NMR spectra of Ar''PH_2, which remained below the detection limit.

The ^{31}P NMR spectrum of this compound shows the chemical shift of the compound has changed quite markedly, (δ = -140.3ppm) from that of the starting material Ar'PCl_2 There is a distinct phosphorus-hydrogen coupling, giving a triplet of septets ($^1J_{P\text{-}H}$ = 216.7Hz, $^4J_{P\text{-}F}$ = 29.4Hz).

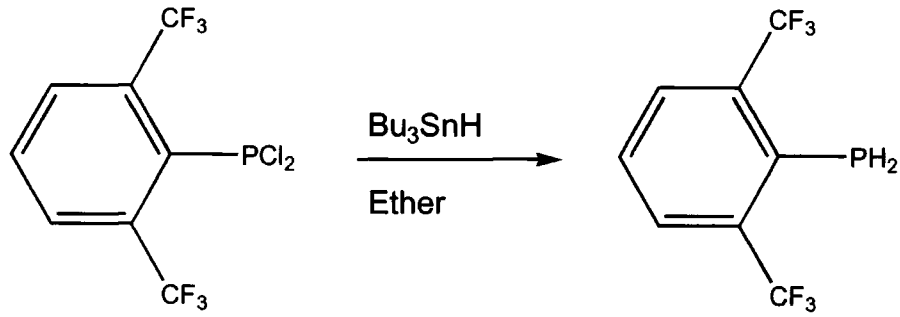

Equation 2.4 – Synthesis of Ar'PH_2

2.2.4 Ar'PF_2

The difluorophosphane was prepared by refluxing a solution of Ar'PCl_2/Ar''PCl_2 in ether with solid SbF_3 over 48 hours at atmospheric pressure. The product was purified by distillation and isolated as a clear colourless oil. The product obtained was Ar'PF_2 only, and showed no signs in its NMR spectra of Ar''PF_2, which remained below the detection limit.

The ^{31}P NMR spectrum of the compound shows distinct P-F coupling caused by both the CF_3 groups and the two new fluorines bonded to the phosphorus itself, again giving rise to a doublet of septets with chemical shift δ = 193.3 ppm ($^1J_{P\text{-}F}$ = 1224 Hz, $^4J_{P\text{-}F}$ = 48.3 Hz).

The ^{19}F NMR spectrum showed a doublet of triplets showing a small amount of F-F interaction and a doublet of septets. The chemical shifts for this compound were δ = -55.5 ppm ($^4J_{P\text{-}F}$ = 48.3 Hz) and δ = -91.85ppm ($^1J_{P\text{-}F}$ = 1224 Hz), ($^5J_{F\text{-}F}$ = 14.1 Hz).

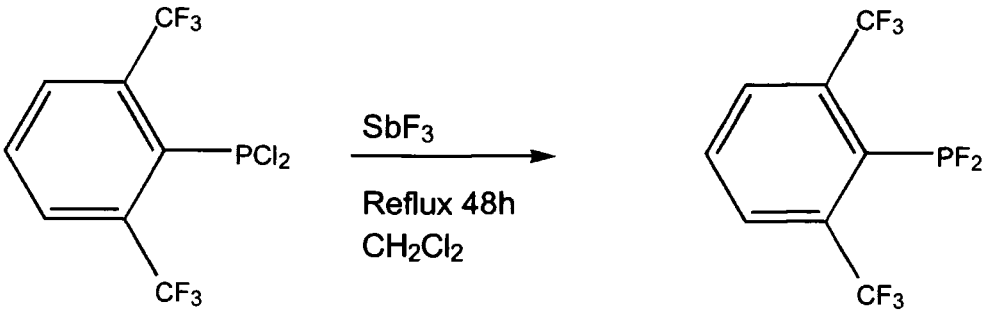

Equation 2.5 – Synthesis of Ar'PF_2

2.2.5 Ar'PBr_2 (Ar''PBr_2)

This compound was prepared in the same manner as Ar'PCl_2 except using PBr_3 instead of PCl_3. Although dibromophosphanes are less common than dichlorophosphanes, the preparation is in principle the same. The product was isolated as a very viscous yellow oil.

As in the case of the preparation of Ar'PCl_2, there is a mixture of inseparable products formed in this reaction (Ar'PBr_2 and Ar''PBr_2). The ^{31}P NMR spectrum of this compounds shows a septet and a quartet, δ = 135.8 ppm ($^4J_{P-F}$ = 62.8 Hz) and δ = 143.9 ppm ($^4J_{P-F}$ = 77.0 Hz).

The ^{19}F NMR spectrum of the two compounds shows two doublets and a singlet. Ar'PBr_2 has one doublet δ = -50.70ppm ($^4J_{P-F}$ = 62.8Hz). Ar''PBr_2 shows a doublet and a singlet, δ = -54.9 ppm ($^4J_{P-F}$ =77.0 Hz) and δ = -61.9 ppm.

This result confirms the result shown for the Ar'PCl_2/Ar''PCl_2 case where the species containing Ar'' had a larger coupling constant that the species containing Ar'. In this case the coupling constant is 23% larger for Ar''PBr_2.

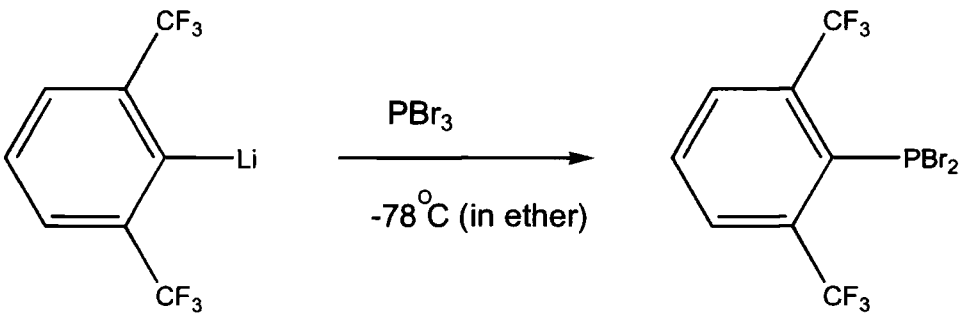

Equation 2.6 – Synthesis of Ar'PBr_2

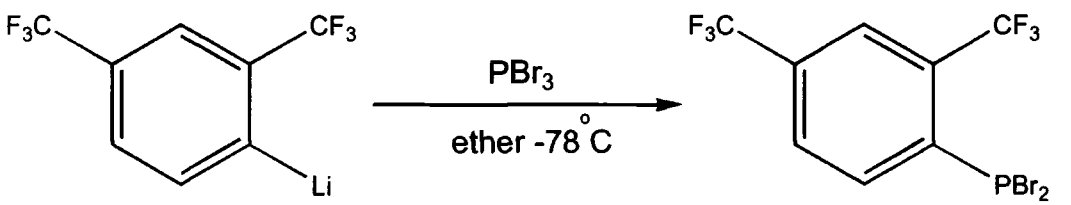

Equation 2.7 – Synthesis of Ar''PBr_2

2.2.6 Ar'P(Cl)$CHCl_2$

This phosphane was produced by the careful reaction of Ar'PCl_2/Ar''PCl_2 with a solution of lithiated CH_2Cl_2 at -130°C in a pentane slush bath. The temperature in this reaction is crucial because lithiated dichloromethane decomposes above –120°C. During the reactions, the solutions must be kept from freezing solid because this would not facilitate transfer through a cannular. This was achieved by a combination of solvents and by vigorous mechanical stirring. There were no signs of the Ar''P(Cl)$CHCl_2$ species from the ^{31}P NMR spectrum. The compound was isolated by distillation yielding a colourless oil.

The ^{31}P NMR spectrum of the product shows a septet with a chemical shift, δ = 65.6 ppm ($^4J_{P-F}$ = 48.6 Hz). The ^{19}F NMR spectrum shows a doublet with chemical shift δ = -53.6 ppm ($^4J_{P-F}$ = 48.6Hz).

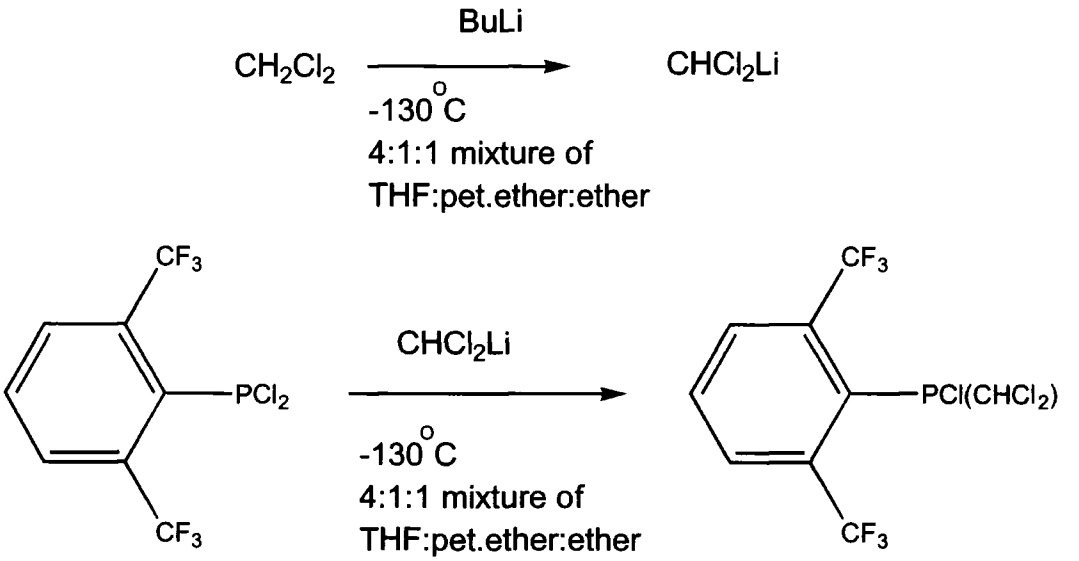

Equation 2.8 – Synthesis of Ar'P(Cl)$CHCl_2$

2.2.7 Ar'P=CCl_2

The synthesis of this compound involves the removal of HCl from Ar'P(Cl)$CHCl_2$ using the tertiary amine base DBU. DBU was used because it is a strong non-nucleophilic base, and as such will not cause a direct reaction with the P-Cl bond. The product is isolated as a colourless oil.

The ^{31}P NMR spectrum of this compound showed a septet with a chemical shift, δ = 206.8 ppm ($^4J_{P-F}$ = 21.5 Hz). The ^{19}F NMR spectrum showed a doublet with a chemical shift, δ = -59.89 ppm ($^4J_{P-F}$ = 21.5 Hz).

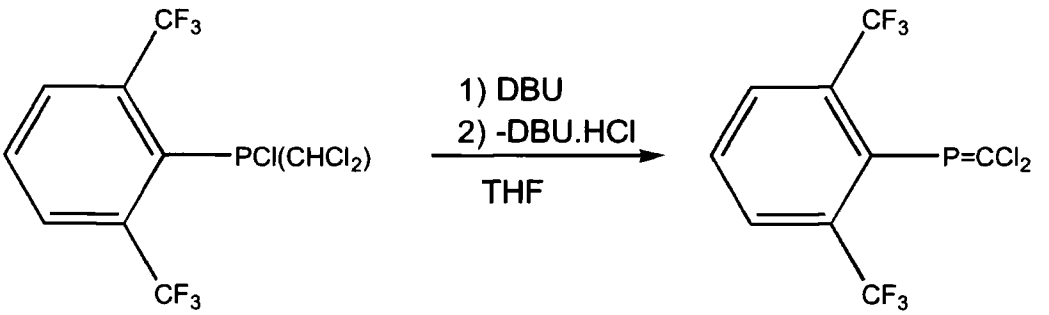

Equation 2.9 – Synthesis of Ar'P=CCl_2

2.2.8 Ar'$_2$PCl (Ar'Ar''PCl)

2.2.8.1 Attempted formation of Ar'$_2$PCl

As shown in Section 2.2.1, when BuLi is added to a solution of Ar'H in ether there are two different lithiated products formed (Ar'Li and Ar''Li). When PCl_3 is added to this solution this facilitates the formation of a number of different products (see Figure 2.4). The formation of the di-substituted products does not appear to be controlled by the ratio of lithiated product to PCl_3.

In the formation of Ar_2PCl (see Section 2.2.11), due to the steric hindrance of surrounding the phosphorus atom with four CF_3 groups, formation of the di-substituted product is difficult and the reaction is slow. In this reaction, however, the formation of the di-substituted product seems to be facilitated more easily than the formation of the mono-substituted product. Even when a large excess of PCl_3 is used a significant quantity of the di-substituted product is formed.

Because Fluoroxyl is more electronegative than chlorine (see Section 1.3.3) the P-Cl bond in $RPCl_2$ will be weaker than in PCl_3. It is reasonable to assume that the newly formed $RPCl_2$ species is more reactive to RLi than PCl_3. In the case of R=Ar this effect is tempered by the steric hindrance of both the CF_3 groups, being in the *ortho* position. The steric effect is less of a consideration if there is only one *ortho* CF_3 group as in the case of Ar''.

There are a number of different possible products obtainable by the addition of PCl_3 to the mixture of Ar'Li and Ar''Li.

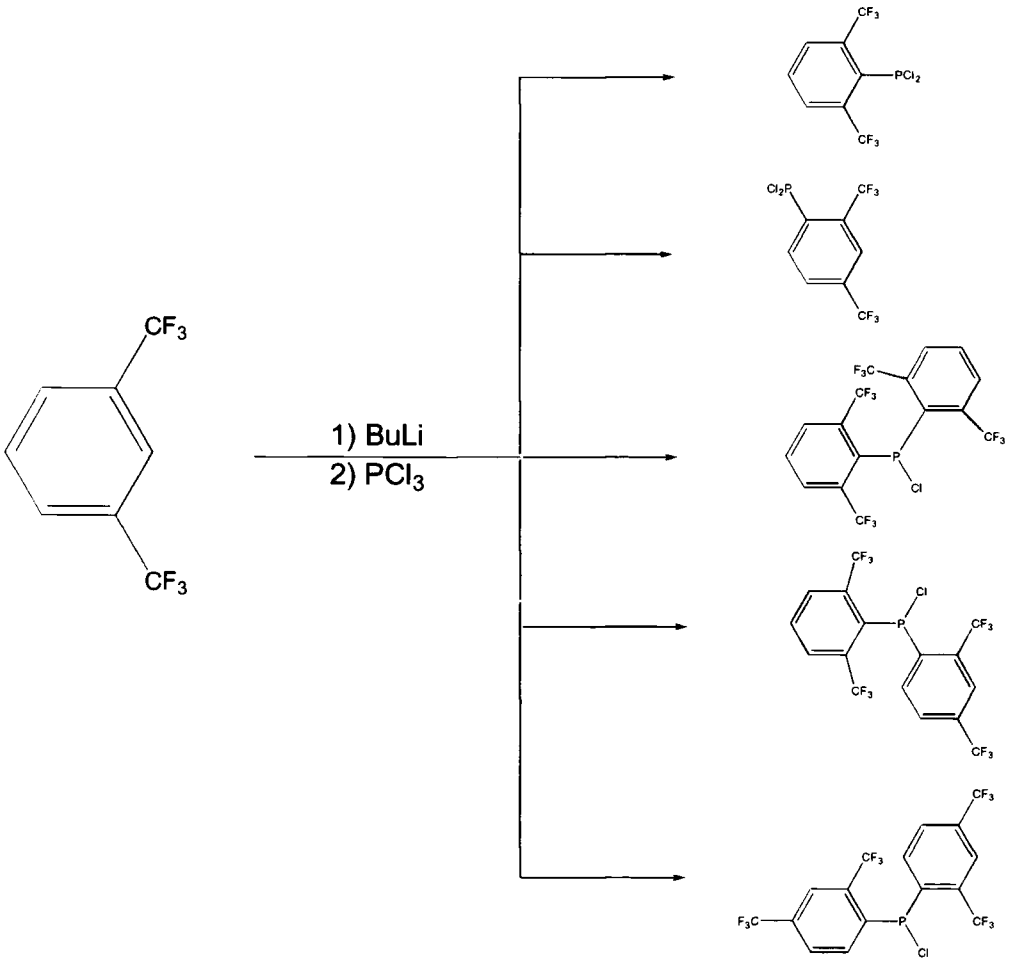

Figure 2.4 – Possible products (mono and disubstituted) formed in the between Ar'H, BuLi and PCl_3

The product was isolated by distillation and a white crystalline solid was purified by recrystallisation from hexanes.

The ^{31}P NMR spectrum of the product showed the existence of only one di-substituted product. The spectrum shows a complicated multiplet and although all the expected peaks are not visible it was possible to obtain a chemical shift δ = 67.3 ppm ($^4J_{P\text{-}F}$ = 67.1 Hz). The expected spectrum would be a septet of quartets due to the six equivalent fluorines on the Ar' CF_3 group and the fluorines on the Ar''CF_3 group.

The structure deduced from the NMR spectra was also confirmed by X-ray crystallographic analysis on crystals of the compound (see Section 2.2.8.3). The ^{19}F spectrum shows a doublet and two singlets (see Equation 2.10).

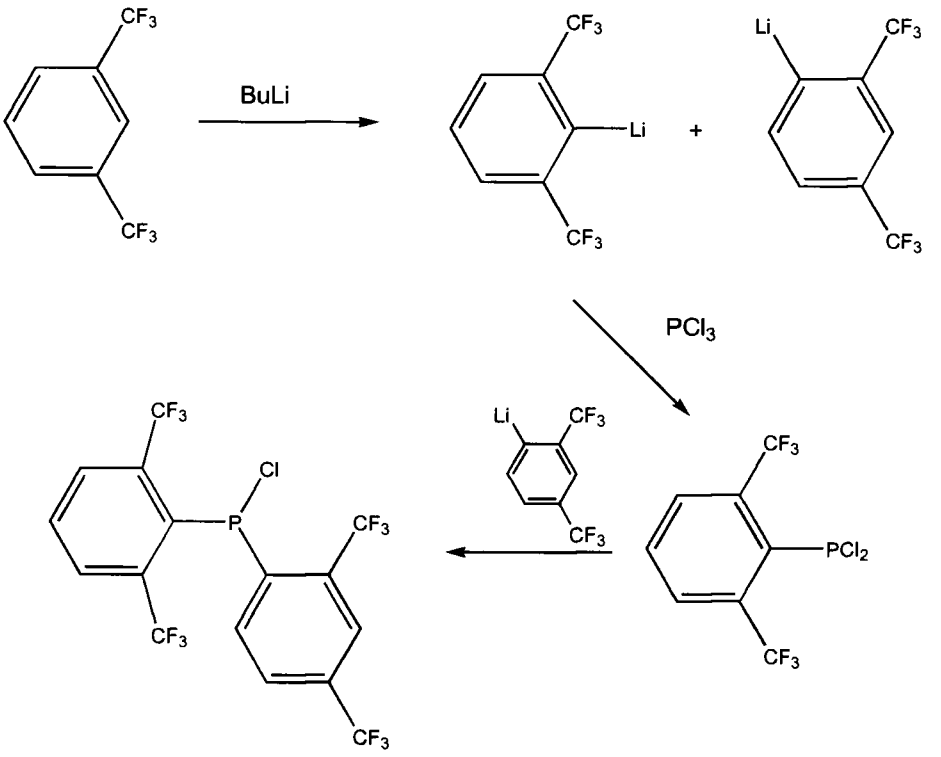

Equation 2.10 – Synthesis of Ar'Ar''PCl

^{19}F NMR studies (see Section 2.2.1.1) have shown that the ratio of lithiated products in the initial reaction is approximately 50:50. This would imply that the most probable di-substituted product would be the mixed Ar'Ar''PCl in preference to Ar''$_2$PCl or Ar'$_2$PCl.

After purification by distillation the ratio of $Ar'PCl_2$ to $Ar''PCl_2$ has been reduced from approximately 50:50 to 66:33 in favour of the more sterically hindered product. Whilst it is fortuitous as that is the desired product, there appears to be a deficit in the amount of Ar'' aryl groups present in the products. The less sterically hindered Ar''Li is more likely to be involved in side reactions, with the possible formation of other coupling products and LiF. After purification the mixture left in the reaction vessel contained a number of different fluorinated species but none containing phosphorus (determined from ^{19}F and ^{31}P NMR studies).

2.2.8.2 Variable temperature ^{19}F NMR studies on Ar'Ar''PCl

The ^{19}F spectrum of Ar'_2PCl would only show a doublet because all the fluorines are equivalent and the signal is coupled to the phosphorus through space. At room temperature, however, the ^{19}F NMR spectrum of Ar'Ar''PCl in toluene shows a doublet with a chemical shift δ = -59.3ppm ($^4J_{P-F}$ = 59.1 Hz) and two singlets, δ = -55.4 (broad peak) and δ = -64.1 ppm (sharp). These peaks are in the ratio 1:2:1, implying that the broad singlet is indeed due to two CF_3 groups rather than one.

From the diagram (Figure 2.5), it is possible that there are four inequivalent CF_3 groups present if the molecule is rigid on the NMR time scale. In this position we would expect to see three doublets and a singlet.

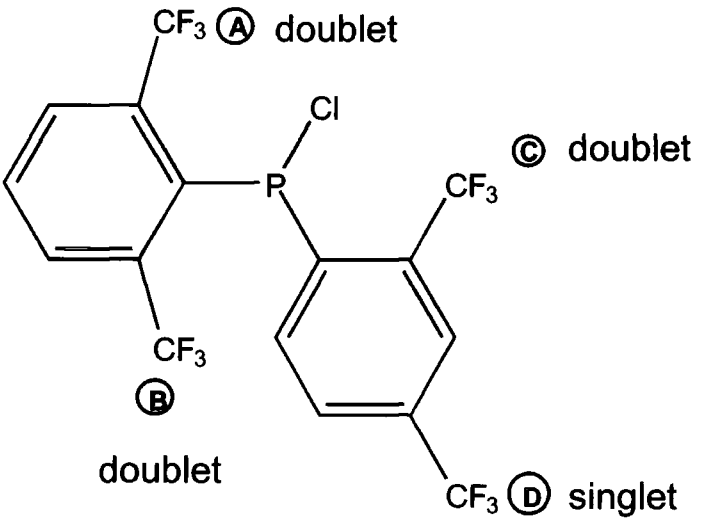

Figure 2.5 – Expected NMR signals for Ar'Ar''PCl

The room temperature spectrum shows three inequivalent CF_3 groups, which can be assigned to a doublet and singlet from the two CF_3 groups on the Ar'' group, and the broad peak arises from both the CF_3 groups from the Ar' group. If these two CF_3 groups were equivalent, a well resolved doublet would be expected; if they were completely (not exchanging), then two doublets would result. What is seen from the resulting spectrum, is that the CF_3 groups become almost equivalent, but not sufficient enough to give a clear doublet in the NMR spectrum.

If the solution (in toluene) is heated to 100°C the ^{19}F NMR spectrum shows a broad doublet in the position where the broad singlet was (δ = -55.0 ppm $^4J_{P-F}$ = 35.3 Hz). This demonstrates that the rotation of the Ar' group about the P-C bond is fast enough on the NMR time scale for the two CF_3 groups to become equivalent.

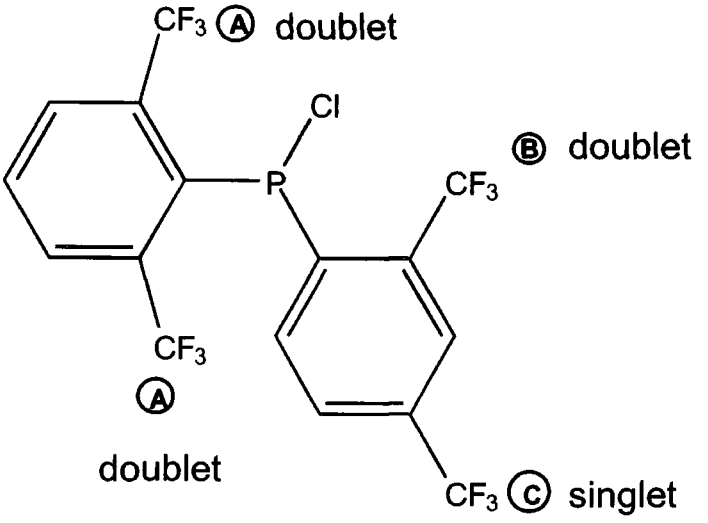

Figure 2.6 – Equivalent CF_3 groups shown in the NMR at 100°C of Ar'Ar''PCl

If the solution is cooled and the rotation of the Ar' group around the P-C bond is slowed significantly on the NMR time scale so that the two CF_3 groups become inequivalent, then the expected spectrum would have 3 separate doublets and a singlet. When the solution is cooled down to –78°C, however, the ^{19}F solution NMR shows two doublets and two singlets. The doublet and singlet, assigned to the Ar'' group from before, are at the same chemical shifts (δ = -59.5 ppm and δ = -64.0 ppm).

The peaks assignable to the CF_3 groups from Ar', however, do not show two separate doublets. The ^{19}F NMR spectrum shows a doublet (δ = -54.5 ppm, $^4J_{P-F}$ = 75.8 Hz) and a singlet (δ = -56.6 ppm). This result implies that not only are the CF_3 groups on the Ar' group inequivalent, it implies that one of the CF_3 groups is significantly further away from the phosphorus atom than the other.

This result is confirmed from the X-ray crystallographic structure of the molecule (see Section 2.2.8.3). The closest contact distance of one of the fluorines in an *ortho* CF_3 group (A) to the phosphorus atom is 2.89Å and the closest distance of a fluorine atom in the CF_3 group (B) is 3.25 Å.

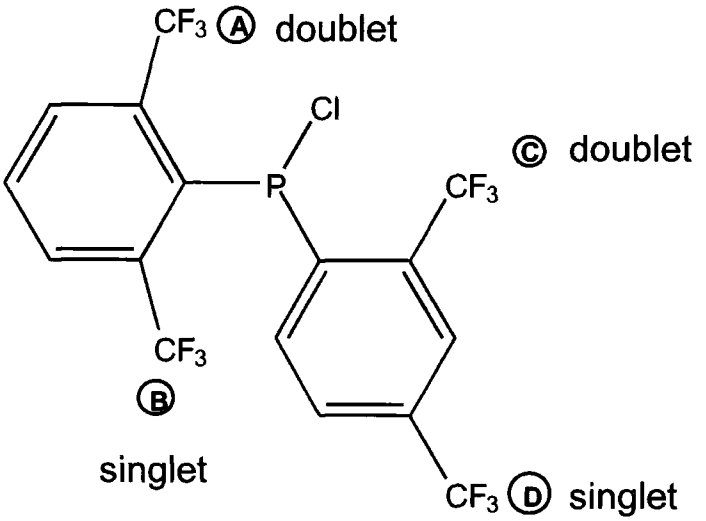

Figure 2.7 – Inequivalent CF_3 groups shown by NMR at –78°C

2.2.8.3 X-ray structure of Ar'Ar''PCl

Data collection and structure solution was performed by Dr A. S. Batsanov.

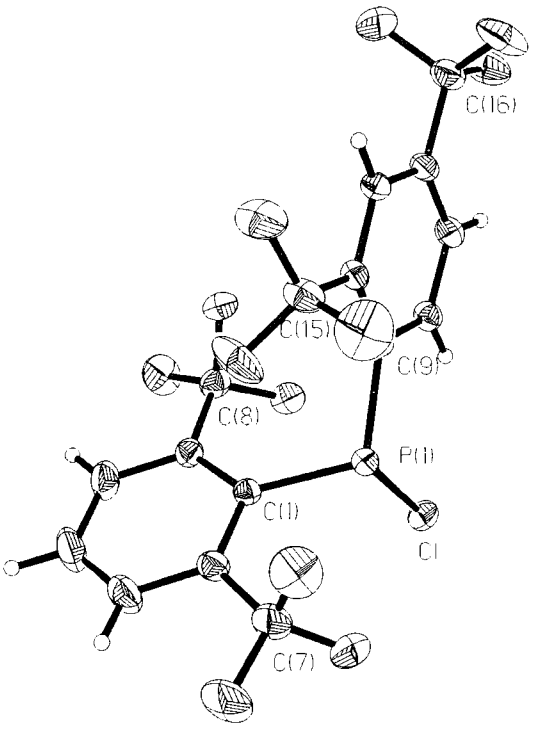

Figure 2.8 – Thermal Ellipsoid diagram at 150K (50% probability) for Ar'Ar''PCl

The structure of this compound shows a number of interesting characteristics. These characteristics are the result of steric interactions and a number of intramolecular interactions between atoms in the same molecule.

- The following diagrams shows differences in the fluorine to phosphorus distances. These differences in distance are shown up in the low temperature solution NMR studies of the compound, which shows two distinct peaks assignable to inequivalent CF_3 groups on the same aryl group (see Section 2.2.8.2).

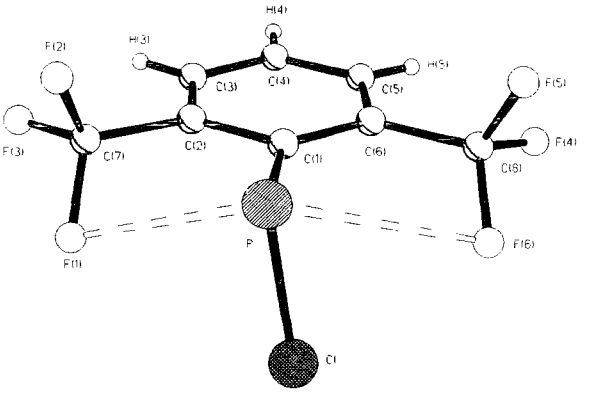

Figure 2.9 – Thermal ellipsoid diagram at 150 (50% probability) showing the inequivalence of the CF_3 groups on the Ar' group in the solid state

Figure 2.10 shows the interactions between some of the fluorine atoms within the CF_3 groups and the phosphorus atom.

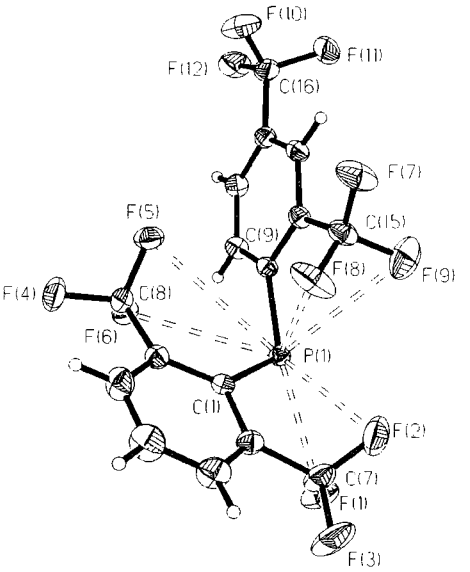

Figure 2.10 – P-F interactions in the solid-state structure of Ar'Ar''PCl
(The chlorine atom (Cl1) has been omitted for clarity)

Table 2.1 shows the comparison between phosphorus fluorine distances from a number of atoms on different CF_3 groups within the molecule. What is immediately apparent from the table is that F(1) and F(2) are significantly closer to the phosphorus atom that F(5) and F(6). This demonstrates the inequality in the two CF_3 groups on the Ar' aryl ring. The distance between the nearest fluorine atom on the Ar'' aryl group and the phosphorus atom [F(8)-P(1)] is also significantly shorter than F(6)-P(1).

Fluorine Atom	**Distance to P(1) (Å)**
F(1)	2.89
F(2)	2.89
F(5)	3.68
F(6)	3.25
F(8)	2.89
F(9)	3.36

Table 2.1 - P-F bond lengths in Ar'Ar''PCl

- There is an interaction between the chlorine and the adjacent hydrogen atom on the Ar'' group. This interaction is possible because the Ar'' group does not have two CF_3 groups *ortho* to the phosphorus atom. The distance between the two atoms is 2.52 Å which is close enough to be considered an intramolecular hydrogen bond[3].

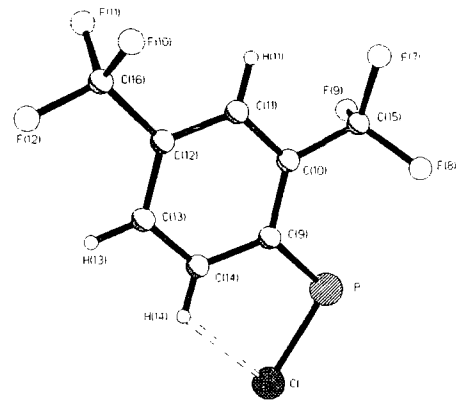

Figure 2.11 – Thermal ellipsoid diagram at 150 (50% probability) showing the interaction between the chlorine atom and the adjacent hydrogen atom on the aryl group Ar''.

- It is also worthy of note that the plane of the aryl ring is the same at the P-Cl...H bond. This is more evidence for the H-Cl interaction as this appears to be determining the conformation of the aryl ring and its position in the structure. The bond angle C(9)-P(1)-Cl(1) is equal to 102° which shows a reduction from the ideal tetrahedral angle of 109°.

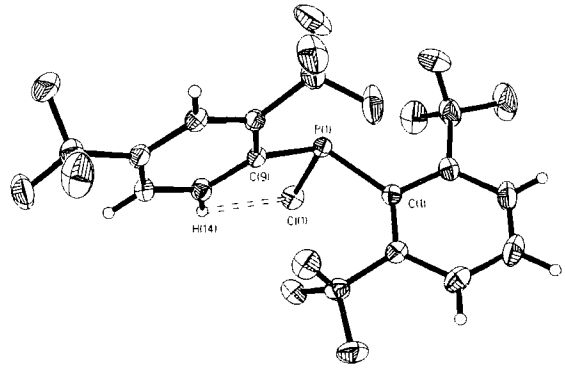

Figure 2.12 – Thermal ellipsoid diagram at 150 (50% probability) showing the P-Cl..H hydrogen bond it's effect on the structure of the molecule

- The steric influences on the molecule are due to the bulky CF_3 groups on the Ar' and Ar'' groups. The angle between the two aryl rings is 94°, which significantly decreases the interaction between the CF_3 groups on different aryl groups.

Crystal data and structure refinement.	
Identification code	Ar'Ar''PCl
Empirical formula	$C_{16}H_6ClF_{12}P$
Formula weight	492.63
Temperature	150(2) K
Wavelength	0.71073 Å
Crystal system	Triclinic
Space group	P-1
Unit cell dimensions	a = 7.949(1) Å α = 104.25(1) °. b = 9.313(1) Å β = 90.49(1) °. c = 12.369(1) Å χ = 96.35(1) °.
Volume	881.4(2) $Å^3$
Z	2
Number of reflections used	Calculation of cell = 512 Total = 10579 Unique = 4735 Obs [I>2σ(I)] = 4285
Crystal description	needle
Crystal colour	colourless
Density (calculated)	1.856 g/cm^3
Absorption coefficient	4.43 cm^{-1}
F(000)	484
Crystal size	0.2 x 0.2 x 0.3 mm
Theta range for data collection	1.70 to 30.44 °.
Index ranges	-11<=h<=10, -13<=k<=12, -17<=l<=16
Experiment device	Siemens SMART
Experiment methods	ω scans
Reflections collected	10579
Independent reflections	4735 [R(int) = 0.0231]
Refinement method	Full-matrix least-squares on F^2
Data / restraints / parameters	4710 / 0 / 295
Goodness-of-fit on F^2	1.094
Final R indices [I>2σ(I)]	R_1 = 0.0324, wR_2 = 0.0761
R indices (all data)	R_1 = 0.0381, wR_2 = 0.0861
Largest diff. peak and hole	0.583 and -0.383 e.$Å^{-3}$

Table 2.2 - Crystal data and structure refinement for Ar'Ar''PCl

	x	y	z	U(eq)
P(1)	6022(1)	3418(1)	3267(1)	19(1)
Cl(1)	8253(1)	4457(1)	4103(1)	26(1)
C(1)	6803(2)	2747(2)	1825(1)	19(1)
C(2)	6975(2)	1203(2)	1530(1)	24(1)
C(3)	7459(2)	490(2)	471(2)	35(1)
C(4)	7757(3)	1277(2)	-331(2)	41(1)
C(5)	7625(2)	2792(2)	-69(1)	33(1)
C(6)	7174(2)	3531(2)	995(1)	22(1)
C(7)	6644(2)	215(2)	2337(2)	35(1)
C(8)	7136(2)	5197(2)	1189(1)	25(1)
C(9)	4803(2)	5012(2)	3308(1)	19(1)
C(10)	3096(2)	4756(2)	2902(1)	20(1)
C(11)	2094(2)	5919(2)	3053(1)	22(1)
C(12)	2748(2)	7352(2)	3647(1)	22(1)
C(13)	4394(2)	7617(2)	4077(1)	24(1)
C(14)	5412(2)	6459(2)	3904(1)	22(1)
C(15)	2254(2)	3215(2)	2335(1)	29(1)
C(16)	1597(2)	8563(2)	3829(1)	28(1)
F(1)	7528(2)	744(1)	3306(1)	44(1)
F(2)	4999(2)	38(1)	2577(1)	48(1)
F(3)	7076(2)	-1158(1)	1917(1)	61(1)
F(4)	7938(2)	5736(1)	393(1)	41(1)
F(5)	5554(1)	5581(1)	1187(1)	31(1)
F(6)	7904(1)	5961(1)	2166(1)	29(1)
F(7)	840(1)	3243(1)	1759(1)	45(1)
F(8)	3259(1)	2427(1)	1616(1)	52(1)
F(9)	1821(2)	2415(1)	3073(1)	58(1)
F(10)	958(2)	8714(1)	2860(1)	49(1)
F(11)	267(1)	8266(1)	4425(1)	47(1)
F(12)	2378(1)	9895(1)	4366(1)	42(1)

Table 2.3 - Atomic coordinates (x 10^4) and equivalent isotropic displacement parameters ($Å^2$ x 10^3) for Ar'Ar''PCl. U(eq) is defined as one third of the trace of the *ortho*gonalized Uij tensor

Bond lengths [Å] and angles [°] for Ar'Ar''PCl.	
P(1)-C(9)	1.8518(14)
P(1)-C(1)	1.8746(14)
P(1)-Cl(1)	2.0608(6)
P(1)-F(1)	2.8903(11)
P(1)-F(8)	2.8969(12)
C(1)-C(6)	1.415(2)
C(1)-C(2)	1.416(2)
C(2)-C(3)	1.394(2)
C(2)-C(7)	1.522(2)
C(3)-C(4)	1.378(3)
C(3)-H(3)	.90(2)
C(4)-C(5)	1.384(3)
C(4)-H(4)	.96(2)
C(5)-C(6)	1.396(2)
C(5)-H(5)	.90(2)
C(6)-C(8)	1.514(2)
C(7)-F(1)	1.338(2)
C(7)-F(3)	1.340(2)
C(7)-F(2)	1.345(2)
C(8)-F(6)	1.345(2)
C(8)-F(5)	1.345(2)
C(8)-F(4)	1.345(2)
C(9)-C(14)	1.398(2)
C(9)-C(10)	1.417(2)
C(10)-C(11)	1.392(2)
C(10)-C(15)	1.511(2)
C(11)-C(12)	1.396(2)
C(11)-H(11)	.94(2)
C(12)-C(13)	1.382(2)
C(12)-C(16)	1.506(2)
C(13)-C(14)	1.395(2)
C(13)-H(13)	.96(2)
C(14)-H(14)	.93(2)
C(15)-F(7)	1.332(2)
C(15)-F(8)	1.337(2)
C(15)-F(9)	1.339(2)
C(16)-F(12)	1.335(2)
C(16)-F(11)	1.336(2)
C(16)-F(10)	1.343(2)
C(9)-P(1)-C(1)	109.23(6)
C(9)-P(1)-Cl(1)	102.10(5)
C(1)-P(1)-Cl(1)	100.23(4)
C(9)-P(1)-F(1)	172.45(5)
C(1)-P(1)-F(1)	75.04(5)
Cl(1)-P(1)-F(1)	82.91(3)
C(9)-P(1)-F(8)	71.98(5)
C(1)-P(1)-F(8)	68.11(5)
Cl(1)-P(1)-F(8)	163.08(3)

Bond lengths [Å] and angles [°] for Ar'Ar''PCl.	
F(1)-P(1)-F(8)	104.75(4)
C(6)-C(1)-C(2)	116.54(12)
C(6)-C(1)-P(1)	129.91(10)
C(2)-C(1)-P(1)	113.50(10)
C(3)-C(2)-C(1)	121.69(14)
C(3)-C(2)-C(7)	115.60(14)
C(1)-C(2)-C(7)	122.70(13)
C(4)-C(3)-C(2)	120.3(2)
C(4)-C(3)-H(3)	119(2)
C(2)-C(3)-H(3)	121(2)
C(3)-C(4)-C(5)	119.7(2)
C(3)-C(4)-H(4)	120.9(14)
C(5)-C(4)-H(4)	119.4(14)
C(4)-C(5)-C(6)	120.8(2)
C(4)-C(5)-H(5)	120(2)
C(6)-C(5)-H(5)	119(2)
C(5)-C(6)-C(1)	120.93(14)
C(5)-C(6)-C(8)	115.71(13)
C(1)-C(6)-C(8)	123.35(12)
F(1)-C(7)-F(3)	105.9(2)
F(1)-C(7)-F(2)	107.3(2)
F(3)-C(7)-F(2)	106.3(2)
F(1)-C(7)-C(2)	112.86(14)
F(3)-C(7)-C(2)	111.82(14)
F(2)-C(7)-C(2)	112.19(14)
F(6)-C(8)-F(5)	107.21(12)
F(6)-C(8)-F(4)	106.26(12)
F(5)-C(8)-F(4)	106.01(12)
F(6)-C(8)-C(6)	112.16(12)
F(5)-C(8)-C(6)	112.85(12)
F(4)-C(8)-C(6)	111.90(12)
C(14)-C(9)-C(10)	117.48(12)
C(14)-C(9)-P(1)	121.50(10)
C(10)-C(9)-P(1)	120.07(10)
C(11)-C(10)-C(9)	120.93(12)
C(11)-C(10)-C(15)	116.81(12)
C(9)-C(10)-C(15)	122.21(12)
C(10)-C(11)-C(12)	119.99(13)
C(10)-C(11)-H(11)	118.6(12)
C(12)-C(11)-H(11)	121.3(12)
C(13)-C(12)-C(11)	119.96(13)
C(13)-C(12)-C(16)	121.82(13)
C(11)-C(12)-C(16)	118.19(13)
C(12)-C(13)-C(14)	120.08(13)
C(12)-C(13)-H(13)	121.7(12)
C(14)-C(13)-H(13)	118.2(12)
C(13)-C(14)-C(9)	121.50(13)
C(13)-C(14)-H(14)	118.2(12)
C(9)-C(14)-H(14)	120.3(12)

Bond lengths [Å] and angles [°] for Ar'Ar''PCl.	
F(7)-C(15)-F(8)	106.46(14)
F(7)-C(15)-F(9)	106.40(14)
F(8)-C(15)-F(9)	106.51(14)
F(7)-C(15)-C(10)	112.86(13)
F(8)-C(15)-C(10)	112.53(12)
F(9)-C(15)-C(10)	111.62(13)
F(12)-C(16)-F(11)	107.12(13)
F(12)-C(16)-F(10)	106.99(13)
F(11)-C(16)-F(10)	106.14(14)
F(12)-C(16)-C(12)	112.84(13)
F(11)-C(16)-C(12)	111.70(13)
F(10)-C(16)-C(12)	111.67(13)
C(7)-F(1)-P(1)	82.33(8)
C(15)-F(8)-P(1)	89.01(9)

Table 2.4 - Bond lengths [Å] and angles [°] for Ar'Ar''PCl

	U11	U22	U33	U23	U13	U12
P(1)	20(1)	19(1)	18(1)	4(1)	2(1)	4(1)
Cl(1)	22(1)	32(1)	23(1)	5(1)	-5(1)	5(1)
C(1)	17(1)	20(1)	19(1)	4(1)	0(1)	4(1)
C(2)	26(1)	21(1)	26(1)	3(1)	-1(1)	4(1)
C(3)	44(1)	25(1)	32(1)	-3(1)	4(1)	7(1)
C(4)	55(1)	39(1)	24(1)	-3(1)	9(1)	9(1)
C(5)	41(1)	39(1)	20(1)	7(1)	6(1)	5(1)
C(6)	21(1)	24(1)	20(1)	5(1)	0(1)	3(1)
C(7)	50(1)	20(1)	37(1)	7(1)	4(1)	9(1)
C(8)	25(1)	27(1)	25(1)	11(1)	2(1)	4(1)
C(9)	18(1)	20(1)	17(1)	3(1)	2(1)	3(1)
C(10)	18(1)	21(1)	19(1)	2(1)	2(1)	2(1)
C(11)	19(1)	26(1)	22(1)	6(1)	3(1)	5(1)
C(12)	24(1)	22(1)	22(1)	6(1)	6(1)	7(1)
C(13)	27(1)	20(1)	24(1)	2(1)	3(1)	3(1)
C(14)	21(1)	22(1)	22(1)	1(1)	-1(1)	2(1)
C(15)	19(1)	25(1)	39(1)	-1(1)	-2(1)	2(1)
C(16)	30(1)	25(1)	32(1)	8(1)	6(1)	10(1)
F(1)	63(1)	40(1)	35(1)	15(1)	-4(1)	21(1)
F(2)	54(1)	35(1)	58(1)	20(1)	12(1)	-7(1)
F(3)	105(1)	23(1)	59(1)	11(1)	14(1)	26(1)
F(4)	53(1)	39(1)	40(1)	23(1)	19(1)	6(1)
F(5)	31(1)	34(1)	32(1)	12(1)	-2(1)	12(1)
F(6)	29(1)	23(1)	33(1)	7(1)	4(1)	1(1)
F(7)	24(1)	39(1)	61(1)	-9(1)	-16(1)	2(1)
F(8)	24(1)	41(1)	67(1)	-29(1)	-1(1)	3(1)
F(9)	68(1)	32(1)	69(1)	17(1)	-2(1)	-16(1)
F(10)	62(1)	51(1)	42(1)	15(1)	-2(1)	32(1)
F(11)	39(1)	40(1)	68(1)	20(1)	30(1)	19(1)
F(12)	43(1)	23(1)	59(1)	2(1)	4(1)	11(1)

Table 2.5 - Anisotropic displacement parameters ($Å^2$ x 10^3) for Ar'Ar''PCl. The anisotropic displacement factor exponent takes the form: $-2\pi^2$ [$h^2 a^2$ U11 + 2 h k a* b* U12]

	x	y	z	U(eq)
H(3)	7525(30)	-494(27)	285(19)	48(6)
H(4)	8075(30)	792(28)	-1064(20)	50(6)
H(5)	7661(29)	3321(26)	-583(19)	47(6)
H(11)	963(26)	5704(22)	2789(16)	32(5)
H(13)	4874(24)	8591(22)	4495(16)	29(5)
H(14)	8519(25)	6673(21)	4197(16)	27(5)

Table 2.6 - Hydrogen coordinates (x 10^4) and isotropic displacement parameters ($Å^2$ x 10^3) for Ar'Ar''PCl.

2.2.9 Ar'Ar''PH

The synthesis of the disubstituted phosphane was not attempted by Goodwin, and this method is analogous to the synthesis of the mono-substituted phosphane ($Ar'PH_2$) where P-Cl bonds are replaced by P-H bonds. Bu_3SnH was added dropwise to a solution of Ar'Ar''PCl in ether at room temperature and pressure. The product was recrystallised from hexanes as a white solid.

The proton decoupled ^{31}P NMR spectrum of the compound in toluene, appears to be a broad multiplet with chemical shift δ = -45.6ppm ($^4J_{P\text{-}F}$ = 39.4 Hz). Again, the expected coupling pattern for this compound would be a septet of quartets, which would explain why the peaks are broad.

When coupled to the proton, the ^{31}P NMR spectrum yields a doublet of multiplets, δ = -45.6ppm ($^1J_{PH}$ = 232.9 Hz).

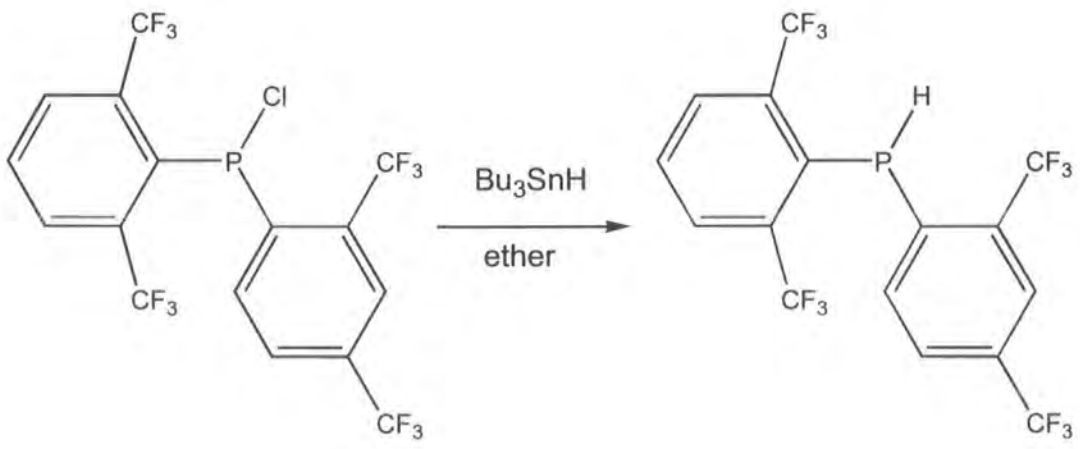

Equation 2.11 – Synthesis of Ar'Ar''PH

2.2.10 $ArPCl_2$

The use of Fluoromes as the aryl ligand instead of the Fluoroxyl species has many advantages in product synthesis and yields, due to the existence of only site for lithiation in the molecule. The work on P(I) compounds described in Chapter 5 was all performed using $ArPCl_2$ as the principal starting material for reasons described therein.

The preparation of $ArPCl_2$ is identical to that of $Ar'PCl_2$ except for the different aryl starting material. There is only one possible lithiation product for Fluoromes which makes the synthesis more efficient and faster.

The ^{31}P NMR spectrum of this compound in dichloromethane yielded a septet with a chemical shift, δ = 144.5 ppm ($^4J_{P-F}$ = 61.5ppm). The ^{19}F spectrum shows a doublet and a singlet, δ = -53.3ppm ($^4J_{P-F}$ = 61.4Hz) and δ = -64.5 ppm.

This NMR data confirms almost exactly the data given by Goodwin in her thesis ($^4J_{P-F}$ = 61.4 Hz).

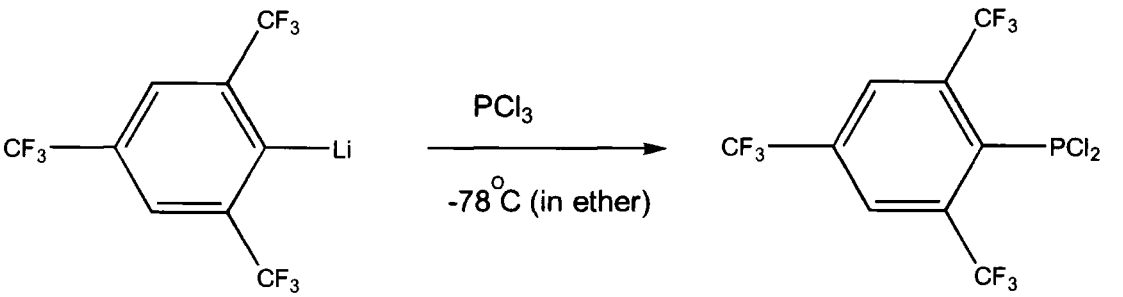

Equation 2.12 – Synthesis of $ArPCl_2$

2.2.11 Ar_2PCl

During the synthesis of $ArPCl_2$ there was very little formation of the di-substituted product. Even when an excess of the lithiated Fluoromes was added there was very little reaction other than mono-substitution. The most effective synthetic method was the addition of a solution of ArLi at room temperature very slowly to a solution of $ArPCl_2$ in ether.

The product was isolated and purified by re-crystallisation from hexanes. Attempts were made to grow crystals suitable for structural X-ray crystallographic analysis, but even after numerous attempts, the crystals grown were unsuitable.

The ^{31}P NMR solution spectrum of this compound yielded a multiplet of thirteen lines, with a chemical shift, δ = 75.5 ppm ($^{4}J_{P-F}$ = 41.2Hz). The ^{19}F NMR spectrum showed a doublet and a singlet with chemical shifts δ = -55.6 ppm (doublet), $^{4}J_{P-F}$ = 41.2Hz, and δ = -65.2 ppm (singlet).

These values again relate closely to the results given by Goodwin (^{31}P: δ = 73.3 ppm, $^{4}J_{P-F}$ = 42.0 Hz).

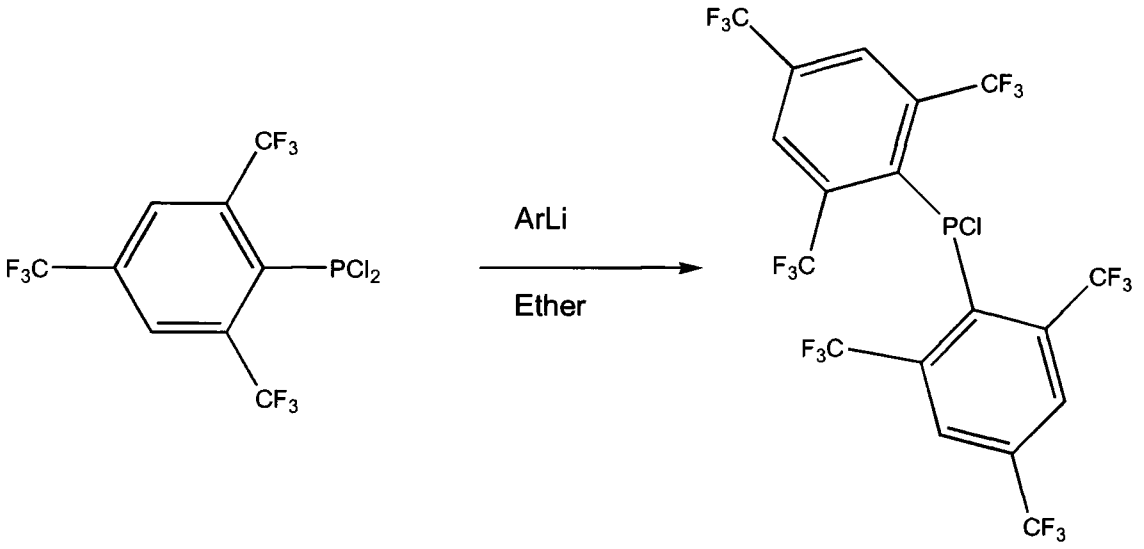

Equation 2.13 – Synthesis of Ar_2PCl

2.2.12 Ar_2PH

This compound is synthesised in the same manner as the analogous compound Ar'Ar''PH. Bu_3SnH is added dropwise to a solution of Ar_2PCl in ether at room temperature and the solution is allowed to stir for 30 minutes. The solvent is removed in *vacuo* and the white crystalline product is isolated by recrystallisation from hexanes.

The ^{31}P NMR solution spectrum shows a doublet of multiplets when the experiment is run proton coupled; this gives the chemical shift of the species δ = -65.7 ppm ($^{1}J_{PH}$ = 249.5Hz) ($^{4}J_{P\text{-}F}$ = 21.21 Hz). The ^{19}F NMR solution spectrum shows a distinct F-H coupling, albeit very small. The spectrum shows a doublet of doublets and a singlet, δ= -60.8 ppm ($^{5}J_{FH}$ = 7.14 Hz) ($^{4}J_{P\text{-}F}$ = 21.21 Hz) and δ = -64.7 ppm.

The synthesis of this phosphane was very important because the P(I) species formed when it is deprotonated is much more stable than the equivalent species synthesised with Fluoroxyl.

Crystals of Ar_2PH were grown by vacuum sublimation and were submitted for X-ray characterisation.

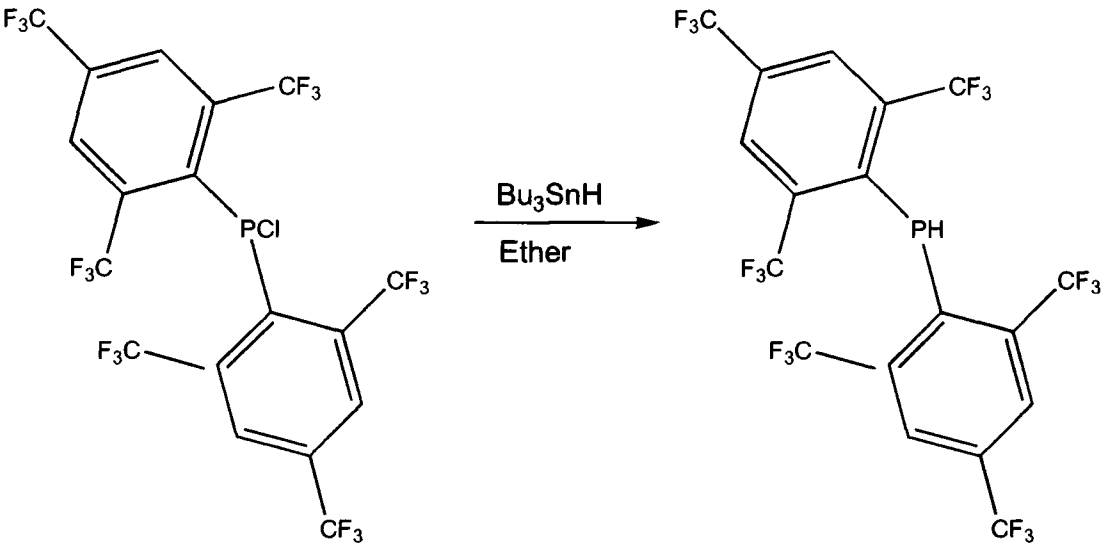

Equation 2.14 – Synthesis of Ar_2PH

2.2.12.1 X-ray structure of Ar_2PH

Crystals submitted for X-ray characterisation were mounted on a glass fibre, introduced onto the diffractometer and diffraction data collected. The structure was subsequently solved. The molecular structure of one of the three molecules in the asymmetric unit is shown in Figure 2.13

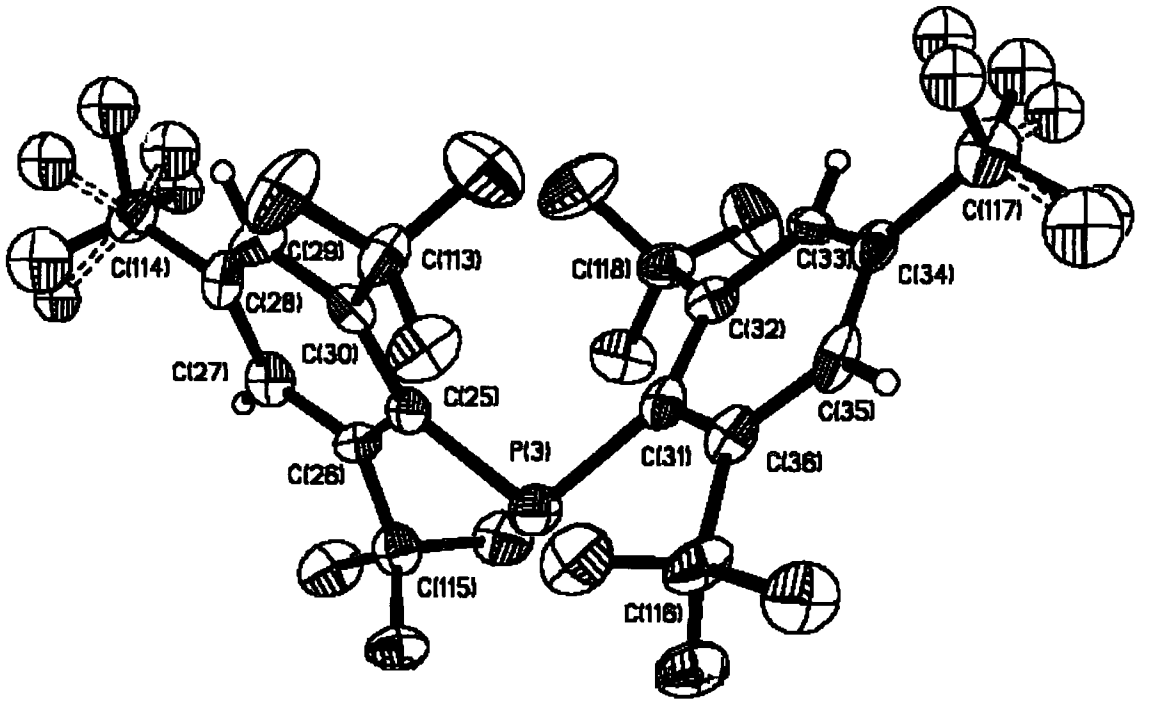

Figure 2.13 – Thermal Ellipsoid diagram at 150K (50% probability) showing one of the three molecules of Ar_2PH in the asymmetric unit.

Unfortunately the structure solution for this compound shows that there are three molecules within the asymmetric unit. With this, there are a number of disordered CF_3 groups on the specific Ar_2PH groups. This leads to problems refining the structure accurately and describing the CF_3 groups accurately. The final R value for the structure using data greater than $2\sigma = 7.15$.

Data were collected on a Siemens 3-circle diffractometer with a CCD area detector, ω scan mode $2\theta \leq 60.2°$. The structure was solved by direct methods and refined by full-matrix least squares against F^2 . Lists of crystal data and refinement parameters, anisotropic displacement parameters, bond lengths and angles, and atomic coordinates are given in Table 2.7 through Table 2.10.

The initial structure solution yielded three independent molecules in the asymmetric unit and refined all the non-Hydrogen atoms. Upon refinement the best solution attainable was all non-H atoms refined with anisotropic displacement parameters.

All the bond lengths quoted have reasonable estimated standard deviation values, although the numbers quoted in the discussion will be concerned with only one of the three molecules listed in the tables below.

The CF_3 groups are disordered, and although there is a significant amount of residual electron density the best model for the groups in this solution is anisotropic. The presence of dynamic disorder of the CF_3 groups was apparent due to the elongated shape of the thermal ellipsoids. The majority of residual electron density in the compound is associated with the disordered CF_3 groups.

What is interesting to note is that there are three molecules in the asymmetric unit. Although this is rare, it is not unprecedented. There is a question over whether or not the solution is in the correct space group, but searches for higher symmetry did not yield better results. Two of the molecules are of a greater proximity to each other than the third. The distances between the molecules, however, are of the order of 3.0Å and are outside the van der Waals radii for two fluorine atoms (2.85 $Å^4$). This closeness would imply that there could have been an interaction between the CF_3 groups on different molecules which is unlikely and adds some weight to the possibility that the space group in this solution may not be correct.

The angle between the planes of the two aryl rings is 67.7°, which is far from ideal. The bulky CF_3 groups on each aryl ring interact with each other due to their close proximity. The conformation of lowest energy, sterically, would be where the two rings are orthogonal to each other.

Crystal data and structure refinement	
Identification code	Ar_2PH
Empirical formula	$C_{18}H_3F_{18}P$
Formula weight	592.17
Temperature	293(2) K
Wavelength	0.71073 Å
Crystal system	Monoclinic
Space group	$P2_1/c$
Unit cell dimensions	a = 15.583(3) Å α = 90 °. b = 23.236(5) Å β = 112.39(3) °. c = 17.869(4) Å γ = 90 °.
Volume	5982(2) $Å^3$
Z	12
Number of reflections used	Calculation of cell = 512 Total = 26813 Unique = 8348 Obs [I>2σ(I)] = 3882
Crystal description	needle
Crystal colour	colourless
Density (calculated)	1.973 g/cm^3
Absorption coefficient	3.10 cm^{-1}
F(000)	3456
Crystal size	0.3 x 0.2 x 0.2 mm
Theta range for data collection	1.48 to 23.02 °.
Index ranges	-17<=h<=12, -25<=k<=25, -19<=l<=19
Experiment device	Siemens SMART
Experiment methods	ω scans
Reflections collected	26813
Independent reflections	8348 [R(int) = 0.1149]
Refinement method	Full-matrix least-squares on F^2
Data / restraints / parameters	8339 / 0 / 992
Goodness-of-fit on F^2	1.223
Final R indices [I>2σ(I)]	R_1 = 0.0715, wR_2 = 0.1493
R indices (all data)	R_1 = 0.1768, wR_2 = 0.1947
Largest diff. peak and hole	0.742 and -0.474 $e.Å^{-3}$

Table 2.7 - Crystal data and structure refinement for Ar_2PH.

	x	y	z	U(eq)
P(1)	890(2)	1644(1)	1196(1)	33(1)
P(2)	5935(2)	-14(1)	2715(1)	33(1)
P(3)	6064(2)	-3321(1)	9586(1)	31(1)
C(1)	129(5)	1840(3)	1733(5)	24(2)
C(2)	350(5)	2335(4)	2239(5)	22(2)
C(3)	-202(6)	2518(4)	2639(5)	28(2)
C(4)	-998(6)	2216(4)	2578(5)	27(2)
C(5)	-1193(6)	1705(4)	2137(5)	26(2)
C(6)	-633(6)	1522(4)	1736(5)	27(2)
C(7)	120(6)	1457(4)	136(5)	25(2)
C(8)	388(6)	984(4)	-220(5)	27(2)
C(9)	-139(6)	811(4)	-1009(5)	32(2)
C(10)	-943(6)	1098(4)	-1479(5)	30(2)
C(11)	-1199(6)	1578(4)	-1147(5)	26(2)
C(12)	-676(6)	1762(4)	-365(5)	29(2)
C(13)	5139(6)	174(4)	1667(5)	25(2)
C(14)	4391(6)	-164(4)	1152(5)	24(2)
C(15)	3834(6)	15(3)	382(5)	22(2)
C(16)	4007(6)	518(4)	59(5)	25(2)
C(17)	4779(6)	836(4)	527(5)	29(2)
C(18)	5331(6)	666(3)	1301(5)	23(2)
C(19)	5219(6)	-220(4)	3290(5)	25(2)
C(20)	5515(6)	-698(3)	3817(5)	22(2)
C(21)	5014(6)	-883(4)	4282(5)	28(2)
C(22)	4225(6)	-608(4)	4250(5)	24(2)
C(23)	3935(6)	-121(4)	3774(5)	21(2)
C(24)	4419(6)	67(3)	3313(5)	27(2)
C(25)	5338(6)	-3109(4)	8535(5)	24(2)
C(26)	5598(5)	-2611(3)	8195(5)	19(2)
C(27)	5108(6)	-2429(4)	7419(5)	28(2)
C(28)	4326(6)	-2723(4)	6931(5)	27(2)
C(29)	4060(6)	-3228(3)	7212(5)	25(2)
C(30)	4571(6)	-3410(3)	7997(5)	22(2)
C(31)	5265(6)	-3524(4)	10102(5)	24(2)
C(32)	4500(6)	-3197(3)	10109(5)	24(2)
C(33)	3963(5)	-3382(4)	10524(5)	21(2)
C(34)	4151(6)	-3893(4)	10955(5)	27(2)
C(35)	4939(6)	-4202(4)	11011(5)	27(2)
C(36)	5477(6)	-4027(3)	10600(5)	25(2)
C(101)	-932(7)	943(4)	1296(6)	37(3)
F(11)	-243(3)	655(2)	1216(3)	38(1)
F(12)	-1606(4)	997(2)	580(3)	58(2)
F(13)	-1267(4)	594(2)	1733(4)	60(2)
C(103)	1221(6)	2681(4)	2388(5)	32(2)
F(17)	1135(3)	3033(2)	1758(3)	49(2)
F(18)	1973(3)	2361(2)	2526(3)	34(1)
F(19)	1424(3)	3022(2)	3034(3)	48(2)
C(104)	-1027(7)	2317(4)	-139(6)	35(2)
F(110)	-342(3)	2638(2)	387(3)	40(1)

	x	y	z	U(eq)
F(111)	-1625(4)	2222(2)	218(4)	56(2)
F(112)	-1449(4)	2649(2)	-769(3)	57(2)
C(105)	-1559(7)	870(5)	-2309(6)	49(3)
F(113)	-1944(8)	1330(5)	-2778(6)	0(3)
F(114)	-2121(9)	513(6)	-2320(7)	1(4)
F(1A)	-2301(8)	1204(5)	-2676(7)	6(3)
F(1B)	-1900(9)	332(6)	-2271(7)	0(4)
F(1C)	-1005(17)	754(13)	-2755(14)	6(5)
F(1Y)	-1202(20)	896(12)	-2753(20)	85(14)
F(1Z)	-909(15)	619(9)	-2608(14)	38(10)
C(102)	-1609(7)	2446(4)	2970(6)	36(3)
F(14)	-1224(10)	2550(6)	3723(8)	43(5)
F(15)	-2015(7)	1996(5)	3223(6)	35(3)
F(16)	-2232(8)	2787(5)	2545(7)	35(4)
F(1D)	-2359(8)	2116(5)	2848(7)	53(4)
F(1E)	-2013(9)	2983(6)	2630(7)	44(4)
F(1F)	-1074(9)	2723(6)	3694(8)	37(4)
C(106)	1261(6)	649(4)	227(6)	30(2)
F(116)	1237(3)	332(2)	832(3)	45(2)
F(117)	2004(3)	994(2)	525(3)	35(1)
F(118)	1466(3)	289(2)	-272(3)	49(2)
C(107)	6394(7)	-1009(4)	3937(6)	37(3)
F(21)	7123(3)	-669(2)	4113(3)	41(1)
F(22)	6347(3)	-1319(2)	3287(3)	50(2)
F(23)	6624(3)	-1399(2)	4544(3)	53(2)
C(108)	3670(8)	-867(5)	4706(6)	53(3)
F(24)	3461(9)	-1403(5)	4533(7)	0(3)
F(24A)	3116(9)	-1242(6)	4394(7)	0(3)
F(25)	3056(13)	-481(8)	4764(12)	24(4)
F(25A)	2775(13)	-667(9)	4367(12)	57(6)
F(25B)	3949(18)	-753(12)	5363(17)	77(9)
F(25C)	3408(13)	-385(7)	5077(10)	24(5)
F(26A)	4265(15)	-956(10)	5532(11)	7(5)
F(26B)	4421(15)	-1088(9)	5462(14)	46(10)
C(111)	3403(6)	726(4)	-746(6)	33(2)
F(213)	2910(9)	1180(6)	-713(8)	35(4)
F(214)	3057(9)	309(6)	-1265(8)	44(5)
F(215)	3965(12)	1026(7)	-1105(10)	53(6)
F(2D)	2786(8)	290(5)	-1193(7)	28(4)
F(2E)	2677(9)	1050(5)	-747(7)	31(4)
F(2F)	3789(10)	912(7)	-1205(9)	31(5)
C(109)	4024(7)	616(4)	2826(6)	33(2)
F(27)	3434(4)	512(2)	2075(3)	52(2)
F(28)	4693(3)	961(2)	2769(3)	40(1)
F(29)	3574(4)	929(2)	3180(3)	55(2)
C(112)	6172(6)	1044(4)	1721(6)	32(2)
F(216)	6953(3)	739(2)	2093(3)	36(1)
F(217)	6071(4)	1381(2)	2289(3)	53(2)
F(218)	6367(3)	1388(2)	1207(3)	49(2)
C(110)	4101(7)	-741(4)	1404(6)	32(2)

	x	y	z	U(eq)
F(210)	3471(4)	-690(2)	1722(4)	54(2)
F(211)	4834(3)	-1018(2)	1942(3)	40(1)
F(212)	3779(4)	-1095(2)	769(3)	54(2)
C(114)	3798(7)	-2500(4)	6103(6)	35(3)
F(34)	2964(8)	-2771(5)	5759(6)	46(3)
F(34A)	3227(9)	-2102(6)	6032(7)	48(4)
F(35B)	3409(7)	-2931(5)	5566(6)	41(3)
F(35A)	4459(7)	-2304(5)	5753(6)	28(3)
F(35)	4156(10)	-2506(6)	5611(8)	58(4)
F(36)	3532(8)	-1929(5)	6150(6)	30(3)
C(116)	6345(6)	-4389(4)	10728(6)	35(3)
F(310)	7108(3)	-4061(2)	10922(3)	38(1)
F(311)	6280(3)	-4698(2)	10081(3)	44(2)
F(312)	6517(3)	-4751(2)	11351(3)	44(1)
C(118)	4211(6)	-2625(4)	9688(6)	32(2)
F(316)	3590(4)	-2678(2)	8940(3)	54(2)
F(317)	4920(3)	-2325(2)	9628(3)	38(1)
F(318)	3840(4)	-2279(2)	10087(3)	51(2)
C(113)	4208(7)	-3975(4)	8195(6)	35(3)
F(31)	3592(4)	-3892(2)	8551(4)	54(2)
F(32)	4879(3)	-4300(2)	8710(3)	38(1)
F(33)	3784(4)	-4295(2)	7545(3)	53(2)
C(115)	6479(6)	-2278(4)	8671(6)	33(2)
F(37)	6405(3)	-1982(2)	9291(3)	41(1)
F(38)	6676(3)	-1894(2)	8208(3)	42(1)
F(39)	7221(3)	-2618(2)	8987(3)	36(1)
C(117)	3525(7)	-4098(4)	11365(6)	37(3)
F(313)	3977(10)	-4275(6)	12119(9)	36(5)
F(314)	3082(9)	-4568(5)	11011(7)	39(4)
F(315)	2902(9)	-3678(6)	11371(8)	46(4)
F(3D)	3193(9)	-3683(5)	11655(7)	37(4)
F(3E)	2792(8)	-4408(5)	10875(7)	36(4)
F(3F)	4070(11)	-4428(7)	12034(10)	60(6)

Table 2.8 - Atomic coordinates (x 10^4) and equivalent isotropic displacement parameters ($Å^2$ x 10^3) for Ar_2PH,. U(eq) is defined as one third of the trace of the *ortho*gonalized Uij tensor.

Bond lengths [Å] and Angles [°]			
P(1)-C(1)	1.845(9)	C(28)-C(114)	1.485(11)
P(1)-C(7)	1.866(8)	C(29)-C(30)	1.389(11)
P(2)-C(19)	1.846(9)	C(30)-C(113)	1.523(12)
P(2)-C(13)	1.861(8)	C(31)-C(32)	1.418(11)
P(3)-C(25)	1.852(8)	C(31)-C(36)	1.429(11)
P(3)-C(31)	1.870(8)	C(32)-C(33)	1.381(11)
C(1)-C(6)	1.400(11)	C(32)-C(118)	1.509(11)
C(1)-C(2)	1.422(10)	C(33)-C(34)	1.385(11)
C(2)-C(3)	1.379(11)	C(34)-C(35)	1.393(11)
C(2)-C(103)	1.512(11)	C(34)-C(117)	1.503(12)
C(3)-C(4)	1.393(11)	C(35)-C(36)	1.370(11)
C(4)-C(5)	1.393(11)	C(36)-C(116)	1.534(12)
C(4)-C(102)	1.481(12)	C(101)-F(12)	1.316(10)
C(5)-C(6)	1.391(11)	C(101)-F(11)	1.318(10)
C(6)-C(101)	1.538(12)	C(101)-F(13)	1.361(10)
C(7)-C(8)	1.410(11)	C(103)-F(18)	1.329(10)
C(7)-C(12)	1.413(11)	C(103)-F(19)	1.336(9)
C(8)-C(9)	1.394(11)	C(103)-F(17)	1.355(10)
C(8)-C(106)	1.506(12)	C(104)-F(112)	1.315(10)
C(9)-C(10)	1.385(11)	C(104)-F(111)	1.334(10)
C(10)-C(11)	1.391(11)	C(104)-F(110)	1.347(10)
C(10)-C(105)	1.521(12)	C(105)-F(1Y)	1.13(3)
C(11)-C(12)	1.389(11)	C(105)-F(1C)	1.40(3)
C(12)-C(104)	1.515(12)	C(105)-F(114)	1.20(2)
C(13)-C(18)	1.404(11)	C(105)-F(113)	1.35(2)
C(13)-C(14)	1.416(11)	C(105)-F(1A)	1.338(14)
C(14)-C(15)	1.382(11)	C(105)-F(1Z)	1.44(3)
C(14)-C(110)	1.536(12)	C(105)-F(1B)	1.37(2)
C(15)-C(16)	1.376(11)	F(113)-F(1A)	.711(13)
C(16)-C(17)	1.388(11)	F(113)-F(1Y)	1.52(3)
C(16)-C(111)	1.468(11)	F(114)-F(1B)	.53(2)
C(17)-C(18)	1.379(11)	F(114)-F(1A)	1.71(2)
C(18)-C(112)	1.518(11)	F(1C)-F(1Z)	.40(4)
C(19)-C(24)	1.429(11)	F(1C)-F(1Y)	.45(4)
C(19)-C(20)	1.414(11)	F(1Y)-F(1Z)	.77(3)
C(20)-C(21)	1.407(11)	C(102)-F(16)	1.259(14)
C(20)-C(107)	1.492(12)	C(102)-F(14)	1.27(2)
C(21)-C(22)	1.368(11)	C(102)-F(1D)	1.345(14)
C(22)-C(23)	1.383(11)	C(102)-F(15)	1.385(13)
C(22)-C(108)	1.521(13)	C(102)-F(1F)	1.40(2)
C(23)-C(24)	1.381(11)	C(102)-F(1E)	1.42(2)
C(24)-C(109)	1.536(11)	F(14)-F(15)	1.77(2)
C(25)-C(30)	1.403(11)	F(15)-F(1D)	.735(13)
C(25)-C(26)	1.436(11)	F(16)-F(1E)	.55(2)
C(26)-C(27)	1.371(11)	F(16)-F(1D)	1.69(2)
C(26)-C(115)	1.523(11)	C(106)-F(116)	1.320(10)
C(27)-C(28)	1.379(11)	C(106)-F(117)	1.341(9)
C(28)-C(29)	1.399(11)	C(106)-F(118)	1.346(9)

Bond lengths [Å] and Angles [°]			
C(107)-F(21)	1.320(10)	C(116)-F(310)	1.342(10)
C(107)-F(22)	1.345(10)	C(118)-F(316)	1.323(9)
C(107)-F(23)	1.353(10)	C(118)-F(318)	1.341(10)
C(108)-F(25B)	1.12(2)	C(118)-F(317)	1.344(9)
C(108)-F(24A)	1.20(2)	C(113)-F(32)	1.333(10)
C(108)-F(24)	1.29(2)	C(113)-F(33)	1.324(10)
C(108)-F(25)	1.35(2)	C(113)-F(31)	1.353(10)
C(108)-F(25A)	1.37(2)	C(115)-F(39)	1.336(9)
C(108)-F(25C)	1.44(2)	C(115)-F(38)	1.331(10)
C(108)-F(26A)	1.43(2)	C(115)-F(37)	1.346(9)
C(108)-F(26B)	1.50(2)	C(117)-F(3D)	1.293(14)
F(24)-F(24A)	.624(14)	C(117)-F(314)	1.317(14)
F(24A)-F(25A)	1.43(2)	C(117)-F(313)	1.32(2)
F(25)-F(25C)	.65(2)	C(117)-F(3E)	1.353(14)
F(25)-F(25A)	.80(2)	C(117)-F(315)	1.38(2)
F(25)-F(25B)	1.53(3)	C(117)-F(3F)	1.40(2)
F(25A)-F(25C)	1.43(2)	F(314)-F(3E)	.56(2)
F(25B)-F(26A)	.67(3)	F(315)-F(3D)	.54(2)
F(25B)-F(26B)	1.04(3)	C(1)-P(1)-C(7)	107.0(4)
F(25B)-F(25C)	1.17(3)	C(19)-P(2)-C(13)	108.0(4)
C(111)-F(2F)	1.26(2)	C(25)-P(3)-C(31)	107.6(4)
C(111)-F(213)	1.32(2)	C(6)-C(1)-C(2)	115.1(8)
C(111)-F(214)	1.31(2)	C(6)-C(1)-P(1)	125.9(6)
C(111)-F(2E)	1.36(2)	C(2)-C(1)-P(1)	118.9(6)
C(111)-F(2D)	1.42(2)	C(3)-C(2)-C(1)	122.1(8)
C(111)-F(215)	1.45(2)	C(3)-C(2)-C(103)	116.1(8)
C(109)-F(28)	1.349(10)	C(1)-C(2)-C(103)	121.7(8)
C(109)-F(27)	1.329(10)	C(2)-C(3)-C(4)	121.1(8)
C(109)-F(29)	1.325(10)	C(5)-C(4)-C(3)	118.0(8)
C(112)-F(218)	1.337(10)	C(5)-C(4)-C(102)	122.4(8)
C(112)-F(216)	1.344(9)	C(3)-C(4)-C(102)	119.6(8)
C(112)-F(217)	1.337(10)	C(4)-C(5)-C(6)	120.5(8)
C(110)-F(210)	1.313(10)	C(1)-C(6)-C(5)	122.7(8)
C(110)-F(212)	1.336(10)	C(1)-C(6)-C(101)	123.5(8)
C(110)-F(211)	1.344(9)	C(5)-C(6)-C(101)	113.8(8)
C(114)-F(35)	1.209(14)	C(8)-C(7)-C(12)	116.3(8)
C(114)-F(34A)	1.257(14)	C(8)-C(7)-P(1)	116.9(6)
C(114)-F(34)	1.362(13)	C(12)-C(7)-P(1)	126.6(7)
C(114)-F(35B)	1.360(13)	C(9)-C(8)-C(7)	121.4(8)
C(114)-F(36)	1.402(14)	C(9)-C(8)-C(106)	116.9(8)
C(114)-F(35A)	1.466(14)	C(7)-C(8)-C(106)	121.8(8)
F(34)-F(35B)	.958(12)	C(8)-C(9)-C(10)	121.5(9)
F(34)-F(34A)	1.64(2)	C(11)-C(10)-C(9)	117.9(8)
F(34A)-F(36)	.60(2)	C(11)-C(10)-C(105)	121.2(9)
F(35B)-F(35)	1.51(2)	C(9)-C(10)-C(105)	120.8(9)
F(35A)-F(35)	.64(2)	C(10)-C(11)-C(12)	121.5(8)
C(116)-F(311)	1.331(10)	C(11)-C(12)-C(7)	121.3(8)
C(116)-F(312)	1.338(9)		

Bond lengths [Å] and Angles [°]			
C(11)-C(12)-C(104)	113.4(8)	C(33)-C(32)-C(31)	121.4(8)
C(7)-C(12)-C(104)	125.2(8)	C(33)-C(32)-C(118)	114.6(8)
C(18)-C(13)-C(14)	114.7(7)	C(31)-C(32)-C(118)	124.0(8)
C(18)-C(13)-P(2)	118.7(6)	C(32)-C(33)-C(34)	121.5(8)
C(14)-C(13)-P(2)	126.2(7)	C(33)-C(34)-C(35)	118.4(8)
C(15)-C(14)-C(13)	121.9(8)	C(33)-C(34)-C(117)	120.2(8)
C(15)-C(14)-C(110)	114.3(8)	C(35)-C(34)-C(117)	121.3(8)
C(13)-C(14)-C(110)	123.7(8)	C(36)-C(35)-C(34)	120.7(8)
C(16)-C(15)-C(14)	121.7(8)	C(35)-C(36)-C(31)	122.3(8)
C(15)-C(16)-C(17)	117.5(8)	C(35)-C(36)-C(116)	116.2(8)
C(15)-C(16)-C(111)	122.4(8)	C(31)-C(36)-C(116)	121.5(8)
C(17)-C(16)-C(111)	120.1(8)	F(12)-C(101)-F(11)	109.0(8)
C(18)-C(17)-C(16)	121.3(9)	F(12)-C(101)-F(13)	106.0(8)
C(17)-C(18)-C(13)	122.5(8)	F(11)-C(101)-F(13)	105.4(8)
C(17)-C(18)-C(112)	115.0(8)	F(12)-C(101)-C(6)	112.8(8)
C(13)-C(18)-C(112)	122.5(8)	F(11)-C(101)-C(6)	113.5(8)
C(24)-C(19)-C(20)	114.4(8)	F(13)-C(101)-C(6)	109.5(8)
C(24)-C(19)-P(2)	127.9(6)	F(18)-C(103)-F(19)	105.6(7)
C(20)-C(19)-P(2)	117.5(6)	F(18)-C(103)-F(17)	107.1(7)
C(21)-C(20)-C(19)	121.4(8)	F(19)-C(103)-F(17)	106.0(8)
C(21)-C(20)-C(107)	116.9(8)	F(18)-C(103)-C(2)	113.8(8)
C(19)-C(20)-C(107)	121.7(8)	F(19)-C(103)-C(2)	111.6(8)
C(22)-C(21)-C(20)	121.6(8)	F(17)-C(103)-C(2)	112.1(7)
C(21)-C(22)-C(23)	119.1(8)	F(112)-C(104)-F(111)	107.1(8)
C(21)-C(22)-C(108)	118.5(8)	F(112)-C(104)-F(110)	106.1(8)
C(23)-C(22)-C(108)	122.3(8)	F(111)-C(104)-F(110)	105.6(8)
C(22)-C(23)-C(24)	120.0(8)	F(112)-C(104)-C(12)	112.6(8)
C(23)-C(24)-C(19)	123.4(8)	F(111)-C(104)-C(12)	112.1(8)
C(23)-C(24)-C(109)	114.2(8)	F(110)-C(104)-C(12)	112.8(8)
C(19)-C(24)-C(109)	122.5(8)	F(1Y)-C(105)-F(1C)	16(2)
C(30)-C(25)-C(26)	114.5(7)	F(1Y)-C(105)-F(114)	125(2)
C(30)-C(25)-P(3)	126.5(7)	F(1C)-C(105)-F(114)	117.2(14)
C(26)-C(25)-P(3)	118.8(6)	F(1Y)-C(105)-F(113)	75(2)
C(27)-C(26)-C(25)	122.6(8)	F(1C)-C(105)-F(113)	91(2)
C(27)-C(26)-C(115)	116.4(8)	F(114)-C(105)-F(113)	112.8(12)
C(25)-C(26)-C(115)	120.9(7)	F(1Y)-C(105)-F(1A)	101(2)
C(28)-C(27)-C(26)	120.3(9)	F(1C)-C(105)-F(1A)	116(2)
C(27)-C(28)-C(29)	120.0(8)	F(114)-C(105)-F(1A)	84.5(11)
C(27)-C(28)-C(114)	118.5(8)	F(113)-C(105)-F(1A)	30.7(6)
C(29)-C(28)-C(114)	121.5(8)	F(1Y)-C(105)-F(1Z)	32(2)
C(30)-C(29)-C(28)	119.0(8)	F(1C)-C(105)-F(1Z)	16.1(14)
C(29)-C(30)-C(25)	123.5(8)	F(114)-C(105)-F(1Z)	108.9(14)
C(29)-C(30)-C(113)	112.2(7)	F(113)-C(105)-F(1Z)	107.5(13)
C(25)-C(30)-C(113)	124.4(8)	F(1A)-C(105)-F(1Z)	130.8(14)
C(32)-C(31)-C(36)	115.4(8)	F(1Y)-C(105)-F(1B)	113(2)
C(32)-C(31)-P(3)	126.1(7)	F(1C)-C(105)-F(1B)	100.7(14)
C(36)-C(31)-P(3)	118.3(7)	F(114)-C(105)-F(1B)	22.5(8)

Bond lengths [Å] and Angles [°]			
F(113)-C(105)-F(1B)	131.6(12)	C(102)-F(14)-F(15)	51.0(7)
F(1A)-C(105)-F(1B)	105.8(11)	F(1D)-F(15)-C(102)	71.4(14)
F(1Z)-C(105)-F(1B)	89.4(12)	F(1D)-F(15)-F(14)	108(2)
F(1Y)-C(105)-C(10)	112(2)	C(102)-F(15)-F(14)	45.4(6)
F(1C)-C(105)-C(10)	108.9(11)	F(1E)-F(16)-C(102)	96(2)
F(1A)-F(113)-C(105)	74(2)	F(1E)-F(16)-F(1D)	144(3)
F(1A)-F(113)-F(1Y)	112(2)	C(102)-F(16)-F(1D)	51.9(7)
C(105)-F(113)-F(1Y)	45.8(13)	F(15)-F(1D)-C(102)	77(2)
F(1B)-F(114)-C(105)	97(3)	F(15)-F(1D)-F(16)	121(2)
F(1B)-F(114)-F(1A)	144(3)	C(102)-F(1D)-F(16)	47.4(7)
C(105)-F(114)-F(1A)	51.1(8)	F(16)-F(1E)-C(102)	62(2)
F(113)-F(1A)-C(105)	76(2)	F(116)-C(106)-F(117)	107.3(7)
F(113)-F(1A)-F(114)	117(2)	F(116)-C(106)-F(118)	106.6(7)
C(105)-F(1A)-F(114)	44.4(7)	F(117)-C(106)-F(118)	104.3(7)
F(114)-F(1B)-C(105)	60(2)	F(116)-C(106)-C(8)	114.9(7)
F(1Z)-F(1C)-F(1Y)	131(10)	F(117)-C(106)-C(8)	111.7(8)
F(1Z)-F(1C)-C(105)	86(6)	F(118)-C(106)-C(8)	111.3(7)
F(1Y)-F(1C)-C(105)	45(6)	F(21)-C(107)-F(22)	106.6(7)
F(1C)-F(1Y)-C(105)	119(8)	F(21)-C(107)-F(23)	105.6(7)
F(1C)-F(1Y)-F(1Z)	23(5)	F(22)-C(107)-F(23)	104.2(8)
C(105)-F(1Y)-F(1Z)	96(4)	F(21)-C(107)-C(20)	113.8(8)
F(1C)-F(1Y)-F(113)	174(7)	F(22)-C(107)-C(20)	113.0(8)
C(105)-F(1Y)-F(113)	59(2)	F(23)-C(107)-C(20)	112.9(8)
F(1Z)-F(1Y)-F(113)	155(5)	F(25B)-C(108)-F(24A)	126(2)
F(1C)-F(1Z)-F(1Y)	26(6)	F(25B)-C(108)-F(24)	116(2)
F(1C)-F(1Z)-C(105)	78(6)	F(24A)-C(108)-F(24)	28.6(7)
F(1Y)-F(1Z)-C(105)	52(3)	F(25B)-C(108)-F(25)	76(2)
F(16)-C(102)-F(14)	117.7(11)	F(24A)-C(108)-F(25)	96.4(14)
F(16)-C(102)-F(1D)	80.7(10)	F(24)-C(108)-F(25)	122.6(14)
F(14)-C(102)-F(1D)	108.2(11)	F(25B)-C(108)-F(25A)	108(2)
F(16)-C(102)-F(15)	109.2(10)	F(24A)-C(108)-F(25A)	67.2(12)
F(14)-C(102)-F(15)	83.6(10)	F(24)-C(108)-F(25A)	95.7(14)
F(1D)-C(102)-F(15)	31.2(6)	F(25)-C(108)-F(25A)	34.3(9)
F(16)-C(102)-F(1F)	108.7(11)	F(25B)-C(108)-F(25C)	53(2)
F(14)-C(102)-F(1F)	19.8(9)	F(24A)-C(108)-F(25C)	119.8(13)
F(1D)-C(102)-F(1F)	126.0(11)	F(24)-C(108)-F(25C)	140.3(12)
F(15)-C(102)-F(1F)	103.3(10)	F(25)-C(108)-F(25C)	26.9(9)
F(16)-C(102)-F(1E)	22.8(7)	F(25A)-C(108)-F(25C)	61.3(11)
F(14)-C(102)-F(1E)	103.8(10)	F(25B)-C(108)-F(26A)	27(2)
F(1D)-C(102)-F(1E)	102.5(10)	F(24A)-C(108)-F(26A)	116.3(13)
F(15)-C(102)-F(1E)	128.2(10)	F(24)-C(108)-F(26A)	96.5(13)
F(1F)-C(102)-F(1E)	90.2(9)	F(25)-C(108)-F(26A)	103(2)
F(16)-C(102)-C(4)	115.4(9)	F(25A)-C(108)-F(26A)	131(2)
F(14)-C(102)-C(4)	116.2(10)	F(25C)-C(108)-F(26A)	79.8(14)
F(1D)-C(102)-C(4)	113.0(9)	F(25B)-C(108)-F(26B)	44(2)
F(15)-C(102)-C(4)	109.7(8)	F(24A)-C(108)-F(26B)	110(2)
F(1F)-C(102)-C(4)	109.9(9)	F(24)-C(108)-F(26B)	85.7(13)
F(1E)-C(102)-C(4)	112.0(9)	F(25)-C(108)-F(26B)	120(2)

Bond lengths [Å] and Angles [°]			
F(25A)-C(108)-F(26B)	145.6(14)	F(2F)-C(111)-F(2E)	114.4(11)
F(25C)-C(108)-F(26B)	96.5(13)	F(213)-C(111)-F(2E)	19.6(8)
F(26A)-C(108)-F(26B)	17.0(12)	F(214)-C(111)-F(2E)	107.0(10)
F(25B)-C(108)-C(22)	113(2)	F(2F)-C(111)-F(2D)	105.4(11)
F(24A)-C(108)-C(22)	119.6(10)	F(213)-C(111)-F(2D)	108.4(10)
F(24)-C(108)-C(22)	113.4(9)	F(214)-C(111)-F(2D)	20.1(8)
F(25)-C(108)-C(22)	110.1(11)	F(2E)-C(111)-F(2D)	90.6(9)
F(25A)-C(108)-C(22)	108.6(11)	F(2F)-C(111)-F(215)	13.9(11)
F(25C)-C(108)-C(22)	104.9(10)	F(213)-C(111)-F(215)	95.5(11)
F(26A)-C(108)-C(22)	109.5(11)	F(214)-C(111)-F(215)	101.4(12)
F(26B)-C(108)-C(22)	102.2(12)	F(2E)-C(111)-F(215)	112.1(11)
F(24A)-F(24)-C(108)	68(2)	F(2D)-C(111)-F(215)	119.3(11)
F(24)-F(24A)-C(108)	84(2)	F(2F)-C(111)-C(16)	117.5(10)
F(24)-F(24A)-F(25A)	146(3)	F(213)-C(111)-C(16)	112.7(9)
C(108)-F(24A)-F(25A)	62.1(11)	F(214)-C(111)-C(16)	112.8(10)
F(25C)-F(25)-F(25A)	159(4)	F(2E)-C(111)-C(16)	114.0(9)
F(25C)-F(25)-C(108)	85(3)	F(2D)-C(111)-C(16)	111.2(9)
F(25A)-F(25)-C(108)	75(2)	F(215)-C(111)-C(16)	108.8(9)
F(25C)-F(25)-F(25B)	46(2)	F(28)-C(109)-F(27)	106.8(7)
F(25A)-F(25)-F(25B)	116(3)	F(28)-C(109)-F(29)	106.0(8)
C(108)-F(25)-F(25B)	45.2(10)	F(27)-C(109)-F(29)	107.1(8)
F(25)-F(25A)-C(108)	71(2)	F(28)-C(109)-C(24)	112.4(7)
F(25)-F(25A)-F(25C)	9(2)	F(27)-C(109)-C(24)	113.3(8)
C(108)-F(25A)-F(25C)	61.6(11)	F(29)-C(109)-C(24)	110.8(7)
F(25)-F(25A)-F(24A)	114(2)	F(218)-C(112)-F(216)	104.7(7)
C(108)-F(25A)-F(24A)	50.7(10)	F(218)-C(112)-F(217)	107.2(8)
F(25C)-F(25A)-F(24A)	105.9(14)	F(216)-C(112)-F(217)	106.3(7)
F(26A)-F(25B)-F(26B)	16(3)	F(218)-C(112)-C(18)	112.6(7)
F(26A)-F(25B)-C(108)	103(4)	F(216)-C(112)-C(18)	112.9(8)
F(26B)-F(25B)-C(108)	88(2)	F(217)-C(112)-C(18)	112.6(7)
F(26A)-F(25B)-F(25C)	179(4)	F(210)-C(110)-F(212)	108.9(8)
F(26B)-F(25B)-F(25C)	165(3)	F(210)-C(110)-F(211)	107.8(7)
C(108)-F(25B)-F(25C)	78(2)	F(212)-C(110)-F(211)	104.8(7)
F(26A)-F(25B)-F(25)	158(4)	F(210)-C(110)-C(14)	113.6(8)
F(26B)-F(25B)-F(25)	145(3)	F(212)-C(110)-C(14)	110.2(7)
C(108)-F(25B)-F(25)	59(2)	F(211)-C(110)-C(14)	111.2(8)
F(25C)-F(25B)-F(25)	23.5(12)	F(35)-C(114)-F(34A)	116.1(12)
F(25)-F(25C)-F(25B)	111(3)	F(35)-C(114)-F(34)	107.0(11)
F(25)-F(25C)-C(108)	69(2)	F(34A)-C(114)-F(34)	77.2(9)
F(25B)-F(25C)-C(108)	49.5(14)	F(35)-C(114)-F(35B)	71.6(9)
F(25)-F(25C)-F(25A)	12(2)	F(34A)-C(114)-F(35B)	111.3(11)
F(25B)-F(25C)-F(25A)	101(2)	F(34)-C(114)-F(35B)	41.2(6)
C(108)-F(25C)-F(25A)	57.2(10)	F(35)-C(114)-F(36)	106.4(11)
F(25B)-F(26A)-C(108)	50(3)	F(34A)-C(114)-F(36)	25.1(7)
F(25B)-F(26B)-C(108)	48(2)	F(34)-C(114)-F(36)	102.2(9)
F(2F)-C(111)-F(213)	100.7(11)	F(35B)-C(114)-F(36)	132.5(10)
F(2F)-C(111)-F(214)	87.8(11)	F(35)-C(114)-F(35A)	25.6(8)
F(213)-C(111)-F(214)	122.3(11)	F(34A)-C(114)-F(35A)	108.3(10)

Bond lengths [Å] and Angles [°]			
F(34)-C(114)-F(35A)	130.9(10)	F(3D)-C(117)-F(313)	87.9(11)
F(35B)-C(114)-F(35A)	97.1(9)	F(314)-C(117)-F(313)	102.1(11)
F(36)-C(114)-F(35A)	90.2(8)	F(3D)-C(117)-F(3E)	106.7(11)
F(35)-C(114)-C(28)	119.2(11)	F(314)-C(117)-F(3E)	24.4(7)
F(34A)-C(114)-C(28)	117.3(10)	F(313)-C(117)-F(3E)	118.9(11)
F(34)-C(114)-C(28)	111.1(9)	F(3D)-C(117)-F(315)	22.8(8)
F(35B)-C(114)-C(28)	112.1(8)	F(314)-C(117)-F(315)	110.4(11)
F(36)-C(114)-C(28)	109.6(8)	F(313)-C(117)-F(315)	108.3(11)
F(35A)-C(114)-C(28)	108.7(8)	F(3E)-C(117)-F(315)	87.6(10)
F(35B)-F(34)-C(114)	69.3(10)	F(3D)-C(117)-F(3F)	105.7(12)
F(35B)-F(34)-F(34A)	110.0(12)	F(314)-C(117)-F(3F)	89.6(10)
C(114)-F(34)-F(34A)	48.5(7)	F(313)-C(117)-F(3F)	17.9(10)
F(36)-F(34A)-C(114)	91(2)	F(3E)-C(117)-F(3F)	110.4(11)
F(36)-F(34A)-F(34)	145(3)	F(315)-C(117)-F(3F)	125.3(12)
C(114)-F(34A)-F(34)	54.3(8)	F(3D)-C(117)-C(34)	113.1(9)
F(34)-F(35B)-C(114)	69.5(10)	F(314)-C(117)-C(34)	110.3(9)
F(34)-F(35B)-F(35)	112.2(13)	F(313)-C(117)-C(34)	113.7(10)
C(114)-F(35B)-F(35)	49.6(7)	F(3E)-C(117)-C(34)	113.5(9)
F(35)-F(35A)-C(114)	54(2)	F(315)-C(117)-C(34)	111.7(9)
F(35A)-F(35)-C(114)	100(2)	F(3F)-C(117)-C(34)	107.2(10)
F(35A)-F(35)-F(35B)	159(2)	F(3E)-F(314)-C(117)	81(2)
C(114)-F(35)-F(35B)	58.9(9)	F(3D)-F(315)-C(117)	69(2)
F(34A)-F(36)-C(114)	64(2)	F(315)-F(3D)-C(117)	88(3)
F(311)-C(116)-F(312)	107.9(8)	F(314)-F(3E)-C(117)	74(2)
F(311)-C(116)-F(310)	107.3(8)		
F(312)-C(116)-F(310)	105.3(7)		
F(311)-C(116)-C(36)	113.3(7)		
F(312)-C(116)-C(36)	110.7(8)		
F(310)-C(116)-C(36)	111.8(8)		
F(316)-C(118)-F(318)	107.2(7)		
F(316)-C(118)-F(317)	106.0(7)		
F(318)-C(118)-F(317)	105.4(7)		
F(316)-C(118)-C(32)	112.7(7)		
F(318)-C(118)-C(32)	111.7(8)		
F(317)-C(118)-C(32)	113.4(7)		
F(32)-C(113)-F(33)	106.6(8)		
F(32)-C(113)-F(31)	105.5(7)		
F(33)-C(113)-F(31)	106.6(8)		
F(32)-C(113)-C(30)	112.7(8)		
F(33)-C(113)-C(30)	112.6(7)		
F(31)-C(113)-C(30)	112.3(8)		
F(39)-C(115)-F(38)	107.0(7)		
F(39)-C(115)-F(37)	106.6(7)		
F(38)-C(115)-F(37)	106.4(7)		
F(39)-C(115)-C(26)	112.7(8)		
F(38)-C(115)-C(26)	111.5(7)		
F(37)-C(115)-C(26)	112.2(7)		

Table 2.9 - Bond lengths [Å] and angles [°] for Ar_2PH.

	U11	U22	U33	U23	U13	U12
P(1)	25(2)	38(2)	33(2)	-13(1)	9(1)	-3(1)
P(2)	28(2)	39(2)	30(2)	13(1)	8(1)	1(1)
P(3)	29(2)	36(2)	28(1)	11(1)	10(1)	0(1)
C(1)	25(6)	11(5)	27(5)	-5(4)	-2(4)	-1(4)
C(2)	18(5)	25(6)	23(5)	-1(4)	9(4)	1(4)
C(3)	39(6)	13(5)	23(5)	-5(4)	1(5)	-5(4)
C(4)	40(6)	18(6)	28(5)	7(4)	19(5)	5(4)
C(5)	33(6)	13(5)	28(5)	-3(4)	9(5)	-6(4)
C(6)	23(6)	21(6)	32(6)	-8(4)	6(5)	-9(4)
C(7)	34(6)	15(5)	25(5)	-4(4)	10(4)	3(4)
C(8)	39(6)	15(6)	30(6)	-7(4)	15(5)	0(4)
C(9)	38(7)	23(6)	40(6)	-3(5)	20(5)	-7(5)
C(10)	28(6)	34(6)	24(5)	2(5)	7(5)	-4(5)
C(11)	27(6)	20(6)	30(6)	0(5)	9(5)	6(4)
C(12)	28(6)	24(6)	37(6)	-9(5)	16(5)	-6(4)
C(13)	32(6)	17(5)	28(5)	1(4)	12(5)	6(4)
C(14)	35(6)	14(5)	27(6)	-1(4)	15(5)	3(4)
C(15)	25(6)	17(6)	26(5)	-11(5)	12(5)	-6(4)
C(16)	15(5)	32(6)	29(6)	2(5)	9(4)	7(4)
C(17)	35(6)	11(6)	47(7)	5(5)	22(5)	7(4)
C(18)	25(6)	12(5)	25(5)	1(4)	2(4)	2(4)
C(19)	29(6)	11(5)	29(5)	1(4)	5(4)	2(4)
C(20)	22(5)	10(5)	31(5)	2(4)	7(4)	3(4)
C(21)	30(6)	16(6)	28(5)	0(5)	1(5)	-9(4)
C(22)	32(6)	12(5)	29(5)	-3(4)	12(5)	0(4)
C(23)	25(6)	20(6)	20(5)	0(4)	10(4)	-1(4)
C(24)	38(6)	10(5)	27(5)	2(4)	6(5)	3(4)
C(25)	25(5)	20(6)	28(5)	-12(4)	10(4)	-1(4)
C(26)	20(5)	8(5)	28(5)	-2(4)	6(4)	-3(4)
C(27)	41(6)	11(5)	35(6)	0(5)	16(5)	4(4)
C(28)	44(6)	15(6)	22(5)	2(4)	13(5)	3(5)
C(29)	26(6)	11(5)	31(6)	0(4)	3(5)	-6(4)
C(30)	26(6)	16(5)	29(5)	2(4)	15(5)	1(4)
C(31)	31(6)	19(6)	20(5)	-8(4)	6(4)	-11(4)
C(32)	25(6)	14(5)	29(5)	-3(4)	6(4)	-3(4)
C(33)	15(5)	25(6)	25(5)	-2(4)	8(4)	0(4)
C(34)	30(6)	29(6)	17(5)	-4(4)	4(4)	-14(5)
C(35)	48(7)	12(6)	16(5)	1(4)	6(5)	-5(5)
C(36)	35(6)	12(5)	23(5)	-3(4)	5(5)	-1(4)
C(101)	43(7)	29(7)	42(7)	-2(5)	21(6)	-14(5)
F(11)	44(4)	16(3)	61(4)	-10(3)	29(3)	-3(2)
F(12)	51(4)	35(4)	62(4)	-23(3)	-8(3)	-6(3)
F(13)	84(5)	32(4)	89(5)	-21(3)	61(4)	-26(3)
C(103)	30(6)	27(6)	28(6)	-11(5)	-1(5)	-11(5)
F(17)	46(4)	34(4)	63(4)	17(3)	15(3)	-12(3)
F(18)	25(3)	25(3)	45(3)	-9(3)	6(3)	-5(2)
F(19)	40(3)	38(4)	64(4)	-31(3)	17(3)	-16(3)
C(104)	39(7)	29(6)	34(6)	-7(5)	10(6)	16(5)
F(110)	49(4)	22(3)	40(3)	-10(3)	7(3)	3(3)

	U11	U22	U33	U23	U13	U12
F(111)	52(4)	40(4)	86(5)	-16(3)	39(4)	9(3)
F(112)	70(4)	40(4)	36(3)	0(3)	-7(3)	25(3)
C(106)	32(6)	17(6)	41(6)	-15(5)	14(5)	0(5)
F(116)	44(4)	30(3)	60(4)	22(3)	17(3)	11(3)
F(117)	26(3)	30(3)	44(3)	-6(3)	10(3)	-1(2)
F(118)	40(3)	39(4)	62(4)	-25(3)	13(3)	11(3)
C(107)	45(7)	30(7)	39(7)	1(6)	20(5)	-10(5)
F(21)	33(3)	36(4)	50(4)	10(3)	12(3)	4(3)
F(22)	51(4)	34(4)	59(4)	-12(3)	14(3)	14(3)
F(23)	49(4)	38(4)	69(4)	36(3)	19(3)	15(3)
C(108)	55(8)	89(11)	20(6)	9(6)	21(6)	30(7)
C(109)	32(6)	35(7)	35(6)	6(5)	15(5)	6(5)
F(27)	50(4)	38(4)	44(4)	9(3)	-8(3)	7(3)
F(28)	47(4)	25(3)	50(4)	10(3)	20(3)	5(3)
F(29)	80(4)	32(4)	80(4)	20(3)	62(4)	28(3)
C(112)	32(6)	21(6)	40(6)	2(5)	11(5)	-1(5)
F(216)	33(3)	23(3)	48(3)	8(3)	10(3)	-2(2)
F(217)	53(4)	33(4)	74(4)	-28(3)	24(3)	-11(3)
F(218)	44(4)	35(3)	55(4)	22(3)	5(3)	-15(3)
C(110)	42(7)	18(6)	28(6)	4(5)	5(5)	-1(5)
F(210)	57(4)	36(4)	92(5)	6(3)	52(4)	-8(3)
F(211)	44(4)	20(3)	49(4)	8(3)	8(3)	-3(2)
F(212)	83(4)	24(3)	38(3)	-7(3)	6(3)	-19(3)
C(114)	36(7)	33(7)	30(6)	-5(5)	7(5)	-1(5)
C(116)	33(7)	30(7)	32(6)	20(5)	-1(5)	1(5)
F(310)	32(3)	29(3)	45(3)	12(3)	5(3)	3(3)
F(311)	50(4)	32(4)	43(4)	-9(3)	10(3)	14(3)
F(312)	49(4)	28(3)	51(4)	23(3)	16(3)	8(3)
C(118)	26(6)	30(6)	36(6)	8(5)	7(5)	0(5)
F(316)	52(4)	34(4)	50(4)	13(3)	-10(3)	5(3)
F(317)	38(3)	21(3)	57(4)	13(3)	19(3)	3(2)
F(318)	72(4)	31(4)	67(4)	9(3)	45(3)	21(3)
C(113)	41(7)	35(7)	23(6)	0(5)	5(5)	-7(5)
F(31)	62(4)	33(4)	84(5)	6(3)	46(4)	-10(3)
F(32)	45(4)	17(3)	42(3)	10(3)	6(3)	-5(3)
F(33)	75(4)	30(3)	37(3)	-6(3)	2(3)	-31(3)
C(115)	38(7)	27(6)	35(6)	0(5)	16(5)	3(5)
F(37)	41(3)	28(3)	52(4)	-12(3)	15(3)	-10(2)
F(38)	45(3)	29(3)	47(3)	13(3)	12(3)	-13(3)
F(39)	26(3)	31(3)	45(3)	10(3)	7(3)	2(2)
C(117)	51(7)	17(6)	38(6)	-9(5)	12(6)	-16(5)

Table 2.10 - Anisotropic displacement parameters ($Å^2$ x 10^3) for Ar_2PH. The anisotropic displacement factor exponent takes the form: $-2\pi^2 [h^2 a^2 U11 + 2 h k a^* b^* U12]$

2.2.13 Attempted preparation of Ar_2PF

Synthesis of this compound was attempted because of the potentially useful complex it was expected to form with Pt(II), giving interesting NMR and potential anti-cancer applications as well (see Section 3.1).

Ar_2PCl was refluxed in CH_2Cl_2 with SbF_3 (analogous to the preparation of $Ar'PF_2$) for three days. Unfortunately the compound was only formed in very small quantities. This is probably due to the steric hindrance around the P-Cl bond which makes substitution (either S_N1 or S_N2) difficult.

The ^{19}F NMR spectrum of the solution obtained at the end of the reaction showed a small doublet of doublets, the chemical shift of which is δ = -56.3 ppm ($^4J_{P\text{-}F}$ = 16.3Hz) ($^5J_{P\text{-}F}$ = 6.1 Hz). This pattern is what would be expected for the six fluorine atoms of the *ortho* CF_3 groups, the larger coupling constant being $^4J_{P\text{-}F}$ and the smaller one being $^5J_{F\text{-}F}$. The coupling pattern which would be expected for the fluorine atoms attached to the phosphorus would be a doublet of septets, and unfortunately due to the very small amount of the product synthesised, these peaks were not distinguishable from the background. There are a number of particularly small peaks, any one of which could be assigned to the *para* CF_3 group fluorines.

There is enough evidence to speculate that the compound was formed in small quantities, although not enough to characterise it fully.

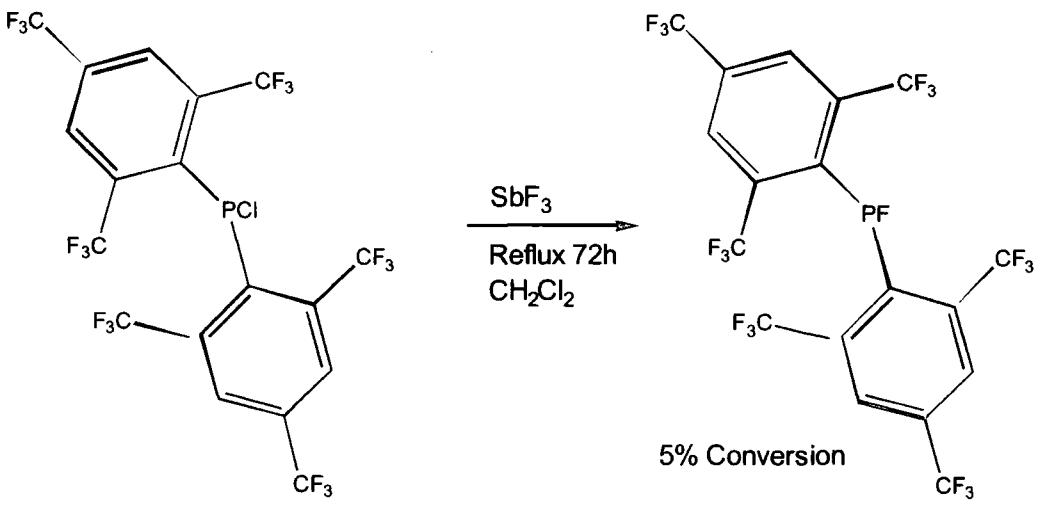

Equation 2.15– Synthesis of Ar_2PF

2.2.14 $ArP(Cl)CHCl_2$

In the analogous reaction to the preparation of $Ar'P(Cl)CHCl_2$, lithiated dichloromethane was added to a solution of $ArPCl_2$ at –130°C in a mixed solvent, with vigorous stirring. Upon warming, the solution went a deep red colour. The solvent was removed in *vacuo* and the remaining colourless oil was purified by distillation.

The ^{31}P NMR spectrum of a solution of the compound in dichloromethane showed the formation of a new septet with chemical shift δ = 62.0 ppm ($^4J_{P-F}$ = 50.6 Hz). The ^{19}F NMR spectrum showed a doublet and a singlet, δ = -54.7 ppm ($^4J_{P-F}$ = 49.8 Hz) and δ = -64.8 Hz.

These results as with those of the starting material $ArPCl_2$ agree with those reported by Goodwin [^{31}P ($CDCl_3$) δ: 63.6ppm, $^4J_{P-F}$ = 49.8 Hz]

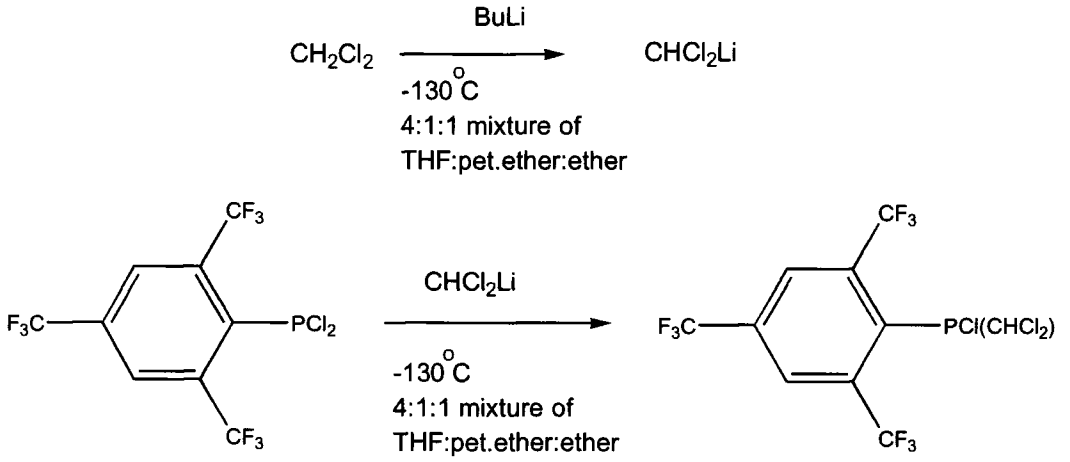

Equation 2.16– Synthesis of $ArPCl(CHCl_2)$

2.2.15 $ArP{=}CCl_2$

DBU was added to a solution of $ArP(Cl)CHCl_2$ in THF at –78°C. A voluminous bright orange precipitate was formed as the solution was allowed to warm to room temperature. The solution was filtered and the solvent removed by distillation at room temperature. The product was purified by distillation, yielding an air stable colourless oil.

The ^{31}P NMR spectrum of a solution of the compound in CH_2Cl_2 showed a septet with a chemical shift δ = 202.9 ppm ($^4J_{P-F}$ = 21.4 Hz). The ^{19}F NMR spectrum showed a doublet and a singlet, δ = -61.0 ppm ($^4J_{P-F}$ = 21.4 Hz) and δ = –65.2 ppm. Compared with Goodwin's results these coupling constants differ by less than 0.2 Hz.

It is worthy of note that the coupling constant $^4J_{P-F}$ in both cases of the phosphaalkenes, Ar'P=CCl_2 and ArP=CCl_2, is significantly smaller than other phosphanes described in this chapter. It should also be noted that the ^{19}F chemical shifts of the CF_3 groups in these two compounds are at lower frequency as well, thus implying more shielding and electron density on the CF_3 groups.

This change may be due in part to the formation of the P=C π double bond. The withdrawal of electrons from the phosphorus atom by the aryl group is more easily facilitated through the π system. The formation of the P=C double bond decreases the p character of the electrons on the phosphorus (sp^3 goes to sp^2), and thus enables more electron density to be delocalised into the ring. This in turn increases the electron density on the CF_3 groups, moving them to a lower frequency in the chemical shift range.

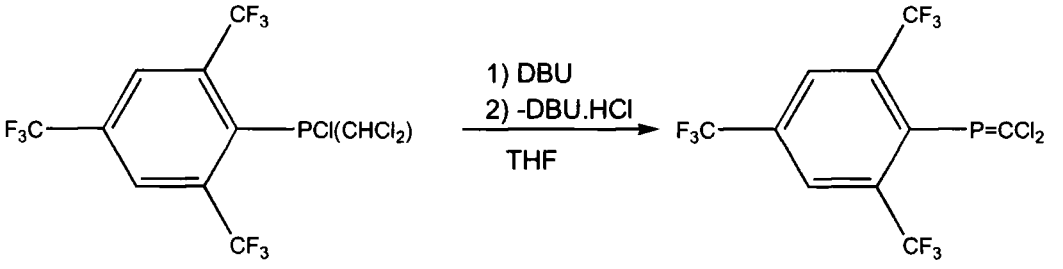

Equation 2.17– Synthesis of ArP=CCl_2

2.3 The resistance of Ar'PH_2 and ArPH_2 to reaction

In the formation of RP=CClH (R = Supermes) (see Section 2.1.2) RPH_2 is reacted with KOH and $CHCl_3$. The crystal structure of the salt RPH[-]K[+] has been published, demonstrating the acidity of the protons bonded to phosphorus in RPH_2.[5]

The Supermes ligand, whilst bulky, effectively donates electron density onto the phosphorus atom, thus making the P-H bonds comparatively stronger and the hydrogens less acidic. They are still, however, acidic enough to react with KOH and are easily lithiated by BuLi (in preference to any other hydrogen in the molecule).

Fluoromes and Fluoroxyl are comparatively more electron withdrawing than Supermes, and this would infer that there would be more electron density withdrawn from the P-H bond, thus making the protons more acidic.

There is no reaction of either $ArPH_2$ or $Ar'PH_2$ with KOH or BuLi, which implies that the protons are much less acidic. The reasons for the apparent lack of reaction could be linked to an interaction, such as H-bonding, between the CF_3 groups and the hydrogens. There may be some close intramolecular contacts in the molecule which prevents cleavage of the P-H bond. The X-ray structure of $ArPH_2$-$PtCl_2(PEt_3)$ gives some insight into this possible interaction. The distances between the fluorine and hydrogen atoms in this structure (2.50/2.56 Å) are within distances which are accepted as those for H-bonds (see Section 3.2.3.1).

2.4 Experimental

2.4.1 Synthesis of Ar'Li and Ar''Li

BuLi (91.2 mmol, 57ml, 1.6M in hexanes) was added dropwise over 10 minutes to a solution of Ar'H (20.03g, 94 mmol) in ether (200ml) at -78°C. The solution was allowed to warm to room temperature and left to stir for four hours. A dark brown solution (Ar'Li + Ar''Li) was formed. The ^{19}F NMR spectrum clearly showed the formation of two separate species. The spectrum showed three singlets in the ratio 2:1:1.

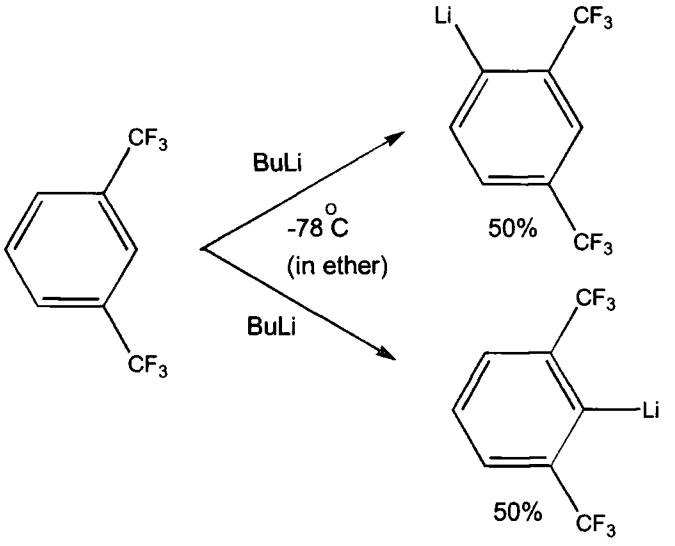

2.4.2 Synthesis of $Ar'PCl_2$/$Ar''PCl_2$

(Ar'Li, 71mmol) was added dropwise to a solution of PCl_3 (16ml, 25.2g, 162mmol) in ether (100ml) slowly over 10 minutes. The solution was allowed to warm to room temperature and a precipitate of LiCl was slowly formed. The solution was then filtered and the solvent and excess PCl_3 were removed *in vacuo*, leaving a brown intractable oil. The products were distilled from this oil under vacuum. Yield (based on Ar'H) 9.46g (42%); Bp 45°C (0.01 mmHg); ^{31}P (CH_2Cl_2) δ = 148.0 ppm (septet), $^4J_{P\text{-}F}$ = 65.2 Hz; ^{19}F δ = -53.0 ppm (doublet), $^4J_{P\text{-}F}$ =65.2 Hz. $Ar''PCl_2$, ^{31}P: δ = 151.1 ppm ($^4J_{P\text{-}F}$ = 84.5 Hz).

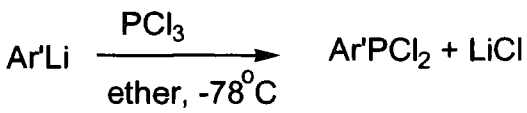

2.4.3 Synthesis of Ar'Ar''PCl

In the synthesis described previously for $Ar'PCl_2$, a large by-product is Ar'Ar''PCl. Using the same synthesis, this product was purified by distillation under vacuum and then by recrystallisation from hexanes. Yield (based on Ar'H) 7.45g (26%); Bp 93°C (0.01mm Hg); ^{31}P (CH_2Cl_2) δ = 67.3 ppm (complex multiplet), $^4J_{P\text{-}F}$ = 67.1 Hz; ^{19}F (room temperature) δ = -59.3 ppm (doublet), $^4J_{P\text{-}F}$ =67.1 Hz, δ = -64.1 (singlet) δ = -55.4 (singlet – broad). Analysis found: %C, 38.94; %H, 1.24; Required for $C_{16}F_{12}H_6PCl$; %C, 41.85; %H, 1.17.

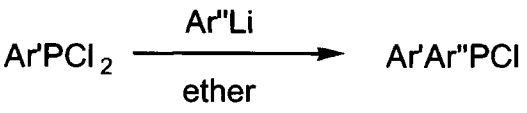

2.4.4 Synthesis of $Ar'PH_2$

Bu_3SnH (9.0ml, 9.2g, 31.6mmol) was added dropwise to a stirred solution of $Ar'PCl_2$ (5.0g, 15.8mmol) in ether (150ml) at room temperature, and the solution was allowed to stir for 30 minutes. The solvent was then removed by distillation at room temperature. The product was purified from the resulting oil by distillation under reduced pressure. Yield 2.81g (71.9%), Bp 46°C (10mm Hg); $^{31}P\{^1H\}$ (CH_2Cl_2) δ = -140.3 ppm (septet), $^4J_{P\text{-}F}$ = 29.4 Hz; ^{19}F δ = -61.5 ppm (doublet of triplets); ^1H δ = 3.9 (doublet) $^1J_{PH}$ = 216.7 Hz.

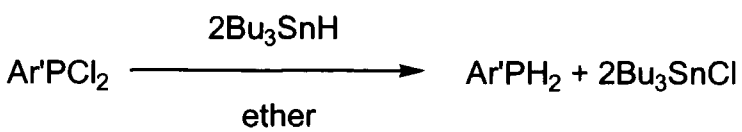

2.4.5 Synthesis of $Ar'PF_2$

SbF_3 (1.5g, 8.45mmol) was added to a solution of $Ar'PCl_2$ (2.1g, 6.65mmol) in $(CHCl_2)_2$ and the resulting mixture was refluxed over three days. The solution was then filtered and the solvent removed by distillation at room temperature. The product was purified by vacuum transfer at room temperature. Yield 1.22g (65%); Bp 63°C (0.03mm Hg); ^{31}P (CH_2Cl_2) δ = 193.3 ppm (triplet of septets), $^1J_{P\text{-}F}$ = 1123.8 Hz, $^4J_{P\text{-}F}$ = 48.3 Hz; ^{19}F δ = -55.5 ppm (doublet of triplets) $^4J_{P\text{-}F}$ = 48.4 Hz; δ = -91.85 ppm, (doublet of septets), $^1J_{P\text{-}F}$ = 1123.8 Hz, $^5J_{F\text{-}F}$ = 14.1 Hz.

$$Ar'PCl_2 \xrightarrow[(CHCl_2)_2]{SbF_3} Ar'PF_2 + SbCl_3$$

2.4.6 Synthesis of $Ar'PBr_2$ and $Ar''PBr_2$

BuLi (78.5ml, 2.5M, 196mmol) was added slowly over 10 minutes to a solution of Ar'H (42g, 196mmol) in ether (250ml) at -78°C. The solution was allowed to warm to room temperature and left to stir for four hours. The solution was then cooled to 0°C and added to a solution of PBr_3 (53g, 18ml, 196mmol) in ether (100ml) dropwise over twenty minutes. A precipitate was immediately formed and the solution was allowed to warm to room temperature and stirred for two hours. The solvent was then removed *in vacuo*. The product was isolated from the remaining brown oil by distillation under vacuum as a yellow oil. Yield 18.7g (29.0%) (mixed $Ar''PBr_2$ and $Ar'PBr_2$); Bp = 70°C (0.05mm Hg), ^{31}P (CH_2Cl_2) δ = 135.8 ppm (septet), ($^4J_{P\text{-}F}$ = 62.8 Hz), δ = 143.9 ppm (quartet) ($^4J_{P\text{-}F}$ = 77.0 Hz); ^{19}F δ = -50.70 ppm (doublet) $^4J_{P\text{-}F}$ = 62.7 Hz ,δ = -61.9 ppm (singlet), δ = -54.9 ppm, (doublet) $^4J_{P\text{-}F}$ = 76.9 Hz.

$$Ar'Li \xrightarrow[\text{ether, -78 °C}]{PBr_3} Ar'PBr_2 + Ar''PBr_2 + LiBr$$

2.4.7 Synthesis of $Ar'P(Cl)CHCl_2$

BuLi (17.1ml, 1.6M in hexanes,27.3mmol) was added dropwise to a solution of CH_2Cl_2 (2.0 ml, 2.66g, 31 mmol) in a 4:1:1 mixture of pentane : THF : diethylether, at -130°C with vigorous stirring. This was allowed to stir for five minutes and was then added rapidly through pre-cooled cannulars to a solution of $Ar'PCl_2$ (6.64g, 27.3mmol) in ether (100ml) also at -130°C. The solution was then allowed to warm up to room temperature and left to stir for two hours. As the solution warmed up it produced a deep red colour and a precipitate of LiCl was formed. The solution was filtered and the solvent was removed *in vacuo*. The product was purified by distillation from the resulting oil to yield a colourless oil. Yield 5.3g (53.3%) Bp 60°C (0.09mm Hg); ^{31}P (CH_2Cl_2) δ = 65.6 ppm (septet), $^4J_{P-F}$ = 48.6Hz; ^{19}F δ = -53.6 ppm (doublet) $^4J_{P-F}$ = 48.6 Hz.

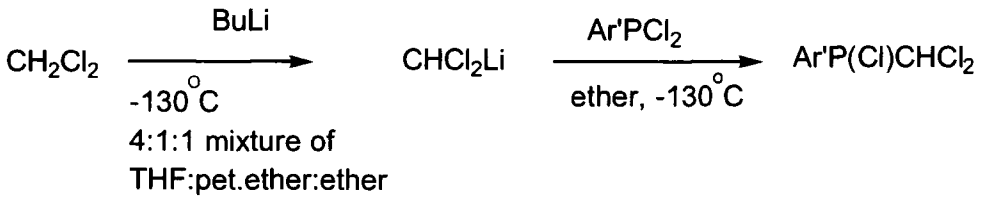

2.4.8 Synthesis of $Ar'P{=}CCl_2$

DBU (3.57g, 23mmol) was added dropwise to a solution of $Ar'P(Cl)CHCl_2$ (6.61g, 23mmol) in THF at -78°C. The reaction was very vigorous and a gelatinous precipitate was formed. The solution was allowed to warm to room temperature and left to stir for two hours. This produced a deep orange colour to the solution. The solvent was removed by distillation at room temperature and the product was purified by distillation under reduced pressure. Yield 5.12g (68%) Bp = 57°C (0.2mm Hg); ^{31}P (CH_2Cl_2) δ = 206.8 ppm (septet), $^4J_{P-F}$ = 21.5 Hz; ^{19}F δ = -59.9 ppm (doublet) $^4J_{P-F}$ = 21.6Hz.

2.4.9 Synthesis of Ar'Ar''PH

Bu_3SnH (2.4ml, 8.4mmol) was added dropwise to a solution of Ar'Ar''PCl (4.01g, 8.13mmol) in ether (100ml) and the solution was allowed to stir for two hours. The solvent was removed *in vacuo* leaving a colourless solution. The product was purified by distillation, producing a clear viscous oil, which solidified on standing. Yield 2.89g (77%) Bp = 48°C (0.01mm Hg); ^{31}P (CH_2Cl_2) δ = -45.6 ppm (complex multiplet), $^1J_{PH}$ = 232.9 Hz, $^4J_{P\text{-}F}$ = 39.4 Hz.

$$\text{Ar'Ar''PCl} \xrightarrow[\text{ether}]{Bu_3SnH} \text{Ar'Ar''PH} + Bu_3SnCl$$

2.4.10 Synthesis of $ArPCl_2$

BuLi (31.2ml, 2.5M in hexanes, 78mmol) was added dropwise over five minutes to a solution of ArH (20.0g, 78mmol) in ether (250ml) at -78°C. The reaction was then allowed to warm to room temperature and stirred for four hours; a gelatinous brown solution was formed. This reaction mixture was then added to a solution of PCl_3 (7ml, 80mmol) in ether (100ml) slowly over ten minutes. A precipitate was formed of LiCl and the reaction was left to stir for two hours. The solution was then filtered and the solvent was removed *in vacuo* leaving an intractable brown oil. The product was purified by distillation yielding a colourless oil. Yield 20.8g (71%) Bp 47°C (0.2mm Hg); ^{31}P (Et_2O) δ = 144.5 ppm (septet), $^4J_{P\text{-}F}$ = 61.5 Hz; ^{19}F δ = -53.3 ppm (doublet), $^4J_{P\text{-}F}$ = 61.4Hz, δ = -64.5 ppm (singlet)

$$\text{ArLi} \xrightarrow[\text{ether, -78°C}]{PCl_3} ArPCl_2 + LiCl$$

2.4.11 Synthesis of $ArP(Cl)CHCl_2$

BuLi (18.95ml, 2.48M in hexanes, 47.0mmol) was added dropwise to a solution of CH_2Cl_2 (3.5ml, 4.7g, 54mmol) in a 4:1:1 mixture of pentane : THF : diethylether, at -130°C with vigorous stirring. This was allowed to stir for five minutes and was then added rapidly through a pre-cooled cannular to a solution of $ArPCl_2$ (17.75g, 47 mmol) in ether (100ml) also at -130°C. The solution was then allowed to warm up to room temperature and left to stir for two hours. As the solution warmed up it produced a deep red colouration and a precipitate was formed of LiCl. The solution was filtered and the solvent was removed *in vacuo*. The product was purified by distillation from the resulting oil to yield a colourless oil. Yield 13.1g (69%) Bp 67°C (0.07mm Hg); ^{31}P (CH_2Cl_2) δ = 62.0 ppm (septet), $^4J_{P-F}$ = 50.6 Hz; ^{19}F δ = -54.7 ppm (doublet) $^4J_{P-F}$ = 50.6 Hz, δ = -64.8 ppm (singlet).

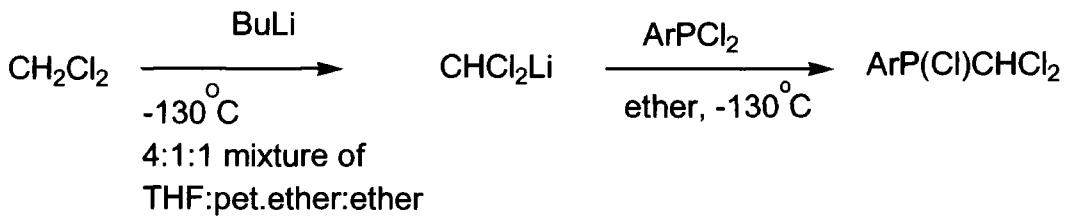

2.4.12 Synthesis of $ArP{=}CCl_2$

DBU (4.67g, 30.8mmol) was added dropwise to a solution of $ArP(Cl)CHCl_2$ (13.0g, 30.8mmols) in THF at -78°C. The reaction was very vigorous and a gelatinous precipitate was formed. The solution was allowed to warm to room temperature and left to stir for two hours. This produced a deep orange colour to the solution. The solvent was removed by distillation at room temperature and the product was purified by distillation under reduced pressure. Yield 5.0g (49%) Bp = 55°C (0.1mm Hg); ^{31}P (CH_2Cl_2) δ = 202.6 ppm (septet), $^4J_{P-F}$ = 21.4 Hz;^{19}F δ = -61.2 ppm (doublet), $^4J_{P-F}$ = 21.4 Hz, δ = -65.2 ppm (singlet).

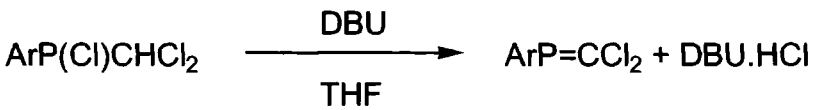

2.4.13 Synthesis of Ar_2PCl

BuLi (12.8ml, 2.5M in hexanes, 32mmol) was added dropwise over five minutes to a solution of ArH (10.0g, 34mmol) in ether (250ml) at -78°C. The solution was then allowed to warm to room temperature and stirred for four hours; a gelatinous brown solution was formed. This reaction mixture was then added to a solution of $ArPCl_2$ (14.6g, 39mmol) in ether (100ml) at room temperature in 5 aliquots of 50ml. The reaction was allowed to stir for twenty minutes after the addition of each aliquot. A precipitate of LiCl was slowly formed. The solution was then filtered and the solvent removed *in vacuo* leaving a brown intractable oil.

The product was purified by distillation to yield a colourless oil, which on standing solidified to give a pale yellow solid. This was then recrystallised from hexanes forming a white crystalline solid. Yield 16.5g (56%) Bp = 95°C (0.05mm Hg); ^{31}P (CH_2Cl_2) δ = 75.5 ppm (septet), $^4J_{P\text{-}F}$ = 41.2Hz; ^{19}F δ = -55.6 ppm (doublet), $^4J_{P\text{-}F}$ = 41.2Hz, δ = -65.2 ppm (singlet).

$$ArPCl_2 \xrightarrow[\text{ether, 297K}]{\text{ArLi}} Ar_2PCl + LiCl$$

2.4.14 Synthesis of Ar_2PH

Bu_3SnH (2.0ml, 7.0mmol) was added to a solution of Ar_2PCl (4.31g, 6.9mmol) in ether (100ml) at room temperature, and the solution was allowed to stir for two hours. The solution was then removed *in vacuo* leaving a colourless solution. The product was then recrystallised from a solution of hexane and then by sublimation. Yield 3.3g (80%) Bp(sublimes) = 62°C (0.08mm Hg); ^{31}P (CH_2Cl_2) δ = -65.7 ppm (doublet of multiplets), $^1J_{P\text{-}F}$ = 251.5 Hz $^4J_{P\text{-}F}$ = 21.2 Hz; ^{19}F δ = -60.8 ppm (doublet of doublets), ($^4J_{P\text{-}F}$ = 21.21 Hz) ($^5J_{FH}$ = 7.14 Hz) and δ = -64.7 ppm (singlet); ^1H δ = 6.22 ppm, $^1J_{PH}$ = 249.4 Hz. Analysis found: %C, 36.25; %H, 0.81; Required for $C_{18}F_{18}H_5P$; %C, 36.38; %H, 0.85.

$$Ar_2PCl \xrightarrow[\text{ether, 297K}]{Bu_3SnH} Ar_2PH + Bu_3SnCl$$

[1] G. M. Kosolapoff., L. Maier., *"Organic phosphorus Compounds"*, Wiley-Interscience. 1972, **4**, 75.
[2] H. P. Goodwin., *Ph.D. Thesis*, Durham, 1990.
[3] G. R. Desiraju., "Crystal Engineering – The design of organic solids", *Material Science Monographs, Elsiever Science Publishers. B. V.*, 1989
[4] H. Bonditi., *J. Phys. Chem.*, 1964, **68**, 441
[5] G. W. Rabe., G. P. A. Yap., A. L. Rheingold., *Inorganic Chemistry*, 1997, **10**, 1990.

Chapter 3

Synthesis and X-ray characterisation of some platinum-phosphane compounds

3.1 Introduction

When considering characterisation of compounds using NMR, bonding any phosphorus containing species directly to platinum has one immediate advantage. Both Pt(0) and Pt(II) in their normal complexes, are diamagnetic, and thus do not broaden the spectrum due to unpaired electrons (Pt (0) = d^{10} and Pt (II) = d^8). The effect is shown in Pt(II) because the complexes are square planar and not tetrahedral.

The diagram below (see Figure 3.1) shows the change in energy of the d orbitals on the metal, as the axial ligands are removed from an octahedral complex. Any orbital containing "z" character (d_{z2} and d_{xz},d_{yz}) lowers in energy, and the other orbitals rise in energy accordingly. This effect causes the crystal field splitting pattern of the d–orbitals to change dramatically, thus causing the pairing of the eight d electrons.

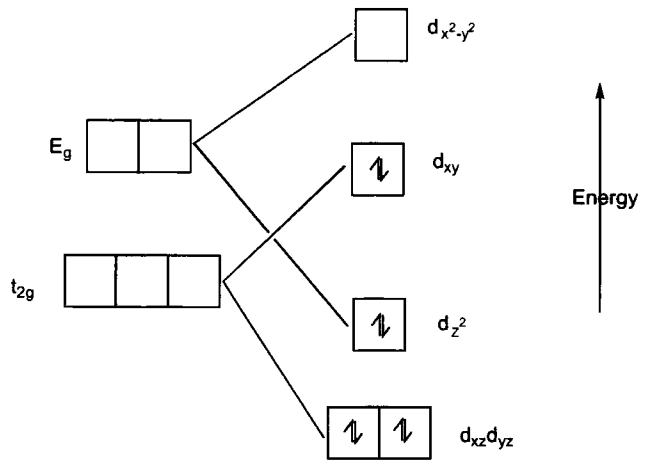

Figure 3.1 – Electron pairing in a square planar complex.

Platinum has an isotope which is NMR active (^{195}Pt, spin = $^1/_2$, abundance = 33.7%), thus in a ^{31}P NMR spectrum there will be two platinum satellites coupled to the phosphorus peak. This makes interpreting the spectrum much easier, as it can be established with certainty which peak is assignable to a phosphorus atom bonded to platinum.

Some of the low coordinate phosphorus species (in which we are interested as a group), when bonded to platinum in the form $PtCl_2(PEt_3)(RP{=}PR)$ (R=Fluoromes), have shown anti-carcinogenic properties when tested against a range of cancers[1]. The anti-carcinogenic properties of platinum(II) complexes have been known for years (e.g. Cis-platin, $PtCl_2(NH_3)_2$)[2]. There has, however, been limited success in the replacement of the nitrogen atoms with phosphorus donors. This has been attributed to a strong *trans* effect exerted in dichloro-Pt(II) compounds. Fluorophosphanes in particular may overcome this effect due to their strong σ-donor and strong π-acceptor properties. We have to thank Johnson Matthey for their loan of platinum and palladium salts.

3.1.1 The "Pt dimer"

The platinum(II) dimer, the formation of which is shown below (see Equation 3.1), was used initially in previous work on these systems[3] because the diphosphene ArP=PAr did not react with similar Pt(II) compounds, (e.g. $PtCl_2$, $PtCl_2(PhCN)_2$). The dimer is easily prepared[4] using a three step method shown below.

$PtCl_2$ was dissolved in a solution of PhCN at 70°C forming a yellow solution. As the solution cooled yellow crystals were formed and then isolated, washed, and dried. The product $[PtCl_2(PhCN)_2]$ was then dissolved in ether and added to a solution of PEt_3 in CH_2Cl_2. The resulting white product was isolated, washed and dried.

It was then dissolved at high temperature in a solution of $PtCl_2$ in $(CHCl_2)_2$ to form the desired product. On cooling the yellow crystalline precipitate was formed and this was isolated, washed and dried.

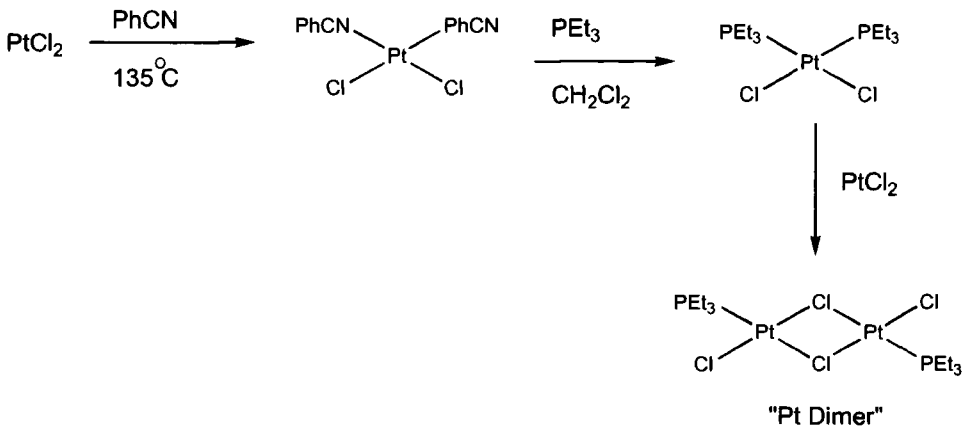

Equation 3.1 – Synthesis of $[(PtCl_2)PEt_3]_2$

3.2 New phosphorus analogues of *cis*-platin

3.2.1 Reaction between the "Pt dimer" and low coordinate phosphorus species

There are two possible isomers formed in this series of reactions, between phosphanes and the dimer, *cis* and *trans*. The actual mechanism for the reaction is likely to be analogous to the normal substitution in a square planar complex[2]. This is by the formation of an initial five coordinate species which then loses one of the original substituents to leave the square planar product.

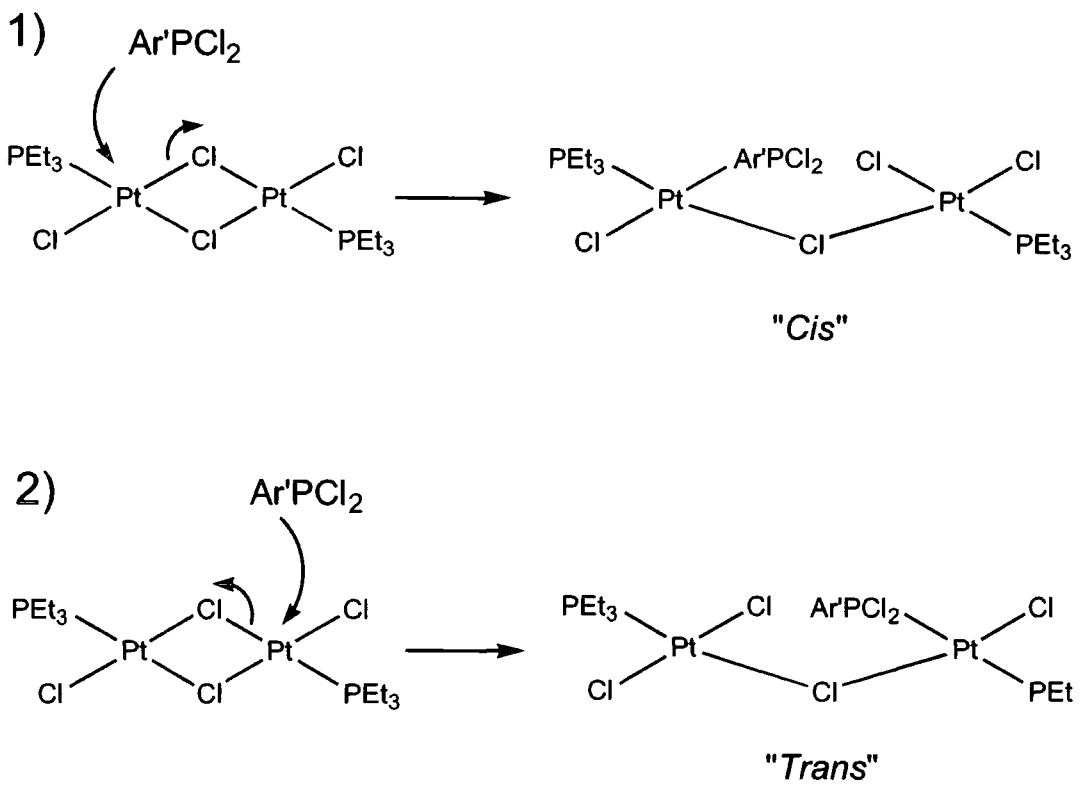

Figure 3.2 – Formation of two possible isomers upon initial reaction between $Ar'PCl_2$ and the dimer

The initial product upon the reaction of the dimer with the phosphane Ar'_xPY_z (X = 1, Y = H, F, Cl, Z = 2) (X = 2, Y = Cl, Z = 1) (X = 1, Y = [=CCl_2], Z = 1) is the kinetic product, the *trans*–isomer. This product then rearranges to give the thermodynamically more favourable product, the *cis*–isomer. The time taken for rearrangement varies with phosphane from a few seconds to days, and in the case of Ar'Ar''PCl the *trans*–isomer is stable over a period of weeks. Evidence for the *cis*–isomer is only visible upon prolonged heating.

> *The trans–influence is defined as "the extent to which that ligand weakens the bond trans to itself in the equilibrium state of the substrate"*[5].

The trans influence exerted by a phosphane is much greater than that of a halide and thus the effect is apparent in these types of systems.

This raises the question as to why the *trans*–isomer is the initial product. The answer comes from studying the Pt dimer. The "*trans* effect" is often seen in reaction of phosphanes with platinum complexes[5], and this trend affects the reaction of the complex in question and the nature of the isomeric products.

Another factor may be that, as can be seen from the diagrams previously shown, if the phosphane approaches on the opposite side of the molecule to the PEt_3 group, it is sterically more favourable, thus forming the *trans* product first.

Because the initial product is the *trans*–isomer, it can be inferred that the initial platinum–chlorine bond which is cleaved is the bond which is *trans* to the PEt_3 group. This ties in with the "*trans* effect" described above.

The time taken to rearrange from the *trans*-isomer to give the thermodynamically more stable product (*cis* isomer) varies with each phosphane. This means that there must be an overriding energy barrier which must be overcome for rearrangement to occur. This could be due to more than one reason:

1) During the rearrangement, the steric bulk of the phosphane may influence the approach of the detached PEt_3 group. The larger the steric bulk of the phosphane, the more likely the PEt_3 group is to coordinate in the *trans* position. (see Figure 3.3).
2) The strength of the Pt–P bond may directly influence the formation of the necessary intermediate. The relative strength of the Pt–P bond is related to the length of the Pt–P bond and thus to the size of the coupling constant $^1J_{P-Pt}$ (see Section 3.4).
3) There may well be a balance between factors 1 and 2 above.

The intermediate species formed in these types of re-arrangements have been shown to be three–coordinate species[2]. This is formed by the loss of the weakest ligand on the platinum centre. The Pt–Cl bonds are stronger than the Pt–P bonds and X–ray crystallographic studies on the compounds have shown that the PEt_3 groups bonded to the platinum are more loosely bound than the phosphanes(phosphaalkene). This would imply that the weakest bond in the complex is the Pt–PEt_3 bond. (The average bond length of the PEt_3 groups bonded to platinum is 2.31 Å, and in the case of the other phosphane groups in the compounds studied, the average bond length is 2.18 Å).

Once the PEt_3 bond has cleaved, the PEt_3 group is then free to couple with the intermediate to form either a *cis* or *trans* isomer. The *cis* isomer is the thermodynamically more stable compound as there is no P–Pt–P interaction caused by the *trans* influence. The *cis* compound is therefore less likely to lose a PEt_3 group and form the three–coordinate species. This in turn eventually realises the total rearrangement from the *trans* to the *cis* isomer.

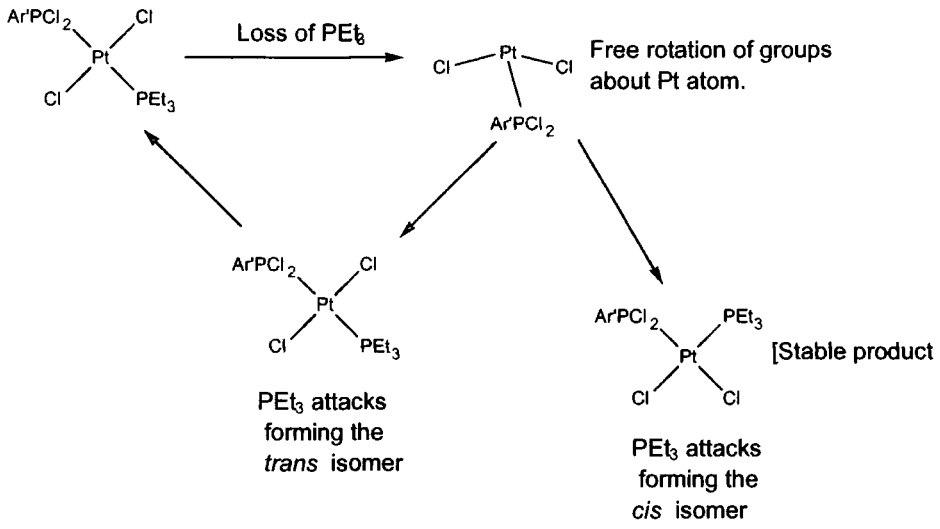

Figure 3.3 – Rearrangement of the initial *trans* product to give the kinetically more stable *cis* product

3.2.2 Reaction between $[PtCl_2(PEt_3)]_2$ and $(C_8H_3F_6)PCl_2$

During the formation of the starting material ($Ar'PCl_2$), the formation of the undesired phosphane $Ar''PCl_2$ is unavoidable (see Section 2.2.1). Purification of these materials proved impossible and thus upon addition of this mixture to the "platinum dimer" a mixture of products is to be expected. Both phosphane groups are similar in nature and will form similar products with the platinum species. This is apparent from the ^{31}P and the ^{19}F NMR spectra of the reaction mixture. Due to the similarities in the two compounds (again isolation of the pure products was impossible), crystals were obtained from the mixture using a layering technique (see Appendix 1) and submitted for X-ray analysis (see Section 3.2.2.1).

$Ar'PCl_2$ ($Ar''PCl_2$) was added to a solution of $[PtCl_2(PEt_3)]_2$ in $(CCl_2H)_2$ and allowed to stir for a period of a few days. Over this time there was a visible change in the ^{31}P NMR spectrum. Initially there were two sets of peaks in the spectrum, the signals corresponding to the dimer itself and the phosphanes. After a number of days, the formation of a number of new peaks at a lower frequency to that of the starting phosphorus halides became apparent. These can be assigned to the new compounds formed between the phosphanes and the platinum complex. The peaks corresponding to the new species formed had distinctive satellites, due to the coupling to active platinum atoms.

The reaction between a phosphane and the "Pt dimer" has two possible isomeric products (*cis* and *trans)*. The initial isomer formed was the *trans* isomer (^{31}P δ = 142.7 ppm $^{2}J_{P-P}$ = 678.4Hz). There are of course two possible *trans* isomers; however, the greater concentration of the Ar'PCl_2 as compared to Ar''PCl_2 was such that it was assumed that the visible product was that due to the Ar'PCl_2. Unfortunately, the resonances associated with the *trans* isomer was so small they were indistiguishable from the backgroud and it was impossible to determine the coupling constant ($^{1}J_{P-Pt}$). Values for the chemical shift and coupling constant assignable to the PEt_3 group in the compound were unobtainable due to the large number of peaks and low concentrations.

This value concurs with the value for the analogous ArPCl_2 compound recorded by H. Goodwin ($^{2}J_{P-P}$ = 694 Hz)[3].

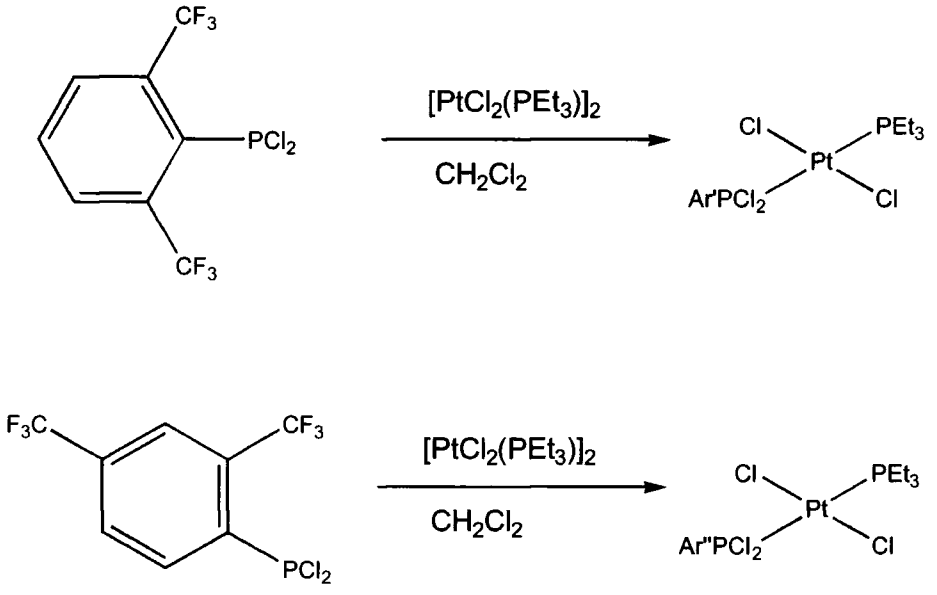

Equation 3.2 – Synthesis of *trans* Ar'PCl_2 and Ar''PCl_2 derivatives of the dimer

These resonances were then superseded by the formation of new resonances assignable to the *cis*-isomers. The reaction was complete after 72 hours with only the *cis*-isomers present (^{31}P δ = 97.9 ppm $^{1}J_{P-Pt}$ = 5488.1 Hz, singlet with Pt satellites, δ = 19.54 ppm $^{1}J_{P-Pt}$ = 3444.7 Hz, singlet with Pt satellites) for (Ar''PCl_2) and (δ = 94.5 ppm, $^{1}J_{P-Pt}$ = 5260 Hz, singlet with Pt satellites, δ = 20.14 ppm $^{1}J_{P-Pt}$ = 2916.1 Hz, singlet with Pt satellites) for (Ar'PCl_2).

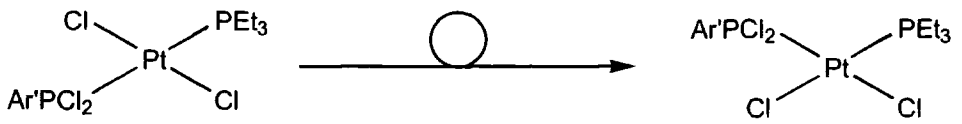

Equation 3.3 – Re-arrangement of *trans* $(Ar'PCl_2)PtCl_2(PEt_3)$

This drawing is equally applicable to the rearrangement of the *trans* Ar''PCl_2–Pt compound.

The product was isolated as an impure white powder which was recrystallised using a layering technique (see Appendix 1). The crystals were submitted for X-ray crystallographic studies and the crystal structure partially solved (see Section 3.2.2.1). The crystal structure ascertained from these crystals was not as accurate as one would expect. This may be due to some impurities in the crystal caused by the Ar''PCl_2–Pt compound also formed in this reaction.

3.2.2.1 Molecular structure of $[PtCl_2(PEt_3)(C_8H_3F_6)PCl_2]$

Crystals submitted for X-ray characterisation were mounted on a glass fibre, introduced onto the diffractometer and diffraction data collected. The structure was subsequently solved and refined; the molecular structure is shown below in Figure 3.4.

Data were collected on a Siemens 3-circle diffractometer with a CCD area detector, ω scan mode $2\theta \leq 60.2°$. The structure was solved by direct methods and refined by full-matrix least squares against F^2. Lists of crystal data and refinement parameters, anisotropic displacement parameters, bond lengths and angles, and atomic coordinates are given in Table 3.1 through Table 3.5.

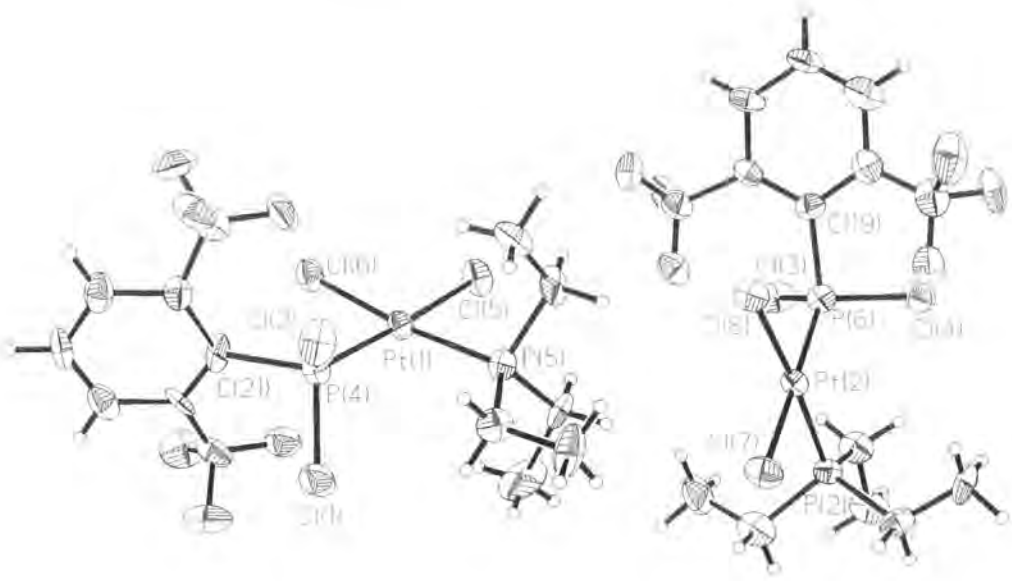

Figure 3.4 – Thermal ellipsoid diagram at 150K (50% Probability) for $[PtCl_2(PEt_3)(Ar'PCl_2)]$

The ESDs for the bond lengths not including platinum are only accurate to two decimal places. This inaccuracy may be caused by a large quantity of unassigned electron density in the difference map of the crystal structure. Residual unassigned electron density may be caused by a number of factors, including crystal degradation in the beam, twinning of the crystal, impurities in the crystal, or the incorrect space group.

Although the structure has been included, none of the data has been used in comparisons with other structures due to the inaccuracy of the data. Time did not allow for the structure to be further resolved or for data to be collected again.

Crystal data and structure refinement	
Identification code	$Ar'PCl_2$
Empirical formula	$C_{14}H_{16}Cl_4F_6P_2Pt$
Formula weight	699.11
Temperature	150(2) K
Wavelength	0.71073 Å
Crystal system	Monoclinic
Space group	$P2_1/c$
Unit cell dimensions	a = 26.8126(1) Å α = 90 °. b = 7.7868(1) Å β = 115.276(1) °. c = 23.5307(3) Å χ = 90 °.
Volume	4442.49(8) $Å^3$
Z	8
Number of reflections used	Calculation of cell = 512 Total = 19445 Unique = 7573 Obs [I>2σ(I)] = 6242
Crystal description	needle
Crystal colour	pale orange
Density (calculated)	2.091 g/cm^3
Absorption coefficient	69.89 cm^{-1}
F(000)	2656
Crystal size	0.2 x 0.1 x 0.4 mm
Theta range for data collection	0.84 to 25.67 °.
Index ranges	−28<=h<=30, −9<=k<=4, −27<=l<=24
Experiment device	Siemens SMART
Experiment methods	ω scans
Reflections collected	18715
Independent reflections	7573 [R(int) = 0.1236]
Refinement method	Full-matrix least-squares on F^2
Data / restraints / parameters	7463 / 0 / 493
Goodness-of-fit on F^2	1.275
Final R indices [I>2σ(I)]	R_1 = 0.1027, wR_2 = 0.2559
R indices (all data)	R_1 = 0.1190, wR_2 = 0.3038
Largest diff. peak and hole	3.584 and −4.282 $e.Å^{-3}$

Table 3.1 – Crystal data and structure refinement for $[PtCl_2(PEt_3)(Ar'PCl_2)]$

	x	y	z	U(eq)
Pt(2)	1554(1)	4272(1)	3995(1)	27(1)
Pt(1)	3423(1)	5150(1)	7449(1)	26(1)
P(3)	972(3)	2283(9)	3975(3)	31(1)
P(2)	3008(3)	6408(10)	6481(3)	33(2)
Cl(1)	3747(3)	3638(9)	8405(3)	37(2)
Cl(5)	1292(3)	5863(9)	4678(3)	37(2)
P(1)	4007(3)	7201(9)	7955(3)	32(2)
Cl(6)	2144(3)	6538(9)	4045(4)	43(2)
P(4)	1890(3)	2974(9)	3360(3)	31(2)
Cl(8)	395(3)	1537(11)	3113(3)	46(2)
Cl(2)	2829(3)	2839(8)	6985(3)	40(2)
Cl(4)	3699(3)	9566(9)	7950(3)	48(2)
Cl(7)	1264(3)	-86(9)	4289(4)	46(2)
Cl(3)	4553(3)	7863(11)	7596(4)	51(2)
C(13)	3262(12)	8508(39)	6361(14)	41(7)
C(27)	1749(12)	4274(37)	2678(13)	40(7)
C(9)	3010(13)	5028(43)	5866(12)	44(7)
C(28)	1144(12)	4667(41)	2285(12)	42(7)
C(14)	2971(15)	9268(41)	5716(13)	56(9)
C(25)	2637(12)	2821(44)	3759(15)	49(8)
C(23)	1649(11)	824(39)	3093(15)	43(7)
C(12)	2214(11)	8075(40)	6763(15)	46(8)
C(26)	2831(13)	1648(60)	4326(16)	71(12)
C(11)	2296(10)	6802(40)	6317(13)	41(7)
C(24)	1935(14)	-28(38)	2710(16)	47(8)
C(10)	3607(17)	4638(54)	5948(18)	71(12)
F(6)	4798(7)	4502(23)	8089(8)	46(4)
F(5)	1657(6)	2223(21)	5329(8)	42(4)
F(4)	1334(6)	39(21)	5617(9)	51(5)
F(3)	5548(8)	5897(25)	8431(9)	57(5)
F(2)	1361(7)	2473(33)	6031(8)	68(6)
C(16)	681(10)	2152(34)	5012(12)	30(6)
C(7)	5206(12)	5159(39)	8620(14)	41(7)
C(1)	4470(11)	6948(32)	8802(11)	31(6)
C(2)	5018(9)	6249(35)	9006(13)	33(6)
C(15)	522(11)	2664(37)	4390(12)	35(6)
C(22)	1291(11)	1779(42)	5510(14)	43(7)
C(20)	-29(11)	3424(40)	4068(13)	43(7)
C(6)	4336(11)	7502(37)	9269(12)	35(6)
C(4)	5285(11)	7347(39)	10054(13)	41(7)
C(5)	4734(12)	7825(37)	9889(13)	42(7)
C(3)	5425(12)	6515(41)	9618(13)	44(7)
F(12)	181(7)	5059(22)	3324(7)	45(4)
F(11)	3350(6)	7341(24)	8669(8)	47(4)
F(10)	3678(6)	9571(24)	9256(9)	52(5)
F(9)	-480(9)	5861(25)	3545(9)	66(6)
F(8)	-578(6)	3639(25)	2972(8)	54(5)
F(7)	3684(7)	7164(28)	9683(9)	59(5)
F(1)	5493(8)	3760(26)	8953(9)	61(5)

	x	y	z	U(eq)
C(17)	294(11)	2024(35)	5270(15)	38(7)
C(8)	3759(12)	7895(35)	9211(16)	44(8)
C(21)	-194(13)	4465(41)	3488(14)	46(7)
C(18)	-255(11)	2591(42)	4910(15)	43(7)
C(19)	-394(14)	3334(49)	4345(17)	57(9)

Table 3.2 – Atomic coordinates (x 10^4) and equivalent isotropic displacement parameters ($Å^2$ x 10^3) for $[PtCl_2(PEt_3)(Ar'PCl_2)]$. U(eq) is defined as one third of the trace of the orthogonalized Uij tensor.

Bond lengths [A] and angles [°]	
Pt(2)–P(3)	2.186(7)
Pt(2)–P(4)	2.282(7)
Pt(2)–Cl(6)	2.339(7)
Pt(2)–Cl(5)	2.362(7)
Pt(1)–P(1)	2.198(7)
Pt(1)–P(2)	2.284(7)
Pt(1)–Cl(2)	2.342(6)
Pt(1)–Cl(1)	2.354(6)
P(3)–C(15)	1.87(3)
P(3)–Cl(7)	2.017(10)
P(3)–Cl(8)	2.041(10)
P(2)–C(9)	1.80(3)
P(2)–C(11)	1.81(3)
P(2)–C(13)	1.84(3)
P(1)–C(1)	1.85(2)
P(1)–Cl(4)	2.016(10)
P(1)–Cl(3)	2.045(10)
P(4)–C(27)	1.80(3)
P(4)–C(23)	1.81(3)
P(4)–C(25)	1.82(3)
C(13)–C(14)	1.50(4)
C(27)–C(28)	1.52(4)
C(9)–C(10)	1.56(5)
C(25)–C(26)	1.51(5)
C(23)–C(24)	1.56(4)
C(12)–C(11)	1.53(4)
F(6)–C(7)	1.36(3)
F(5)–C(22)	1.27(3)
F(4)–C(22)	1.37(4)
F(3)–C(7)	1.31(3)
F(2)–C(22)	1.28(3)
C(16)–C(15)	1.39(4)
C(16)–C(17)	1.41(4)
C(16)–C(22)	1.58(4)
C(7)–F(1)	1.37(4)
C(7)–C(2)	1.48(4)
C(1)–C(6)	1.37(4)
C(1)–C(2)	1.44(3)
C(2)–C(3)	1.40(4)
C(15)–C(20)	1.47(4)
C(20)–C(19)	1.39(4)
C(20)–C(21)	1.48(4)
C(6)–C(5)	1.41(4)
C(6)–C(8)	1.53(4)
C(4)–C(3)	1.39(4)
C(4)–C(5)	1.41(4)
F(12)–C(21)	1.31(4)
F(11)–C(8)	1.35(4)
F(10)–C(8)	1.33(3)

Bond lengths [A] and angles [°]	
F(9)–C(21)	1.37(3)
F(8)–C(21)	1.37(3)
F(7)–C(8)	1.34(4)
C(17)–C(18)	1.42(4)
C(18)–C(19)	1.35(5)
P(3)–Pt(2)–P(4)	98.6(2)
P(3)–Pt(2)–Cl(6)	175.8(3)
P(4)–Pt(2)–Cl(6)	85.4(3)
P(3)–Pt(2)–Cl(5)	88.2(2)
P(4)–Pt(2)–Cl(5)	173.1(2)
Cl(6)–Pt(2)–Cl(5)	87.8(2)
P(1)–Pt(1)–P(2)	99.2(3)
P(1)–Pt(1)–Cl(2)	175.4(3)
P(2)–Pt(1)–Cl(2)	85.4(3)
P(1)–Pt(1)–Cl(1)	87.6(2)
P(2)–Pt(1)–Cl(1)	172.7(2)
Cl(2)–Pt(1)–Cl(1)	87.8(2)
C(15)–P(3)–Cl(7)	100.9(10)
C(15)–P(3)–Cl(8)	100.4(9)
Cl(7)–P(3)–Cl(8)	96.6(4)
C(15)–P(3)–Pt(2)	119.4(9)
Cl(7)–P(3)–Pt(2)	118.6(4)
Cl(8)–P(3)–Pt(2)	117.0(4)
C(9)–P(2)–C(11)	107.1(14)
C(9)–P(2)–C(13)	106.2(14)
C(11)–P(2)–C(13)	104.1(14)
C(9)–P(2)–Pt(1)	112.2(10)
C(11)–P(2)–Pt(1)	107.8(10)
C(13)–P(2)–Pt(1)	118.7(10)
C(1)–P(1)–Cl(4)	100.9(9)
C(1)–P(1)–Cl(3)	101.6(9)
Cl(4)–P(1)–Cl(3)	97.5(5)
C(1)–P(1)–Pt(1)	120.1(8)
Cl(4)–P(1)–Pt(1)	117.7(4)
Cl(3)–P(1)–Pt(1)	115.4(4)
C(27)–P(4)–C(23)	107.7(14)
C(27)–P(4)–C(25)	105(2)
C(23)–P(4)–C(25)	105.7(14)
C(27)–P(4)–Pt(2)	110.1(10)
C(23)–P(4)–Pt(2)	117.1(10)
C(25)–P(4)–Pt(2)	110.3(10)
C(14)–C(13)–P(2)	116(2)
C(28)–C(27)–P(4)	115(2)
C(10)–C(9)–P(2)	112(2)
C(26)–C(25)–P(4)	113(2)
C(24)–C(23)–P(4)	114(2)
C(12)–C(11)–P(2)	114(2)
C(15)–C(16)–C(17)	121(2)
C(15)–C(16)–C(22)	126(2)
C(17)–C(16)–C(22)	113(2)

Bond lengths [A] and angles [°]	
F(3)–C(7)–F(6)	105(2)
F(3)–C(7)–F(1)	104(2)
F(6)–C(7)–F(1)	105(2)
F(3)–C(7)–C(2)	115(3)
F(6)–C(7)–C(2)	115(2)
F(1)–C(7)–C(2)	111(2)
C(6)–C(1)–C(2)	116(2)
C(6)–C(1)–P(1)	123(2)
C(2)–C(1)–P(1)	121(2)
C(3)–C(2)–C(1)	121(3)
C(3)–C(2)–C(7)	113(2)
C(1)–C(2)–C(7)	125(2)
C(16)–C(15)–C(20)	117(2)
C(16)–C(15)–P(3)	122(2)
C(20)–C(15)–P(3)	122(2)
F(5)–C(22)–F(2)	113(3)
F(5)–C(22)–F(4)	108(2)
F(2)–C(22)–F(4)	106(3)
F(5)–C(22)–C(16)	114(3)
F(2)–C(22)–C(16)	109(2)
F(4)–C(22)–C(16)	107(2)
C(19)–C(20)–C(15)	120(3)
C(19)–C(20)–C(21)	118(3)
C(15)–C(20)–C(21)	122(3)
C(1)–C(6)–C(5)	123(3)
C(1)–C(6)–C(8)	127(3)
C(5)–C(6)–C(8)	110(3)
C(3)–C(4)–C(5)	120(2)
C(4)–C(5)–C(6)	119(3)
C(4)–C(3)–C(2)	119(3)
C(16)–C(17)–C(18)	119(3)
F(10)–C(8)–F(7)	105(3)
F(10)–C(8)–F(11)	107(2)
F(7)–C(8)–F(11)	107(2)
F(10)–C(8)–C(6)	112(2)
F(7)–C(8)–C(6)	110(2)
F(11)–C(8)–C(6)	114(2)
F(12)–C(21)–F(9)	106(3)
F(12)–C(21)–F(8)	107(2)
F(9)–C(21)–F(8)	103(2)
F(12)–C(21)–C(20)	120(3)
F(9)–C(21)–C(20)	108(3)
F(8)–C(21)–C(20)	112(3)
C(19)–C(18)–C(17)	120(3)
C(18)–C(19)–C(20)	122(3)

Table 3.3 – Atomic Selected bond lengths [Å] and angles [°] for $[PtCl_2(PEt_3)(Ar'PCl_2)]$

	U11	U22	U33	U23	U13	U12
Pt(2)	22(1)	27(1)	31(1)	-1(1)	9(1)	-1(1)
Pt(1)	20(1)	27(1)	30(1)	1(1)	5(1)	-1(1)
P(3)	30(3)	28(3)	33(3)	-3(3)	13(3)	-2(3)
P(2)	32(3)	35(4)	28(3)	-1(3)	8(3)	1(3)
Cl(1)	26(3)	42(4)	35(3)	6(3)	4(3)	-4(3)
Cl(5)	33(3)	34(4)	43(4)	-10(3)	16(3)	-3(3)
P(1)	28(3)	29(4)	32(3)	3(3)	6(3)	-3(3)
Cl(6)	38(4)	36(4)	57(4)	-7(3)	22(3)	-12(3)
P(4)	25(3)	34(4)	34(3)	1(3)	13(3)	0(3)
Cl(8)	34(3)	59(5)	40(4)	-16(3)	12(3)	-6(3)
Cl(2)	35(3)	23(3)	47(4)	-3(3)	5(3)	-7(3)
Cl(4)	59(5)	30(4)	43(4)	3(3)	10(3)	9(3)
Cl(7)	56(4)	33(4)	63(5)	6(3)	37(4)	7(3)
Cl(3)	34(4)	64(5)	48(4)	15(4)	13(3)	-8(4)
C(13)	39(15)	41(17)	46(16)	11(14)	20(13)	12(14)
C(27)	50(17)	32(15)	42(15)	6(13)	25(14)	4(13)
C(9)	53(18)	55(19)	17(12)	0(12)	10(12)	4(15)
C(28)	48(17)	48(18)	22(13)	10(12)	9(12)	11(14)
C(14)	71(23)	36(17)	33(16)	11(14)	-4(15)	-2(16)
C(25)	39(16)	53(20)	59(19)	-21(16)	26(15)	-2(15)
C(23)	28(14)	43(17)	55(18)	-4(14)	15(13)	5(13)
C(12)	23(13)	45(18)	63(19)	14(15)	12(13)	1(13)
C(26)	32(17)	110(34)	56(21)	7(22)	5(15)	21(20)
C(11)	23(13)	47(17)	35(14)	5(13)	-4(11)	23(13)
C(24)	54(19)	28(15)	64(20)	-11(14)	28(16)	0(14)
C(10)	90(28)	79(28)	67(23)	-15(21)	55(22)	24(24)
F(6)	44(9)	48(10)	53(10)	-6(8)	27(8)	-11(8)
F(5)	25(8)	41(9)	55(10)	9(8)	13(7)	3(7)
F(4)	27(8)	34(9)	70(12)	21(9)	0(8)	8(7)
F(3)	53(11)	56(12)	80(13)	-2(10)	47(10)	-3(9)
F(2)	40(10)	123(19)	30(9)	-6(11)	5(8)	-6(12)
C(16)	21(12)	31(14)	37(14)	1(11)	10(11)	1(11)
C(7)	33(15)	38(16)	56(18)	-9(14)	22(14)	-9(13)
C(1)	35(14)	23(13)	24(12)	-12(10)	3(11)	-14(11)
C(2)	6(10)	34(14)	49(16)	2(12)	4(10)	4(10)
C(15)	32(14)	40(16)	36(14)	-5(12)	17(12)	-5(12)
C(22)	23(13)	51(19)	47(17)	-6(15)	8(12)	2(13)
C(20)	32(14)	44(17)	40(15)	15(13)	4(12)	-21(13)
C(6)	27(13)	37(15)	33(14)	-2(12)	5(11)	2(12)
C(4)	24(14)	45(17)	33(14)	-3(13)	-8(11)	-5(12)
C(5)	45(17)	34(16)	33(14)	-3(12)	4(13)	-8(13)
C(3)	30(14)	48(18)	41(16)	16(14)	2(12)	-4(14)
F(12)	36(9)	43(10)	42(9)	6(8)	4(7)	-11(8)
F(11)	14(7)	66(12)	51(10)	-15(9)	2(7)	3(8)
F(10)	25(8)	54(11)	77(13)	-11(10)	21(8)	2(8)
F(9)	75(13)	49(11)	54(11)	5(9)	8(10)	28(11)
F(8)	28(8)	61(12)	43(9)	-11(9)	-13(7)	-9(8)
F(7)	54(11)	84(15)	57(11)	0(10)	42(9)	7(11)
F(1)	50(11)	60(12)	78(13)	16(11)	32(10)	26(10)

	U11	U22	U33	U23	U13	U12
C(17)	27(13)	31(15)	62(18)	1(13)	24(13)	7(12)
C(8)	32(15)	22(14)	80(23)	-5(14)	26(16)	5(12)
C(21)	42(17)	45(18)	45(17)	-8(14)	13(14)	8(15)
C(18)	24(13)	52(19)	60(19)	1(15)	24(13)	0(13)
C(19)	46(18)	66(23)	64(21)	-1(19)	27(17)	-3(17)

Table 3.4 – Anisotropic displacement parameters ($Å^2$ x 10^3) for $[PtCl_2(PEt_3)(Ar'PCl_2)]$. The anisotropic displacement factor exponent takes the form: $-2\pi^2 [h^2 a^{*2} U11 + 2 h k a^* b^* U12]$

	x	y	z	U(eq)
H(12A)	3234(12)	9328(39)	6667(14)	49
H(12B)	3658(12)	8391(39)	6457(14)	49
H(11A)	1951(12)	5373(37)	2815(13)	47
H(11B)	1896(12)	3681(37)	2409(13)	47
H(10A)	2822(13)	3936(43)	5870(12)	52
H(10B)	2800(13)	5586(43)	5454(12)	52
H(9A)	1103(14)	5340(224)	1915(51)	62
H(9B)	999(24)	5325(226)	2536(33)	62
H(9C)	938(18)	3589(41)	2148(79)	62
H(8A)	3120(73)	10414(139)	5711(34)	84
H(8B)	2576(21)	9357(295)	5606(49)	84
H(8C)	3026(86)	8531(173)	5411(21)	84
H(7A)	2778(12)	2386(44)	3460(15)	59
H(7B)	2793(12)	3982(44)	3896(15)	59
H(6A)	1713(11)	97(39)	3463(15)	51
H(6B)	1246(11)	863(39)	2828(15)	51
H(5A)	1824(19)	8097(206)	6683(70)	69
H(5B)	2328(83)	9223(65)	6695(70)	69
H(5C)	2438(69)	7721(157)	7199(15)	69
H(4A)	3235(13)	1651(293)	4536(81)	106
H(4B)	2699(101)	478(96)	4190(22)	106
H(4C)	2684(99)	2055(224)	4618(65)	106
H(3A)	2102(10)	7242(40)	5882(13)	49
H(3B)	2122(10)	5697(40)	6338(13)	49
H(2A)	1819(71)	-1231(87)	2625(90)	71
H(2B)	2336(14)	27(253)	2953(47)	71
H(2C)	1829(73)	585(179)	2312(48)	71
H(1A)	3591(18)	3922(308)	5599(75)	107
H(1B)	3809(42)	4028(325)	6346(68)	107
H(1C)	3796(41)	5718(58)	5952(132)	107
H(15A)	5562(11)	7591(39)	10463(13)	49
H(14A)	4631(12)	8352(37)	10188(13)	50
H(13A)	5792(12)	6134(41)	9733(13)	53
H(28A)	400(11)	1564(35)	5679(15)	46
H(25A)	-525(11)	2448(42)	5068(15)	52
H(24A)	-753(14)	3810(49)	4129(17)	69

Table 3.5 – Hydrogen coordinates (x 10^4) and isotropic displacement parameters ($Å^2$ x 10^3) for $[PtCl_2(PEt_3)(Ar'PCl_2)]$

3.2.3 Reaction between $[PtCl_2(PEt_3)]_2$ and $(C_8H_3F_6)PH_2$

$Ar'PH_2$ was added to a solution of $[PtCl_2(PEt_3)]_2$ in CH_2Cl_2 and allowed to stir. The ^{31}P NMR spectrum shows no formation of the *trans* isomer and only the formation of the *cis*–isomer. The proton decoupled ^{31}P NMR spectrum of the compound shows a new peak (δ = -79.9 ppm) which is assignable to the *cis* isomer, due to the lack of distinct P–P coupling, which would be expected in the *trans* compound. The value for the P–Pt coupling constant confirms this as being significantly larger than the coupling expected from a *trans* compound. ($^1J_{P-Pt}$ = 3834 Hz). Unfortunately due to an oversight these are the only values recorded for this compound.

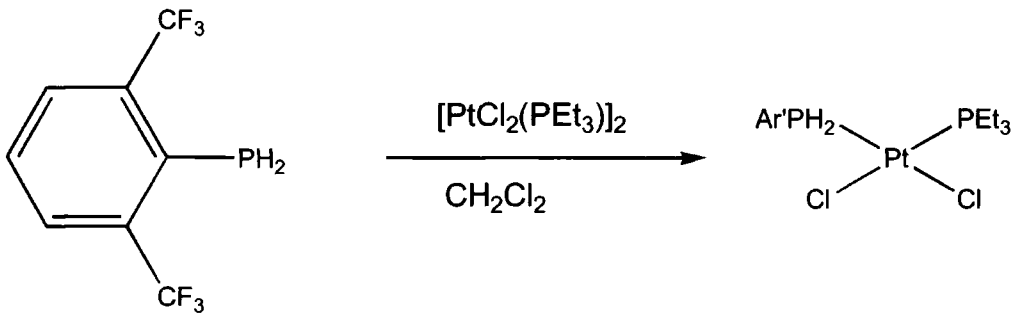

Equation 3.4 – Synthesis of *cis*–$[PtCl_2(PEt_3)(Ar'PH_2)]$

This reaction is analogous to the previous one; the main difference between the two reactions is that in this case the shift of the signals associated with the $Ar'PH_2$ phosphorus atom in the complex is at higher frequency than that of the starting material ($Ar'PH_2$). This implies that there is an overall deshielding of the phosphane which accompanies the bonding to platinum. There will also be some back donation into the LUMO on the phosphorus, although this is not as significant in this case as compared with the $Ar'PCl_2$ bonded to platinum species. (see Section 3.5). This effect means that comparatively there is less electron density associated with the phosphorus atom after bonding to the platinum, rather than before.

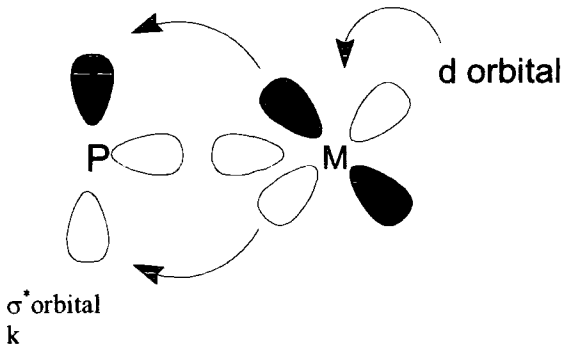

Figure 3.5 – Back donation of electron density from the metal centre to unoccupied π^* orbitals on the phosphorus atom

Another explanation for this phenomenon could be that $Ar'PH_2$ is a unique case in itself because of the nature of the two P–H bonds. $Ar'PH_2$ and $ArPH_2$ are non–volatile liquids at room temperature and for mono–substituted phosphanes they are exceptionally stable. The shielding of the phosphane is due to the comparative lack of electron density in the P–H bonds.

The product was isolated as a white powder which was recrystallised using a layering technique (see Appendix 1). The crystals were submitted for X–ray crystallographic studies and the crystal structure solved.

3.2.3.1 The molecular structure of $[PtCl_2(PEt_3)(C_8H_3F_6)PH_2]$

Crystals submitted for X–ray characterisation were mounted on a glass fibre, introduced onto the diffractometer and diffraction Data were collected. The structure was subsequently solved; the molecular structure is shown below in Figure 3.6.

Data were collected on a Siemens 3–circle diffractometer with a CCD area detector, ω scan mode $2\theta \leq 60.2°$. The structure was solved by direct methods and refined by full–matrix least squares against F^2 . Lists of crystal data and refinement parameters, anisotropic displacement parameters, bond lengths and angles, and atomic coordinates are given in Table 3.6 through Table 3.10.

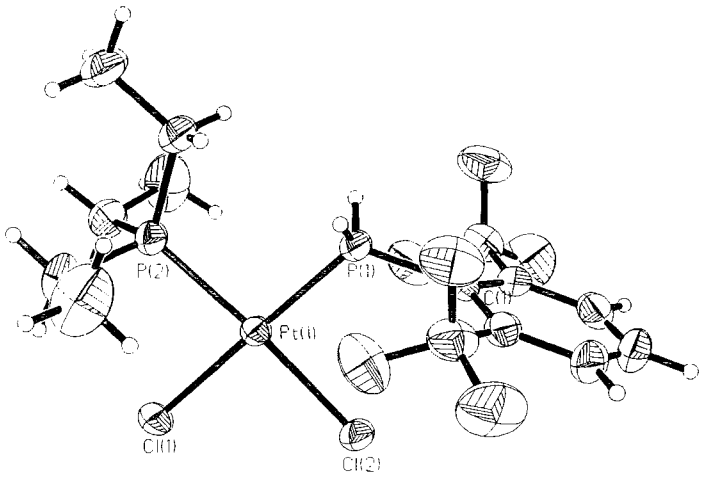

Figure 3.6 – Thermal ellipsoid diagram at 150K (50% Probability) for $[PtCl_2(PEt_3)(Ar'PH_2)]$

What is interesting to note from the structure is the lengthening of the P(1)–Pt bond and the decrease in coupling constant with respect to the $Ar'PCl_2$ case. This comparison is discussed in more detail later (see Section 3.4).

The distance between the hydrogen atoms attached to phosphorus(1) and the closest fluorine atoms on the CF_3 groups is within the range of distances that would signify an interaction and probable intramolecular hydrogen bond (H(1A)–(F4) = 2.56 Å, H(1B)–F(3) = 2.50 Å)[6].

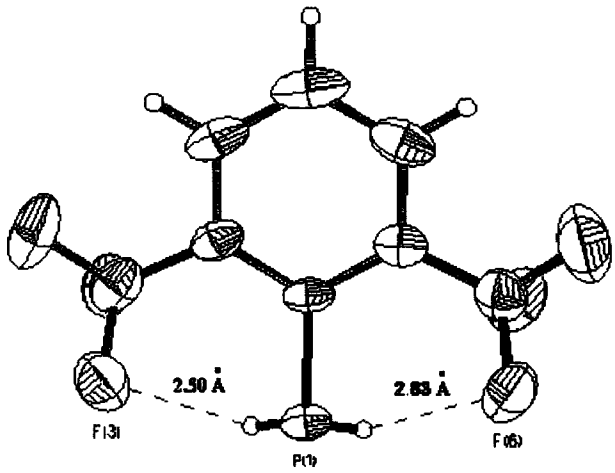

Figure 3.7 – Thermal ellipsoid diagram at 150K (50% Probability) showing the interactions between hydrogen and fluorine atoms in the molecule

These results confirm one of the hypotheses put forward regarding the lack of reaction between $Ar'PH_2$ and bases (see Section 2.3). The interactions between the hydrogens and fluorines will cause them to be less acidic and also potentially more sterically protected from attack by a nucleophile or base.

Crystal data and structural refinment	
Identification code	Ar'PH_2–Dimer
Empirical formula	$C_{14}H_{20}Cl_2F_6P_2Pt$
Formula weight	630.23
Temperature	293(2) K
Wavelength	0.71073 Å
Crystal system	Monoclinic
Space group	$P2_1/c$
Unit cell dimensions	a = 14.069(3) Å α = 90 °. b = 12.676(3) Å β = 117.20(3) °. c = 13.620(3) Å χ = 90 °.
Volume	2160.4(7) $Å^3$
Z	4
Number of reflections used	Calculation of cell = 512 Total = 9226 Unique = 3595 Obs [I>2σ(I)] = 3097
Crystal description	needle
Crystal colour	colourless
Density (calculated)	1.938 g/cm^3
Absorption coefficient	69.36 cm^{-1}
F(000)	1200
Crystal size	0.2 x 0.1 x 0.4 mm
Theta range for data collection	1.63 to 25.39 °.
Index ranges	–12<=h<=16, –15<=k<=15, –16<=l<=15
Experiment device	Siemens SMART
Experiment methods	ω scans
Reflections collected	8977
Independent reflections	3595 [R(int) = 0.0417]
Refinement method	Full-matrix least-squares on F^2
Data / restraints / parameters	3577 / 0 / 229
Goodness-of-fit on F^2	1.088
Final R indices [I>2σ(I)]	R_1 = 0.0287, wR_2 = 0.0670
R indices (all data)	R_1 = 0.0373, wR_2 = 0.0878
Largest diff. peak and hole	.679 and –1.368 e.$Å^{-3}$

Table 3.6 – Crystal data and structure refinement for $[PtCl_2(PEt_3)(Ar'PH_2)]$

	x	y	z	U(eq)
Pt(1)	2220(1)	7077(1)	1688(1)	27(1)
Cl(2)	3381(1)	7912(1)	1112(1)	36(1)
P(1)	2973(1)	7963(1)	3263(1)	33(1)
Cl(1)	1434(1)	6137(1)	16(1)	37(1)
P(2)	1106(1)	6185(1)	2155(1)	37(1)
F(1)	5438(4)	7224(4)	5340(3)	63(1)
F(2)	6419(4)	7119(4)	4517(4)	78(2)
F(6)	2066(3)	9776(4)	1845(3)	62(1)
C(1)	4071(4)	8855(5)	3474(4)	30(1)
F(4)	2427(4)	10607(4)	3335(4)	69(1)
F(5)	2773(5)	11309(4)	2118(5)	88(2)
C(2)	5139(5)	8495(6)	3957(5)	37(2)
C(4)	5770(6)	10200(8)	3812(6)	61(2)
C(5)	4741(6)	10578(6)	3325(6)	49(2)
F(3)	4775(4)	6655(4)	3683(4)	64(1)
C(14)	456(8)	5844(9)	3827(7)	87(3)
C(11)	-282(5)	6442(6)	1187(6)	47(2)
C(6)	3888(5)	9916(5)	3140(5)	36(2)
C(9)	1279(6)	4767(5)	2110(6)	48(2)
C(8)	2796(6)	10389(6)	2615(6)	49(2)
C(3)	5969(5)	9163(7)	4119(6)	49(2)
C(7)	5432(6)	7378(7)	4372(5)	48(2)
C(13)	1236(7)	6435(7)	3522(6)	64(2)
C(12)	598(7)	7596(7)	1184(11)	90(3)
C(10)	2381(7)	4379(8)	2889(9)	87(3)

Table 3.7 – Atomic coordinates (x 10^4) and equivalent isotropic displacement parameters ($Å^2$ x 10^3) for $[PtCl_2(PEt_3)(Ar'PH_2)]$. U(eq) is defined as one third of the trace of the orthogonalized Uij tensor

Bond lengths [Å] and angles [°]	
Pt(1)–P(1)	2.215(2)
Pt(1)–P(2)	2.248(2)
Pt(1)–Cl(1)	2.351(2)
Pt(1)–Cl(2)	2.361(2)
P(1)–C(1)	1.828(6)
P(2)–C(13)	1.812(7)
P(2)–C(11)	1.818(7)
P(2)–C(9)	1.819(7)
F(1)–C(7)	1.329(8)
F(2)–C(7)	1.350(8)
F(6)–C(8)	1.332(8)
C(1)–C(6)	1.405(9)
C(1)–C(2)	1.413(9)
F(4)–C(8)	1.331(8)
F(5)–C(8)	1.342(9)
C(2)–C(3)	1.376(9)
C(2)–C(7)	1.510(11)
C(4)–C(3)	1.368(12)
C(4)–C(5)	1.374(11)
C(5)–C(6)	1.389(9)
F(3)–C(7)	1.335(9)
C(14)–C(13)	1.535(10)
C(11)–C(12)	1.528(11)
C(6)–C(8)	1.493(10)
C(9)–C(10)	1.506(11)
P(1)–Pt(1)–P(2)	93.87(6)
P(1)–Pt(1)–Cl(1)	179.54(5)
P(2)–Pt(1)–Cl(1)	86.52(6)
P(1)–Pt(1)–Cl(2)	89.85(6)
P(2)–Pt(1)–Cl(2)	175.87(6)
Cl(1)–Pt(1)–Cl(2)	89.76(6)
C(1)–P(1)–Pt(1)	117.5(2)
C(13)–P(2)–C(11)	106.6(4)
C(13)–P(2)–C(9)	104.8(4)
C(11)–P(2)–C(9)	105.6(3)
C(13)–P(2)–Pt(1)	116.5(2)
C(11)–P(2)–Pt(1)	111.1(3)
C(9)–P(2)–Pt(1)	111.5(2)
C(6)–C(1)–C(2)	117.2(6)
C(6)–C(1)–P(1)	121.7(5)
C(2)–C(1)–P(1)	121.1(5)
C(3)–C(2)–C(1)	121.3(7)
C(3)–C(2)–C(7)	116.8(6)
C(1)–C(2)–C(7)	121.8(6)
C(3)–C(4)–C(5)	120.3(7)
C(4)–C(5)–C(6)	120.6(7)
C(12)–C(11)–P(2)	112.9(6)
C(5)–C(6)–C(1)	120.3(6)
C(5)–C(6)–C(8)	117.3(6)

Bond lengths [Å] and angles [°]	
C(1)–C(6)–C(8)	122.4(6)
C(10)–C(9)–P(2)	114.2(6)
F(4)–C(8)–F(6)	106.3(6)
F(4)–C(8)–F(5)	105.3(6)
F(6)–C(8)–F(5)	106.2(6)
F(4)–C(8)–C(6)	113.2(6)
F(6)–C(8)–C(6)	113.4(6)
F(5)–C(8)–C(6)	111.9(6)
C(4)–C(3)–C(2)	120.2(7)
F(1)–C(7)–F(3)	106.6(6)
F(1)–C(7)–F(2)	106.2(6)
F(3)–C(7)–F(2)	105.7(6)
F(1)–C(7)–C(2)	112.7(6)
F(3)–C(7)–C(2)	113.5(5)
F(2)–C(7)–C(2)	111.7(6)
C(14)–C(13)–P(2)	116.3(5)

Table 3.8 – Atomic Selected bond lengths [Å] and angles [°] for $[PtCl_2(PEt_3)(Ar'PH_2)]$

	U11	U22	U33	U23	U13	U12
Pt(1)	26(1)	32(1)	24(1)	-3(1)	12(1)	-4(1)
Cl(2)	37(1)	46(1)	31(1)	-4(1)	20(1)	-9(1)
P(1)	32(1)	44(1)	28(1)	-7(1)	17(1)	-12(1)
Cl(1)	39(1)	44(1)	30(1)	-12(1)	16(1)	-7(1)
P(2)	36(1)	43(1)	32(1)	-9(1)	17(1)	-13(1)
F(1)	71(3)	76(3)	36(2)	10(2)	21(2)	15(2)
F(2)	52(3)	98(4)	83(3)	4(3)	29(3)	31(3)
F(6)	47(3)	70(3)	53(2)	-13(2)	9(2)	14(2)
C(1)	30(3)	39(4)	25(3)	-12(3)	16(2)	-13(3)
F(4)	58(3)	93(4)	61(3)	-20(3)	31(2)	17(3)
F(5)	95(4)	62(3)	104(4)	30(3)	44(3)	22(3)
C(2)	29(3)	51(4)	31(3)	-10(3)	13(3)	-7(3)
C(4)	47(5)	83(7)	58(5)	-24(5)	29(4)	-34(4)
C(5)	70(5)	41(4)	49(4)	-15(3)	38(4)	-19(4)
F(3)	74(3)	47(3)	50(3)	-2(2)	12(2)	6(2)
C(14)	104(7)	124(9)	61(5)	-36(5)	62(5)	-68(7)
C(11)	34(4)	54(5)	57(4)	-8(4)	23(3)	-5(3)
C(6)	40(4)	42(4)	34(3)	-9(3)	23(3)	-8(3)
C(9)	45(4)	38(4)	58(4)	7(3)	21(3)	-7(3)
C(8)	56(5)	44(4)	48(4)	-8(4)	25(4)	1(4)
C(3)	30(4)	73(6)	39(4)	-13(4)	12(3)	-14(3)
C(7)	40(4)	68(5)	33(4)	-3(3)	13(3)	6(4)
C(13)	76(6)	81(6)	52(4)	-25(4)	45(4)	-45(5)
C(12)	54(5)	59(6)	165(11)	-13(7)	56(6)	8(5)
C(10)	70(6)	75(7)	104(7)	39(6)	29(6)	18(5)

Table 3.9 – Anisotropic displacement parameters ($Å^2$ x 10^3) for $[PtCl_2(PEt_3)(Ar'PH_2)]$. The anisotropic displacement factor exponent takes the form: $-2\pi^2 [h^2 a^{*2} U11 + 2 h k a^* b^* U12]$

	x	y	z	U(eq)
H(1A)	2420(1)	8373(1)	3325(1)	40
H(1B)	3236(1)	7455(1)	3862(1)	40
H(4)	6335(6)	10651(8)	3934(6)	73
H(5)	4614(6)	11283(6)	3118(6)	59
H(14A)	647(40)	5968(52)	4590(19)	130
H(14B)	492(45)	5102(10)	3707(61)	130
H(14C)	-257(12)	6093(43)	3375(46)	130
H(11A)	-401(5)	6250(6)	450(6)	57
H(11B)	-738(5)	6001(6)	1374(6)	57
H(9A)	764(6)	4414(5)	2286(6)	57
H(9B)	1122(6)	4569(5)	1363(6)	57
H(3)	6666(5)	8910(7)	4438(6)	59
H(13A)	1959(7)	6253(7)	4058(6)	77
H(13B)	1146(7)	7185(7)	3589(6)	77
H(12A)	-1292(30)	7715(17)	576(40)	135
H(12B)	-84(37)	8043(8)	1110(69)	135
H(12C)	-618(62)	7753(19)	1864(29)	135
H(10A)	2412(19)	3628(11)	2820(44)	130
H(10B)	2537(24)	4554(51)	3633(10)	130
H(10C)	2896(10)	4709(44)	2709(39)	130

Table 3.10 – Hydrogen coordinates (x 10^4) and isotropic displacement parameters ($Å^2$ x 10^3) for $[PtCl_2(PEt_3)(Ar'PH_2)]$

3.2.4 Reaction between $[PtCl_2(PEt_3)]_2$ and $(C_8H_3F_6)PF_2$

$Ar'PF_2$ was added to a solution of $[PtCl_2(PEt_3)]_2$ in $(CHCl_2)_2$ and the solution was allowed to stir. The ^{31}P NMR spectrum of this product is more complex than some of the other products due to the P–F couplings as well as P–Pt. It is interesting to note that in the ^{19}F NMR spectrum it is possible to observe F–Pt coupling as well as the F–P coupling for the two fluorine atoms bonded to the phosphorus atom.

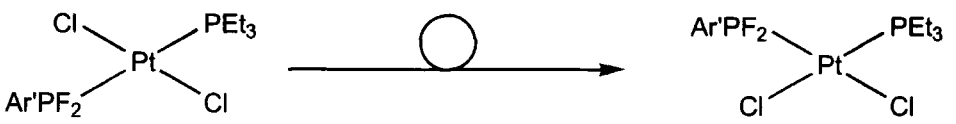

Equation 3.5 – Rearrangement of *trans*–$[PtCl_2(PEt_3)(Ar'PF_2)]$

In this case the *trans* isomer was comparatively stable for a number of hours and was characterised. The ^{31}P NMR spectrum of the compound shows the initial formation of the *trans* isomer. The peaks associated with this species form a doublet of triplets, each with its corresponding platinum satellite. The spectrum shows the species to have chemical shift values δ = 163.1 ppm ($^1J_{P-Pt}$ = 2723 Hz, $^1J_{P-F}$ = 1207.5 Hz, $^2J_{P-P}$ = 692 Hz doublet of triplets with Pt satellites) and δ = 18.75 ppm ($^1J_{P-Pt}$ = 1091.0 Hz, $^2J_{P-P}$ = 690.6 Hz, doublet with Pt satellites).

What is interesting to note from these results is that the coupling constant ($^1J_{P-Pt}$ = 2723 Hz) is at the upper end of expected values for *trans* complexes (2200–2800 Hz). This high value implies that the distance between the phosphorus atom and the platinum atom is significantly shorter than in other species discussed in this chapter. This result is confirmed by the coupling constant for the *cis* compound and the associated P–Pt bond length ascertained from X-ray crystallographic analysis.

The ^{31}P NMR spectrum of the resulting *cis* compound shows a triplet, with each of the peaks having the corresponding Pt satellites, giving the impression of a triplet of triplets. The coupling constant for this compound, as with the *trans* compound, is higher than normally observed for a *cis* compound. The signals associated with the PEt_3 groups shows a singlet with Pt satellites. The compound has chemical shift values δ = 135.6 ppm ($^1J_{P-Pt}$ = 6194.8 Hz, $^1J_{P-F}$ = 1140 Hz, $^2J_{P-P}$ = 42.6Hz) and δ = 20.51 ppm ($^1J_{P-Pt}$ = 2916.2 Hz, $^2J_{P-P}$ = 42.8 Hz).

The ^{19}F NMR spectrum shows a number of peaks corresponding to the different fluorine species in the compound, the CF_3 groups on the aryl group producing a singlet (δ = -55.8 ppm). The signal assignable to the fluorine atoms bonded directly to the phosphorus atom gives a number of peaks due to coupling to the phosphorus atom, the platinum atom and a very small coupling to the CF_3 groups. The chemical shift of the fluorine is δ = -75.7 ppm ($^1J_{P-F}$ = 1207.4 Hz) ($^2J_{F-Pt}$ = 150.6 Hz) ($^5J_{F-F}$ = 19.77 Hz).

The product was isolated as a white powder which was recrystallised using a layering technique (see Appendix 1). The crystals were submitted for X-ray crystallographic studies and the crystal structure solved.

3.2.4.1 *The molecular structure of $[PtCl_2(PEt_3)(C_8H_3F_6)PF_2]$*

Crystals submitted for X–ray characterisation were mounted on a glass fibre, introduced onto the diffractometer, and Data were collected. The structure was subsequently solved and refined; the molecular structure is shown below with a table of significant bond length within the structure.

Data were collected on a Siemens 3–circle diffractometer with a CCD area detector, ω scan mode $2\theta \leq 60.2°$. The structure was solved by direct methods and refined by full–matrix least squares against F^2 . Lists of crystal data and refinement parameters, anisotropic displacement parameters, bond lengths and angles, and atomic coordinates are given in Table 3.11 through Table 3.15.

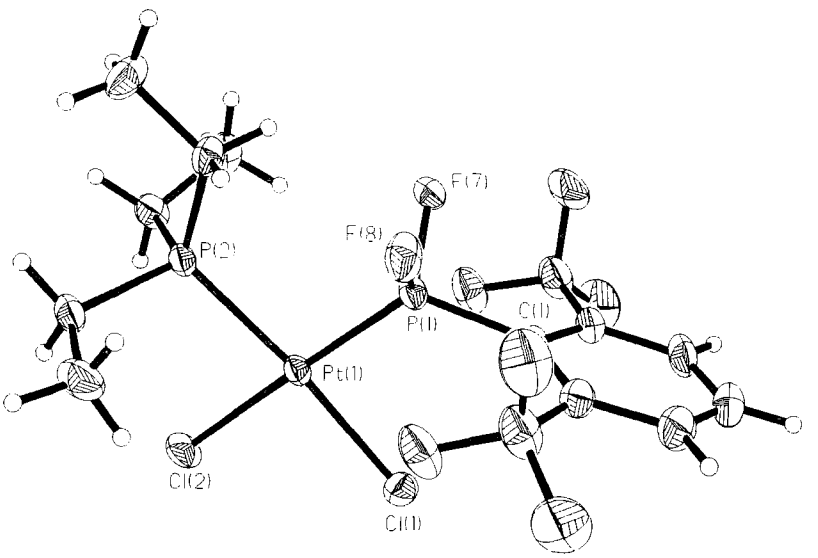

Figure 3.8 – Thermal ellipsoid diagram at 150K (50% probability) for $[PtCl_2(PEt_3)(Ar'PF_2)]$

Crystal data and structural refinement	
Identification code	Ar'PF_2–dimer
Empirical formula	$C_{14}H_{18}Cl_2F_8P_2Pt(CH_2Cl_2)$
Formula weight	751.14
Temperature	150(2) K
Wavelength	0.71073 Å
Crystal system	$P2_12_12_1$
Space group	Orthogonal
Unit cell dimensions	a = 7.3197(3) Å α = 90 °. b = 14.2513(5) Å β = 90 °. c = 23.2656(8) Å χ = 90 °.
Volume	2427.0(2) $Å^3$
Z	4
Number of reflections used	Calculation of cell = 512 Total = 17182 Unique = 6540 Obs [I>2σ(I)] = 6160
Crystal description	needle
Crystal colour	colourless
Density (calculated)	2.056 g/cm^3
Absorption coefficient	64.16 cm^{-1}
F(000)	1432
Crystal size	0.2 x 0.1 x 0.4 mm
Theta range for data collection	1.68 to 30.31 °.
Index ranges	–10<=h<=9, –11<=k<=19, –28<=l<=33
Experiment device	Siemens SMART
Experiment methods	ω scans
Reflections collected	17125
Independent reflections	6540 [R(int) = 0.0547]
Refinement method	Full–matrix least–squares on F^2
Data / restraints / parameters	6528 / 0 / 265
Goodness–of–fit on F^2	1.141
Final R indices [I>2σ(I)]	R_1 = 0.0363, wR_2 = 0.0780
R indices (all data)	R_1 = 0.0419, wR_2 = 0.0835
Absolute structure parameter	–0.007(7)
Largest diff. peak and hole	1.671 and –1.729 e.$Å^{-3}$

Table 3.11 – Crystal data and structure refinement for $[PtCl_2(PEt_3)(Ar'PF_2)]$

	x	y	z	U(eq)
Pt(1)	-16130(1)	4602(1)	-3975(1)	19(1)
Cl(1)	-13633(2)	4871(1)	-3354(1)	28(1)
P(2)	-18451(2)	4195(1)	-4575(1)	21(1)
P(1)	-17044(2)	6019(1)	-3824(1)	23(1)
F(8)	-19020(6)	6149(3)	-3593(2)	35(1)
F(7)	-17270(7)	6638(3)	-4372(2)	33(1)
C(1)	-15766(10)	6818(4)	-3352(3)	25(1)
C(9)	-20363(9)	4993(5)	-4637(3)	26(1)
C(11)	-17585(11)	4028(5)	-5306(3)	28(2)
F(6)	-13754(8)	6482(3)	-4417(2)	40(1)
F(5)	-14575(8)	7922(3)	-4529(2)	45(1)
C(6)	-16180(13)	6896(5)	-2768(3)	31(1)
C(7)	-13631(13)	7341(5)	-4186(3)	38(2)
C(2)	-14339(10)	7381(5)	-3571(3)	27(1)
F(4)	-11884(8)	7595(4)	-4215(2)	54(1)
C(13)	-19447(11)	3071(5)	-4370(3)	29(2)
C(10)	-21815(10)	4710(6)	-5076(3)	38(2)
C(5)	-15332(13)	7561(6)	-2428(3)	39(2)
C(4)	-13992(14)	8137(5)	-2646(3)	42(2)
C(3)	-13475(12)	8034(5)	-3218(3)	37(2)
C(12)	-17022(12)	4940(6)	-5602(3)	36(2)
F(3)	-17668(7)	5410(3)	-2672(2)	42(1)
F(2)	-19280(7)	6655(4)	-2489(2)	51(1)
F(1)	-17189(9)	6210(4)	-1904(2)	57(2)
C(8)	-17610(13)	6300(6)	-2468(4)	40(2)
Cl(2)	-14990(3)	3093(1)	-4142(1)	32(1)
C(14)	-19983(12)	3018(6)	-3741(4)	39(2)
C(15)	-12178(25)	4835(12)	-1956(7)	110(5)
Cl(3)	-11572(6)	3883(3)	-1473(2)	60
Cl(3')	-11241(20)	3956(8)	-1713(7)	60
Cl(4)	-12499(6)	5904(3)	-1592(2)	60
Cl(4')	-13249(20)	5631(10)	-1719(6)	60

Table 3.12 – Atomic coordinates (x 10^4) and equivalent isotropic displacement parameters ($Å^2$ x 10^3) for $[PtCl_2(PEt_3)(Ar'PF_2)]$.U(eq) is defined as one third of the trace of the orthogonalized Uij tensor.

Bond lengths [Å] and angles [°]	
Pt(1)–P(1)	2.157(2)
Pt(1)–P(2)	2.275(2)
Pt(1)–Cl(2)	2.339(2)
Pt(1)–Cl(1)	2.360(2)
P(2)–C(9)	1.809(7)
P(2)–C(13)	1.824(7)
P(2)–C(11)	1.830(7)
P(1)–F(8)	1.554(5)
P(1)–F(7)	1.558(4)
P(1)–C(1)	1.838(6)
C(1)–C(6)	1.396(9)
C(1)–C(2)	1.413(10)
C(9)–C(10)	1.529(9)
C(11)–C(12)	1.528(10)
F(6)–C(7)	1.339(8)
F(5)–C(7)	1.341(9)
C(6)–C(5)	1.382(11)
C(6)–C(8)	1.518(12)
C(7)–F(4)	1.331(10)
C(7)–C(2)	1.523(10)
C(2)–C(3)	1.394(10)
C(13)–C(14)	1.518(11)
C(5)–C(4)	1.376(13)
C(4)–C(3)	1.390(11)
F(3)–C(8)	1.356(9)
F(2)–C(8)	1.324(11)
F(1)–C(8)	1.353(10)
C(15)–Cl(4')	1.49(2)
C(15)–Cl(3')	1.54(2)
C(15)–Cl(4)	1.76(2)
C(15)–Cl(3)	1.82(2)
P(1)–Pt(1)–P(2)	96.11(6)
P(1)–Pt(1)–Cl(2)	177.13(7)
P(2)–Pt(1)–Cl(2)	86.00(6)
P(1)–Pt(1)–Cl(1)	89.35(6)
P(2)–Pt(1)–Cl(1)	174.51(6)
Cl(2)–Pt(1)–Cl(1)	88.57(6)
C(9)–P(2)–C(13)	105.3(3)
C(9)–P(2)–C(11)	106.0(3)
C(13)–P(2)–C(11)	105.5(3)
C(9)–P(2)–Pt(1)	117.8(2)
C(13)–P(2)–Pt(1)	111.2(2)
C(11)–P(2)–Pt(1)	110.2(3)
F(8)–P(1)–F(7)	96.7(3)
F(8)–P(1)–C(1)	101.2(3)
F(7)–P(1)–C(1)	101.1(3)
F(8)–P(1)–Pt(1)	117.1(2)
F(7)–P(1)–Pt(1)	115.5(2)
C(1)–P(1)–Pt(1)	121.3(2)

Bond lengths [Å] and angles [°]	
C(6)–C(1)–C(2)	117.8(6)
C(6)–C(1)–P(1)	121.4(6)
C(2)–C(1)–P(1)	120.8(5)
C(10)–C(9)–P(2)	115.1(5)
C(12)–C(11)–P(2)	113.7(5)
C(5)–C(6)–C(1)	120.9(8)
C(5)–C(6)–C(8)	115.5(7)
C(1)–C(6)–C(8)	123.6(7)
F(4)–C(7)–F(6)	107.0(7)
F(4)–C(7)–F(5)	107.3(6)
F(6)–C(7)–F(5)	106.9(6)
F(4)–C(7)–C(2)	111.3(7)
F(6)–C(7)–C(2)	112.9(6)
F(5)–C(7)–C(2)	111.1(7)
C(3)–C(2)–C(1)	120.2(7)
C(3)–C(2)–C(7)	115.1(6)
C(1)–C(2)–C(7)	124.7(6)
C(14)–C(13)–P(2)	113.5(6)
C(4)–C(5)–C(6)	121.3(7)
C(5)–C(4)–C(3)	118.9(7)
C(4)–C(3)–C(2)	120.7(8)
F(2)–C(8)–F(1)	106.5(7)
F(2)–C(8)–F(3)	108.4(7)
F(1)–C(8)–F(3)	105.0(7)
F(2)–C(8)–C(6)	113.9(7)
F(1)–C(8)–C(6)	110.0(7)
F(3)–C(8)–C(6)	112.5(6)
Cl(4')–C(15)–Cl(3')	136.0(2)
Cl(4)–C(15)–Cl(3)	112.4(9)

Table 3.13 – Atomic Selected bond lengths [Å] and angles [°] for $[PtCl_2(PEt_3)(Ar'PF_2)]$

	U11	U22	U33	U23	U13	U12
Pt(1)	26(1)	14(1)	18(1)	-1(1)	1(1)	1(1)
Cl(1)	31(1)	27(1)	27(1)	-2(1)	-3(1)	3(1)
P(2)	29(1)	15(1)	18(1)	-1(1)	0(1)	-2(1)
P(1)	29(1)	16(1)	23(1)	-3(1)	-1(1)	2(1)
F(8)	31(2)	31(2)	43(2)	-15(2)	2(2)	3(2)
F(7)	53(3)	18(2)	27(2)	2(2)	-12(2)	1(2)
C(1)	39(4)	13(3)	23(3)	-2(2)	-6(3)	-2(3)
C(9)	27(3)	26(3)	26(3)	8(3)	0(3)	-1(3)
C(11)	43(4)	22(3)	19(3)	-3(3)	3(3)	4(3)
F(6)	62(3)	25(2)	33(2)	-3(2)	15(2)	-2(2)
F(5)	74(4)	26(2)	35(2)	15(2)	2(2)	-5(2)
C(6)	42(4)	25(3)	25(3)	-5(2)	-2(3)	3(3)
C(7)	50(5)	24(3)	39(4)	1(3)	5(4)	-5(3)
C(2)	31(4)	20(3)	31(3)	-1(3)	-3(3)	-4(3)
F(4)	51(3)	54(3)	57(3)	2(3)	16(3)	-15(3)
C(13)	40(4)	19(3)	30(3)	3(3)	-2(3)	-7(3)
C(10)	36(4)	46(5)	32(3)	-15(4)	-10(3)	1(4)
C(5)	58(5)	33(4)	25(4)	-7(3)	0(3)	3(4)
C(4)	61(5)	27(3)	37(4)	-7(3)	-9(4)	-6(4)
C(3)	56(5)	19(3)	37(4)	-2(3)	-3(3)	-11(3)
C(12)	46(5)	34(4)	27(3)	-2(3)	4(3)	-9(3)
F(3)	61(3)	25(2)	41(2)	1(2)	18(2)	-4(2)
F(2)	52(3)	49(3)	52(3)	-16(2)	22(2)	7(2)
F(1)	85(4)	56(3)	29(2)	6(2)	17(3)	-2(3)
C(8)	56(5)	29(4)	35(4)	-3(3)	16(4)	-2(4)
Cl(2)	45(1)	18(1)	32(1)	-3(1)	-1(1)	9(1)
C(14)	40(5)	35(4)	43(4)	18(4)	2(4)	-4(4)

Table 3.14 – Anisotropic displacement parameters ($Å^2$ x 10^3) for $[PtCl_2(PEt_3)(Ar'PF_2)]$. The anisotropic displacement factor exponent takes the form: $-2\pi^2 [h^2 a^{*2} U11 + 2 h k a^* b^* U12]$

	x	y	z	U(eq)
H(9A)	-20942(9)	5047(5)	-4263(3)	31
H(9B)	-19900(9)	5608(5)	-4739(3)	31
H(11A)	-16538(11)	3612(5)	-5292(3)	34
H(11B)	-18522(11)	3725(5)	-5535(3)	34
H(13A)	-20521(11)	2957(5)	-4604(3)	35
H(13B)	-18573(11)	2577(5)	-4452(3)	35
H(10A)	-22705(49)	5202(21)	-5110(20)	57
H(10B)	-22405(61)	4143(26)	-4952(14)	57
H(10C)	-21246(16)	4607(44)	-5443(7)	57
H(5)	-15675(13)	7621(6)	-2045(3)	47
H(4)	-13440(14)	8588(5)	-2415(3)	50
H(3)	-12542(12)	8406(5)	-3366(3)	45
H(12A)	-16447(70)	4799(6)	-5963(12)	54
H(12B)	-16181(61)	5276(20)	-5362(11)	54
H(12C)	-18085(15)	5320(18)	-5669(22)	54
H(14A)	-18905(13)	3041(44)	-3507(4)	59
H(14B)	-20623(76)	2442(21)	-3670(7)	59
H(14C)	-20762(71)	3539(25)	-3648(8)	59
H(15A)	-11219(25)	4911(12)	-2239(7)	132
H(15B)	-13294(25)	4673(12)	-2158(7)	132

Table 3.15 – Hydrogen coordinates (x 10^4) and isotropic displacement parameters ($Å^2$ x 10^3) for $[PtCl_2(PEt_3)(Ar'PF_2)]$

3.2.5 Reaction between $[PtCl_2(PEt_3)]_2$ and $(C_8H_3F_6)P{=}CCl_2$

Ar'P=CCl_2 was added to a solution of $[PtCl_2(PEt_3)]_2$ in $(CHCl_2)_2$ and the solution was allowed to stir. The time period over which the *trans* isomer is visible in this reaction is fairly short and rearrangement is complete within five minutes. This was visible in the ^{31}P NMR spectrum only by performing an NMR scale reaction and then running a spectrum immediately. The phosphaalkene and platinum starting material are both consumed within 30 minutes and the *cis* isomer is the sole product visible in the NMR spectrum.

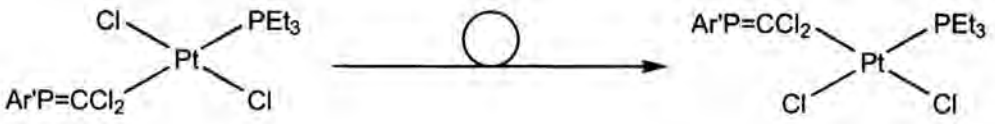

Equation 3.6 – Re-arrangement of *trans*-$[PtCl_2(PEt_3)(Ar'P{=}CCl_2)]$

The ^{31}P NMR spectrum of this product shows a doublet with Pt satellites, which signifies the formation of the *trans* isomer. This is not present in large yields and at the time it was not possible to determine an accurate value for the P-Pt coupling constant. It is possible to ascertain an approximate value from the spectrum. The *trans* species has a chemical shift value δ = 184.5 ppm ($^1J_{P-Pt} \approx 2400$ Hz) ($^2J_{P-P}$ = 580.2 Hz).

The ^{31}P NMR spectrum also shows a number of peaks assignable to the PEt_3 groups *trans* to the phosphane in question. Again, unfortunately these peaks are small and the coupling constants are impossible to determine accurately. Approximate values for the coupling constants were, however, determined manually δ = 18.3 ppm ($^1J_{P-Pt} \approx 2900$ Hz) ($^2J_{P-P}$ = 579.9 Hz).

After a short period of time, the ^{31}P NMR spectrum shows two singlets with associated Pt satellites, assigned to the *cis* species. There is a small amount of coupling visible between the *cis* phosphorus species although it is very small as compared with the *trans* isomer. The chemical shift values for the *cis* compound are δ = 155.3 ppm ($^{1}J_{P-Pt}$ = 3143 Hz, $^{2}J_{P-P}$ = 19.2 Hz) (doublet with Pt satellites) and δ = 12.9 Hz ($^{1}J_{P-Pt}$ = 3030 Hz, $^{2}J_{P-P}$ = 19.8 Hz) (doublet with Pt satellites). The ^{19}F spectrum shows a singlet with chemical shift value δ = -57.1 ppm.

The product was isolated as a white powder which was recrystallised using a layering technique (see Appendix 1). The crystals were submitted for X-ray crystallographic studies and the crystal structure solved.

3.2.5.1 The molecular structure of $[PtCl_2(PEt_3)(C_8H_3F_6)P{=}CCl_2]$

Crystals submitted for X-ray characterisation were mounted on a glass fibre, introduced onto the diffractometer, and Data were collected. The structure was subsequently solved and refined; the molecular structure is shown below in Figure 3.9.

Data were collected on a Siemens 3-circle diffractometer with a CCD area detector, ω scan mode $2\theta \leq 60.2°$. The structure was solved by direct methods and refined by full-matrix least squares against F^2 . Lists of crystal data and refinement parameters, anisotropic displacement parameters, bond lengths and angles, and atomic coordinates are given in Table 3.16 through Table 3.21.

The solid state X-ray crystal structure of this compound reveals that the angle between the P=C bond and the aryl ring is 68.7°. This is far from ideal, and the most significant factor may be the steric interactions with the CF_3 groups *cis* to the phosphorus. The angle between the square planar platinum ($PtCl_2(PEt_3)$) and the plane of the aryl ring is only 13.1°.

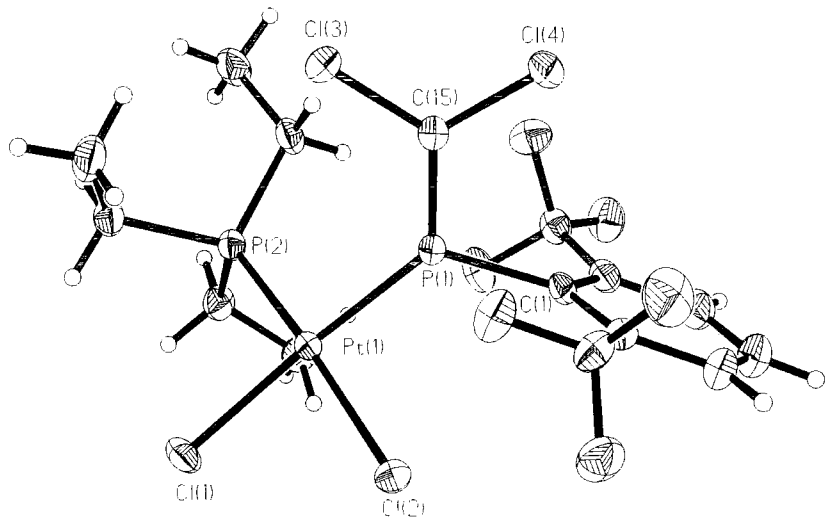

Figure 3.9 – Thermal ellipsoid diagram at 150K (50% probability) for $[PtCl_2(PEt_3)(Ar'P{=}CCl_2)]$

Crystals data and structure refinement	
Identification code	Ar'P=CCl_2–dimer
Empirical formula	$C_{15}H_{18}Cl_4F_8P_2Pt$
Formula weight	711.12
Temperature	150(2) K
Wavelength	0.71073 Å
Crystal system	Monoclinic
Space group	$P2_1/n$
Unit cell dimensions	a = 8.0329(1) Å α = 90 °. b = 20.2638(3) Å β = 94.728(2) °. c = 13.7371(2) Å χ = 90 °.
Volume	2228.48(5) $Å^3$
Z	4
Number of reflections used	Calculation of cell = 512 Total = 13434 Unique = 4235 Obs [I>2σ(I)] = 3760
Crystal description	needle
Crystal colour	pale
Density (calculated)	2.120 g/cm^3
Absorption coefficient	69.69 cm^{-1}
F(000)	1352
Crystal size	0.28 x 0.09 x 0.09 mm
Theta range for data collection	1.80 to 27.98 °.
Index ranges	–9<=h<=9, –23<=k<=22, –15<=l<=17
Experiment device	Siemens SMART
Experiment methods	ω scans
Reflections collected	13167
Independent reflections	4235 [R(int) = 0.0449]
Refinement method	Full–matrix least–squares on F^2
Data / restraints / parameters	4227 / 0 / 256
Goodness–of–fit on F^2	1.074
Final R indices [I>2σ(I)]	R_1 = 0.0271, wR_2 = 0.0567
R indices (all data)	R_1 = 0.0343, wR_2 = 0.0621
Largest diff. peak and hole	.692 and –1.025 e.$Å^{-3}$

Table 3.16 – Crystal data and structure refinement for [$PtCl_2(PEt_3)$(Ar'P=CCl_2)]

	x	y	z	U(eq)
Pt(1)	5303(1)	3031(1)	7739(1)	18(1)
Cl(1)	4459(2)	1973(1)	7264(1)	31(1)
P(1)	6334(1)	4025(1)	8056(1)	18(1)
Cl(3)	8538(2)	3761(1)	9856(1)	27(1)
Cl(2)	6151(2)	3219(1)	6155(1)	27(1)
Cl(4)	8526(2)	5068(1)	8994(1)	30(1)
P(2)	4151(2)	2805(1)	9158(1)	20(1)
F(1)	9176(4)	4115(2)	6947(2)	33(1)
F(5)	2140(4)	5464(2)	8109(2)	36(1)
F(6)	2656(4)	4422(2)	8074(2)	35(1)
F(4)	4203(4)	5068(2)	9019(2)	33(1)
F(3)	8710(4)	4376(2)	5429(2)	37(1)
F(2)	9886(4)	5073(2)	6449(2)	43(1)
C(1)	5956(6)	4741(2)	7239(3)	19(1)
C(2)	7004(6)	4913(2)	6518(3)	22(1)
C(8)	8673(6)	4609(3)	6347(3)	28(1)
C(3)	6590(7)	5434(3)	5876(4)	32(1)
C(4)	5138(7)	5795(3)	5947(4)	36(1)
C(5)	4116(7)	5646(3)	6673(4)	32(1)
C(6)	4505(6)	5129(2)	7321(3)	23(1)
C(7)	3375(6)	5022(2)	8123(3)	24(1)
C(9)	5056(6)	2084(2)	9792(4)	27(1)
C(10)	6912(7)	2133(3)	10129(4)	35(1)
C(11)	1974(6)	2567(3)	8904(3)	26(1)
C(12)	947(7)	2986(3)	8140(4)	31(1)
C(13)	4130(6)	3480(2)	10029(3)	26(1)
C(14)	3687(8)	3298(3)	11058(4)	38(1)
C(15)	7749(6)	4275(2)	8942(3)	21(1)

Table 3.17 – Atomic coordinates (x 10^4) and equivalent isotropic displacement parameters ($Å^2$ x 10^3) for $[PtCl_2(PEt_3)(Ar'P{=}CCl_2)]$.U(eq) is defined as one third of the trace of the orthogonalized Uij tensor.

Selected Bond lengths [Å] and angles [°]	
Pt(1)–P(1)	2.2082(12)
Pt(1)–P(2)	2.2735(11)
Pt(1)–Cl(1)	2.3257(12)
Pt(1)–Cl(2)	2.3632(11)
P(1)–C(15)	1.673(5)
P(1)–C(1)	1.844(5)
Cl(3)–C(15)	1.712(5)
Cl(4)–C(15)	1.723(5)
P(1)–Pt(1)–P(2)	100.76(4)
P(1)–Pt(1)–Cl(1)	172.98(4)
P(2)–Pt(1)–Cl(1)	85.69(4)
P(1)–Pt(1)–Cl(2)	84.43(4)
P(2)–Pt(1)–Cl(2)	172.22(4)
Cl(1)–Pt(1)–Cl(2)	89.44(4)
C(15)–P(1)–C(1)	105.8(2)
C(15)–P(1)–Pt(1)	129.9(2)
C(1)–P(1)–Pt(1)	123.9(2)

Table 3.18 – Atomic Selected bond lengths [Å] and angles [°] for $[PtCl_2(PEt_3)(Ar'P{=}CCl_2)]$

Bond lengths [Å] and angles [°]	
Pt(1)–P(1)	2.2082(12)
Pt(1)–P(2)	2.2735(11)
Pt(1)–Cl(1)	2.3257(12)
Pt(1)–Cl(2)	2.3632(11)
P(1)–C(15)	1.673(5)
P(1)–C(1)	1.844(5)
Cl(3)–C(15)	1.712(5)
Cl(4)–C(15)	1.723(5)
P(2)–C(13)	1.818(5)
P(2)–C(11)	1.820(5)
P(2)–C(9)	1.821(5)
F(1)–C(8)	1.337(6)
F(5)–C(7)	1.335(5)
F(6)–C(7)	1.346(6)
F(4)–C(7)	1.353(5)
F(3)–C(8)	1.349(6)
F(2)–C(8)	1.353(6)
C(1)–C(2)	1.396(6)
C(1)–C(6)	1.418(7)
C(2)–C(3)	1.398(7)
C(2)–C(8)	1.512(7)
C(3)–C(4)	1.386(8)
C(3)–H(3)	.93
C(4)–C(5)	1.377(8)
C(4)–H(4)	.93
C(5)–C(6)	1.393(7)
C(5)–H(5)	.93
C(6)–C(7)	1.501(7)
C(9)–C(10)	1.527(7)
C(9)–H(9A)	.97
C(9)–H(9B)	.97
C(10)–H(10A)	.96
C(10)–H(10B)	.96
C(10)–H(10C)	.96
C(11)–C(12)	1.537(7)
C(11)–H(11A)	.97
C(11)–H(11B)	.97
C(12)–H(12A)	.96
C(12)–H(12B)	.96
C(12)–H(12C)	.96
C(13)–C(14)	1.532(6)
C(13)–H(13A)	.97
C(13)–H(13B)	.97
C(14)–H(14A)	.96
C(14)–H(14B)	.96
C(14)–H(14C)	.96
P(1)–Pt(1)–P(2)	100.76(4)
P(1)–Pt(1)–Cl(1)	172.98(4)
P(2)–Pt(1)–Cl(1)	85.69(4)

Bond lengths [Å] and angles [°]	
P(1)–Pt(1)–Cl(2)	84.43(4)
P(2)–Pt(1)–Cl(2)	172.22(4)
Cl(1)–Pt(1)–Cl(2)	89.44(4)
C(15)–P(1)–C(1)	105.8(2)
C(15)–P(1)–Pt(1)	129.9(2)
C(1)–P(1)–Pt(1)	123.9(2)
C(13)–P(2)–C(11)	105.4(2)
C(13)–P(2)–C(9)	108.3(2)
C(11)–P(2)–C(9)	102.6(2)
C(13)–P(2)–Pt(1)	116.1(2)
C(11)–P(2)–Pt(1)	110.0(2)
C(9)–P(2)–Pt(1)	113.4(2)
C(2)–C(1)–C(6)	117.7(4)
C(2)–C(1)–P(1)	123.3(4)
C(6)–C(1)–P(1)	118.9(3)
C(1)–C(2)–C(3)	120.7(4)
C(1)–C(2)–C(8)	127.1(4)
C(3)–C(2)–C(8)	112.2(4)
F(1)–C(8)–F(3)	106.6(4)
F(1)–C(8)–F(2)	106.1(4)
F(3)–C(8)–F(2)	105.6(4)
F(1)–C(8)–C(2)	115.9(4)
F(3)–C(8)–C(2)	112.1(4)
F(2)–C(8)–C(2)	109.9(4)
C(4)–C(3)–C(2)	120.7(5)
C(4)–C(3)–H(3)	119.6(3)
C(2)–C(3)–H(3)	119.6(3)
C(5)–C(4)–C(3)	119.4(5)
C(5)–C(4)–H(4)	120.3(3)
C(3)–C(4)–H(4)	120.3(3)
C(4)–C(5)–C(6)	120.8(5)
C(4)–C(5)–H(5)	119.6(3)
C(6)–C(5)–H(5)	119.6(3)
C(5)–C(6)–C(1)	120.6(4)
C(5)–C(6)–C(7)	117.5(4)
C(1)–C(6)–C(7)	121.9(4)
F(5)–C(7)–F(6)	106.9(4)
F(5)–C(7)–F(4)	106.0(4)
F(6)–C(7)–F(4)	106.6(4)
F(5)–C(7)–C(6)	112.7(4)
F(6)–C(7)–C(6)	112.1(4)
F(4)–C(7)–C(6)	112.1(4)
C(10)–C(9)–P(2)	115.8(4)
C(10)–C(9)–H(9A)	108.3(3)
P(2)–C(9)–H(9A)	108.3(2)
C(10)–C(9)–H(9B)	108.3(3)
P(2)–C(9)–H(9B)	108.3(2)
H(9A)–C(9)–H(9B)	107.4
C(9)–C(10)–H(10A)	109.5(3)
C(9)–C(10)–H(10B)	109.5(3)

Bond lengths [Å] and angles [°]	
H(10A)–C(10)–H(10B)	109.5
C(9)–C(10)–H(10C)	109.5(3)
H(10A)–C(10)–H(10C)	109.5
H(10B)–C(10)–H(10C)	109.5
C(12)–C(11)–P(2)	115.9(3)
C(12)–C(11)–H(11A)	108.3(3)
P(2)–C(11)–H(11A)	108.3(2)
C(12)–C(11)–H(11B)	108.3(3)
P(2)–C(11)–H(11B)	108.3(2)
H(11A)–C(11)–H(11B)	107.4
C(11)–C(12)–H(12A)	109.5(3)
C(11)–C(12)–H(12B)	109.5(3)
H(12A)–C(12)–H(12B)	109.5
C(11)–C(12)–H(12C)	109.5(3)
H(12A)–C(12)–H(12C)	109.5
H(12B)–C(12)–H(12C)	109.5
C(14)–C(13)–P(2)	116.2(4)
C(14)–C(13)–H(13A)	108.2(3)
P(2)–C(13)–H(13A)	108.2(2)
C(14)–C(13)–H(13B)	108.2(3)
P(2)–C(13)–H(13B)	108.2(2)
H(13A)–C(13)–H(13B)	107.4
C(13)–C(14)–H(14A)	109.5(3)
C(13)–C(14)–H(14B)	109.5(3)
H(14A)–C(14)–H(14B)	109.5
C(13)–C(14)–H(14C)	109.5(3)
H(14A)–C(14)–H(14C)	109.5
H(14B)–C(14)–H(14C)	109.5
P(1)–C(15)–Cl(3)	122.5(3)
P(1)–C(15)–Cl(4)	122.3(3)
Cl(3)–C(15)–Cl(4)	115.2(3)

Table 3.19 –Bond lengths [Å] and angles [°] for $[PtCl_2(PEt_3)(Ar'P{=}CCl_2)]$

	U11	U22	U33	U23	U13	U12
Pt(1)	22(1)	15(1)	16(1)	-1(1)	1(1)	0(1)
Cl(1)	46(1)	18(1)	30(1)	-6(1)	6(1)	-7(1)
P(1)	21(1)	15(1)	18(1)	2(1)	0(1)	-1(1)
Cl(3)	31(1)	26(1)	22(1)	3(1)	-5(1)	2(1)
Cl(2)	37(1)	25(1)	18(1)	0(1)	6(1)	0(1)
Cl(4)	34(1)	22(1)	31(1)	0(1)	-6(1)	-9(1)
P(2)	24(1)	17(1)	20(1)	1(1)	3(1)	-1(1)
F(1)	30(2)	37(2)	33(2)	11(1)	8(1)	7(1)
F(5)	32(2)	32(2)	43(2)	4(1)	7(1)	10(1)
F(6)	33(2)	23(2)	50(2)	1(1)	8(1)	-7(1)
F(4)	33(2)	41(2)	26(1)	-3(1)	2(1)	3(1)
F(3)	46(2)	40(2)	27(2)	1(1)	11(1)	7(2)
F(2)	31(2)	46(2)	53(2)	5(2)	7(1)	-14(2)
C(1)	21(2)	14(2)	22(2)	0(2)	0(2)	-5(2)
C(2)	28(3)	19(3)	18(2)	0(2)	2(2)	0(2)
C(8)	29(3)	34(3)	21(2)	6(2)	4(2)	-1(2)
C(3)	42(3)	27(3)	26(2)	7(2)	3(2)	-3(2)
C(4)	44(3)	29(3)	33(3)	9(2)	-1(2)	2(3)
C(5)	33(3)	26(3)	36(3)	2(2)	-6(2)	3(2)
C(6)	26(3)	19(3)	25(2)	-2(2)	3(2)	-2(2)
C(7)	20(2)	21(3)	31(2)	0(2)	-2(2)	2(2)
C(9)	33(3)	21(3)	28(2)	2(2)	3(2)	5(2)
C(10)	39(3)	28(3)	38(3)	9(2)	-4(2)	4(2)
C(11)	27(3)	25(3)	28(2)	4(2)	2(2)	-6(2)
C(12)	28(3)	34(3)	30(2)	2(2)	3(2)	0(2)
C(13)	33(3)	17(3)	28(2)	0(2)	8(2)	-4(2)
C(14)	67(4)	24(3)	26(3)	-5(2)	16(3)	-1(3)
C(15)	25(2)	18(3)	21(2)	1(2)	0(2)	1(2)

Table 3.20 – Anisotropic displacement parameters ($Å^2$ x 10^3) for $[PtCl_2(PEt_3)(Ar'P{=}CCl_2)]$. The anisotropic displacement factor exponent takes the form: $-2\pi^2 [h^2 a^{*2} U11 + 2 h k a^* b^* U12]$

	x	y	z	U(eq)
H(3)	7297(7)	5541(3)	5396(4)	38
H(4)	4857(7)	6134(3)	5507(4)	43
H(5)	3154(7)	5893(3)	6731(4)	38
H(9A)	4444(6)	2001(2)	10360(4)	32
H(9B)	4893(6)	1706(2)	9363(4)	32
H(10A)	7273(13)	1729(7)	10446(25)	53
H(10B)	7090(9)	2493(12)	10579(21)	53
H(10C)	7540(8)	2206(19)	9574(5)	53
H(11A)	1939(6)	2112(3)	8686(3)	32
H(11B)	1436(6)	2585(3)	9511(3)	32
H(12A)	-189(12)	2834(11)	8080(19)	46
H(12B)	1412(28)	2947(14)	7521(7)	46
H(12C)	976(37)	3440(4)	8341(13)	46
H(13A)	5225(6)	3685(2)	10081(3)	31
H(13B)	3336(6)	3808(2)	9766(3)	31
H(14A)	3700(48)	3689(4)	11455(9)	57
H(14B)	4490(28)	2988(15)	11342(11)	57
H(14C)	2594(21)	3104(18)	11024(5)	57

Table 3.21 – Hydrogen coordinates (x 10^4) and isotropic displacement parameters (Å^2 x 10^3) for $[PtCl_2(PEt_3)(Ar'P{=}CCl_2)]$

3.2.6 Reaction between $[PtCl_2(PEt_3)]_2$ and $(C_8H_3F_6)_2PCl$

Ar'Ar''PCl was added to a solution of $[PtCl_2(PEt_3)]_2$ in $(CHCl_2)_2$ and the solution was allowed to stir. This reaction shows a distinct difference to the previous ones in that the *trans* isomer did not rearrange over time. This is probably due to the steric bulk of the phosphane itself which inhibits the formation of the *cis* isomer, due to interaction with the PEt_3 group.

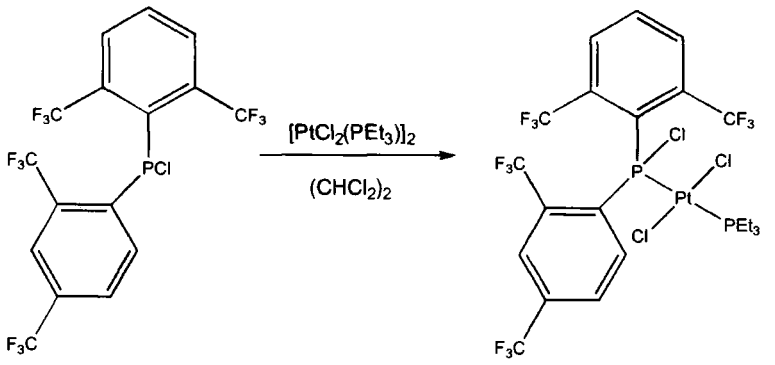

Equation 3.7 – Synthesis of *trans*–$[PtCl_2(PEt_3)(Ar'Ar''PCl)]$

The ^{31}P NMR spectrum shows a doublet and the associated Pt satellites for both the phosphane in question (Ar'Ar''PCl) and the PEt_3 group, signifying the formation of the *trans* compound. The chemical shifts of the species has values δ = 94.5 ppm ($^1J_{P-Pt}$ = 2531.4 Hz, $^2J_{P-P}$ = 562.0 Hz) and δ = 21.19 ppm ($^1J_{P-Pt}$ = 2765.3 Hz, $^2J_{P-P}$ = 561.8 Hz).

The ^{19}F NMR spectrum is more interesting in that it shows a distinct difference in the coupling from the CF_3 groups on the Ar' group and the *cis* CF_3 group on the Ar'' group. The spectrum shows two doublets and two singlets. This result confirms the interesting NMR results for the Ar'Ar''PCl phosphane itself (see Section 2.2.8.2). All the CF_3 groups are unique on the NMR time scale and the coupling constants are significantly different from one CF_3 group to the next.

The expected signals would be three doublets and one singlet, but as in the case of the free phosphane, one CF_3 group is reasonably far away from the phosphorus atom to reduce the coupling significantly enough, that it only appears as a singlet in the spectrum.

The chemical shift values for the species are δ = -52.8 ppm (singlet), δ = - 53.4 ppm (doublet) ($^4J_{P-F}$ = 12.7 Hz), δ = -55.1 ppm (singlet) and δ = -56.4 ppm (doublet) ($^4J_{P-F}$ = 61.19 Hz).

In the X-ray structure of the ligand Ar'Ar''PCl, it is apparent that one of the CF_3 groups in the Ar' aryl group is significantly further away from the phosphorus atom than the other, and this causes there to be no P-F coupling due to that interaction. In this case, not only is this observation confirmed, but also the P-F coupling constant between the phosphorus and the *cis* CF_3 group on the Ar'' group is significantly smaller than that of the Ar'(CF_3)-P interaction. This implies that the fluorine atoms on this CF_3 group are also on average further away from the phosphorus. Unfortunately the crystals grown of this compound were not suitable for X-ray analysis so it is impossible to confirm this deduction at present.

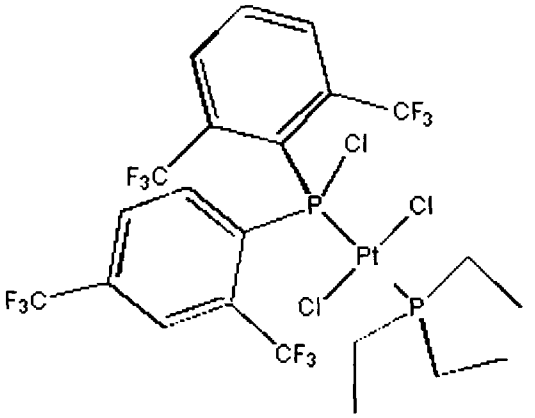

Figure 3.10 – *Trans*-[$PtCl_2(PEt_3)$(Ar'Ar''PCl)]

This result does, however, show that there must be significant steric hindrance around the P-Pt bond which would help to explain the apparent lack of rearrangement from the *trans* to the *cis* complex in this case.

The *trans* compound was heated for four days at 45°C and a small quantity was observed to rearrange to the *cis* compound. The formation of a number of other products was also apparent from the ^{31}P NMR spectrum and although the species was identified from the ^{31}P NMR spectrum, the ^{19}F NMR spectrum was too complex to determine exactly which peaks were significant. This formation of a number of products is probably due to the decomposition of the Ar'Ar''PCl species and the subsequent formation of platinum compounds of the by-products.

The ^{31}P NMR spectrum of the *cis* compound shows the formation of a singlet with the corresponding platinum satellites and the decrease in size of the doublet of triplets associated with the *trans* isomer. The chemical shift of the *cis* isomer has a value $\delta = 69.3$ ppm ($^{1}J_{P-Pt} = 4783.3$ Hz).

Isolation and purification of the *cis* compound could not be achieved and crystals of the compound were not obtained.

3.2.7 Attempted reaction between $[PtCl_2(PEt_3)]_2$ and Ar'Ar''PH

Ar'Ar''PH was added to a solution of $[PtCl_2(PEt_3)]_2$ in $(CHCl_2)_2$ and allowed to stir. No reaction was apparent from the ^{31}P NMR spectrum even after extended refluxing over a number of days.

3.2.8 Attempted reaction between $[PtCl_2(PEt_3)]_2$ and Ar_2PH

Ar_2PH was added to a solution of $[PtCl_2(PEt_3)]_2$ in $(CHCl_2)_2$ and allowed to stir. No reaction was apparent from the ^{31}P NMR spectrum even after extended refluxing over a number of days.

3.3 Results

3.3.1 A comparison of coupling constants

Complexes were prepared by reaction of the "Pt dimer" and the following compounds, $Ar'PH_2$, $Ar'PF_2$, $Ar'PCl_2$, $Ar'P{=}CCl_2$, and Ar'Ar''PCl. The results are shown in Table 3.22.

Species reacted with Pt dimer	Isomer	Coupling constant $^{1}J_{P-Pt}$ [Hz]	Bond length Pt–P(1) [Å]
$Ar'PH_2$	*cis*	3809	2.215(2)
	trans		
$Ar'PCl_2$	*cis*	5511	2.186(7)
	trans	678.4	
$Ar'PF_2$	*cis*	6252	2.157(2)
	trans	2723.3	
$Ar'P{=}CCl_2$	*cis*	3143	2.2082(12)
	trans	2340	
Ar'Ar''PCl	*cis*	4783.3	
	trans	2531.6	

Table 3.22 – Coupling constants and P–Pt bond lengths for a series of synthesised platinum phosphane complexes

As can be seen from Table 3.22 the largest coupling constants are formed in the compounds where there is the greatest electron withdrawal from the groups attached to the phosphorus. The coupling constants for the *cis* compounds range from 3100 Hz to over 6100 Hz. This increase is due to the amount of back donation occurring from the platinum to the phosphorus atom. This in turn shortens the P–Pt bond length (see Section 3.4).

3.4 Comparison between coupling constants and Pt–P bond length

Many studies[7] have been carried out which show conclusively that the coupling constant $^1J_{Pt-P}$ is directly comparable to the Pt–P bond length. This trend is indicative of the factors which determine the magnitude of the coupling constant.

In NMR studies, the electrons which give rise to this effect are the s electrons. It is the s electrons and the amount of s character in the bonding orbital which gives rise to the coupling constants. Interaction between s–electrons from two different atoms give rise to the coupling. As the s electrons on the platinum and the s electrons on the phosphorus become closer, the coupling constant increases[8].

We must now consider what actually causes the bond length to be shorter and thus the coupling constant to be greater. An average coupling constant for $^1J_{Pt-P}$ for an η^1 complex is in the region of 2000–4000Hz; however, some of the values for the compounds discussed in Table 3.22 are relatively larger than this.

As discussed in the introduction, there are two main interactions in phosphane bonding, σ–bond donation from the phosphane to the metal and π–back–donation from the metal to the phosphane. The greater the back donation then the stronger the bond and thus the greater the coupling constant. In this comparison the extent of back donation is wholly dependent on the phosphane, as in all cases the $PtCl_2(PEt_3)$ moiety remains constant. The greater the π–electron withdrawing capacity of the ligand the greater the back donation. The phosphanes concerned all have the Fluoroxyl group, which as discussed earlier (Chapter 2) is electron withdrawing, and the varying factor is the other substituents on phosphorus. In the series $Ar'PH_2$ < $Ar'PCl_2$ < $Ar'PF_2$ the coupling constant increases while the bond length decreases. This can be attributed to the electronegativity of the attached X group.

In the other cases, however, (Ar'Ar''PCl, $Ar'P{=}CCl_2$) there may be further factors involved, such as steric hindrance which may affect the bond length.

3.5 Changes in the chemical shifts upon bonding

When discussing bonding in phosphane–platinum (II) complexes there are two factors to consider; firstly the contribution to bonding from the σ bond, and secondly the contribution of the back donation from the platinum atom into the LUMO on the phosphorus atom.

With the exception of $Ar'PH_2$, the chemical shift moves to a lower frequency on bonding to Pt(II). This implies that there is an increase in electron density at the phosphorus centre. It can therefore be reasonably assumed that the back donation of electrons from the platinum contributes more to the shielding than the electrons from the phosphorus in the σ bond.

In the case of the compound formed with $Ar'PH_2$, however, the shift is to a higher frequency thus implying that the dominant factor in bonding is the σ bond, comparative to the back donation from the platinum atom.

This can be explained by looking at the substituents on the phosphorus atom. Halogen atoms bonded to phosphorus cause an overall effect of electron withdrawal from the s and more importantly p orbitals on the phosphorus atom itself. This increases the capacity for the phosphorus to accept electron density from the platinum in the form of back donation to the LUMO (π^*).

Hydrogen, however, has approximately the same electronegativity as phosphorus[5] and as such does not aid back donation from the platinum atom. The aryl group will withdraw some electrons but this is an equal factor when looking at the series of compounds.

This feature of back donation also ties in with the fact that the bond lengths become shorter $Ar'PF_2 < Ar'PCl_2 < Ar'PH_2$ and the coupling constants decrease.

3.5.1 Change in chemical shift upon bonding to platinum

Phosphane	Chemical shift (δ) prior to bonding (ppm)	Chemical shift (δ) of the *cis* platinum compound (ppm)	Change in Chemical shift upon bonding (ppm)
$Ar'PH_2$	-140.3	-79.9	+ 60.4
$Ar'PCl_2$	148.0	142.7	- 5.3
$Ar'PF_2$	193.3	163.1	- 30.2

Table 3.23 – Changes in chemical shift upon bonding to platinum

As can be seen from Table 3.23, there would seem to be no correlation between the change in chemical shift of the phosphane, upon bonding to the platinum and the strength of the bond formed. What it does demonstrate is the vast change in electron density around the phosphorus atom upon bonding in certain cases. In the case of $Ar'PH_2$ the electron density is reduced on the phosphorus and in the case of the $Ar'PF_2$ phosphane electron density is greatly increased upon bonding.

3.6 Variations in the delocalisation of electrons in the aryl ring

Table 3.24 shows the variation in carbon–carbon bond lengths within each of the aryl rings once bonded to the platinum atom. The information given in the table reveals that the electronic distribution is far from uniform.

The carbon atoms connected to the CF_3 group are most affected by the electron withdrawal. The expected pattern is that the bond lengths around atoms C(2) and C(6) would be shortest and the bonds around C(4) would be longest.

If the results for the Ar'PCl_2 compound are not included in the comparisons (they are only accurate to two decimal places and not three like the others), it is clear that the shortest bond lengths in the compounds are those between C(4)–C(5) and C(3)–C(4) and that the longest bond lengths in the compounds are those between C(1)–C(6) and C(1)–C(2).

There are other influences on the carbon C(1) as it is bonded to phosphorus directly; however, this shows that the stronger bonds (shorter C–C bond lengths) are between those atoms furthest away from the CF_3 groups in the ring.

Compound	C(1)–C(2)	C(1)–C(6)	C(2)–C(3)	C(5)–C(6)	C(3)–C(4)	C(4)–C(5)
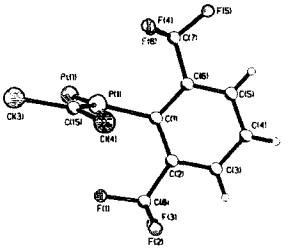 Ave. C–C bond length = 1.395	1.396(6)	1.418(7)	1.398(7)	1.393(7)	1.386(8)	1.377(8)
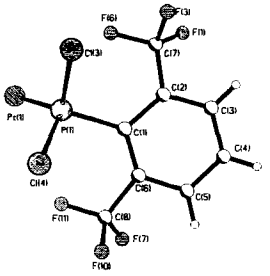 Ave. C–C bond length = 1.40	1.44(3)	1.37(4)	1.40(4)	1.41(4)	1.39(4)	1.41(4)
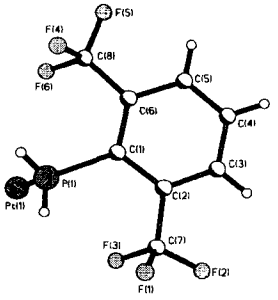 Ave. C–C bond length = 1.388	1.413(5)	1.405(9)	1.376(9)	1.389(9)	1.368(12)	1.374(11)
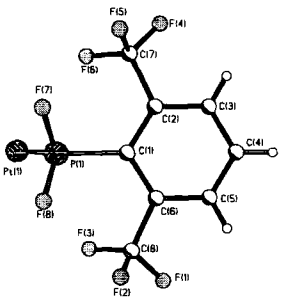 Ave. C–C bond length = 1.391	1.413(10)	1.396(9)	1.394(10)	1.382(11)	1.390(11)	1.376(13)

Table 3.24 – Comparison between carbon–carbon bond lengths in the aryl rings

3.7 Experimental

3.7.1 The "Platinum dimer" *trans*-$[PtCl_2(PEt_3)]_2$

3.7.1.1 Synthesis of cis-*$[PtCl_2(PhCN)_2]$*

$PtCl_2$ (2.0g, 7.5mmol) was added to PhCN (20ml) and was heated to 100°C for ten minutes, yielding a bright yellow solution which upon cooling gave a bright yellow precipitate. The solution was filtered and the crystals were washed with petroleum ether and dried *in vacuo*. Yield 2.5g (90%).

$$PtCl_2 \xrightarrow{\text{xs PhCN}} PtCl_2(PhCN)_2$$

3.7.1.2 Synthesis of cis-*$[PtCl_2(PEt_3)_2]$*

PEt_3 (1.3ml, 4.2mmol) was added to a solution of *cis*-$[PtCl_2(PhCN)_2]$ (1.0g, 2.1mmol) dissolved CH_2Cl_2 (5ml) and the reaction was stirred for three hours at room temperature. The solvent was removed *in vacuo* and the resulting white crystals were washed with hexane and dried *in vacuo*. Yield 0.8g (97%)

$$PtCl_2(PhCN)_2 \xrightarrow[-\ 2\ PhCN]{2\ PEt_3} PtCl_2(PEt_3)_2$$

3.7.1.3 Synthesis of trans-$[PtCl_2(PEt_3)]_2$

cis-$[PtCl_2(PEt_3)_2]$ (2.2g, 4.4mmol) was added to a solution of $PtCl_2$ (1.6g, 6.02 mmol) in $(CHCl_2)_2$ (5ml) and heated to 150°C for 1 hour. The solution turned bright orange. Upon cooling pale yellow crystals were formed. The solvent was removed carefully *in vacuo* and the product was purified by recrystallisation from CH_2Cl_2. Yield 3.5g (80%).

$$PtCl_2(PEt_3)_2 \xrightarrow{PtCl_2} \textit{trans}\text{-}[PtCl_2(PEt_3)]_2$$

3.7.2 Synthesis of *cis*-$[PtCl_2(PEt_3)(Ar'PCl_2)]$

A mixture of Ar''PCl_2 and Ar'PCl_2 (0.40g) and $[PtCl_2(PEt_3)]_2$ (0.49g, 0.7mmol) was dissolved in CH_2Cl_2 (25ml) and left to react for three days. A white precipitate was formed and the solution was filtered and washed with hexanes. Crystals of the resulting product were grown by layering hexanes above a solution of the product in $(CHCl_2)_2$. Yield 0.7 g; ^{31}P δ = 97.9 ppm $^1J_{P-Pt}$ = 5488.1 Hz, singlet with Pt satellites, δ = 19.54 ppm $^1J_{P-Pt}$ = 3444.7 Hz, singlet with Pt satellites) for (Ar''PCl_2) and (δ = 94.5 ppm, $^1J_{P-Pt}$ = 5260 Hz, singlet with Pt satellites, δ = 20.14 ppm $^1J_{P-Pt}$ = 2916.1 Hz, singlet with Pt satellites) for (Ar'PCl_2). Analysis found: %C, 22.97; %H, 2.93; Required for $C_{14}F_6H_{18}P_2PtCl_4$; %C, 24.05; %H, 2.60.

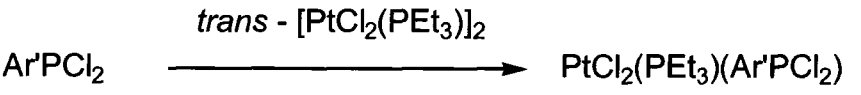

3.7.3 Synthesis of *cis*-$[PtCl_2(PEt_3)(Ar'PH_2)]$

Ar'PH_2 (0.30g, 1.2mmol) and $[PtCl_2(PEt_3)]_2$ (0.46g, 0.6mmol) were dissolved in CH_2Cl_2 (25ml) and left to react for three days. A white precipitate was formed and the solution was filtered and washed with hexanes. Yield 0.5g; ^{31}P $\{^1H\}$ (CH_2Cl_2) δ = – 79.9 ppm
($^1J_{P-Pt}$ = 3834 Hz).

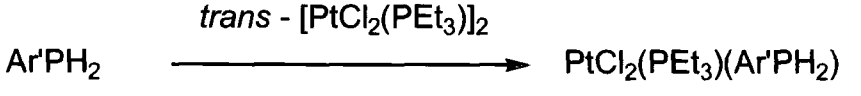

3.7.4 Synthesis of *cis*-[$PtCl_2(PEt_3)(Ar'PF_2)$]

$Ar'PF_2$ (0.35g, 1.2mmol) and $[PtCl_2(PEt_3)]_2$ (0.46g, 0.6mmol) were dissolved in CH_2Cl_2 (25ml) and left to react for three days. A white precipitate was formed and the solution was filtered and washed with hexanes. Crystals of the resulting product were grown by layering hexanes above a solution of the product in $(CHCl_2)_2$. ^{31}P $(CHCl_2)_2$ δ = 135.6 ppm ($^1J_{P-Pt}$ = 6194.8 Hz, $^1J_{P-F}$ = 1140 Hz, $^2J_{P-P}$ = 4.26Hz) (triplet with Pt satellites),

δ = 20.51 ppm ($^1J_{P-Pt}$ = 2916.2 Hz, $^2J_{P-P}$ = 42.8 Hz) (singlet with Pt satellites). ^{19}F: (CH_2Cl_2) δ = –75.7 ppm (doublet and Pt satellites, $^1J_{P-F}$ = 1207.4 Hz, $^2J_{F-Pt}$ = 150.6 Hz, $^5J_{F-F}$ = 19.77 Hz).

$$Ar'PF_2 \xrightarrow{\textit{trans}\text{-}[PtCl_2(PEt_3)]_2} PtCl_2(PEt_3)(Ar'PF_2)$$

3.7.5 Synthesis of *cis*-[$PtCl_2(PEt_3)(Ar'P{=}CCl_2)$]

$Ar'P{=}CCl_2$ (0.46g, 1.4mmol) and $[PtCl_2(PEt_3)]_2$ (0.4g, 0.52mmol) were dissolved in a solution of CH_2Cl_2 and left to react for three days. An orange precipitate formed and the solution was filtered and washed with hexanes. Crystals of the resulting product were grown by layering hexanes above a solution of the product in $(CHCl_2)_2$. ^{31}P (CH_2Cl_2) δ = 155.3 ppm ($^1J_{P-Pt}$ = 3143.8 Hz, $^2J_{P-P}$ = 19.24 Hz) (doublet with Pt satellites). ^{19}F (CH_2Cl_2) δ = –57.1 ppm (singlet).

$$Ar'P{=}CCl_2 \xrightarrow{\textit{trans}\text{-}[PtCl_2(PEt_3)]_2} PtCl_2(PEt_3)(Ar'P{=}CCl_2)$$

3.7.6 Synthesis of trans-[$PtCl_2(PEt_3)(Ar'Ar''PCl)$]

Ar'Ar''PCl (0.50g, 0.1mmol) was added to a solution of $[PtCl_2(PEt_3)]_2$ (0.39g, 0.05mmol) in $(CHCl_2)_2$. The solution was allowed to stir for ten days. Attempts to grow crystals suitable for X-ray analysis were unsuccessful. ^{31}P (CH_2Cl_2) δ = 94.5 ppm ($^1J_{P-Pt}$ = 1265.7 Hz) ($^2J_{P-P}$ = 562.0 Hz) (doublet with Pt satellites), δ = 21.19 ppm ($^1J_{P-Pt}$ = 2765.3 Hz, $^2J_{P-P}$ = 561.8 Hz). ^{19}F (CH_2Cl_2) δ = -52.8 ppm (singlet), δ = - 53.4 ppm (doublet) ($^4J_{P-F}$ = 12.7 Hz), δ = -55.1 ppm (singlet) and δ = -56.4 ppm (doublet) ($^4J_{P-F}$ = 61.19 Hz).

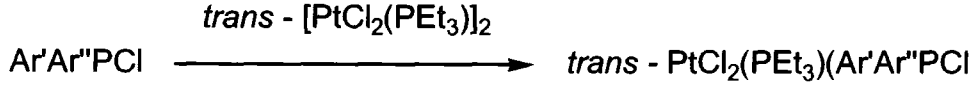

3.7.7 Synthesis of *cis*-[$PtCl_2(PEt_3)(Ar'Ar''PCl)$]

A solution of *trans*-$PtCl_2(PEt_3)(Ar'Ar''PCl)$ in $(CHCl_2)_2$ was heated to 45°C for four days. Attempts to grow crystals suitable for X-ray analysis were not successful. ^{31}P [$(CHCl_2)_2$] δ = 69.3 ppm ($^1J_{P-Pt}$ = 4783.3 Hz).

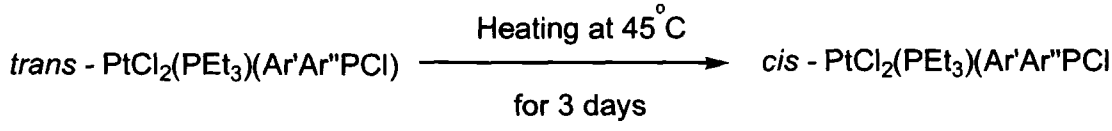

---

[1] H. P. Goodwin., K. B. Dillon., B. Murrer, *Unpublished Work.*
[2] N. N. Greenwood., A. Earnshaw., *Chemistry of the Elements*, Pergamon Press, Oxford, 1989.
[3] H. P. Goodwin., *Ph.D thesis.*, 1990.
[4] J. Chatt., L. M. Venanzi., *J. Am. Chem. Soc.*, 1955, 2787.
[5] J. E. Huheey., "Inorganic Chemistry (third edition)"., *Harper and Row* 1983.
[6] G. R. Desiraju., "Crystal Engineering – The design of organic solids", *Material Science Monographs, Elsiever Science Publishers. B. V.,* 1989
[7] J. G. Verkade., L. D. Quin., "Phosphorus-31 NMR Spectroscopy in Stereochemical Analysis of Organic Compounds and Metal Complexes", *VCH Publishers*, 1987
[8] Unidentate Phosphorus Ligands", P. S. Pregosin, in Phosphorus–31 NMR Spectroscopy in Stereochemical Analysis Organic Compounds and Metal Complexes", J. G. Verkade and L. D. Quin (eds), VCH Publishers, 1987, 509 – 511

Chapter 4

Synthesis of novel vinyl platinum complexes

4.1 Introduction

The synthesis of the phosphaalkyne R-CP (where R = Supermes), by the reaction of the phosphaalkene $RP{=}CCl_2$ with $Pd(PPh_3)_4$, was reported by Sanchez *et al*[1], with a proposed mechanism involving the rearrangement of the intermediate species [RP=C:].

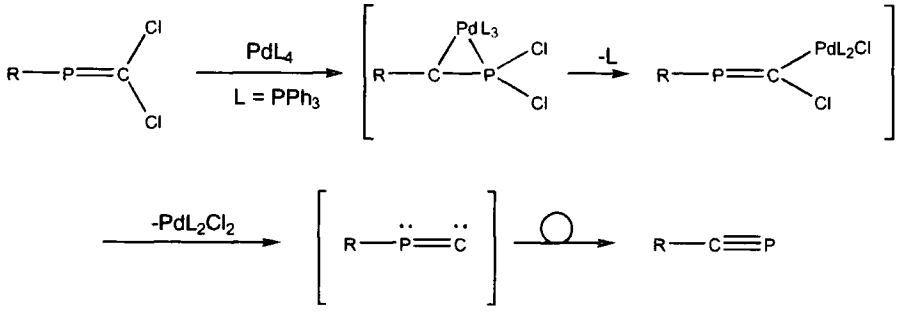

Equation 4.1 – Proposed mechanism for the synthesis of a phosphaalkyne using PdL_4 and $RP{=}CCl_2$

A more detailed literature search revealed that this reaction was identical to work published subsequently by Angelici *et al* in 1994[2]. The major difference is that Angelici had X-ray structures for the intermediates in the reaction with Pd(0) and Pt(0) which shows the formation of a four-membered ring between a C=C bond in the aryl ring and the P=C phosphaalkene bond.

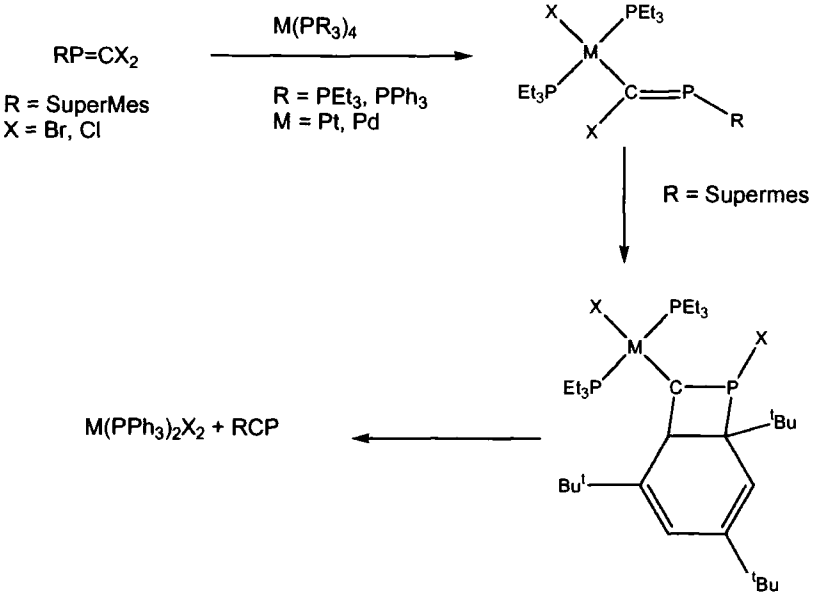

Equation 4.2 –Mechanism demonstrated by Angelici with the isolation of intermediates

The phosphaalkene $ArP{=}CCl_2$ was first prepared by Goodwin[3] by the removal of HCl from a substituted phosphane $[ArP(Cl)CHCl_2]$. It was proposed that the reaction between this phosphaalkene and Pd(0) and Pt(0) compounds would potentially facilitate a simple synthesis of a new phosphaalkene Ar-CP. There was also the possibility for the formation of η^2 complexes as well of the type $Pt(L_2)(\eta^2\text{-}ArP{=}CCl_2)$.

4.2 Phosphaalkenes

4.2.1 Synthesis of $Ar'P{=}CCl_2$

4.2.1.1 $Ar'P(Cl)CHCl_2$

The synthesis and characterisation of the compound is described in Section 2.2.6.

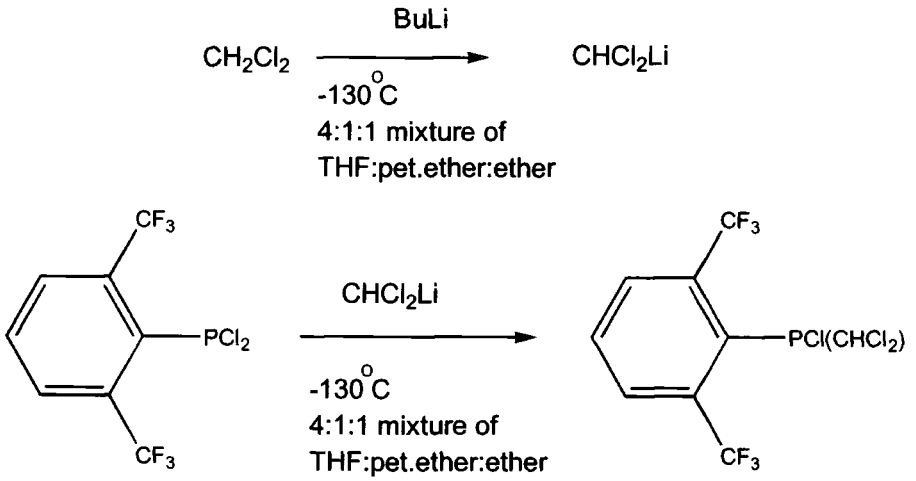

Equation 4.3 – Preparation of $Ar'PCl(CHCl_2)$

4.2.1.2 *Reaction between Ar'P(Cl)CHCl$_2$ and DBU*

The formation of this phosphaalkene is described in Section 2.2.7.

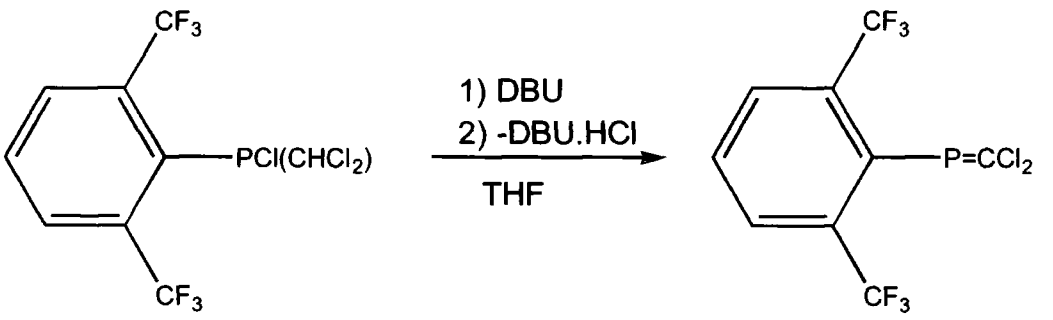

Equation 4.4 – Preparation of Ar'P=CCl$_2$

As described in Section 2.2.7 this low coordinate phosphorus species is stabilised by the steric bulk of the Fluoroxyl group and the electron withdrawing effects of that group.

The analogous compounds RP=CCl$_2$ (R = 2,4,6-tris(tritertiarybutyl)phenyl and R=^{t}Bu) are well known [4] and their chemistry has been extensively studied. The reactions described in this chapter were performed to see if the perfluorinated aryl species would react in an analogous fashion to their non-fluorinated partners.

4.2.2 Formation of ArP=CCl$_2$

The analogous phosphaalkene was prepared by the same method described above, using Fluoromes as the aryl group instead of Fluoroxyl. This compound was synthesised because the extra CF_3 group on the aryl group would not only produce a more electronically stable compound but there would also be less chance of side reactions in the *para* position.

4.3 Attempted synthesis of η^2-bonded phosphaalkene complexes

This section concerns the reaction of Ar'P=CCl_2 and ArP=CCl_2 with a number of different Pt(0) and Pd(0) compounds, in the attempt to make η^2 – bonded species. It was also expected that if the synthesis followed the same mechanism as Angelici's reaction, that it may in turn provide a method of synthesis for phosphaalkynes.

4.3.1 Reaction between Ar'P=CCl_2 and $Pt(PPh_3)_4$

Ar'P=CCl_2 was added to a solution of $Pt(PPh_3)_4$ in toluene, which produced an orange colour to the solution. Orange crystals were formed over a few days and these were isolated and submitted for X-ray crystallographic characterisation.

This reaction was an attempt to form an η^2-complex of the phosphaalkene. It did not, however, yield this product. The novel vinyl platinum species, *trans* PtCl(CCl=PAr')$(PPh_3)_2$ was formed. The reaction is analogous to a reaction performed using the Supermes R group described in Section 4.1.

The ^{31}P NMR spectrum showed the formation of a number of new peaks; a septet with platinum satellites (δ = 201.93 ppm $^1J_{P\text{-}Pt}$ = 413.1 Hz). ($^4J_{P\text{-}F}$ = 19.7 Hz) which is assignable to the phosphaalkene ligand, and two peaks associated with the PPh_3 groups still bonded to the platinum. The first PPh_3 ligand shows no P-P coupling (δ = 13.63 ppm $^1J_{P\text{-}Pt}$ = 4019.8 Hz) (singlet and platinum satellites). The second PPh_3 ligand does show some P-P interaction (δ = 16.12 ppm $^1J_{P\text{-}Pt}$ = 1846.9 Hz, $^3J_{P\text{-}P}$ = 44.4 Hz) (doublet with platinum satellites). There is also a signal for free PPh_3 (δ = -2.75 ppm).

It is interesting to note the difference in the coupling constant between the two PPh_3 groups and the platinum. Both the ligands are *cis* to the phosphaalkene derivative and yet one of the species clearly shows P-P coupling and a significantly smaller P-Pt coupling constant. The P-P interaction must therefore be a through space interaction similar to that seen between the phosphorus atoms and the CF_3 groups on the aryl species.

The size of the coupling constant is directly related to the bond length P-Pt. The crystal structure shown in Section 4.3.1.1 demonstrates that the difference in P-Pt bond lengths is negligible (2.32Å and 2.33Å). This implies that there is significant interaction between one of the PPh_3 groups and the phosphaalkene derivative. The P-P distances in the molecule are P(1)-P(2) = 3.76Å and P(1)-P(3) = 4.48 Å.

If we consider the sizes of the coupling constants, the interaction of 4019 Hz is typical of a *cis* complex and the interaction of 1846 Hz is typical of a *trans* complex.

In Angelici's paper[2] he describes the formation of both the *cis* and *trans* isomers upon initial addition of the two reactants. Taking that into consideration in this case, it would suggest that we have formed the two separate isomers. There is no evidence, however, for two signals assignable to the phosphaalkene derivative and there would also be more peaks assignable to inequivalent PPh_3 groups.

Assuming that we have only formed the *trans* isomer, as the NMR and X-ray structure suggest, we have to consider the difference in the signals assignable to the PPh_3 groups. If we consider the PPh_3 group closest to P(1) to be comparable to being *cis* and the PPh_3 group containing P(3) to be comparable to a *trans* complex this would go some way to describe the spectrum. The P-P coupling constant for a *trans* complex is normally of the order of 5-600 Hz and negligible for *cis* complexes. The coupling constant in this case is only of the order of 50 Hz.

We believe that the signal with $^1J_{P\text{-}Pt}$ = 1846 Hz and $^3J_{P\text{-}P}$ to be assignable to the PPh_3 group containing P(3) and the signal with $^1J_{P\text{-}Pt}$ = 4019 Hz to be assignable to the PPh_3 groups containing P(2) and being closer to the phosphorus atom in the phosphaalkene derivative.

The crystal structure also shows that there is no rotation of the phosphaalkene derivative about the Pt-C bond due to steric interactions. The distance between P(1) and P(2) is much smaller than that between P(1) and P(3)

The ^{19}F spectrum showed a large number of indistinguishable peaks possibly due to decomposition and side reactions involving the product. Unfortunately none of the peaks could be identified accurately as those relating to the peaks in the ^{31}P NMR spectrum.

Orange plate-like crystals were grown from toluene using the layering technique described in Appendix 1. The crystals were submitted for X-ray structural characterisation.

$$Ar'P{=}CCl_2 \xrightarrow[-\ PPh_3]{Pt(PPh_3)_4} PtCl(CCl{=}PAr')(PPh_3)_2$$

Equation 4.5 – Preparation of *trans*-[PtCl(CCl=PAr')$(PPh_3)_2$]

4.3.1.1 The molecular structure of [PtCl(CCl=PAr')$(PPh_3)_2$]

Crystals submitted for X-ray characterisation were mounted on a glass fibre, introduced onto the diffractometer, and diffraction data were collected. The structure was subsequently solved and refined; the molecular structure is shown in Figure 4.1.

Data were collected on a Siemens 3-circle diffractometer with a CCD area detector, ω scan mode $2\theta \leq 60.2°$. The structure was solved by direct methods and refined by full-matrix least squares against F^2 . Lists of crystal data and refinement parameters, anisotropic displacement parameters, bond lengths and angles, and atomic coordinates are given in tables 4.1 through 4.5.

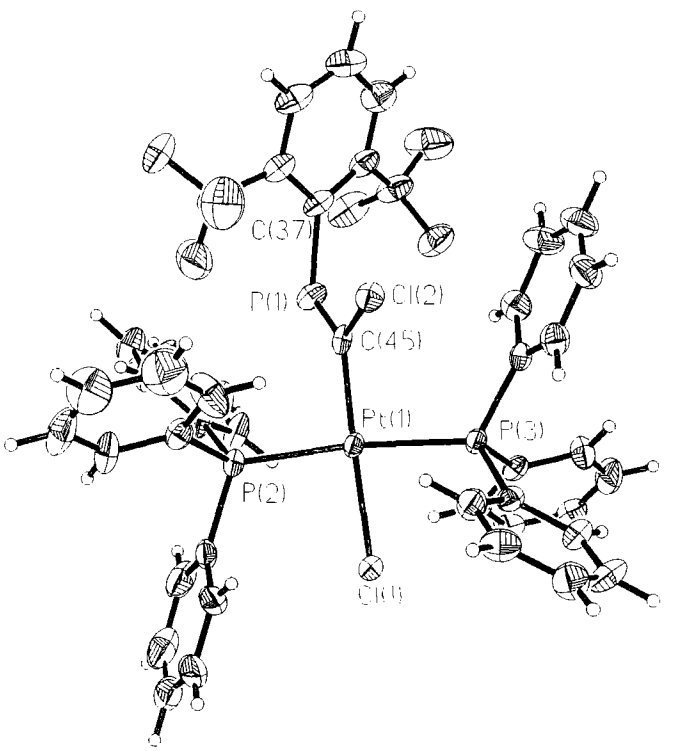

Figure 4.1 – Thermal ellipsoid diagram 150(2)K (50% probability) showing *trans*-[PtCl(CCl=PAr')$(PPh_3)_2$]

A significant factor in the structure of this compound is the steric hindrance. There is a large interaction is between the CF_3 groups on the aryl ring and the chlorine atom bonded to the phosphaalkene fragment [Cl(2)]. To minimise interaction the plane of the aryl ring is orthogonal to the plane of the Pt-C-Cl bonds.

This is not the case as can be seen from Figure 4.2, which is shown in the plane of the six carbons of the aryl ring.

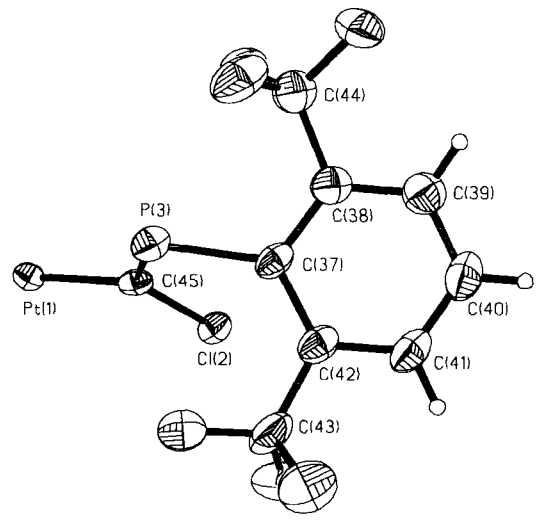

Figure 4.2 – Thermal ellipsoid diagram at 150(2)K (50% probability) showing the angle between the C=P plane and the aryl ring.
(The Figure is shown in the plane of the aryl ring)

The electronic effects in the structure would be at a maximum if the ring interacts with the lone pair on the phosphorus atom [P(1)] which would also mean that the plane of the aryl ring would be orthogonal to the Pt-C-Cl bonds.

The actual angle between the plane of the aryl ring and the plane of the Pt-C-Cl bonds is 76.1°. This suggests that there is also an interaction between the CF_3 groups and the PPh_3 groups.

It is worth noting from the structure that the two PPh_3 groups adopt a "*trans*" conformation which minimises any steric interaction between these two groups. This implies that the structure is based more around the steric positioning of the Fluoroxyl group than the PPh_3 groups.

Crystal data and structure refinement	
Identification code	$Ar'P=C(Cl)Pt(PPh_3)_2Cl$
Empirical formula	$C_{45}H_{33}Cl_2F_6P_3Pt$
Formula weight	1046.61
Temperature	150(2) K
Wavelength	0.71073 Å
Crystal system	Triclinic
Space group	P-1
Unit cell dimensions	a = 9.4710(2) Å α = 104.76 °. b = 11.6532(1) Å β = 91.851(1) °. c = 21.3936(3) Å χ = 105.36 °.
Volume	2188.95(6) $Å^3$
Z	2
Number of reflections used	Calculation of cell = 512 Total = 16114 Unique = 11479 Obs [I>2σ(I)] = 8413
Crystal description	needle
Crystal colour	orange
Density (calculated)	1.588 g/cm^3
Absorption coefficient	34.93 cm^{-1}
F(000)	1028
Crystal size	0.2 x 0.2 x 0.4 mm
Theta range for data collection	0.99 to 30.49 °.
Index ranges	-12<=h<=10 -16<=k<=15 -29<=l<=28
Experiment device	Siemens SMART
Experiment methods	ω scans
Reflections collected	16114
Independent reflections	11497 [R(int) = 0.0288]
Refinement method	Full-matrix least-squares on F^2
Data / restraints / parameters	11488 / 0 / 512
Goodness-of-fit on F^2	0.990
Final R indices [I>2σ(I)]	R_1 = 0.0417, wR_2 = 0.0832
R indices (all data)	R_1 = 0.0679, wR_2 = 0.0965
Largest diff. peak and hole	1.879 and -1.499 e.$Å^{-3}$

Table 4.1 - Crystal data and structure refinement for $[PtCl(CCl=PAr')(PPh_3)_2]$

	x	y	z	U(eq)
Pt(1)	10957(1)	2138(1)	13075(1)	22(1)
P(3)	10825(1)	127(1)	13111(1)	22(1)
P(2)	11247(1)	4214(1)	13156(1)	23(1)
C(30)	12894(6)	6072(5)	12644(3)	41(2)
C(7)	12648(5)	32(5)	13340(2)	26(1)
C(45)	9883(5)	1588(4)	12166(2)	23(1)
C(1)	9615(5)	-395(5)	13690(2)	24(1)
C(2)	9231(5)	463(5)	14187(2)	29(1)
C(8)	12872(6)	-778(5)	13693(3)	33(1)
C(13)	10217(6)	-1150(5)	12365(2)	27(1)
C(32)	9145(6)	5123(5)	12602(3)	31(1)
C(19)	12166(6)	5304(5)	13931(3)	31(1)
C(24)	13646(6)	5431(5)	14077(3)	38(1)
C(25)	12413(5)	4815(5)	12579(3)	30(1)
C(31)	9478(6)	4524(5)	13054(3)	30(1)
C(4)	7854(6)	-1165(6)	14616(3)	36(1)
C(3)	8353(6)	68(6)	14644(3)	36(1)
C(26)	12886(7)	4026(6)	12097(3)	54(2)
C(12)	13846(6)	710(5)	13107(3)	34(1)
C(23)	14417(8)	6231(6)	14654(3)	53(2)
C(9)	14265(6)	-905(6)	13798(3)	46(2)
C(6)	9094(6)	-1647(5)	13663(3)	37(1)
C(5)	8234(7)	-2017(6)	14127(3)	45(2)
Cl(1)	12253(2)	2709(1)	14123(1)	38(1)
C(18)	8747(6)	-1506(5)	12103(3)	35(1)
C(14)	11183(6)	-1722(5)	12019(3)	35(1)
C(11)	15244(6)	580(6)	13210(3)	42(2)
C(16)	9276(7)	-2969(6)	11185(3)	48(2)
C(15)	10703(7)	-2629(5)	11439(3)	44(2)
C(17)	8280(7)	-2398(6)	11515(3)	47(2)
C(33)	7729(6)	5246(6)	12531(3)	42(2)
C(36)	8406(6)	4081(6)	13428(3)	44(2)
C(34)	6689(7)	4832(6)	12916(3)	52(2)
C(35)	7015(7)	4242(7)	13365(3)	57(2)
Cl(2)	10851(1)	879(1)	11563(1)	31(1)
P(3)	8220(2)	1773(1)	11993(1)	31(1)
F(3)	6002(4)	-785(3)	11832(2)	52(1)
F(2)	4855(4)	461(4)	11628(2)	56(1)
F(1)	4297(4)	-1420(4)	11040(2)	71(1)
C(37)	7730(6)	1003(5)	11094(2)	30(1)
C(29)	13830(7)	6523(7)	12214(4)	55(2)
C(20)	11471(8)	5982(6)	14378(3)	52(2)
C(42)	8482(6)	1409(6)	10595(3)	35(1)
C(44)	5438(7)	-457(6)	11339(3)	45(2)
C(22)	13719(11)	6903(6)	15090(3)	71(2)
C(38)	6526(6)	-72(5)	10884(3)	35(1)
F(6)	9805(5)	3411(4)	11275(2)	71(1)
F(5)	9220(5)	3240(4)	10279(2)	73(1)
F(4)	10944(4)	2547(4)	10545(2)	72(1)

	x	y	z	U(eq)
C(39)	6225(6)	-764(6)	10242(3)	44(2)
C(28)	14269(8)	5744(7)	11734(4)	64(2)
C(40)	7081(7)	-406(6)	9779(3)	46(2)
C(41)	8173(7)	704(6)	9958(3)	44(2)
C(43)	9596(8)	2649(6)	10690(3)	48(2)
C(21)	12261(10)	6784(7)	14961(3)	68(2)
C(27)	13823(9)	4497(8)	11666(4)	74(2)
C(10)	15429(7)	-245(6)	13551(3)	47(2)
Cl(3)	16004(6)	4366(5)	10175(3)	230(2)
C(46)	14049(25)	4218(23)	10033(11)	126(8)

Table 4.2 - Atomic coordinates (x 10^4) and equivalent isotropic displacement parameters ($Å^2$ x 10^3) for [PtCl(CCl=PAr')(PPh_3)$_2$]. U(eq) is defined as one third of the trace of the orthogonalized Uij tensor

Bond lengths [Å] and Angles [°]	
Pt(1)-C(45)	2.030(5)
Pt(1)-P(2)	2.3219(13)
Pt(1)-P(3)	2.3341(12)
Pt(1)-Cl(1)	2.3671(13)
P(3)-C(7)	1.819(5)
P(1)-C(1)	1.824(5)
P(3)-C(13)	1.836(5)
P(2)-C(31)	1.823(5)
P(2)-C(25)	1.830(5)
P(2)-C(19)	1.834(6)
C(30)-C(25)	1.382(7)
C(30)-C(29)	1.402(8)
C(7)-C(12)	1.387(7)
C(7)-C(8)	1.401(7)
C(45)-P(1)	1.688(5)
C(45)-Cl(2)	1.767(5)
C(1)-C(2)	1.392(7)
C(1)-C(6)	1.395(7)
C(2)-C(3)	1.392(7)
C(8)-C(9)	1.384(7)
C(13)-C(14)	1.394(7)
C(13)-C(18)	1.397(7)
C(32)-C(33)	1.393(7)
C(32)-C(31)	1.401(7)
C(19)-C(20)	1.380(8)
C(19)-C(24)	1.387(8)
C(24)-C(23)	1.386(8)
C(25)-C(26)	1.370(8)
C(31)-C(36)	1.386(7)
C(4)-C(3)	1.373(8)
C(4)-C(5)	1.375(8)
C(26)-C(27)	1.410(9)
C(12)-C(11)	1.388(7)
C(23)-C(22)	1.364(10)
C(9)-C(10)	1.372(8)
C(6)-C(5)	1.386(7)
C(18)-C(17)	1.384(8)
C(14)-C(15)	1.379(8)
C(11)-C(10)	1.389(8)
C(16)-C(15)	1.356(8)
C(16)-C(17)	1.403(9)
C(33)-C(34)	1.373(8)
C(36)-C(35)	1.386(8)
C(34)-C(35)	1.385(8)
P(1)-C(37)	1.886(5)
F(3)-C(44)	1.350(6)
F(2)-C(44)	1.353(7)
F(1)-C(44)	1.335(7)
C(37)-C(38)	1.412(8)

Bond lengths [Å] and Angles [°]	
C(37)-C(42)	1.414(7)
C(29)-C(28)	1.343(10)
C(20)-C(21)	1.402(10)
C(42)-C(41)	1.377(8)
C(42)-C(43)	1.507(9)
C(44)-C(38)	1.501(8)
C(22)-C(21)	1.363(11)
C(38)-C(39)	1.379(8)
F(6)-C(43)	1.309(7)
F(5)-C(43)	1.339(6)
F(4)-C(43)	1.352(7)
C(39)-C(40)	1.378(8)
C(28)-C(27)	1.370(10)
C(40)-C(41)	1.379(9)
Cl(3)-C(46)	1.82(2)
Cl(3)-C(46)	1.83(2)
C(46)-Cl(3)	1.83(2)
C(45)-Pt(1)-P(2)	92.66(13)
C(45)-Pt(1)-P(3)	93.93(13)
P(2)-Pt(1)-P(3)	173.39(5)
C(45)-Pt(1)-Cl(1)	177.59(13)
P(2)-Pt(1)-Cl(1)	89.34(5)
P(3)-Pt(1)-Cl(1)	84.05(4)
C(7)-P(3)-C(1)	107.5(2)
C(7)-P(3)-C(13)	102.2(2)
C(1)-P(3)-C(13)	103.3(2)
C(7)-P(3)-Pt(1)	109.9(2)
C(1)-P(3)-Pt(1)	113.4(2)
C(13)-P(3)-Pt(1)	119.4(2)
C(31)-P(2)-C(25)	108.0(2)
C(31)-P(2)-C(19)	105.0(3)
C(25)-P(2)-C(19)	101.1(3)
C(31)-P(2)-Pt(1)	111.5(2)
C(25)-P(2)-Pt(1)	114.5(2)
C(19)-P(2)-Pt(1)	115.8(2)
C(25)-C(30)-C(29)	120.2(6)
C(12)-C(7)-C(8)	118.9(5)
C(12)-C(7)-P(3)	118.3(4)
C(8)-C(7)-P(3)	122.6(4)
P(3)-C(45)-Cl(2)	122.5(3)
P(3)-C(45)-Pt(1)	123.9(3)
Cl(2)-C(45)-Pt(1)	113.6(2)
C(2)-C(1)-C(6)	118.4(5)
C(2)-C(1)-P(3)	120.1(4)
C(6)-C(1)-P(3)	121.5(4)
C(1)-C(2)-C(3)	120.1(5)
C(9)-C(8)-C(7)	120.2(5)
C(14)-C(13)-C(18)	118.1(5)
C(14)-C(13)-P(3)	122.8(4)
C(18)-C(13)-P(3)	118.8(4)

Bond lengths [Å] and Angles [°]	
C(33)-C(32)-C(31)	119.1(5)
C(20)-C(19)-C(24)	118.4(6)
C(20)-C(19)-P(2)	124.1(5)
C(24)-C(19)-P(2)	117.5(4)
C(23)-C(24)-C(19)	121.0(6)
C(26)-C(25)-C(30)	119.0(5)
C(26)-C(25)-P(2)	120.2(4)
C(30)-C(25)-P(2)	120.7(4)
C(36)-C(31)-C(32)	119.7(5)
C(36)-C(31)-P(2)	116.9(4)
C(32)-C(31)-P(2)	123.4(4)
C(3)-C(4)-C(5)	119.1(5)
C(4)-C(3)-C(2)	121.1(5)
C(25)-C(26)-C(27)	120.0(6)
C(7)-C(12)-C(11)	121.0(5)
C(22)-C(23)-C(24)	120.0(7)
C(10)-C(9)-C(8)	120.0(5)
C(5)-C(6)-C(1)	120.4(5)
C(4)-C(5)-C(6)	120.9(6)
C(17)-C(18)-C(13)	120.3(5)
C(15)-C(14)-C(13)	121.2(5)
C(12)-C(11)-C(10)	118.9(5)
C(15)-C(16)-C(17)	119.7(6)
C(16)-C(15)-C(14)	120.5(6)
C(18)-C(17)-C(16)	120.1(6)
C(34)-C(33)-C(32)	120.6(5)
C(35)-C(36)-C(31)	120.5(5)
C(33)-C(34)-C(35)	120.5(5)
C(34)-C(35)-C(36)	119.6(5)
C(45)-P(3)-C(37)	104.9(2)
C(38)-C(37)-C(42)	115.5(5)
C(38)-C(37)-P(3)	119.2(4)
C(42)-C(37)-P(3)	125.3(4)
C(28)-C(29)-C(30)	120.6(6)
C(19)-C(20)-C(21)	120.1(7)
C(41)-C(42)-C(37)	121.4(6)
C(41)-C(42)-C(43)	113.9(5)
C(37)-C(42)-C(43)	124.7(5)
F(1)-C(44)-F(3)	105.7(5)
F(1)-C(44)-F(2)	105.9(5)
F(3)-C(44)-F(2)	105.1(5)
F(1)-C(44)-C(38)	112.8(5)
F(3)-C(44)-C(38)	114.5(5)
F(2)-C(44)-C(38)	112.0(5)
C(21)-C(22)-C(23)	120.1(7)
C(39)-C(38)-C(37)	121.9(5)
C(39)-C(38)-C(44)	116.6(5)
C(37)-C(38)-C(44)	121.3(5)
C(40)-C(39)-C(38)	120.6(6)
C(29)-C(28)-C(27)	120.2(6)

Bond lengths [Å] and Angles [°]	
C(39)-C(40)-C(41)	118.8(6)
C(42)-C(41)-C(40)	121.2(5)
F(6)-C(43)-F(5)	107.0(6)
F(6)-C(43)-F(4)	105.6(6)
F(5)-C(43)-F(4)	104.3(5)
F(6)-C(43)-C(42)	116.3(5)
F(5)-C(43)-C(42)	110.4(5)
F(4)-C(43)-C(42)	112.4(6)
C(22)-C(21)-C(20)	120.4(7)
C(28)-C(27)-C(26)	120.0(8)
C(9)-C(10)-C(11)	121.0(6)
C(46)-Cl(3)-C(46)#1	75.5(12)
Cl(3)-C(46)-Cl(3)#1	104.5(12)

Table 4.3 - Bond lengths [Å] and angles [°] for [PtCl(CCl=PAr')(PPh_3)$_2$]

	U11	U22	U33	U23	U13	U12
Pt(1)	24(1)	20(1)	27(1)	10(1)	0(1)	7(1)
P(3)	23(1)	20(1)	26(1)	10(1)	1(1)	7(1)
P(2)	26(1)	21(1)	28(1)	12(1)	7(1)	10(1)
C(30)	36(3)	35(3)	63(4)	31(3)	16(3)	14(3)
C(7)	29(3)	30(3)	21(3)	8(2)	3(2)	11(2)
C(45)	25(3)	21(3)	31(3)	15(2)	9(2)	11(2)
C(1)	17(2)	31(3)	28(3)	14(2)	3(2)	8(2)
C(2)	27(3)	29(3)	30(3)	6(2)	-2(2)	9(2)
C(8)	35(3)	40(3)	32(3)	17(3)	4(2)	16(3)
C(13)	32(3)	21(3)	29(3)	13(2)	4(2)	4(2)
C(32)	33(3)	29(3)	39(3)	15(3)	7(2)	14(2)
C(19)	48(4)	19(3)	28(3)	8(2)	6(2)	12(2)
C(24)	47(4)	26(3)	33(3)	8(2)	-1(3)	-1(3)
C(25)	25(3)	35(3)	34(3)	18(3)	8(2)	8(2)
C(31)	32(3)	30(3)	40(3)	18(3)	14(2)	18(2)
C(4)	28(3)	49(4)	34(3)	19(3)	2(2)	8(3)
C(3)	30(3)	52(4)	27(3)	10(3)	3(2)	15(3)
C(26)	53(4)	38(4)	57(4)	3(3)	31(3)	-7(3)
C(12)	28(3)	32(3)	42(3)	15(3)	-1(2)	3(2)
C(23)	74(5)	31(3)	44(4)	16(3)	-7(3)	-9(3)
C(9)	48(4)	66(5)	37(4)	25(3)	0(3)	29(3)
C(6)	46(4)	25(3)	41(4)	11(3)	12(3)	10(3)
C(5)	47(4)	37(4)	57(4)	28(3)	10(3)	5(3)
Cl(1)	50(1)	25(1)	36(1)	10(1)	-17(1)	6(1)
C(18)	33(3)	34(3)	36(3)	11(3)	9(3)	4(3)
C(14)	34(3)	33(3)	41(4)	10(3)	6(3)	15(3)
C(11)	26(3)	53(4)	41(4)	9(3)	1(3)	7(3)
C(16)	61(4)	41(4)	29(3)	1(3)	5(3)	0(3)
C(15)	54(4)	33(3)	41(4)	2(3)	7(3)	13(3)
C(17)	35(3)	52(4)	36(4)	4(3)	-3(3)	-9(3)
C(33)	39(4)	48(4)	56(4)	27(3)	9(3)	27(3)
C(36)	42(4)	53(4)	63(4)	42(4)	26(3)	29(3)
C(34)	37(4)	70(5)	75(5)	42(4)	22(3)	36(3)
C(35)	46(4)	74(5)	80(5)	47(4)	39(4)	37(4)
Cl(2)	34(1)	32(1)	30(1)	11(1)	9(1)	13(1)
P(3)	27(1)	41(1)	29(1)	15(1)	4(1)	13(1)
F(3)	52(2)	65(3)	45(2)	31(2)	4(2)	12(2)
F(2)	41(2)	93(3)	50(2)	35(2)	15(2)	29(2)
F(1)	43(2)	92(3)	53(3)	21(2)	-2(2)	-21(2)
C(37)	30(3)	44(3)	24(3)	17(3)	5(2)	15(3)
C(29)	38(4)	61(5)	83(6)	55(4)	11(3)	9(3)
C(20)	84(5)	50(4)	39(4)	20(3)	14(3)	41(4)
C(42)	34(3)	47(4)	30(3)	19(3)	4(2)	15(3)
C(44)	34(3)	64(5)	37(4)	22(3)	-6(3)	8(3)
C(22)	136(8)	35(4)	37(4)	11(3)	-16(5)	18(5)
C(38)	29(3)	45(4)	35(3)	20(3)	-1(2)	11(3)
F(6)	102(3)	48(2)	49(3)	19(2)	15(2)	-6(2)
F(5)	106(3)	60(3)	61(3)	41(2)	-4(2)	17(2)
F(4)	57(3)	71(3)	91(3)	38(3)	26(2)	5(2)

	U11	U22	U33	U23	U13	U12
C(39)	35(3)	52(4)	44(4)	16(3)	2(3)	10(3)
C(28)	56(5)	76(6)	58(5)	28(4)	32(4)	0(4)
C(40)	45(4)	65(5)	29(3)	8(3)	2(3)	20(3)
C(41)	45(4)	65(4)	29(3)	21(3)	8(3)	20(3)
C(43)	67(5)	55(4)	29(4)	22(3)	13(3)	19(4)
C(21)	142(8)	50(5)	31(4)	12(3)	18(4)	59(5)

Table 4.4 - Anisotropic displacement parameters ($Å^2$ x 10^3) for $[PtCl(CCl{=}PAr')(PPh_3)_2]$. The anisotropic displacement factor exponent takes the form: $-2\ pi^2\ [\ h^2\ a^2\ U11 + ... + 2\ h\ k\ a^*\ b^*\ U12\ ]$

	x	y	z	U(eq)
H(30A)	12595(6)	6619(5)	12975(3)	49
H(2A)	9561(5)	1302(5)	14213(2)	35
H(8A)	12081(6)	-1231(5)	13858(3)	40
H(32A)	9859(6)	5435(5)	12354(3)	38
H(24A)	14129(6)	4973(5)	13784(3)	45
H(4A)	7267(6)	-1421(6)	14923(3)	43
H(3A)	8101(6)	648(6)	14973(3)	43
H(26A)	12589(7)	3179(6)	12053(3)	65
H(12A)	13712(6)	1260(5)	12879(3)	41
H(23A)	15410(8)	6310(6)	14744(3)	64
H(9A)	14412(6)	-1437(6)	14036(3)	55
H(6A)	9324(6)	-2236(5)	13331(3)	44
H(5A)	7910(7)	-2852(6)	14109(3)	54
H(18A)	8079(6)	-1142(5)	12325(3)	42
H(14A)	12170(6)	-1488(5)	12182(3)	42
H(11A)	16042(6)	1038(6)	13052(3)	50
H(16A)	8959(7)	-3579(6)	10793(3)	58
H(15A)	11362(7)	-3010(5)	11222(3)	53
H(17A)	7304(7)	-2620(6)	11337(3)	56
H(33A)	7486(6)	5611(6)	12219(3)	51
H(36A)	8622(6)	3673(6)	13724(3)	53
H(34A)	5760(7)	4948(6)	12875(3)	63
H(35A)	6305(7)	3956(7)	13622(3)	68
H(29A)	14150(7)	7370(7)	12261(4)	66
H(20A)	10477(8)	5907(6)	14292(3)	62
H(22A)	14239(11)	7443(6)	15475(3)	85
H(39A)	5438(6)	-1479(6)	10122(3)	52
H(28A)	14877(8)	6052(7)	11446(4)	77
H(40A)	6925(7)	-904(6)	9353(3)	56
H(41A)	8710(7)	981(6)	9642(3)	52
H(21A)	11787(10)	7237(7)	15261(3)	81
H(27A)	14138(9)	3960(8)	11337(4)	89
H(10A)	16357(7)	-353(6)	13613(3)	56

Table 4.5 - Hydrogen coordinates (x 10^4) and isotropic displacement parameters ($Å^2$ x 10^3) for $[PtCl(CCl{=}PAr')(PPh_3)_2]$

4.3.2 Reaction between $ArP{=}CCl_2$ and $Pt(PPh_3)_4$

In an analogous reaction to the previous one the Fluoromes phosphaalkene was added to a solution of $Pt(PPh_3)_4$ in toluene and the solution was allowed to stir. The solution became dark orange in colour.

The ^{31}P NMR spectrum showed the formation of a number of new peaks; a septet with platinum satellites (δ = 197.8ppm $^2J_{P\text{-}Pt}$ = 404.2 Hz) which can be assigned to the phosphaalkene ligand ($^4J_{P\text{-}F}$ = 18.9 Hz), and two peaks associated with the PPh_3 groups still bonded to the platinum. The first PPh_3 group shows no P-P coupling (δ = 15.67 ppm $^1J_{P\text{-}Pt}$ = 4015.0 Hz) (singlet and platinum satellites), but the second PPh_3 ligand does show some P-P interaction (δ = 18.22 ppm $^1J_{P\text{-}Pt}$ = 1923.8 Hz, $^2J_{P\text{-}P}$ = 44.6 Hz) (doublet with platinum satellites). There is also a signal for free PPh_3 (δ = -2.67 ppm).

This reaction is analogous to that of the compound containing Ar' (see Section 4.3.1). The same effect of differing coupling constants for the two PPh_3 groups can clearly be seen. Unfortunately, no crystallographic data were obtained due to a poor crystal structure solution. A number of crystals were submitted for structure solution and none of them gave a satisfactory solution. In one case the solution appeared to be a compound with the PPh_3 ligands *cis* to each other, which is inconsistent with the NMR studies which indicated a compound with the PPh_3 groups *trans* to each other at all times.

The ^{19}F NMR spectrum shows the formation of a new doublet (δ = -58.0ppm, $^4J_{P\text{-}F}$ = 18.9 Hz). Over a period of time, however, a number of new peaks appeared. Unfortunately these were not assignable to anything indicating the formation of a single new product.

It is worth noting that although there is a difference in chemical shift for the compounds, the coupling constants between the phosphorus atom and the platinum are almost identical. This would imply that the *para* CF_3 group on the compound has little or no influence over bonding or the coupling constant.

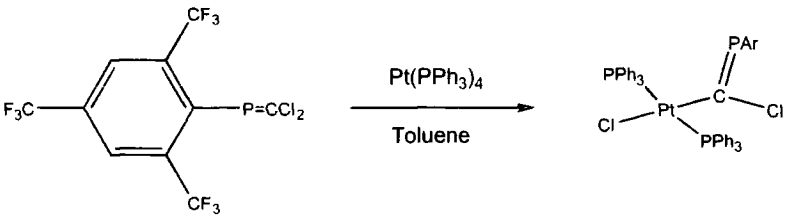

Equation 4.6 – Preparation of *trans*-[PtCl(CCl=PAr)(PPh_3)$_2$]

4.3.2.1 *Molecular structure of trans-[PtCl(CCl=PAr)(PPh_3)$_2$]*

Orange plate-like crystals were grown from toluene using the layering technique described in Appendix 1. The crystals were submitted for X-ray structural characterisation.

The data collection and structure solution was performed by Miss C. Broder.

Unfortunately the structure solution of this compound is not complete and cannot be included. A preliminary ORTEP diagram is shown below. The R value for the structural refinement is 4.7% although the residual electron density peaks in the density map are of the order of two electrons which is too great to be ignored.

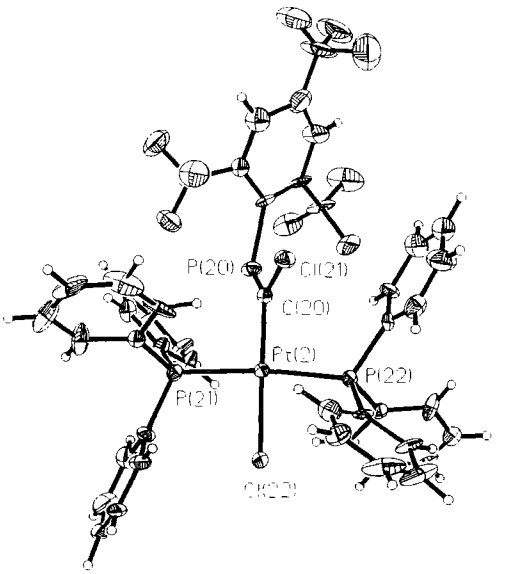

Figure 4.3 – Thermal ellipsoid diagram 150(2)K (50% probability) showing *trans*-[PtCl(CCl=PAr)(PPh_3)$_2$]

4.3.3 Reaction between Ar'P=CCl_2 and $Pd(PPh_3)_4$

Ar'P=CCl_2 was added to a solution of $Pd(PPh_3)_4$ in toluene and the reaction was allowed to stir. The solution changed colour from bright yellow to dark orange. The ^{31}P NMR spectrum showed the formation of a new septet in the spectrum. The chemical shift value for this compound is δ = 199.5 ppm ($^4J_{P-F}$ = 24.8 Hz). The ^{19}F NMR spectrum show the formation of a new doublet, δ = -59.6 ppm ($^4J_{P-F}$ = 24.7Hz).

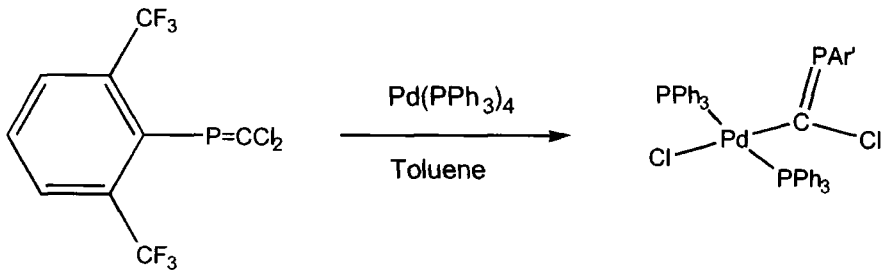

Equation 4.7 – Preparation of *trans*-[PdCl(PPh$_3$)$_2$(CCl=PAr')]

From the ^{31}P NMR spectrum it is apparent that a similar type of reaction has occurred to that in the Platinum reaction see Section 4.3.1. This palladium compound appears to be comparatively more unstable than the analogous Platinum compound, and after only a few hours the NMR spectrum becomes more complex as other species are formed.

Unfortunately the crystals grown of this product were not suitable for X-ray crystallographic studies.

4.3.4 Reaction between $ArP{=}CCl_2$ and $Pd(PPh_3)_4$

$ArP{=}CCl_2$ was added to a solution of $Pd(PPh_3)_4$ in toluene and the reaction was allowed to stir. The solution changed colour from bright yellow to dark orange. The ^{31}P NMR spectrum showed the formation of a new septet in the spectrum which correlates to the formation of a similar type of compound to those described in Section 4.3.3. The chemical shift value for the new compound is δ = 195.3 ppm ($^4J_{P\text{-}F}$ = 22.4 Hz). The ^{19}F NMR spectrum shows the formation of a new doublet and singlet, corresponding to the new compound. The chemical shift values are δ = -54.0 ppm ($^4J_{P\text{-}F}$ = 22.2Hz) (doublet) and δ = -63.8 ppm (singlet).

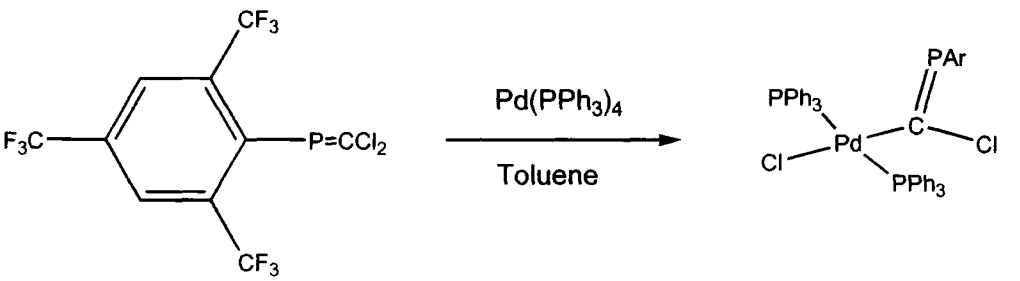

Equation 4.8 – Preparation of *trans*-$[PdCl(PPh_3)_2(CCl{=}PAr)]$

After a short period of time a doublet formed in the spectrum at a higher frequency to that of the new septet. This new compound was unstable and after only a matter of minutes the signal was lost from the spectrum and the formation of a number of new peaks was visible, all of which were unassignable.

4.4 Synthesis of other phosphaalkenes

4.4.1 Reaction between Ar'P=CCl_2, Bu_3SnH and DBU

An NMR scale reaction was carried out to try and determine whether or not it was possible to create the two phosphaalkenes Ar'P=C(H)Cl and Ar'P=CH_2. The standard synthesis of these two compounds is the reaction between RPH_2, base and CH_2Cl_2 [5]. This works for other large aryl groups such as supermesitylene and mesitylene, but not for Fluoroxyl or Fluoromes.

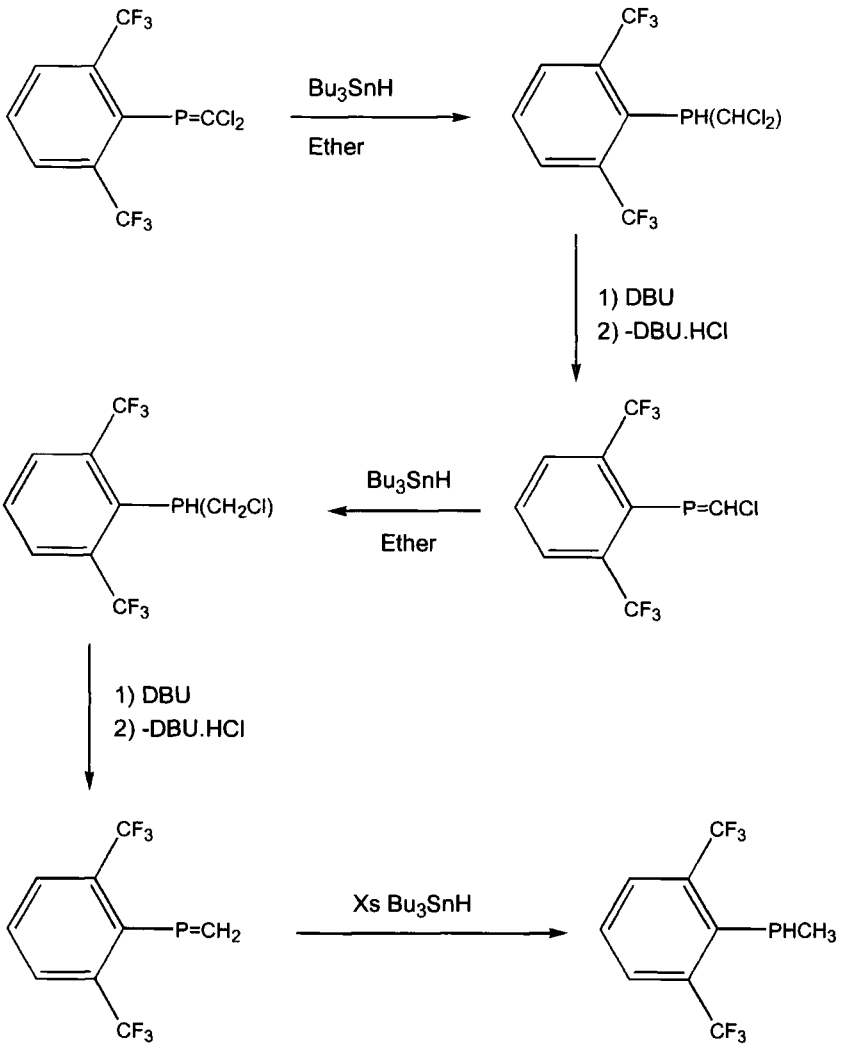

Equation 4.9 – Preparation of a number of phosphaalkenes

It has been shown that the phosphaalkene RP=C(H)Cl can lose HCl when irradiated with UV. With this in mind, an attempt to prepare Ar'P=C(H)Cl *via* this route was made.

Bu_3SnH was added dropwise into a solution containing Ar'P=CCl_2 and DBU in ether, reducing the P=C bond and forming the compound Ar'PH-$CHCl_2$ (δ = 38.6ppm). It then reacted with the DBU in solution to form the phosphaalkene Ar'P=C(H)Cl. (δ = 252.3ppm).

This compound then in turn was reduced again by the Bu_3SnH to form Ar'PH-CH_2Cl (δ = -56.6ppm). It then reacted with DBU to form the phosphaalkene Ar'P=CH_2 (δ = 288.0 ppm). If an excess of Bu_3SnH had been added, the final product would have been Ar'PH-CH_3 because without chlorine atoms remaining on the phosphorus or carbon atoms, it wouldn't react with DBU.

Going from Ar'P=CCl_2 to Ar'P=C(H)Cl and Ar'P=CH_2 there is a shift to higher frequency in the ^{31}P NMR spectrum.

Due to the yields in the formation of the initial phosphaalkene (Ar'P=CCl_2) these reactions were not performed on a larger scale due to the quantity of available starting material.

4.5 Experimental

4.5.1 Preparation of [PtCl(CCl=PAr')(PPh_3)$_2$]

A solution of Ar'P=CCl_2 (0.5g 1.5mmol) in toluene (50ml) was added to a solution of $Pt(PPh_3)_4$ (1.89g 1.5mmol) in toluene (50ml) and the solution was allowed to stir. The solution turned dark orange in colour and an orange precipitate was formed. The product was then recrystallised from a solution of toluene.. Yield 1.2g (73%) ^{31}P (CH_2Cl_2) δ = 201.9 ppm ($^2J_{P\text{-}Pt}$ = 406 Hz) (Septet with Pt satellites)

$$Ar'P{=}CCl_2 \xrightarrow[-\ PPh_3]{Pt(PPh_3)_4} PtCl(CCl{=}PAr')(PPh_3)_2$$

4.5.2 Preparation of [PtCl(CCl=PAr)(PPh_3)$_2$]

A solution of ArP=CCl_2 (0.5g 1.2mmol) in toluene (50ml) was added to a solution of $Pt(PPh_3)_4$ (1.49g 1.2mmol) in toluene (50ml) and the solution was allowed to stir. The solution turned dark orange in colour and an orange precipitate was formed. The product was then recrystallised from a solution of toluene. ^{31}P: δ = 197.8ppm $^1J_{P\text{-}Pt}$ = 202 Hz ($^4J_{P\text{-}F}$ = 23.8 Hz) (Singlet with Pt Satellites).^{19}F δ = 55.9 ppm (23.7 Hz) (doublet), δ = -61.1ppm (singlet). Yield 0.6g (57%).

$$ArP{=}CCl_2 \xrightarrow[-\ PPh_3]{Pt(PPh_3)_4} PtCl(CCl{=}PAr)(PPh_3)_2$$

4.5.3 Preparation of $[PdCl(CCl=PAr')(PPh_3)_2]$

A solution of $Ar'P=CCl_2$ (0.5g 1.5mmol) in toluene (50ml) was added to a solution of $Pd(PPh_3)_4$ (1.73g 1.5mmol) in toluene (50ml) and the solution was allowed to stir. The solution turned dark orange in colour. ^{31}P: δ = 199.5 ppm ($^4J_{P-F}$ = 24.8 Hz) (multiplet), ^{19}F: δ = -59.6 ppm ($^4J_{P-F}$ = 24.7Hz) (doublet).

$$Ar'P=CCl_2 \xrightarrow[-\ PPh_3]{Pd(PPh_3)_4} PdCl(CCl=PAr')(PPh_3)_2$$

4.5.4 Preparation of $[PdCl(CCl=PAr)(PPh_3)_2]$

A solution of $ArP=CCl_2$ (0.5g 1.2mmol) in toluene (50ml) was added to a solution of $Pd(PPh_3)_4$ (1.73g 1.5mmol) in toluene (50ml) and the solution was allowed to stir. The solution turned dark orange in colour. ^{31}P: δ = 195.3 ppm ($^4J_{P-F}$ = 22.4 Hz) (singlet), ^{19}F: δ = -54.0 ppm ($^4J_{P-F}$ = 22.2 Hz) (doublet) and δ = -63.8 ppm (singlet).

$$ArP=CCl_2 \xrightarrow[-\ PPh_3]{Pd(PPh_3)_4} PdCl(CCl=PAr)(PPh_3)_2$$

---

[1] V. D. Romanenko., M. Sanchez., T. V. Sarina., M-R. Mazieres., R. Wolf., *Tetrahedron Lett.*, **33**, 2981, 1992.
[2] R. J. Angelici., H. Jun., V. G. Young., *Organometallics*, 1994, **13**, 2444.
[3] H. P. Goodwin., *Ph.D. Thesis.*, Durham, 1990.
[4] J. F. Nixon., *Chem. Rev.*, 1988, **88**, 1327.
[5] R. Appel., C. Casser., M. Immelkeppel., F. Knoch., *Angew. Chem. Ed. Engl.*, 1984, **23**, 895.

Chapter 5

Synthesis and characterisation of novel P(I) compounds

5.1 Introduction

Metal phosphides have been known in the literature for some time now[1]. There have been a number of synthetic strategies employed, although none are analogous to a substitution reaction commonly used in metal-amide chemistry. In metal-amide chemistry, substitution of the amide ligand is possible by the reaction with an amine which is more acidic than the amine formed upon protonation of the amide ligand (HN^tBu_2 is more acidic than $HNMe_2$).

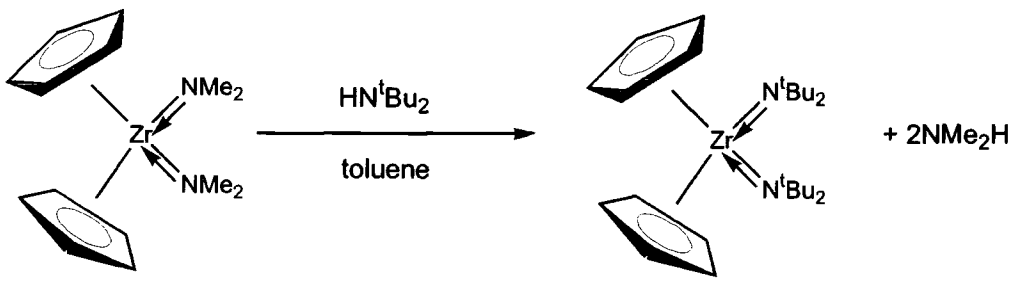

Equation 5.1 – Substitution of amines in metal-amide chemistry

No reaction between PPh_2H and a metal amide has been reported as far as we are aware. This is probably due to the weakly acidic proton on PPh_2H, rather than availability of the reagent.

The most commonly used reagent in P(I) chemistry is $LiPPh_2$ which is formed by the reaction of BuLi with PPh_2H. This reagent is then used in reaction with metal chloride bonds in an analogous way to lithiated amides, releasing LiCl and forming the desired metal phosphide.

5.2 Starting materials

5.2.1 Fluoroxyl disubstituted phosphanes

Ar'Ar''PCl and Ar'Ar''PH were both prepared as described in sections 2.2.8 and 2.2.9, where both compounds were used in the attempt to make P(I) compounds. Ar' has the major disadvantage over Ar in that it has a potential reaction site easily accessible by both electrophiles and nucleophiles. All attempts to make stable P(I) complexes have resulted in a large mixture of products, probably due to reaction of the P(I) species with other components of the reaction mixture.

5.2.2 Fluoromes disubstituted phosphanes

Ar_2PCl and Ar_2PH were both prepared as described before in sections 2.2.11 and 2.2.12. Both Ar_2PCl and Ar_2PH can be used to produce relatively stable P(I) complexes although the stability of some of the products is solvent dependent (see section 5.4). The stability of these compounds is much greater than that of the Fluoroxyl derivative, and they can be isolated and characterised. Ar_2PLi has not been isolable, however, due to the reasons discussed later (see sections 5.4.1 through 5.4.3).

5.3 The anionic P(I) species $Ar_2P^{(-)}$

The phosphorus (I) species $Ar_2P^{(-)}$ is very intensely coloured. It is dichroic, appearing dark blue (λ_{max} = 583nm , 599nm, 615nm) in concentrated solutions and red (λ_{max} = 383nm) in weaker concentrations. The intense blue colour is an indication of the formation of the species and it has been used qualitatively to see if the species has been produced. The species can be prepared by two basic methods:

1) Deprotonation of the disubstituted phosphane Ar_2PH. This can be observed with a reasonably weak base (e.g. pyrrolidine pK_b = 11.3). With weaker bases such as NEt_3 (pK_b= 9.81) the blue colour indicating the existence of the species can be facilitated if the solution is cooled in liquid nitrogen (see section 5.3.1).
2) Removal of the chlorine from the disubstituted phosphane Ar_2PCl in a redox reaction with a number of different low oxidation state metals compounds [e.g. Pt(0), Pd(0)]

UV studies on some of the blue solutions formed in these reactions (bases used NEt_3, N^iPr_3, DBU) showed that the blue colours were not identical. The maximum absorbance for the three solutions tested varied from 583nm to 615nm. This change implies that the anion and solvent may have some bearing on the colour.

The colour may be due to internal electron delocalisation in the $Ar_2P^{(-)}$ anion, possibly between π and π^* orbitals, though no modelling of the anion was performed.

In the literature[2] the standard preparation of a P(I) species is the lithiation of diphenyl phosphane, which forms the stable, yellow crystalline product $LiPPh_2$.

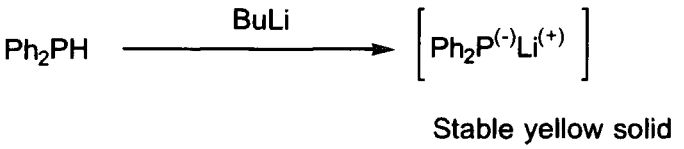

Equation 5.2 – Synthesis of $PPh_2^{(-)}Li^{(+)}$

The lithiation of Ar_2PH, however, presents a problem not encountered in the above example (equation 5.2). As seen in the lithiation of Fluoromes (see section 1.4) care must be taken to ensure that there is not an excess of BuLi otherwise there is the explosive risk of the formation of LiF. In the formation of $Ar_2P^{(-)}$ an extreme canonical form can be drawn which implies that some of the electron density associated with the negative charge of the $P^{(-)}$ species is delocalised on to the CF_3 groups. It then makes them even more susceptible to attack by the electrophilic $Li^{(+)}$. In the formation of Ar_2PLi a species is being formed which is very reactive towards itself, leading to the formation of coupling products and LiF.

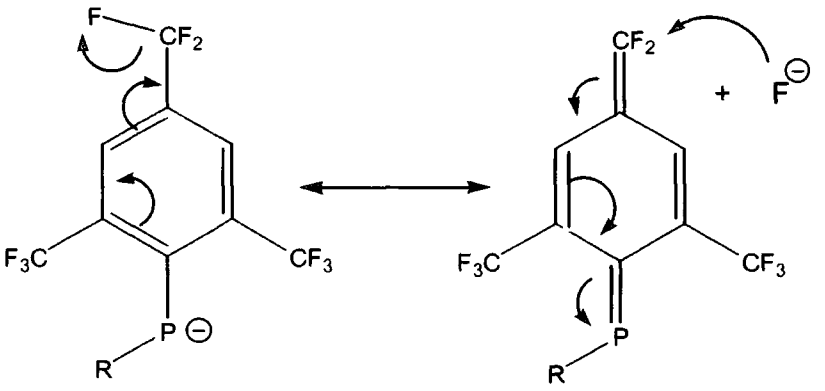

Figure 5.1 – A canonical form of $RP^{(-)}Fmes$

The stability of the Ar_2PLi species is solvent dependent, and it has proved to be impossible to isolate. Due to the instability of this compound and its potentially explosive nature, characterising NMR data were not recorded.

5.3.1 The appearance of the blue colour at low temperature

Equilibrium constants for acids and bases in solution determine the proton-donating (or accepting) ability at equilibrium. In a situation where the dissociation constant for the acid is much greater than that for the base, there will be little or no reaction (see equation 5.2).

$$Ar_2PH + NEt_3 \underset{k_b}{\overset{k_a}{\rightleftharpoons}} HNEt_3^{(+)} + Ar_2P^{(-)}$$

Equation 5.3 – Equilibrium in the reaction between Ar_2PH and NEt_3

In the reaction between Ar_2PH and NEt_3 at room temperature there is no sign of any blue colour, so it is reasonable to assume that NEt_3 is not a strong enough base to remove a proton from Ar_2PH in the solution (toluene). The equilibrium constants for the reaction K_a and K_b are defined in Figure 5.2.

$$K_a = \frac{[(HNEt_3)]^{(+)}\,[(Ar_2P)]^{(-)}}{[(NEt_3)]\,[(Ar_2PH)]} \qquad K_b = \frac{[(NEt_3)]\,[(Ar_2PH)]}{[(HNEt_3)]^{(+)}\,[(Ar_2P)]^{(-)}}$$

Figure 5.2 – Equilibrium constants for the reaction between Ar_2PH and NEt_3

The concentration of the Ar_2PH and NEt_3 is much greater than that of the anions and thus there is no colour visible. When the solution is cooled, however, a blue colour is observed. The temperature at which this colour is apparent depends on the solvent, and the base involved (not always NEt_3). The colder the temperature the more intense the colour.

The blue colour is very intense and if, as predicted, the $Ar_2P^{(-)}$ anion is coloured due to charge transfer, then only a very small amount need be present in the solution to produce a visible colour.

At room temperature there will be "some" of the anions present as is required if we assume an equilibrium. The concentration is so small and the length of time of their existence is so short that the blue colour is not visible. As the solution is cooled, the rate of exchange is lowered. This means that the length of time in which the very small concentration of these anions is present, becomes longer.

As the solution is cooled, there comes a point where enough of the $Ar_2P^{(-)}$ anion is present that it can be detected. To prove the existence of anions in the solution, if a conductimetry experiment were to be conducted, as the solution cooled, the conductance of the solution should be seen to rise. This type of experiment was not possible in the time frame of the experimental for this thesis.

This effect shows the existence of an equilibrium even when a strong acid and weak base are mixed together.

5.4 Reactions between Ar_2PH and selected bases

5.4.1 Attempted preparation of Ar_2PLi (in hexanes)

BuLi was added to a solution of Ar_2PH in hexanes at room temperature with the reaction vessel open to the mercury bubbler at all times. The solution became a very intense purple colour which almost instantly dissipated. The resulting solution showed no signs of any new phosphorus species according to the solution ^{31}P NMR spectrum.

BuLi was added to a solution of Ar_2PH in hexane at -78°C. The solution turned a very pale pink colour and over time did not darken. Upon warming the pink colour dissipated at approximately –30°C and the ^{31}P NMR spectrum showed no products other than the starting material present in the final solution.

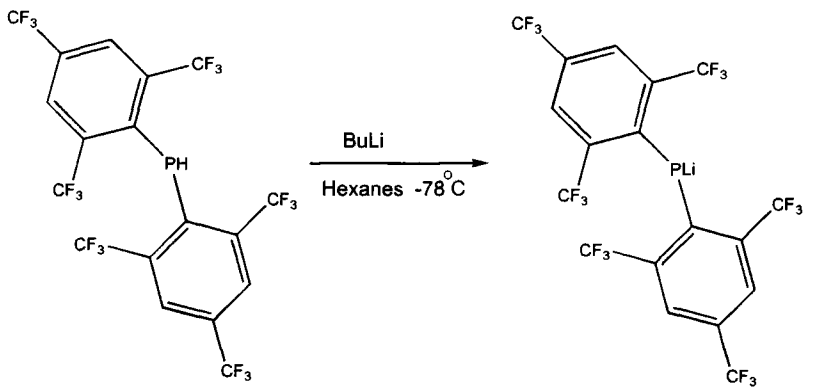

Equation 5.4 – Possible product formed by the lithiation in hexanes of Ar_2PH at –78°C

5.4.2 Preparation of Ar_2PLi (in THF)

BuLi was added to Ar_2PH in a solution of THF at -78°C. The solution turned a deep blue colour and was allowed to warm to room temperature, the solution remaining deep blue in colour. After approximately two hours, the solution turned dark brown in colour and there were no tangible products distinguishable in the ^{31}P NMR spectrum (other than the starting material). The ^{19}F NMR spectrum of the final solution showed the formation of a number of new species, none of which were distinguishable. Due to inherent instability of the compound, it was decided not to perform an NMR experiment on the blue solutions and so there are no characterising data on this compound.

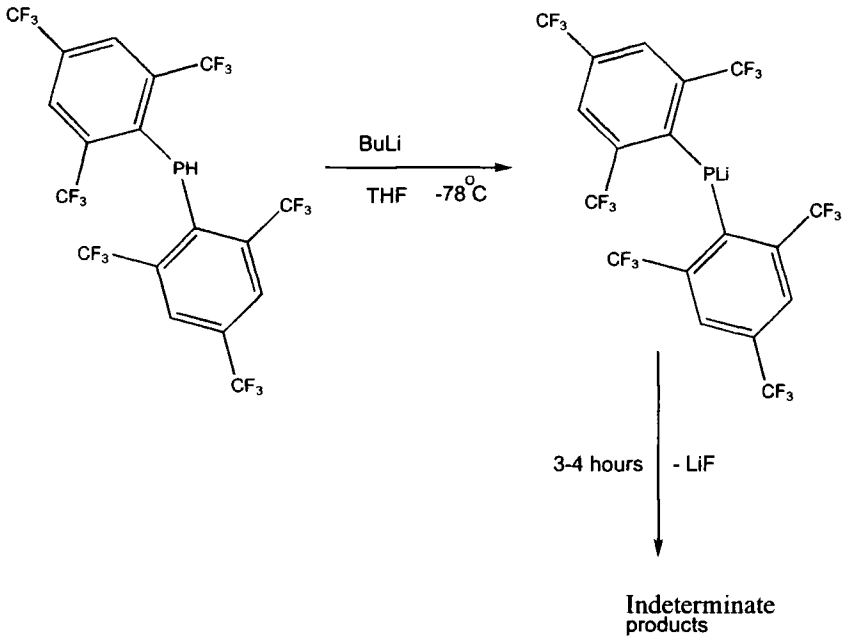

Equation 5.5 – Lithiation in THF of Ar_2PH at –78°C

5.4.3 Attempted stabilisation of Ar_2Li using PMDETA

PMDETA (pentamethyldiethylenetriamine) has been reported in the literature to stabilise the species $Li(PPh_3)_2$,[3] and has also been used extensively by Davidson *et al* [4]to stabilise lithiated species in solution.

BuLi was added to a solution containing an equimolar ratio of Ar_2PH and PMDETA in toluene at -78°C. The solution turned a dark blue colour and was allowed to warm to room temperature. The solution was allowed to stir for 30 minutes and then was placed in the freezer at -30°C in an attempt to freeze out the product. After eight hours the blue colour had dissipated from the solution and a brown slurry was left.

Again, due to the instability it was decided not to perform an NMR experiment on the blue solution so there are no NMR data on this compound.

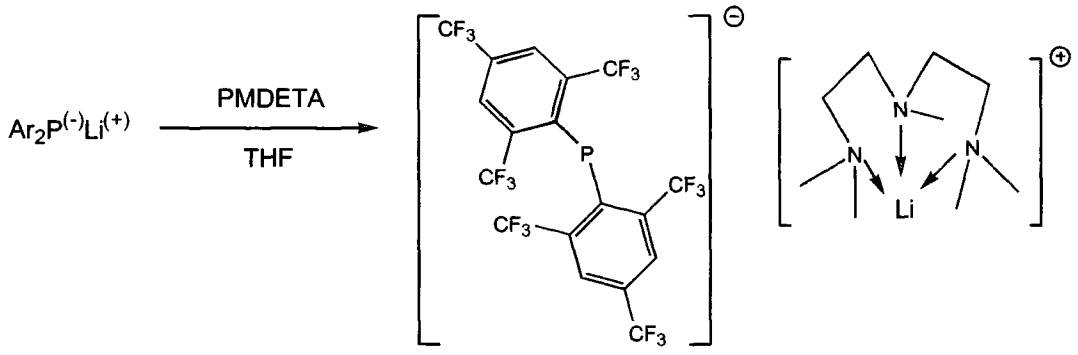

Equation 5.6 – Predicted products formed in the lithiation Ar_2PH using PMDETA to stabilise the lithium ion

The use of PMDETA was an attempt to coordinate the lithium ion in the product, and thus prevent it from attacking the CF_3 groups on a neighbouring molecule. This appears to slow down the process but does not prevent coupling and loss of LiF.

Again the ^{31}P NMR spectrum of the resulting final solution (not blue) showed no new species, whilst the ^{19}F NMR spectrum showed the formation of a number of indeterminate new fluorine species.

5.4.4 Reaction between Ar_2PH and pyrrolidine

Equimolar quantities of Ar_2PH and pyrrolidine were reacted together in toluene and a pale blue colour was observed. Upon being heated to 80°C the colour was almost entirely removed. The colour returned to the solution when cooled. The reaction was cooled in the freezer which resulted in the solution becoming more intensely coloured and resulted in the formation of crystals.

Upon warming to room temperature, the crystals turned from dark blue to a pale red colour and degenerated into a non-crystalline material before redesolving.

On examination under the microscope, under cooled conditions the blue crystals were not suitable for X-ray crystallography analysis.

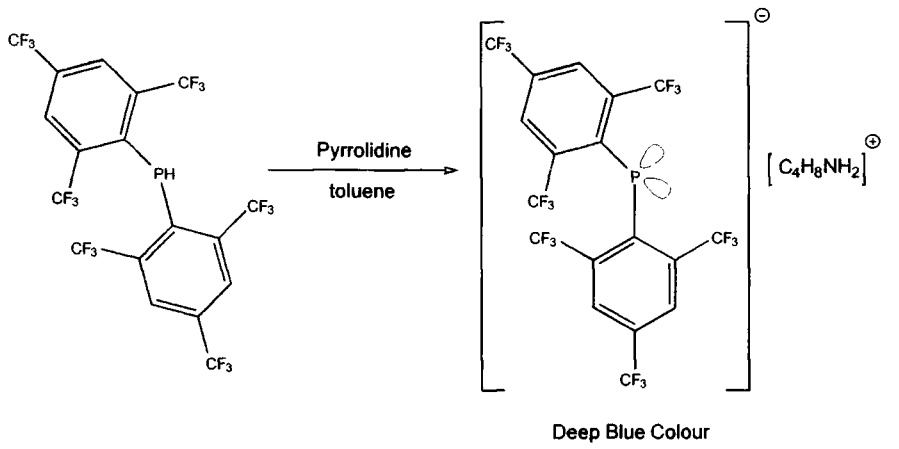

Equation 5.7 – Speculated products formed in the synthesis of $Ar_2P^{(-)}[pyrrolidineH]^{(+)}$

5.4.5 Reaction between Ar_2PH and $Ph_3P{=}CH_2$

A solution of Ar_2PH in toluene was added to an equimolar solution of the unstabilised ylide ($Ph_3P{=}CH_2$) in toluene. The solution produced a deep blue colour. From this reaction, very deep red crystals were formed and the compound was characterised by X-ray analysis. This reaction was performed by Miss S. Lamb.

The ^{31}P NMR solution spectrum shows the formation of $Ar_2P^{(-)}$ δ = 21.0 ppm (multiplet, $^4J_{P\text{-}F}$ = 32.6 Hz) and the phosphonium salt $[Ph_3PCH_3]^{(+)}$ δ = 21.6 ppm. The ^{19}F NMR spectrum shows a doublet and a singlet δ = -61.2 ppm ($^4J_{P\text{-}F}$ = 32.6 Hz) and δ = -63.3 ppm, respectively.

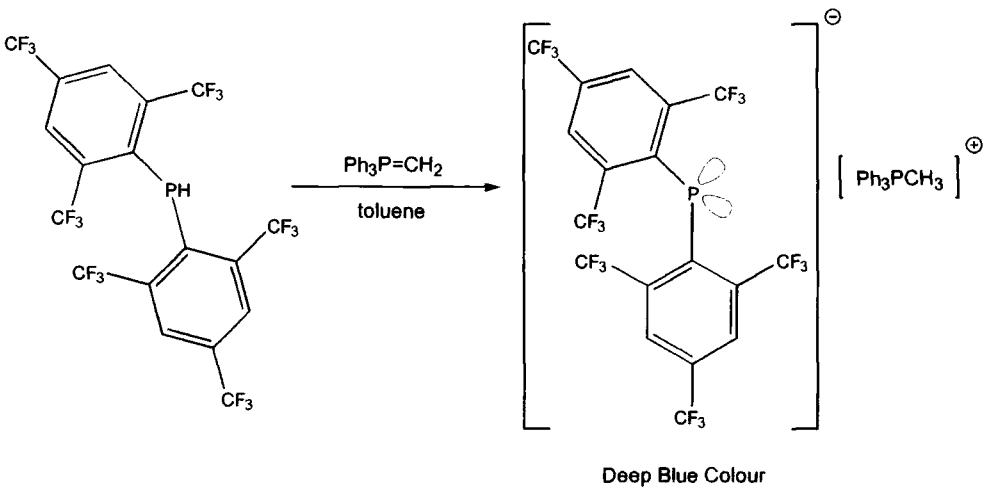

Equation 5.8 – Synthesis of $Ar_2P^{(-)}[PPh_3CCH_3]^{(+)}$

5.3.1.1 The molecular structure of $[C_6H_2(CF_3)_3]_2P^{(-)}$ $[Ph_3PCH_3]^{(+)}$

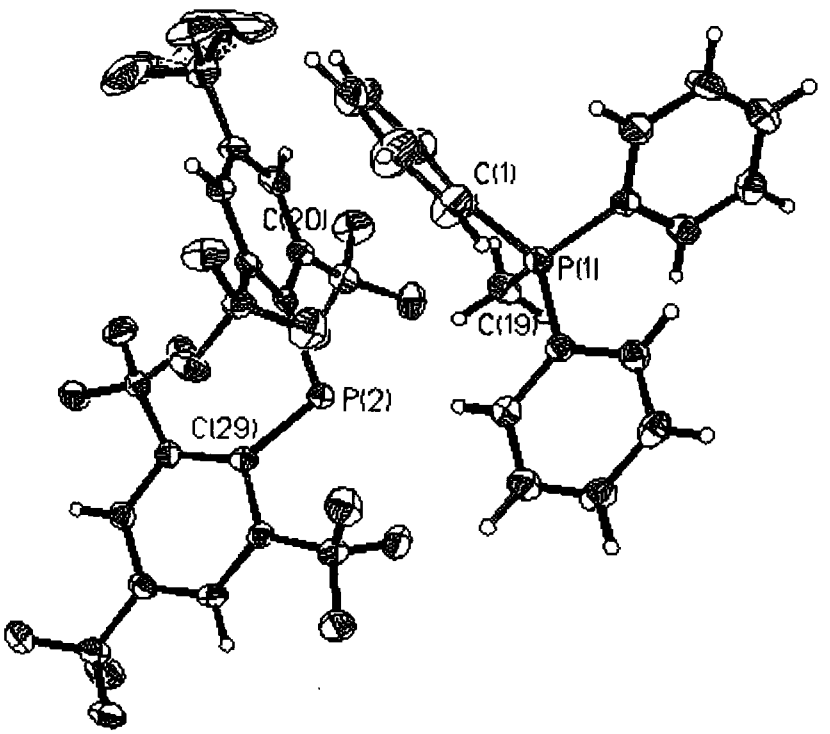

Figure 5.3 – Thermal Ellipsoid diagram for $Ar_2P^{(-)}[PPh_3CCH_3]^{(+)}$

Data were collected on a Siemens 3-circle diffractometer with a CCD area detector, ω scan mode $2\theta \leq 60.2°$. The structure was solved by direct methods and refined by full-matrix least squares against F^2 . Lists of crystal data and refinement parameters, anisotropic displacement parameters, bond lengths and angles, and atomic coordinates are given in tables 5.1 to 5.5.

Crystal data and structure refinement	
Identification code	Ar_2P-PPh_3CH_3
Empirical formula	$C_{37}H_{30}F_{18}P_2$
Formula weight	868.47
Temperature	150(2) K
Wavelength	0.71073 Å
Crystal system	triclinic
Space group	P-1
Unit cell dimensions	a = 11.532(2) Å, α = 110.21(3) °. b = 12.625(3) Å, β = 102.85(3) °. c = 13.579(3) Å, χ = 96.96(3) °.
Volume	1765.7(6) $Å^3$
Z	2
Number of reflections used	Calculation of cell = 512 Total = 12640 Unique = 9504 Obs [I>2σ] = 4709
Crystal description	cube shaped
Crystal colour	dark red
Density (calculated)	1.633 g/cm^3
Absorption coefficient	2.47 cm^{-1}
F(000)	868
Crystal size	0.1 x 0.2. x 0.1 mm
Theta range for data collection	1.67 to 30.09 °.
Index ranges	-14<=h<=16, -17<=k<=12, -10<=l<=18
Experiment device	Siemens SMART
Experiment methods	ω scans
Reflections collected	12640
Independent reflections	9054 [R(int) = 0.0290]
Refinement method	Full-matrix least-squares on F^2
Data / restraints / parameters	9044 / 0 / 537
Goodness-of-fit on F^2	0.929
Final R indices [I>2σ(I)]	R_1 = 0.0461, wR_2 = 0.0758
R indices (all data)	R_1 = 0.1182, wR_2 = 0.0999
Largest diff. peak and hole	0.374 and -0.319 e.($Å^{-3}$)

Table 5.1 - Crystal data and structure refinement for $(Ar_2P)(PPh_3CH_3)$

	x	y	z	U(eq)
P(1)	7796(1)	7494(1)	2572(1)	24(1)
C(1)	6834(2)	6318(2)	2654(2)	26(1)
C(2)	7325(3)	5587(2)	3118(2)	34(1)
P(2)	8488(1)	9427(1)	6606(1)	24(1)
C(3)	6584(3)	4633(2)	3104(2)	40(1)
C(4)	5351(3)	4399(3)	2629(2)	44(1)
C(5)	4841(3)	5115(3)	2175(3)	54(1)
C(6)	5580(3)	6074(2)	2180(2)	43(1)
C(7)	8391(2)	6931(2)	1424(2)	22(1)
C(8)	7930(2)	5807(2)	656(2)	33(1)
C(9)	8391(3)	5402(2)	-229(2)	39(1)
C(10)	9308(2)	6116(2)	-350(2)	33(1)
C(11)	9768(2)	7230(2)	406(2)	30(1)
C(12)	9321(2)	7644(2)	1300(2)	28(1)
C(13)	6937(2)	8535(2)	2386(2)	22(1)
C(14)	6584(2)	8622(2)	1373(2)	26(1)
C(15)	5962(2)	9459(2)	1251(2)	30(1)
C(16)	5683(2)	10212(2)	2148(2)	32(1)
C(17)	6015(2)	10123(2)	3153(2)	32(1)
C(18)	6650(2)	9289(2)	3282(2)	29(1)
C(19)	9028(2)	8190(2)	3791(2)	31(1)
C(20)	8466(2)	7916(2)	6448(2)	19(1)
C(21)	9561(2)	7506(2)	6568(2)	23(1)
F(101)	11696(1)	7718(1)	6865(1)	43(1)
F(102)	11097(1)	9177(1)	7807(1)	40(1)
F(103)	10834(1)	8749(1)	6083(1)	36(1)
C(22)	9569(2)	6367(2)	6452(2)	27(1)
C(23)	8494(2)	5581(2)	6187(2)	27(1)
C(24)	7395(2)	5918(2)	5972(2)	24(1)
C(25)	7369(2)	7048(2)	6068(2)	20(1)
F(107)	6041(1)	7709(1)	4921(1)	39(1)
F(108)	5240(1)	6325(1)	5293(1)	39(1)
F(109)	5796(1)	8044(1)	6518(1)	36(1)
C(26)	10783(2)	8286(2)	6837(2)	28(1)
C(28)	6133(2)	7294(2)	5705(2)	28(1)
C(29)	7798(2)	10091(2)	7666(2)	21(1)
C(30)	7831(2)	9940(2)	8682(2)	22(1)
C(31)	7515(2)	10730(2)	9527(2)	24(1)
C(32)	7114(2)	11692(2)	9440(2)	24(1)
C(33)	6991(2)	11843(2)	8463(2)	23(1)
C(34)	7294(2)	11070(2)	7596(2)	21(1)
C(35)	8278(2)	8970(2)	8939(2)	26(1)
F(118)	7510(1)	7924(1)	8335(1)	36(1)
F(117)	8387(1)	9103(1)	9985(1)	36(1)
F(116)	9372(1)	8849(1)	8788(1)	35(1)
C(36)	6882(3)	12563(2)	10401(2)	31(1)
F(113)	7916(1)	13301(1)	11125(1)	44(1)

	x	y	z	U(eq)
F(114)	6343(2)	12083(1)	10974(1)	43(1)
F(115)	6160(1)	13237(1)	10117(1)	39(1)
C(37)	7019(2)	11284(2)	6552(2)	29(1)
F(112)	8030(1)	11563(1)	6259(1)	37(1)
F(111)	6283(1)	10372(1)	5691(1)	38(1)
F(110)	6452(2)	12171(1)	6627(1)	43(1)
C(27)	8507(3)	4371(3)	6110(3)	38(1)
F(104)	9421(3)	3970(3)	5697(6)	64(2)
F(105)	8663(8)	4251(3)	7031(3)	83(2)
F(106)	7513(3)	3603(4)	5418(4)	51(1)
F(202)	9584(9)	4291(13)	6668(26)	93(8)
F(201)	7873(20)	4192(14)	6829(18)	97(7)
F(200)	8066(39)	3622(15)	5257(12)	185(14)

Table 5.2 - Atomic coordinates (x 10^4) and equivalent isotropic displacement parameters ($Å^2$ x 10^3) for $(Ar_2P)(PPh_3CH_3)$. U(eq) is defined as one third of the trace of the orthogonalized Uij tensor

Bond lengths [Å] and angles [°]	
P(1)-C(19)	1.782(3)
P(1)-C(13)	1.791(2)
P(1)-C(1)	1.793(3)
P(1)-C(7)	1.799(2)
C(1)-C(6)	1.393(4)
C(1)-C(2)	1.394(3)
C(2)-C(3)	1.380(4)
P(2)-C(29)	1.802(2)
P(2)-C(20)	1.841(2)
C(3)-C(4)	1.373(4)
C(4)-C(5)	1.378(4)
C(5)-C(6)	1.391(4)
C(7)-C(8)	1.390(3)
C(7)-C(12)	1.393(3)
C(8)-C(9)	1.383(3)
C(9)-C(10)	1.381(4)
C(10)-C(11)	1.376(3)
C(11)-C(12)	1.385(3)
C(13)-C(14)	1.391(3)
C(13)-C(18)	1.397(3)
C(14)-C(15)	1.382(3)
C(15)-C(16)	1.393(3)
C(16)-C(17)	1.380(3)
C(17)-C(18)	1.390(3)
C(20)-C(21)	1.419(3)
C(20)-C(25)	1.433(3)
C(21)-C(22)	1.393(3)
C(21)-C(26)	1.508(3)
F(101)-C(26)	1.344(3)
F(102)-C(26)	1.341(3)
F(103)-C(26)	1.351(3)
C(22)-C(23)	1.381(3)
C(23)-C(24)	1.387(3)
C(23)-C(27)	1.497(4)
C(24)-C(25)	1.391(3)
C(25)-C(28)	1.508(3)
F(107)-C(28)	1.329(3)
F(108)-C(28)	1.356(3)
F(109)-C(28)	1.350(3)
C(29)-C(30)	1.448(3)
C(29)-C(34)	1.451(3)
C(30)-C(31)	1.389(3)
C(30)-C(35)	1.503(3)
C(31)-C(32)	1.383(3)
C(32)-C(33)	1.383(3)
C(32)-C(36)	1.491(3)
C(33)-C(34)	1.391(3)
C(34)-C(37)	1.506(3)
C(35)-F(116)	1.341(3)

Bond lengths [Å] and angles [°]	
C(35)-F(117)	1.345(3)
C(35)-F(118)	1.358(3)
C(36)-F(114)	1.344(3)
C(36)-F(115)	1.350(3)
C(36)-F(113)	1.354(3)
C(37)-F(111)	1.344(3)
C(37)-F(110)	1.348(3)
C(37)-F(112)	1.358(3)
C(27)-F(200)	1.17(2)
C(27)-F(105)	1.287(4)
C(27)-F(106)	1.326(5)
C(27)-F(202)	1.339(13)
C(27)-F(104)	1.371(4)
C(27)-F(201)	1.403(14)
F(104)-F(202)	1.20(3)
F(104)-F(200)	1.49(4)
F(105)-F(201)	.88(2)
F(105)-F(202)	1.268(14)
F(106)-F(200)	.72(4)
F(106)-F(201)	1.73(2)
C(19)-P(1)-C(13)	108.70(12)
C(19)-P(1)-C(1)	110.81(13)
C(13)-P(1)-C(1)	110.01(12)
C(19)-P(1)-C(7)	109.33(12)
C(13)-P(1)-C(7)	109.45(11)
C(1)-P(1)-C(7)	108.53(11)
C(6)-C(1)-C(2)	118.8(2)
C(6)-C(1)-P(1)	120.0(2)
C(2)-C(1)-P(1)	121.1(2)
C(3)-C(2)-C(1)	120.7(3)
C(29)-P(2)-C(20)	109.09(11)
C(4)-C(3)-C(2)	120.0(3)
C(3)-C(4)-C(5)	120.5(3)
C(4)-C(5)-C(6)	119.9(3)
C(5)-C(6)-C(1)	120.1(3)
C(8)-C(7)-C(12)	119.7(2)
C(8)-C(7)-P(1)	121.3(2)
C(12)-C(7)-P(1)	119.1(2)
C(9)-C(8)-C(7)	120.1(2)
C(10)-C(9)-C(8)	119.9(2)
C(11)-C(10)-C(9)	120.3(2)
C(10)-C(11)-C(12)	120.3(2)
C(11)-C(12)-C(7)	119.6(2)
C(14)-C(13)-C(18)	119.9(2)
C(14)-C(13)-P(1)	121.0(2)
C(18)-C(13)-P(1)	119.1(2)
C(15)-C(14)-C(13)	120.4(2)
C(14)-C(15)-C(16)	119.5(3)
C(17)-C(16)-C(15)	120.5(2)
C(16)-C(17)-C(18)	120.2(2)

Bond lengths [Å] and angles [°]	
C(17)-C(18)-C(13)	119.5(2)
C(21)-C(20)-C(25)	115.2(2)
C(21)-C(20)-P(2)	120.9(2)
C(25)-C(20)-P(2)	123.4(2)
C(22)-C(21)-C(20)	122.0(2)
C(22)-C(21)-C(26)	116.4(2)
C(20)-C(21)-C(26)	121.6(2)
C(23)-C(22)-C(21)	120.7(2)
C(22)-C(23)-C(24)	119.3(2)
C(22)-C(23)-C(27)	120.7(2)
C(24)-C(23)-C(27)	120.0(2)
C(23)-C(24)-C(25)	120.7(2)
C(24)-C(25)-C(20)	121.5(2)
C(24)-C(25)-C(28)	116.5(2)
C(20)-C(25)-C(28)	121.9(2)
F(102)-C(26)-F(101)	105.7(2)
F(102)-C(26)-F(103)	106.3(2)
F(101)-C(26)-F(103)	105.6(2)
F(102)-C(26)-C(21)	114.2(2)
F(101)-C(26)-C(21)	112.2(2)
F(103)-C(26)-C(21)	112.1(2)
F(107)-C(28)-F(109)	106.9(2)
F(107)-C(28)-F(108)	105.9(2)
F(109)-C(28)-F(108)	104.6(2)
F(107)-C(28)-C(25)	113.2(2)
F(109)-C(28)-C(25)	114.1(2)
F(108)-C(28)-C(25)	111.6(2)
C(30)-C(29)-C(34)	113.1(2)
C(30)-C(29)-P(2)	130.7(2)
C(34)-C(29)-P(2)	115.3(2)
C(31)-C(30)-C(29)	122.1(2)
C(31)-C(30)-C(35)	114.4(2)
C(29)-C(30)-C(35)	123.4(2)
C(32)-C(31)-C(30)	122.1(2)
C(31)-C(32)-C(33)	118.4(2)
C(31)-C(32)-C(36)	120.0(2)
C(33)-C(32)-C(36)	121.5(2)
C(32)-C(33)-C(34)	121.2(2)
C(33)-C(34)-C(29)	122.8(2)
C(33)-C(34)-C(37)	115.5(2)
C(29)-C(34)-C(37)	121.6(2)
F(116)-C(35)-F(117)	105.7(2)
F(116)-C(35)-F(118)	106.2(2)
F(117)-C(35)-F(118)	104.6(2)
F(116)-C(35)-C(30)	113.9(2)
F(117)-C(35)-C(30)	112.5(2)
F(118)-C(35)-C(30)	113.1(2)
F(114)-C(36)-F(115)	106.5(2)
F(114)-C(36)-F(113)	105.9(2)
F(115)-C(36)-F(113)	105.5(2)

Bond lengths [Å] and angles [°]	
F(114)-C(36)-C(32)	113.0(2)
F(115)-C(36)-C(32)	112.7(2)
F(113)-C(36)-C(32)	112.7(2)
F(111)-C(37)-F(110)	105.6(2)
F(111)-C(37)-F(112)	106.5(2)
F(110)-C(37)-F(112)	105.3(2)
F(111)-C(37)-C(34)	113.1(2)
F(110)-C(37)-C(34)	112.3(2)
F(112)-C(37)-C(34)	113.4(2)
F(200)-C(27)-F(105)	124.5(12)
F(200)-C(27)-F(106)	33(2)
F(105)-C(27)-F(106)	107.3(4)
F(200)-C(27)-F(202)	115.2(12)
F(105)-C(27)-F(202)	57.7(9)
F(106)-C(27)-F(202)	133.9(7)
F(200)-C(27)-F(104)	72(2)
F(105)-C(27)-F(104)	106.0(4)
F(106)-C(27)-F(104)	103.1(3)
F(202)-C(27)-F(104)	52.6(11)
F(200)-C(27)-F(201)	108(2)
F(105)-C(27)-F(201)	37.7(7)
F(106)-C(27)-F(201)	78.5(10)
F(202)-C(27)-F(201)	95.2(9)
F(104)-C(27)-F(201)	137.3(6)
F(200)-C(27)-C(23)	117.8(9)
F(105)-C(27)-C(23)	114.3(3)
F(106)-C(27)-C(23)	113.7(3)
F(202)-C(27)-C(23)	111.9(6)
F(104)-C(27)-C(23)	111.6(3)
F(201)-C(27)-C(23)	106.2(6)
F(202)-F(104)-C(27)	62.3(5)
F(202)-F(104)-F(200)	103.1(11)
C(27)-F(104)-F(200)	47.8(8)
F(201)-F(105)-F(202)	141(2)
F(201)-F(105)-C(27)	78.3(12)
F(202)-F(105)-C(27)	63.2(9)
F(200)-F(106)-C(27)	61(2)
F(200)-F(106)-F(201)	109(2)
C(27)-F(106)-F(201)	52.8(6)
F(104)-F(202)-F(105)	118.6(13)
F(104)-F(202)-C(27)	65.1(11)
F(105)-F(202)-C(27)	59.1(4)
F(105)-F(201)-C(27)	63.9(9)
F(105)-F(201)-F(106)	102.9(13)
C(27)-F(201)-F(106)	48.8(6)
F(106)-F(200)-C(27)	86(2)
F(106)-F(200)-F(104)	143(2)
C(27)-F(200)-F(104)	60.6(14)

Table 5.3 - Bond lengths [Å] and angles [°] for $(Ar_2P)(PPh_3CH_3)$

	U11	U22	U33	U23	U13	U12
P(1)	24(1)	23(1)	24(1)	9(1)	8(1)	7(1)
C(1)	27(2)	28(1)	26(1)	12(1)	12(1)	8(1)
C(2)	36(2)	34(2)	35(2)	16(1)	11(1)	10(1)
P(2)	30(1)	18(1)	23(1)	6(1)	11(1)	5(1)
C(3)	59(2)	32(2)	38(2)	19(1)	21(2)	14(2)
C(4)	56(2)	36(2)	42(2)	12(2)	25(2)	-2(2)
C(5)	34(2)	54(2)	76(2)	34(2)	12(2)	-1(2)
C(6)	34(2)	44(2)	58(2)	30(2)	10(2)	7(2)
C(7)	20(1)	21(1)	23(1)	9(1)	5(1)	7(1)
C(8)	37(2)	26(2)	35(2)	9(1)	15(1)	2(1)
C(9)	46(2)	26(2)	34(2)	-2(1)	14(2)	5(1)
C(10)	31(2)	39(2)	28(2)	8(1)	13(1)	12(1)
C(11)	23(2)	36(2)	33(2)	15(1)	10(1)	6(1)
C(12)	28(2)	25(1)	27(2)	6(1)	7(1)	4(1)
C(13)	21(1)	22(1)	25(1)	10(1)	7(1)	6(1)
C(14)	25(2)	27(1)	27(2)	11(1)	10(1)	6(1)
C(15)	25(2)	35(2)	36(2)	20(1)	7(1)	6(1)
C(16)	25(2)	31(2)	48(2)	22(1)	13(1)	12(1)
C(17)	32(2)	30(2)	36(2)	12(1)	15(1)	13(1)
C(18)	35(2)	28(2)	29(2)	14(1)	13(1)	10(1)
C(19)	29(2)	35(2)	25(2)	7(1)	5(1)	8(1)
C(20)	20(1)	20(1)	14(1)	4(1)	5(1)	4(1)
C(21)	22(1)	24(1)	18(1)	5(1)	3(1)	6(1)
F(101)	21(1)	44(1)	63(1)	20(1)	7(1)	9(1)
F(102)	33(1)	38(1)	28(1)	-2(1)	2(1)	-9(1)
F(103)	30(1)	43(1)	35(1)	17(1)	10(1)	2(1)
C(22)	22(2)	28(2)	30(2)	9(1)	7(1)	11(1)
C(23)	30(2)	19(1)	31(2)	8(1)	9(1)	9(1)
C(24)	28(2)	18(1)	25(1)	5(1)	8(1)	2(1)
C(25)	22(1)	21(1)	19(1)	6(1)	8(1)	7(1)
F(107)	32(1)	49(1)	40(1)	25(1)	3(1)	12(1)
F(108)	21(1)	26(1)	56(1)	8(1)	1(1)	0(1)
F(109)	29(1)	33(1)	42(1)	4(1)	12(1)	15(1)
C(26)	24(2)	29(2)	28(2)	8(1)	5(1)	5(1)
C(28)	27(2)	22(1)	31(2)	7(1)	7(1)	4(1)
C(29)	19(1)	17(1)	21(1)	3(1)	2(1)	1(1)
C(30)	22(1)	21(1)	19(1)	6(1)	5(1)	1(1)
C(31)	26(2)	23(1)	21(1)	6(1)	7(1)	2(1)
C(32)	24(2)	21(1)	24(1)	5(1)	9(1)	5(1)
C(33)	21(1)	16(1)	30(2)	6(1)	6(1)	5(1)
C(34)	20(1)	19(1)	25(1)	10(1)	7(1)	2(1)
C(35)	35(2)	25(2)	20(1)	8(1)	11(1)	8(1)
F(118)	50(1)	20(1)	35(1)	9(1)	10(1)	5(1)
F(117)	58(1)	38(1)	22(1)	15(1)	16(1)	23(1)
F(116)	35(1)	47(1)	34(1)	21(1)	14(1)	22(1)

	U11	U22	U33	U23	U13	U12
C(36)	36(2)	24(2)	33(2)	7(1)	14(1)	9(1)
F(113)	41(1)	36(1)	34(1)	-6(1)	7(1)	4(1)
F(114)	83(1)	34(1)	42(1)	12(1)	34(1)	14(1)
F(115)	46(1)	30(1)	42(1)	8(1)	19(1)	20(1)
C(37)	32(2)	27(2)	34(2)	15(1)	12(1)	12(1)
F(112)	43(1)	40(1)	45(1)	28(1)	24(1)	15(1)
F(111)	40(1)	45(1)	26(1)	12(1)	3(1)	11(1)
F(110)	57(1)	47(1)	44(1)	28(1)	22(1)	33(1)
F(104)	53(2)	36(2)	106(4)	20(2)	34(2)	24(2)
F(105)	178(6)	31(2)	31(2)	14(1)	8(3)	26(3)
F(106)	41(2)	18(2)	78(4)	13(2)	-1(2)	-1(1)
F(202)	37(6)	66(8)	208(25)	90(13)	28(9)	32(5)
F(201)	125(14)	60(7)	177(18)	80(10)	103(13)	58(9)
F(200)	456(41)	52(11)	14(6)	-11(6)	9(18)	115(20)

Table 5.4 - Anisotropic displacement parameters ($Å^2$ x 10^3) for $(Ar_2P)(PPh_3CH_3)$. The anisotropic displacement factor exponent takes the form: $-2\pi^2$ [$h^2 a^2$ U11 + ... + 2 h k a* b* U12]

	x	y	z	U(eq)
H(2A)	8160(3)	5742(2)	3442(2)	41
H(3A)	6821(3)	4150(2)	3415(2)	47
H(4A)	4856(3)	3751(3)	2614(2)	53
H(5A)	4003(3)	4958(3)	1865(3)	64
H(6A)	5237(3)	6554(2)	1866(2)	52
H(8A)	7310(2)	5327(2)	736(2)	40
H(9A)	8085(3)	4649(2)	-741(2)	47
H(10A)	9615(2)	5842(2)	-946(2)	40
H(11A)	10382(2)	7707(2)	317(2)	35
H(12A)	9641(2)	8395(2)	1815(2)	34
H(14A)	6769(2)	8115(2)	775(2)	31
H(15A)	5731(2)	9518(2)	574(2)	36
H(16A)	5270(2)	10780(2)	2070(2)	38
H(17A)	5814(2)	10622(2)	3745(2)	38
H(18A)	6881(2)	9233(2)	3960(2)	34
H(19A)	9496(2)	7640(2)	3900(2)	47
H(19B)	8713(2)	8498(2)	4404(2)	47
H(19C)	9539(2)	8807(2)	3726(2)	47
H(22A)	10306(2)	6133(2)	6554(2)	32
H(24A)	6667(2)	5382(2)	5761(2)	29
H(31A)	7573(2)	10608(2)	10172(2)	29
H(33A)	6701(2)	12474(2)	8385(2)	28

Table 5.5 - Hydrogen coordinates (x 10^4) and isotropic displacement parameters ($Å^2$ x 10^3) for $(Ar_2P)(PPh_3CH_3)$

There are some very interesting things to note concerning the anion in the molecular structure of $[CH_3PPh_3]^{(+)}Ar_2P^{(-)}$. The structure of the phosphonium cation shows no interesting variations from other compounds containing this species. There are, however, a number of notable points in the structure of the anion as compared with the $(PPh_2)^{(+)}$ anion.

The geometry of the anion is influenced by the steric bulk of the aryl groups. The structural orientation of the molecule is such that the interaction between neighbouring *ortho* CF_3 groups on the two aryl groups is at a minimum. The angle between the planes of the two aryl rings is 86.4°

This factor in itself causes two phenomena: the angle (C-P-C) between the two aryl groups is larger than in equivalent compounds recorded in the CSD[5], and the angle between the two planes containing the aryl groups is significantly larger.

The twisting of the aryl groups would also appear to have some electronic consequences. There is a distinct difference in the length of the two P-C bonds [1.802(2) and 1.841(2)Å], and both aryl groups are inequivalent. The aryl group associated with the longer P-C bond is not in the same plane as this bond and the ring itself is not planar. This would suggest that there is significantly more delocalisation of the negative charge onto this aryl group, rather than equal delocalisation onto both groups.

Figure 5.4 shows the deviation of one of the aryl rings from planarity. The diagram was composed by superimposing one aryl ring on the top of the other one, so comparing the planarity of each ring.

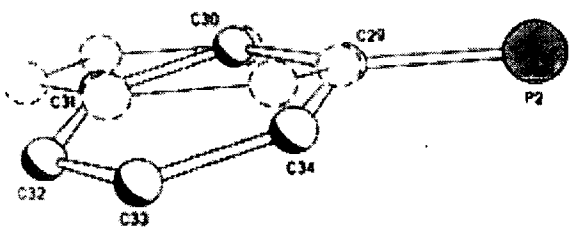

Figure 5.4 – Superimposition of the two aryl rings, highlighting the distortion from planarity

Delocalisation of electron density from the lone pair into the aryl groups is shown in the irregularity of the carbon-carbon bond lengths in the two aryl groups. The carbon-carbon bonds which are adjacent to the phosphorus atom are significantly longer than other bonds in the aryl ring (see Table 5.6).

C-C bonds in aryl group 1	C-C Bond length (Å)	C-C bonds in aryl group 2	C-C Bond length (Å)
C(20)-C(21)	1.419(3)	C(29)-C(30)	1.448(3)
C(25)-C(20)	1.433(3)	C(29)-C(34)	1.451(3)
C(21)-C(22)	1.393(3)	C(30)-C(31)	1.389(3)
C(22)-C(23)	1.381(3)	C(31)-C(32)	1.383(3)
C(23)-C(24)	1.387(3)	C(32)-C(33)	1.383(3)
C(24)-C(25)	1.391(3)	C(33)-C(34)	1.391(3)

Table 5.6 - Comparisons of carbon-carbon bond lengths in the aryl rings

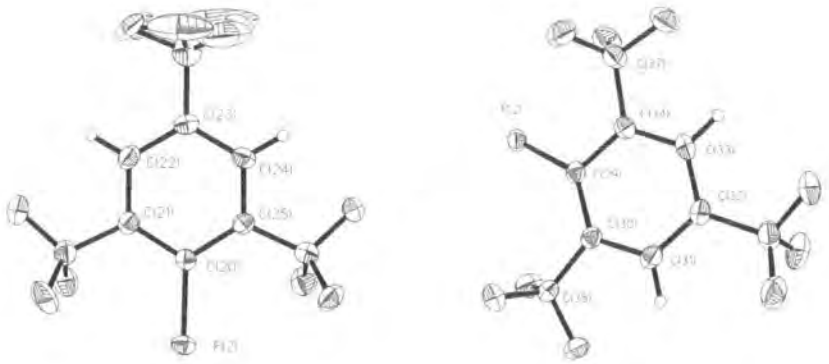

Aryl ring (1) Aryl ring (2)

Figure 5.5 – The two aryl rings in the compound $Ar_2P^{(-)}$

The angle (C-P-C) between the two aryl groups in Ar_2PH is 107.5°, and this increases slightly to 109.1° upon deprotonation. This is probably due to an electronic effect and allows a greater interaction between the lone pair of electrons on the phosphorus and the aryl rings.

If we consider the plane of the aryl ring (1), which is the non-deformed ring, and assume the other ring (2) is twisted away from that one, it is possible to draw some conclusions about the electronic properties of the system.

The aryl ring (2) is not in the same plane as the C-P-C bonds, and the ring itself is also slightly buckled, which would imply a greater change in hybridisation of C(29) than C(20). Because the ring is twisted almost 90^{o} away from the lone pairs, there is very little direct delocalisation arising from the π-π interactions between the lone pair and the ring. If we infer that the oxidation state of the phosphorus in $Ar_2P^{(-)}$ is P(I) then it may be regarded as sp^3 hybridised. Due to the twisting of the rings significantly away from the planar system from an expected sp^3 hybrid phosphorus atom, it is possible to infer that the terms hybridisation and oxidation are not the best ways to describe the electronic effects inherent in the system. Although the removal of hydrogen is intrinsically known as oxidation, calling the oxidation state of the phosphorus atom in $Ar_2P^{(-)}$ "P(I)" does not tell the whole story.

The formation of this compound illustrates the possibility for the formation of a number of stable $Ar_2P^{(-)}$ species and comparisons thereof. The phosphonium ion is bulky and there are a number of hydrogen bonded interactions between the anion and cation which also contribute to stability. Thus far, this is the only successful X-ray structure of the anion despite numerous attempts to grow crystals of other materials.

5.4.6 Reaction between Ar_2PH and DBU

DBU was added to a solution of Ar_2PH in toluene, resulting in a deep blue colour. The ^{31}P NMR spectrum of this solution showed the complete reaction of the Ar_2PH and the formation of a new resonance which was shifted significantly to a higher frequency (δ = 30.2 ppm) ($^{4}J_{P\text{-}F}$ = 36.7 Hz) (complex multiplet). The ^{19}F Spectrum shows the formation of two new sets of peaks, a doublet (δ = -59.4 ppm) ($^{4}J_{P\text{-}F}$ = 37.5 Hz) and a singlet (δ = -60.7ppm).

This species appeared to be more stable than the secondary amine derivative formed using pyrrolidine. The species is relatively stable in solution over a number of days. Unfortunately, during any attempt to isolate the material it decomposes rapidly, producing a large number of peaks in both the ^{31}P and the ^{19}F NMR spectra.

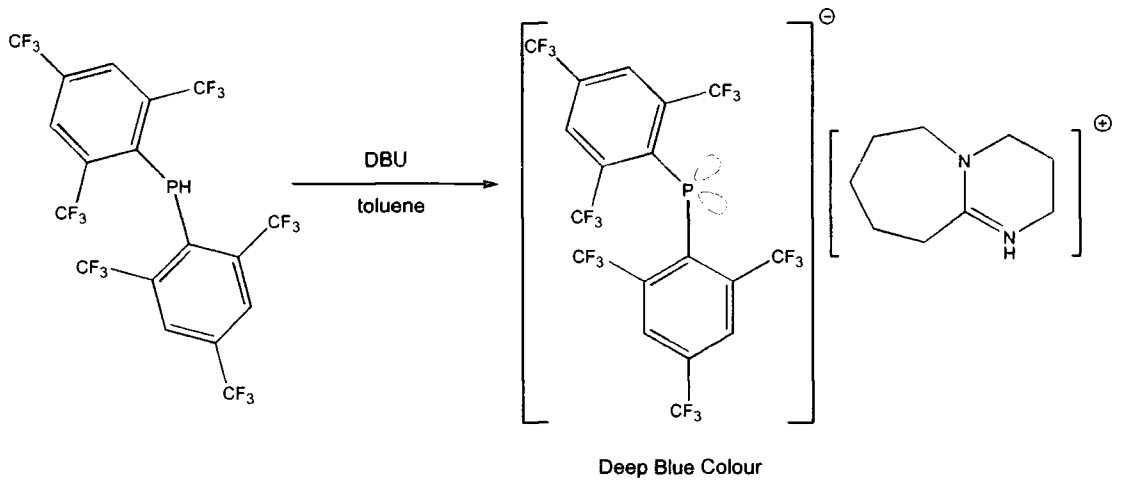

Equation 5.9 – Synthesis of $Ar_2P^{(-)}[DBUH]^{(+)}$

5.5 Results of substitution reactions between Ar_2PH and metal amides

5.5.1 Reaction between Ar_2PH and $Cp_2Zr(NMe_2)_2$

Ar_2PH and $Cp_2Zr(NMe_2)_2$ were added together under an inert atmosphere of N_2 in a glove box; toluene was then added to the solution and the solution turned deep purple in colour. There appeared to be no new products in the ^{31}P NMR spectrum. The reaction was warmed to 60°C, but after a period of hours the purple colour was lost. This was assigned to the instability of the starting materials and products to heat.

As with the formation of $Ar_2P^{(-)}$ the colour is probably due to electron delocalisation within the aryl species. Even a small amount of this compound formed would produce an intense colour.

Attempts to isolate the species resulted in decomposition and the formation of a large number of new species in the ^{31}P and ^{19}F NMR spectra. It is unclear as to whether or not di-substitution was achieved in this reaction. Equation 5.10 highlights the potential products should di-substitution occur.

(In the reaction between Cp_2ZrCl_2 and $2LiPPh_2$, the reaction goes to completion and the formation of the di-phosphide $Cp_2Zr(PPh_2)_2$ may be possible.)

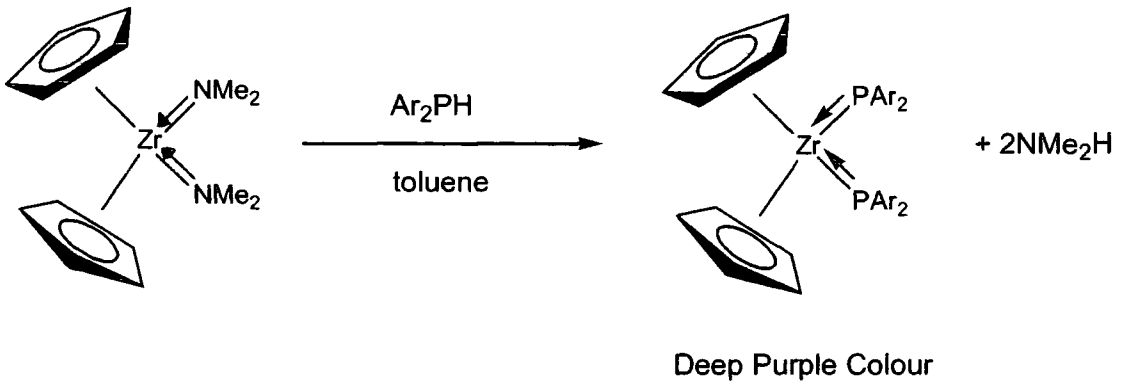

Equation 5.10 – Proposed synthesis of $Cp_2Zr(PAr_2)_2$

5.5.1.1 Mechanism for the substitution of Ar_2PH for NMe_2H

For substitution of this nature to occur, the proton on the phosphane must be more acidic than the proton on the equivalent amine (NMe_2H). Metal phosphides have been prepared by a number of methods[6] and this particular method has not been apparent. This implies that the normal precursor for metal phosphides (Ph_2PH) is not as acidic as the disubstituted amines normally associated with this type of system.

Ar_2PH is comparatively more acidic than Ph_2PH because of the electron withdrawing capacities of the Fluoromes groups compared to the phenyl rings. The electrons are delocalised through the π system of the rings, thus weakening any phosphorus bonds with p character (the P-H bond is formally sp^3).

The mechanism for the reaction[7] involves the coordination of the phosphane ligand to the metal centre and then transfer of the proton from the phosphane to the amide, liberating the amine.

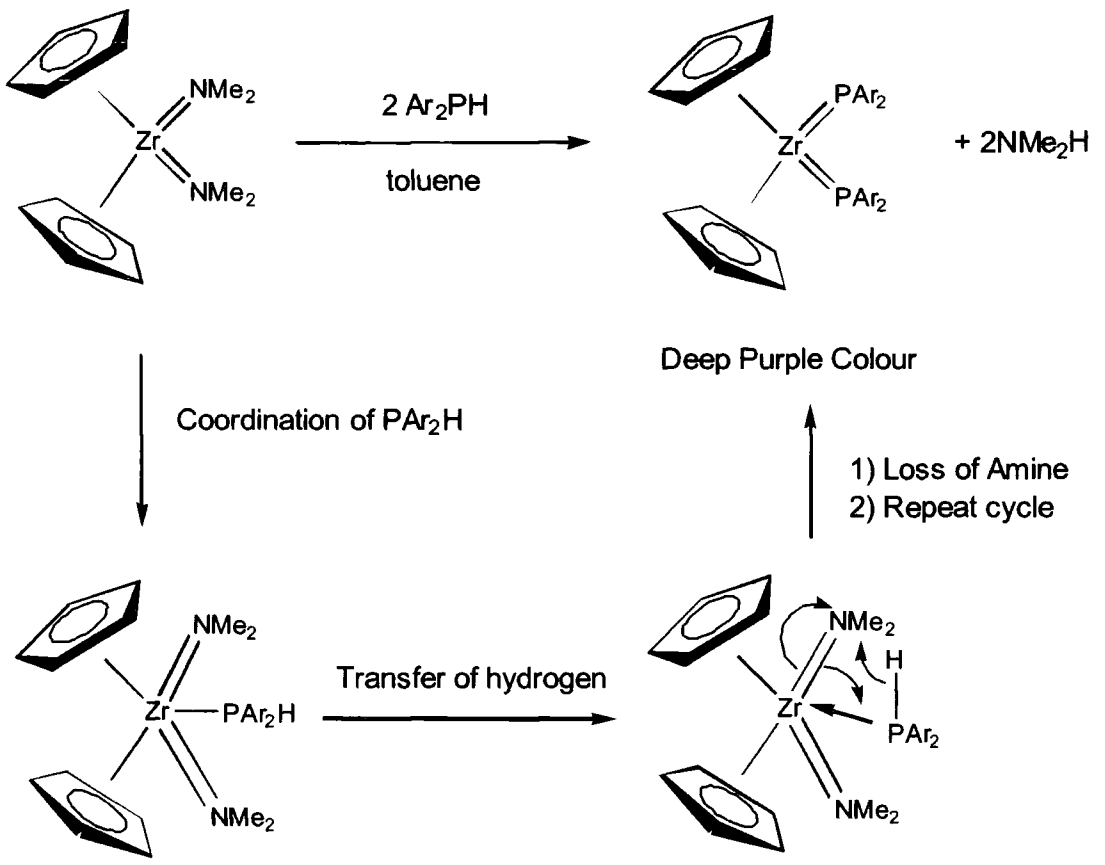

Figure 5.6 – Proposed mechanism for the proton transfer in a reaction between $Cp_2Zr(NMe_2)_2$ and $2Ar_2PH$

5.5.2 Reaction between Ar_2PH and $Ta(NMe_2)_5$

Equimolar quantities of Ar_2PH and the yellow crystalline $Ta(NMe_2)_5$ were dissolved in toluene at room temperature and a dark purple solution was produced. Even before the solvent was added to the reaction it was apparent that there was some reaction between the two solids because there was a faint purple colour to the mixture.

The ^{31}P NMR spectrum of the reaction showed one broad singlet (δ = 112.6 ppm) and the complete removal of the starting material Ar_2PH. This indicates that there is only mono-substitution of the phosphane for the amine. If there were more than one product there would be more than one signal in the phosphorus NMR spectrum.

Unfortunately, the ^{19}F NMR spectrum showed the formation of a large number of new species. Like the phosphide formed with zirconium, this appears to be a very unstable species. What is apparent from the ^{31}P NMR spectrum is the large change in chemical shift, indicating a large decrease in shielding.

The fact that there is only mono-substitution of the amine is due to the steric bulk of the phosphide ligand. For substitution to occur, the phosphane must first bind to the metal before losing the hydrogen (see Equation 5.11). The phosphide is sterically bulkier than the amide ligands and is less likely to facilitate coordination of another phosphane ligand. The structure of $Ta(NMe_2)_5$ is a square based pyramid. One of the NMe_2 groups is more likely to be substituted because of the steric positioning of the other groups around the tantalum atom.

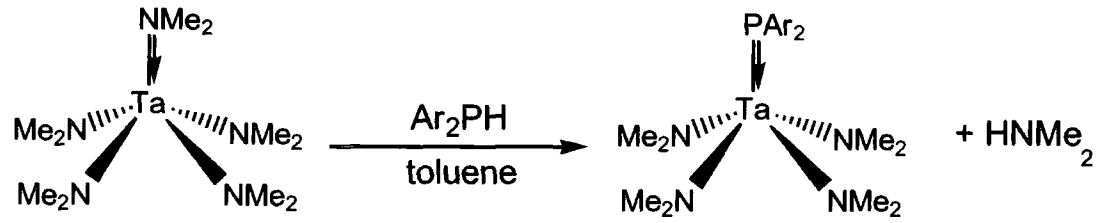

Equation 5.11 – Proposed synthesis of $Ta(NMe_2)_4(PAr_2)$

Attempts were made to isolate the species and record NMR spectra and UV data. The species decomposed almost immediately when these attempts were made. The ^{31}P NMR spectrum of the resulting solution showed the formation of a number of new phosphorus species in the solution. Some of the peaks are close enough together to suggest that they may be coupled. This decomposition may be analogous to the decomposition of unstable metal amide species which results in coupled N-N amine species and the formation of P-P bonds in metal phosphide chemistry[6].

5.6 Reaction of Ar_2PH with low oxidation state transition metals

5.6.1 Reaction of Ar_2PH with $Pt(PPh_3)_4$

Ar_2PH was reacted with $Pt(PPh_3)_4$ in benzene on an NMR scale and a dark orange solution was formed. $Pt(PPh_3)_4$ is known to react with acidic protons[8] to form highly unstable Pt-H species.

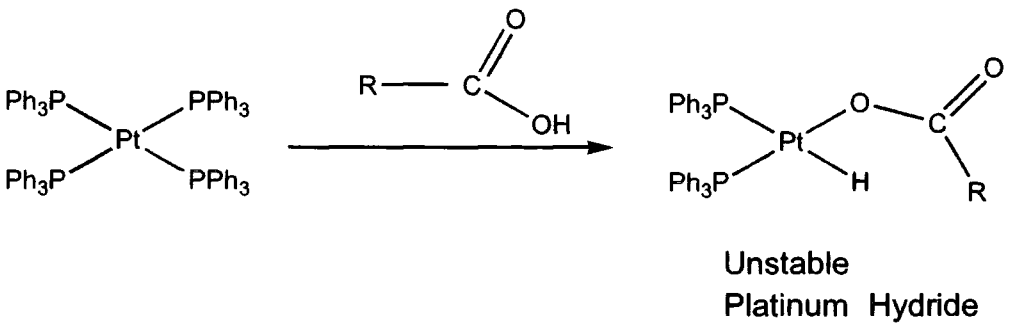

Equation 5.12 – Synthesis of a platinum hydride[8]

The ^{31}P NMR spectrum showed the complete consumption of the Pt(0) species and the formation of a broad peak ($\delta \approx$ 35-40 ppm). This broad peak is probably due to rapid exchange from the platinum of the phosphorus species bonded to it.

The ^{19}F NMR spectrum showed a new doublet and singlet in the spectrum. Although these were very small in comparison to those of the starting material (Ar_2PH), they are distinct. The chemical shift values were δ = -55.7 ppm ($^4J_{P\text{-}F}$ = 39.3 Hz) (doublet) and δ = -63.7 ppm. ^{19}F NMR is a more sensitive tool than ^{31}P and the appearance of these new peaks is an indication of the formation of a new species.

The ^1H NMR spectrum of the solution was attempted, but addition of deuterated solvent to a mixture of the starting material resulted in instant effervescence and there was no peak in the spectrum which could be attributed to having platinum satellites and thus be indicative of a Pt-H species.

Attempts were made to grow crystals from the reaction. When attempts were made to isolate the crystals, the solution effervesced vigorously and became green in appearance. The rapid evolution of gas would suggest the decomposition of a compound which is intrinsically a platinum hydrido complex, although this is only one possibility. This effect may be caused by localised heating or dissolved gases coming out of the solution. Only approximately $0.5cm^3$ of gas would be expected if H_2 was formed by the complete decomposition of the expected product.

5.6.2 Reaction of Ar_2PH with $Pd(PPh_3)_4$

Toluene was added to a mixture of Ar_2PH and $Pd(PPh_3)_4$ in a Schlenk tube. The initial solution formed was dark orange, but effervesced instantaneously and became dark green in colour. The ^{31}P NMR spectrum showed the formation of two new peaks, δ = 25.1 ppm, and δ = -4.8 ppm (free PPh_3). The peak at δ = 25.1 ppm is typical of Pd(II) species such as $Pd(PPh_3)_2X_2$ where X is a halide or organic species. The ^{19}F showed the formation of a number of new species although none of them are high in yield.

5.6.3 Reaction of Ar_2PH with $Pt(dppe)_2$

Toluene was added to a mixture of Ar_2PH and $Pt(dppe)_2$ in a Schlenk tube. The solution became a slightly darker orange colour. The ^{31}P NMR spectrum showed the formation of a broad peak (δ = 41.8 ppm). This again is typical of Pt(0) species in solution, and shows the rapid dissociation and exchange of ligands at the platinum centre. This reaction showed no evidence of effervescence, although when attempts were made to isolate the product, the solution became bright green. This initial spectrum suggests that the Ar_2PH ligands may be exchanging with dppe ligands at the platinum centre, rather than oxidising the Pt(0) to Pt(II).

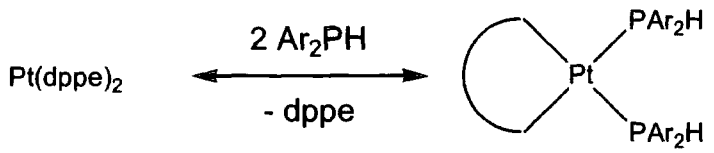

Equation 5.13 – Possible substitution of dppe ligands in the attempted formation of a platinum hydride

5.7 Attempted reaction of Ar_2PH and Ar_2PCl with Pt(II) compounds.

5.7.1 Reaction between Ar_2PH and the "Pt Dimer"

Ar_2PH was refluxed in CH_2Cl_2 in a 2:1 ratio with the platinum dimer $[PtCl_2(PEt_3)]_2$. No reaction was observed even after a few days of heating.

5.7.2 Reaction between Ar_2PH and $PtCl_2(PhCN)_2$

In the second step of the preparation of the "Pt Dimer" (see section 3.7.1), $PtCl_2(PhCN)_2$ is reacted with PEt_3 to form $PtCl_2(PEt_3)_2$. Ar_2PH was refluxed with $PtCl_2(PhCN)_2$ in CH_2Cl_2 for 48 hours. The only species present in the reaction after this time were the starting materials.

5.7.3 Reaction between Ar_2PCl and $Pt(PPh_3)_4$

Under an inert atmosphere of N_2, Ar_2PCl and $Pt(PPh_3)_4$ were added together. The mixture of solids became pale green in colour. Toluene was added to this mixture and the solution immediately became deep blue-green in colour. The initial ^{31}P NMR spectrum showed formation of a new phosphorus peak (δ = 23.7 ppm), although there was no obvious fluorine coupling visible in any of the peaks. After 24 hours, the formation of Ar_2PH was observed in the spectrum (δ = -67ppm) and the ^{19}F spectrum became very complex with a large number of fluorine peaks being observed.

The predicted products for this reaction come from oxidative insertion of platinum into the phosphorus chlorine bonds, analogous to the reaction with Ar_2PH (see section 5.6.1) and the insertion reaction observed upon reaction with $Ar'P{=}CCl_2$ (see section 4.3).

From the ^{31}P and ^{19}F spectra it is apparent that the species formed is unstable with respect to further reaction and can remove a proton from either solvent or one of the other reactants.

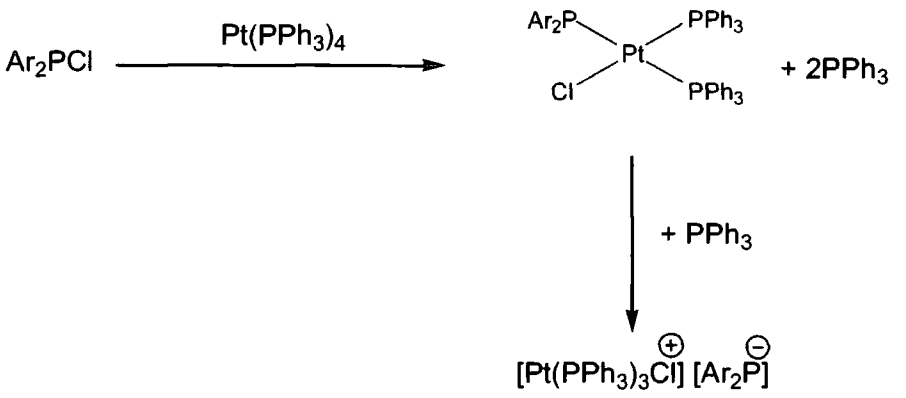

Equation 5.15 – Possible reaction between $Pt(PPh_3)_4$ and Ar_2PH

The deep blue colour of the solution indicates the formation of the $Ar_2P^{(-)}$ anion. This is an indication that the phosphide is not bound to the platinum, (in the case of other reactions the solution is dark orange and not blue). A possible mechanism for the reaction is shown in Equation 5.15.

5.7.4 Reaction between Ar_2PCl and $Pt(dppe)_2$

Toluene was added to a mixture of Ar_2PCl and $Pt(dppe)_2$ in a Schlenk tube. There was no initial reaction. Over a period of three hours the solution became colourless and a very fine dark blue particulate solid was formed. This solid was isolated by filtration. The remaining solution showed only one main peak in the ^{31}P NMR spectrum (δ = 20.6 ppm), which can be attributed to free dppe. The ^{19}F NMR spectrum shows the formation of a large number of new species. Again a number of side reactions appear to have taken place.

The dark blue solid which was formed in this reaction was not soluble in any solvent tried (hexanes, toluene, THF, ether) which implies that it is potentially some form of polymeric species. Due to time constraints, this compound was not characterised further.

From the ^{31}P and ^{19}F spectra it is apparent that the species formed is unstable with respect to further reaction and can remove a proton from either solvent or one of the other reactants.

The deep blue colour of the solution indicates the formation of the $Ar_2P^{(-)}$ anion. This is an indication that the phosphide is not bound to the platinum, (in the case of other reactions the solution is dark orange and not blue).

5.7.4 Reaction between Ar_2PCl and $Pt(dppe)_2$

Toluene was added to a mixture of Ar_2PCl and $Pt(dppe)_2$ in a Schlenk tube. There was no initial reaction. Over a period of three hours the solution became colourless and a very fine dark blue particulate solid was formed. This solid was isolated by filtration. The remaining solution showed only one main peak in the ^{31}P NMR spectrum (δ = 20.6 ppm), which can be attributed to free dppe. The ^{19}F NMR spectrum shows the formation of a large number of new species. Again a number of side reactions appear to have taken place.

The dark blue solid which was formed in this reaction was not soluble in any solvent tried (hexanes, toluene, THF, ether) which implies that it is potentially some form of polymeric species. Due to time constraints, this compound was not characterised further.

5.8 Experimental

5.8.1 Attempted synthesis of $[Ar_2P]^{(-)}[Li]^{(+)}$ in Hexanes

BuLi (0.97ml, 2.41M, 0.23mmol) was added slowly to a solution of Ar_2PH (0.15g, 0.2mmol) in hexanes at –78°C. The solution became very pale pink in colour. Upon warming to room temperature, the pink colour dissipated leaving a colourless solution. The ^{31}P NMR spectrum showed only the starting material and no new species. The ^{19}F NMR spectrum showed the formation of a large number of indeterminate species.

5.8.2 Attempted synthesis of $[Ar_2P]^{(-)}[Li]^{(+)}$ in THF

BuLi (0.97ml, 2.41M, 0.23mmol) was added to a solution of Ar_2PH (0.15g, 0.2mmol) in THF. The solution became an intense dark blue colour and was allowed to warm to room temperature. After two hours the solution became colourless and a brown precipitate was formed. Again, the NMR spectra showed the formation of a large number of indeterminate species.

5.8.3 Attempted synthesis of $[Ar_2P]^{(-)}[Li]^{(+)}$(PMDETA)

BuLi (0.97ml, 2.41M, 0.23mmol) was added to a solution of Ar_2PH (0.15g, 0.2mmol) and a large excess of PMDETA in THF. The solution became dark blue in colour and was allowed to warm to room temperature. After four hours at room temperature, the solution was placed in a fridge at –20°C. After another four hours, the solution became colourless and a brown solid was precipitated. The NMR spectra showed the formation of a number of new indistinguishable peaks.

5.8.4 Attempted synthesis of $[DBUH]^{(+)}[Ar_2P]^{(-)}$

DBU (0.5ml, 0.3mmol) was added to a solution of Ar_2PH (0.2g, 0.3mmol) in toluene. The solution became dark blue in colour, which appeared stable over a number of hours. The product was not isolated. ^{31}P (toluene) δ = 30.2 ppm (13 line multiplet), $^4J_{PF}$ = 36.7 Hz; ^{19}F δ = -59.4 ppm (doublet) ($^4J_{PF}$ = 37.5 Hz), δ = -60.7 ppm (singlet).

5.8.5 Attempted synthesis of $[Ar_2P]^{(-)}[(C_4H_8NH)H]^{(+)}$

Pyrrolidine (0.02g, 0.3mmol) was added to a solution of Ar_2PH (0.2g, 0.3mmol) in toluene. The solution became a pale blue colour, which darkened when cooled in the fridge. A crystalline material was formed although the crystals were not stable enough to be submitted for X-ray crystallographic analysis. Numerous attempts were made to collect NMR data on the compound, but at room temperature the only signal in the ^{31}P NMR spectrum was from the starting material. Facilities for low temperature NMR were not available at the time of the experiment.

5.8.6 Synthesis of $[Ar_2P]^{(-)}[Ph_3PCH_3]^{(+)}$

Toluene (10ml) was added to a Schlenk tube containing $Ph_3P{=}CH_2$ (0.14g, 0.5mmol) and Ar_2PH (0.3g, 0.5mmol). The resulting deep blue coloured solution was stirred at room temperature for 15 minutes, during which time a red precipitate was formed. Upon the addition of more toluene (15ml) and gentle warming, the solid redissolved. Upon standing for three hours deep red crystals were formed. Yield 0.24g, (55%). m. p. 129-130°C. ^{31}P (toluene) δ = (21.0 ppm) (multiplet), $^4J_{PF}$ = 32.6 Hz; ^{19}F δ = -61.2 ppm (doublet), ($^4J_{PF}$ = 32.6 Hz) δ = - 62.3 ppm (singlet).

$$Ar_2PH \xrightarrow{Ph_3P=CH_2} (Ar_2P)^{(-)}(Ph_3PCH_3)^{(+)}$$

5.8.7 Attempted synthesis of $ZrCp_2(PAr_2)_2$

Toluene was added to a mixture of $Cp_2Zr(NMe_2)_2$ (0.093g, 0.3mmol) and Ar_2PH (0.36g, 0.6mmol). The solution became a deep purple colour and was allowed to stir. The mixture was placed in the fridge overnight and crystals grew. When attempts to isolate these crystals were made the solution became pale green and the crystals disintegrated. No NMR spectra were recorded on the purple species in solution.

5.8.8 Attempted synthesis of $Ta(NMe_3)_4(PAr_2)$

Toluene was added to a solution of $Ta(NMe_2)_5$ (0.14 g, 0.35mmol) and Ar_2PH (0.42g, 0.7mmol). The resulting solution was deep purple in colour and the solution was allowed to stir. Attempts to isolate the product resulted in both the loss of the purple colour and the formation of a large numbers of peaks in the ^{19}F NMR spectrum.

The purple solution did yield useful NMR data; ^{31}P (toluene) δ = 112.6 ppm (broad singlet). ^{19}F showed a large number of indistinguishable products.

5.8.9 Attempted synthesis of $[HPt(PPh_3)_2(Ar_2P)]$

Toluene (20ml) was added to a mixture of Ar_2PH (0.10g, 0.17mmol) and $Pt(PPh_3)_4$ (0.20g, 0.17mmol) in a Schlenk tube under an atmosphere of N_2. The solution became dark orange in colour and was stable over time. ^{19}F; δ = -55.7 ppm ($^4J_{P\text{-}F}$ = 39.3 Hz) (doublet) and δ = -63.7 ppm (singlet).

Any attempt to isolate the product resulted in the formation of a dark green solution with rapid effervescence. The resulting solution showed a large number of peaks in the ^{19}F NMR spectrum, although none were assignable.

5.8.10 Attempted synthesis of [PtH(dppe)(Ar_2P)]

Toluene (20ml) was added to a mixture of Ar_2PH (0.10g, 0.17mmol) and $Pt(dppe)_2$ (0.17g, 0.17mmol) in a Schlenk tube under an atmosphere of N_2. The resulting ^{31}P NMR showed the formation of a broad peak (δ = 41.8 ppm). The ^{19}F NMR spectrum showed a large number of non-assignable peaks.

5.8.11 Attempted synthesis of [PdH(PPh_3)$_2$(Ar_2P)]

Toluene (20ml) was added to a mixture of Ar_2PH (0.10g, 0.17mmol) and $Pd(PPh_3)_4$ (0.18g, 0.17mmol) in a Schlenk tube under an atmosphere of N_2. The solution became dark orange in colour and was stable over time. ^{31}P, 25.1 ppm, (singlet) δ = -4.8 ppm (singlet). ^{19}F and ^{1}H NMR showed the formation of a large number of new peaks which were non-assignable. Any attempt to isolate the product resulted in the formation of a dark green solution with rapid effervescence. The resulting solution showed a large number of peaks in the ^{19}F NMR spectrum, although none were assignable.

5.8.12 Attempted synthesis of [PtCl(PPh$_3$)$_2$(Ar$_2$P)]

Under an inert atmosphere of N_2, Ar_2PCl (0.1g, 0.16mmol) and $Pt(PPh_3)_4$ (2.0g, 0.16mmol) were added together. The mixture of solids became pale green. Toluene was added to this mixture and the solution immediately became a deep blue-green colour. ^{31}P : δ = 23.7 ppm (singlet); ^{19}F: Many complex non-assignable peaks.

5.8.13 Attempted synthesis of [PtCl(dppe)(Ar$_2$P)]

Toluene was added to a mixture of Ar_2PCl and $Pt(dppe)_2$ in a Schlenk tube. There was no initial reaction. Over a period of three hours the solution became colourless and a very fine dark blue particulate solid was formed. ^{31}P: δ = 20.6 ppm (singlet = dppe).

---

[1] S. R. Wade., M. G. H. Wallbridge., G. R. Willey., *J. Chem. Soc. Dalton. Trans.*, 1983, 2555.
[2] K. Issleib., H. Hackert., *Z. Naturforsch.*, 1966, **21**, 519.
[3] K. Wade.,W. Clegg., R. Snaith., G. T. Walker., D. R. Armstrong., R. E. Mulvey., *Polyhedron.*, 1987, **7**, 698.
[4] M. G. Davidson., *Private Communication.*
[5] F. H. Allen., O. Kennard., *Chemical Design Automation News.*, 1993, **8**, 31.
[6] Z. Hou., T. L. Breen., D. Stephenson., *Organometallics*, 1993, **12**, 3158.
[7] D. J. Cardin., S. A. Keppie., M. F. Lappert., *J. Chem. Soc(A)*, 1970, 2594.
[8] J. E. Huheey., *Inorganic Chemistry* (third edition)., Harper and Row, London, 1983.

Appendix 1

Crystal growth and crystallographic methods

A.1 Crystal growth and crystallographic methods

A.1.1 Growing Crystals

A.1.1.1 The layering technique

This method of crystallisation was used to grow most of the crystals used for X-ray structural determination described in this thesis. The method employed here is commonly referred to as the "layering technique".

A pure solution of the desired compound in a suitable solvent was introduced into a small capillary tube, diameter of 5-8mm. On top of this, some low boiling petrol was carefully poured so that a distinct interface was visible between the two solvents. The tube was then covered and allowed to stand for a number of days. The two solutions slowly diffused into one another which causes the solute to come out of solutions into a crystalline form.

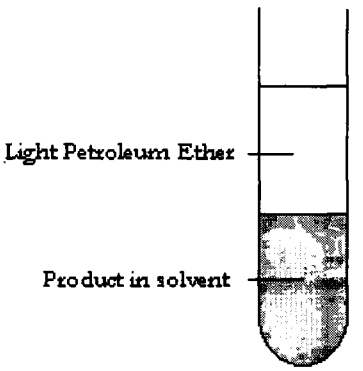

A.1.1.1.1 Pt dimer complexes

In the case of the platinum dimer complexes (see Chapter 3) the solvent used was either CH_2Cl_2 or $(CHCl_2)_2$. The solutions were bright yellow and upon addition of the petrol a small amount of white precipitate was visible on the boundary of the two solvents. After diffusion of the petrol a colourless solution was left and colourless needle like crystals were formed.

A.1.1.1.2 Phosphaalkene-platinum complex

To attain crystals of the complex formed in the reaction between the phosphaalkene $ArP{=}CCl_2$ and $Pt(PPh_3)_4$ (see Chapter 4) the solid product was dissolved in toluene and placed in the capillary tube as before. The solution was a bright orange colour. Petrol was slowly poured onto the top of this and no precipitate was visible.

After a few days, long flat plate-like orange crystals were produced and these were used for X-ray structural determination of the compound.

A.1.1.2 Vacuum sublimation

This method involved the slow growth of crystals in a sealed glass container under vacuum.

A small quantity of solid was placed at the bottom of a glass tube and the system was evacuated. It was then sealed and allowed to warm to room temperature in a shielded area. The tube was then placed in bright sunlight and allowed to stand for a few days. Crystals of the desired product were then formed and used for X-ray characterisation. It was found that better quality crystals were obtained when the heat was less direct and the growth of crystals slower.

This method is only viable if the sublimation temperature of the compound (under vacuum) is not much higher than room temperature. The slower the crystals form the better.

This method was used for growing crystals of Ar_2PH.

A.1.1.3 Recrystallisation

Where laying and vacuum sublimation were not successful or not possible, crystals were grown from a saturated solution in a freezer at -30°C.

A.1.2 Crystallographic methods

All the crystallographic experiments carried out were performed on the Siemens SMART 3-circle diffractometer. The air sensitive crystals were removed from the reaction vessel under a suspension of perfluoropolyether oil which protected the crystals from solvent evaporation and from air or moisture oxidation/hydrolysis.

The crystals were then checked for quality and singularity by rotating them through polarised light using a light microscope. A pure single crystal under a specific orientation will allow all the polarised light to pass through it, giving the appearance under the microscope that the crystal has disappeared.

The X-rays are generated by accelerating electrons (generated from a heated filament) towards a metal target (in this case molybdenum). These are then monochromated to a specific wavelength (K_α = 0.71073Å) and collimated. This collimation produces X-rays of this specific wavelength in a beam approximately 0.5mm in diameter.

After a crystal of a suitable size has been selected (all side lengths <0.5mm) the crystals were then mounted on a glass fibre, on a goniometer head, and placed on the goniometer (see figure A.1). The maximum size of the crystal is determined by the size of the collimated beam. The crystal must remain wholly in the beam under all orientations and thus a crystal of no more than 0.4mm in any one width is preferable.

Figure A.1 – A Goniometer

The goniometer was then placed immediately onto the SMART and the crystal rests in a stream of dry nitrogen produced by an Oxford Cryosystems "N_2 open flow cryostat cooler" (cryostream)[1] at 150K and was allowed to cool.

An initial search for diffracted intensities usually yields at least 20 reflections in the case of a good crystal. Using these intensities, the software calculated the unit cell dimensions. Once it had been established that these were within acceptable parameters, data collection commenced.

Once crystallinity and quality have been established, a "hemisphere" of Data were collected over a period of time using ω scans of an interval of 0.3°. Once the data collection was complete, the Data were integrated, solved, and then refined.

The Data were processed using the SAINT[2] program and after that the space group was determined from the integrated intensities, by the XPREP[3] program. The structure solution was then provided by using the XS[4] package and refined using SHELXL-93[5].

---

[1] J. Cozier., A. M. Glazier., *J. Appl. Cryst.*, **19**, 1986, 105
[2] Siemens SAINT Version 4.050 (Siemens Analytical X-ray Instruments), 1995.
[3] SHELXTL – Sheldrick, G, M., 1994.
[4] SHELXS-86 – Acta., Crystallographica., **A46**, 1990, 467.
[5] SHELXL-93 – Sheldrick, G, M., 1993.

Appendix 2

Crystal structure of compounds completed during the period 1994-1997, not included in the main body of the thesis

A.2 Other crystals structures 1994-1997

A.2.1 1,2,bisdiphenylphosphoniumethylene hydroxide bromide

This compound was synthesised by Miss Jennifer Boon and is a hydrolysis product formed in the reaction between PCl_3 and dppe.

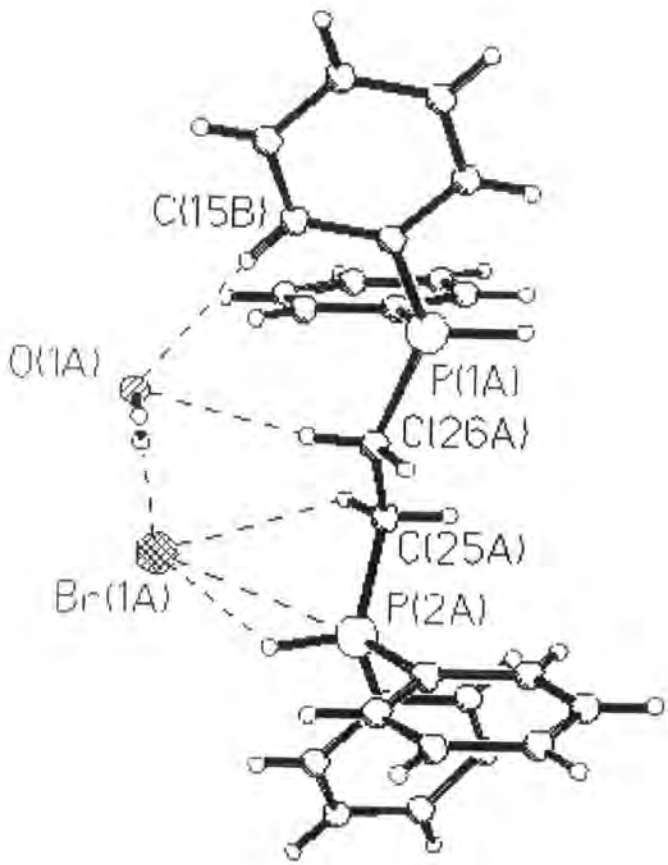

Figure A2.1 – A Diagrammatical representation of the product formed in the reaction between PCl_3 and dppe.

Crystal data and structure refinement.	
Identification code	Jenny Boon
Empirical formula	$C_{26}H_{28}Br_2OP_2$
Formula weight	578.24
Temperature	150(2) K
Wavelength	0.71073 Å
Crystal system	monoclinic
Space group	P2(1)/c
Unit cell dimensions	a = 11.4590(5) Å α = 90 °. b = 14.3115(5) Å β = 100.4620(10) °. c = 15.5895(6) Å χ = 90 °
Volume	2514.1(2) $Å^3$
Z	4
Number of reflexions used	507
Crystal description	needle
Crystal colour	colourless
Density (calculated)	1.528 g/cm^3
Absorption coefficient	33.68 cm^{-1}
F(000)	1168
Crystal size	0.2 x 0.2 x 0.4 mm
Theta range for data collection	1.95 to 25.67 °
Index ranges	-13<=h<=13, -17<=k<=7, -16<=l<=18
Experiment device	Siemens Smart
Experiment methods	ω scans
Reflections collected	10581
Independent reflections	4266 [R(int) = 0.0429]
Refinement method	Full-matrix least-squares on F^2
Data / restraints / parameters	4220 / 0 / 315
Goodness-of-fit on F^2	1.179
Final R indices [I>2σ(I)]	R_1 = 0.0431, wR_2 = 0.0792
R indices (all data)	R_1 = 0.0624, wR_2 = 0.1083
Largest diff. peak and hole	.414 and -.383 e.$Å^{-3}$

Table 1 Crystal data and structural refinement

	x	y	z	U(eq)
P(1)	8639(1)	7214(1)	1451(1)	24(1)
P(2)	8562(1)	6711(1)	4239(1)	23(1)
C(4)	12506(4)	8124(4)	1870(3)	37(1)
C(13)	9291(4)	7435(3)	5110(3)	23(1)
C(19)	6976(4)	6763(3)	4137(3)	24(1)
C(12)	7399(4)	6861(3)	193(3)	28(1)
C(23)	5151(4)	7634(4)	3882(3)	34(1)
C(24)	6370(4)	7612(3)	3952(3)	31(1)
C(15)	10442(4)	7578(4)	6555(3)	32(1)
C(15)	8610(4)	5585(3)	477(3)	30(1)
C(6)	10437(4)	8494(4)	1497(3)	35(1)
C(1)	10164(4)	7560(3)	1585(3)	26(1)
C(17)	9726(4)	8955(4)	5745(3)	33(1)
C(14)	9930(4)	7021(3)	5862(3)	27(1)
C(7)	8175(4)	6487(3)	521(3)	23(1)
C(18)	9200(4)	8408(3)	5052(3)	30(1)
C(11)	7089(4)	6340(4)	-946(3)	33(1)
C(20)	6356(4)	5955(3)	4256(3)	29(1)
C(26)	8411(4)	6630(3)	2430(3)	27(1)
C(21)	5128(4)	5989(3)	4185(3)	30(1)
C(22)	4532(4)	6828(3)	4002(3)	29(1)
C(5)	11615(5)	8771(4)	1633(3)	40(1)
C(9)	8302(4)	5071(3)	-278(3)	32(1)
C(10)	7553(4)	5457(4)	-992(3)	35(1)
C(16)	10320(4)	8540(4)	6500(3)	33(1)
C(2)	11061(4)	6899(3)	1819(3)	34(1)
C(3)	12240(4)	7188(4)	1964(4)	41(1)
C(25)	9022(4)	7126(3)	3264(3)	25(1)
Br(1)	11455(1)	5610(1)	4270(1)	34(1)
Br(2)	7741(1)	9344(1)	2518(1)	36(1)
O(1)	10149(4)	4654(3)	2390(3)	43(1)

Table 2 Atomic coordinates (x 10^4) and equivalent isotropic displacement parameters ($Å^2$ x 10^3) for $C_{26}H_{28}Br_2OP_2$. U(eq) is defined as one third of the trace of the *ortho*gonalized Uij tensor

Bond lengths [Å] and angles [°]	
P(1)-C(7)	1.785(4)
P(1)-C(1)	1.791(4)
P(1)-C(26)	1.801(5)
P(2)-C(13)	1.789(5)
P(2)-C(19)	1.797(4)
P(2)-C(25)	1.797(5)
C(4)-C(5)	1.378(7)
C(4)-C(3)	1.388(7)
C(13)-C(14)	1.396(6)
C(13)-C(18)	1.399(6)
C(19)-C(20)	1.386(6)
C(19)-C(24)	1.404(6)
C(12)-C(11)	1.382(7)
C(12)-C(7)	1.398(6)
C(23)-C(24)	1.382(6)
C(23)-C(22)	1.384(7)
C(15)-C(14)	1.385(6)
C(15)-C(16)	1.385(7)
C(15)-C(9)	1.379(6)
C(15)-C(7)	1.390(6)
C(6)-C(5)	1.385(7)
C(6)-C(1)	1.386(7)
C(1)-C(2)	1.396(6)
C(17)-C(18)	1.381(7)
C(17)-C(16)	1.383(7)
C(11)-C(10)	1.379(7)
C(20)-C(21)	1.392(6)
C(26)-C(25)	1.534(6)
C(21)-C(22)	1.385(7)
C(9)-C(10)	1.391(7)
C(2)-C(3)	1.391(7)
C(7)-P(1)-C(1)	113.3(2)
C(7)-P(1)-C(26)	110.5(2)
C(1)-P(1)-C(26)	108.5(2)
C(13)-P(2)-C(19)	111.6(2)
C(13)-P(2)-C(25)	106.4(2)
C(19)-P(2)-C(25)	111.1(2)
C(5)-C(4)-C(3)	120.6(5)
C(14)-C(13)-C(18)	119.9(4)
C(14)-C(13)-P(2)	119.5(3)
C(18)-C(13)-P(2)	120.5(4)
C(20)-C(19)-C(24)	120.2(4)
C(20)-C(19)-P(2)	119.3(3)
C(24)-C(19)-P(2)	120.5(3)
C(11)-C(12)-C(7)	119.8(4)
C(24)-C(23)-C(22)	120.4(5)
C(23)-C(24)-C(19)	119.4(4)
C(14)-C(15)-C(16)	120.1(5)
C(9)-C(15)-C(7)	119.9(4)
C(5)-C(6)-C(1)	119.5(5)
C(6)-C(1)-C(2)	120.7(4)
C(6)-C(1)-P(1)	119.2(4)
C(2)-C(1)-P(1)	120.0(4)
C(18)-C(17)-C(16)	120.0(5)

Bond lengths [Å] and angles [°]	
C(15)-C(14)-C(13)	119.6(4)
C(15)-C(7)-C(12)	119.9(4)
C(15)-C(7)-P(1)	121.6(3)
C(12)-C(7)-P(1)	118.4(3)
C(17)-C(18)-C(13)	119.8(5)
C(10)-C(11)-C(12)	119.8(5)
C(19)-C(20)-C(21)	119.7(4)
C(25)-C(26)-P(1)	112.9(3)
C(22)-C(21)-C(20)	120.0(5)
C(23)-C(22)-C(21)	120.3(4)
C(4)-C(5)-C(6)	120.3(5)
C(15)-C(9)-C(10)	119.8(5)
C(11)-C(10)-C(9)	120.7(5)
C(17)-C(16)-C(15)	120.5(5)
C(3)-C(2)-C(1)	119.2(5)
C(4)-C(3)-C(2)	119.7(5)
C(26)-C(25)-P(2)	113.9(3)

Table 3 - Bond lengths [Å] and angles [°] for $C_{26}H_{28}Br_2OP_2$

	U11	U22	U33	U23	U13	U12
P(1)	22(1)	22(1)	28(1)	-2(1)	4(1)	-2(1)
P(2)	20(1)	23(1)	25(1)	2(1)	4(1)	2(1)
C(4)	29(3)	52(3)	34(3)	-11(3)	16(2)	-13(3)
C(13)	20(2)	29(2)	21(2)	2(2)	7(2)	2(2)
C(19)	21(2)	28(2)	23(3)	-2(2)	4(2)	2(2)
C(12)	27(2)	27(3)	33(3)	4(2)	9(2)	1(2)
C(23)	27(3)	32(3)	44(3)	0(2)	9(2)	7(2)
C(24)	25(2)	29(3)	41(3)	5(2)	9(2)	0(2)
C(15)	25(2)	43(3)	26(3)	4(2)	0(2)	1(2)
C(15)	31(3)	29(3)	28(3)	2(2)	1(2)	-1(2)
C(6)	25(3)	37(3)	39(3)	7(2)	-2(2)	-4(2)
C(1)	19(2)	29(3)	30(3)	-4(2)	5(2)	-3(2)
C(17)	23(2)	32(3)	44(3)	-2(2)	4(2)	4(2)
C(14)	25(2)	25(3)	30(3)	1(2)	6(2)	-1(2)
C(7)	22(2)	25(2)	23(2)	-1(2)	8(2)	-2(2)
C(18)	27(3)	31(3)	31(3)	0(2)	0(2)	5(2)
C(11)	28(3)	44(3)	25(3)	1(2)	4(2)	-3(2)
C(20)	31(3)	25(2)	29(3)	1(2)	4(2)	3(2)
C(26)	26(2)	30(3)	27(3)	-3(2)	7(2)	-6(2)
C(21)	23(2)	32(3)	35(3)	-4(2)	2(2)	-7(2)
C(22)	20(2)	36(3)	31(3)	-3(2)	4(2)	-1(2)
C(5)	41(3)	40(3)	39(3)	8(3)	9(3)	-14(3)
C(9)	36(3)	24(3)	35(3)	-7(2)	7(2)	0(2)
C(10)	36(3)	40(3)	29(3)	-11(2)	5(2)	-10(2)
C(16)	25(3)	38(3)	35(3)	-12(2)	4(2)	-1(2)
C(2)	31(3)	30(3)	41(3)	-7(2)	10(2)	-2(2)
C(3)	24(3)	49(3)	50(4)	-15(3)	6(2)	2(2)
C(25)	18(2)	30(3)	28(3)	-3(2)	3(2)	0(2)
Br(1)	29(1)	28(1)	46(1)	-1(1)	7(1)	4(1)
Br(2)	39(1)	22(1)	48(1)	-2(1)	12(1)	2(1)

Table 4 Anisotropic displacement parameters ($Å^2$ x 10^3) for $C_{26}H_{28}Br_2OP_2$. The anisotropic displacement factor exponent takes the form: $-2\pi^2 [h^2 a^2 U11 + 2 h k a^* b^* U12]$

	x	y	z	U(eq)
H(18A)	13294(4)	8317(4)	1967(3)	46(16)
H(99A)	7093(4)	7459(3)	-160(3)	16(11)
H(11A)	4743(4)	8193(4)	3753(3)	34(14)
H(12A)	6786(4)	8156(3)	3876(3)	54(17)
H(14A)	10869(4)	7306(4)	7057(3)	25(12)
H(16A)	9108(4)	5328(3)	957(3)	22(12)
H(17A)	9835(4)	8932(4)	1348(3)	35(14)
H(21A)	9662(4)	9603(4)	5703(3)	50(17)
H(25A)	10011(4)	6375(3)	5897(3)	10(10)
H(28A)	8787(4)	8686(3)	4548(3)	37(14)
H(29A)	6568(4)	6585(4)	-1420(3)	41(15)
H(2A)	6759(4)	5394(3)	4382(3)	25(12)
H(3A)	7566(4)	6593(3)	2432(3)	55(17)
H(3B)	8713(4)	5997(3)	2429(3)	50(16)
H(4A)	4708(4)	5448(3)	4260(3)	57(18)
H(5A)	3713(4)	6850(3)	3960(3)	33(13)
H(6A)	11804(5)	9395(4)	1565(3)	57(18)
H(7A)	8594(4)	4468(3)	-310(3)	35(14)
H(8A)	7363(4)	5115(4)	-1507(3)	37(14)
H(9A)	10640(4)	8910(4)	6975(3)	36(14)
H(10A)	10873(4)	6272(3)	1877(3)	38(15)
H(12B)	12847(4)	6756(4)	2123(4)	43(15)
H(20A)	8857(4)	7790(3)	3205(3)	40(14)
H(20B)	9873(4)	7044(3)	3324(3)	38(14)
H(3P)	8020(31)	8020(25)	1293(23)	8(10)
H(4P)	8856(34)	5870(27)	4418(25)	15(10)
H(2W)	9519(60)	4468(45)	2478(42)	76(22)
H(1W)	10608(67)	4964(54)	2985(51)	114(27)

Table 2.5 Hydrogen coordinates (x 10^4) and isotropic displacement parameters ($Å^2$ x 10^3) for $C_{26}H_{28}Br_2OP_2$.

A.2.2 cis-dibromo(triethylphosphane)(1,1-dihydroxy-2,6-bis(trifluoromethyl)phenyl)platinum(II)

This compound is formed by the hydrolysis of the product, formed in the reaction between $Ar'PBr_2/Ar''PBr_2$ and $[PtCl_2(PEt_3)]_2$. The expected product from this reaction would be $RPBr_2[PtCl_2(PEt_3)]$.

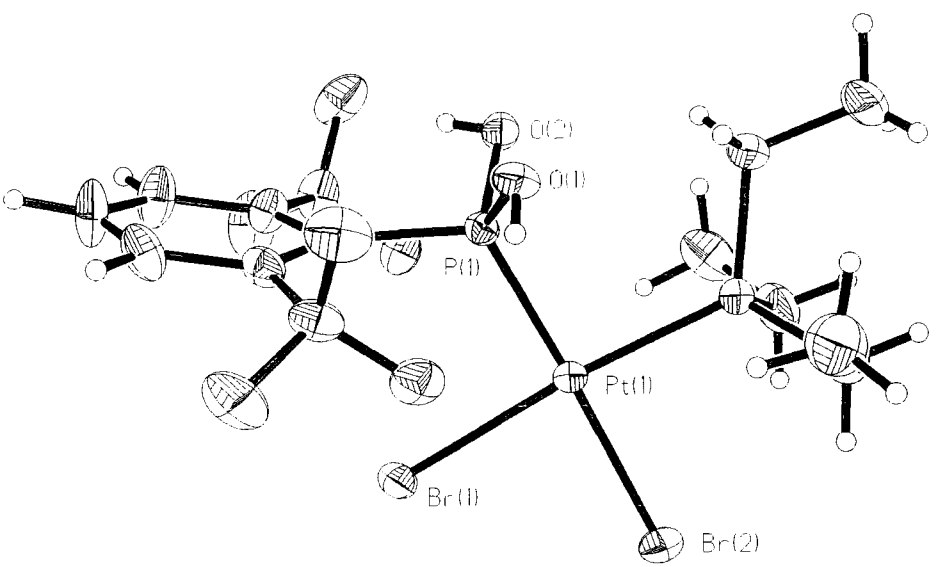

Figure A2.2 – Thermal ellipsoid diagram at 150K (50% Probability) for $Ar'P(OH)_2[PtBr_2(PEt_3)]$

Crystal data and structure refinement	
Identification code	-$PtBr_2$
Empirical formula	$C_{14}H_{20}Br_2F_6O_2P_2Pt$
Formula weight	751.15
Temperature	150(2) K
Wavelength	0.71073 Å
Crystal system	Orthorhombic
Space group	P_{212121}
Unit cell dimensions	a = 19.332(3) Å α = 90 °. b = 19.332(3) Å β = 90 °. c = 12.856(3) Å χ = 90 °
Volume	4804.4(14) $Å^3$
Z	8
Number of reflections used	15711
Crystal description	cube
Crystal colour	colourless
Density (calculated)	2.077 g/cm^3
Absorption coefficient	93.53 cm^{-1}
F(000)	2816
Crystal size	0.2 x 0.2 x 0.2 mm
Theta range for data collection	1.49 to 27.48 °.
Index ranges	-25<=h<=23, -25<=k<=24, -12<=l<=16
Experiment device	Siemens SMART
Experiment methods	ω scans
Reflections collected	15711
Independent reflections	5487 [R(int) = 0.0517]
Refinement method	Full-matrix least-squares on F^2
Data / restraints / parameters	5475 / 0 / 249
Goodness-of-fit on F^2	1.196
Final R indices [I>2σ(I)]	R_1 = 0.0316, wR_2 = 0.0669
R indices (all data)	R_1 = 0.0386, wR_2 = 0.0727
Absolute structure parameter	-.019(8)
Largest diff. peak and hole	.937 and -.699 e.$Å^{-3}$

Table 6 Crystal data and structural refinement

	x	y	z	U(eq)
Pt(1)	3048(1)	3044(1)	4956(1)	21(1)
Br(2)	3533(1)	3640(1)	6506(1)	30(1)
Br(1)	3292(1)	1943(1)	5904(1)	27(1)
F(3)	1602(2)	2101(2)	5324(3)	33(1)
F(2)	846(2)	1679(3)	4255(4)	38(1)
C(6)	1966(4)	1178(4)	4196(6)	25(2)
F(1)	1179(3)	1095(3)	5578(4)	45(1)
C(8)	1405(4)	1529(4)	4830(6)	29(2)
C(1)	2539(4)	1529(3)	3760(5)	20(1)
C(2)	3058(4)	1109(4)	3313(6)	26(2)
P(2)	2961(1)	4099(1)	4194(2)	28(1)
C(4)	2377(5)	81(4)	3563(8)	43(2)
F(6)	3969(2)	1941(2)	3440(4)	31(1)
F(5)	4240(2)	903(3)	3069(5)	51(1)
F(4)	3753(3)	1537(3)	1918(4)	44(1)
C(7)	3740(4)	1389(4)	2923(7)	32(2)
C(3)	2963(4)	403(4)	3206(7)	38(2)
C(13)	2464(5)	4709(4)	4952(8)	43(2)
C(9)	2595(5)	4151(4)	2896(6)	36(2)
C(14)	1712(5)	4538(5)	4978(11)	57(2)
C(12)	4305(5)	4057(5)	3379(8)	52(3)
C(11)	3835(5)	4466(5)	4072(8)	44(2)
C(10)	2535(7)	4884(5)	2449(8)	58(3)
C(5)	1888(4)	469(4)	4084(7)	34(2)
P(1)	2568(1)	2482(1)	3651(1)	20(1)
O(1)	1781(3)	2684(3)	3461(4)	26(1)
O(2)	2932(3)	2603(3)	2565(4)	26(1)

Table 7 Atomic coordinates (x 10^4) and equivalent isotropic displacement parameters ($Å^2$ x 10^3) for $C_{14}H_{20}Br_2F_6O_2P_2Pt$. U(eq) is defined as one third of the trace of the *ortho*gonalized Uij tensor

Bond lengths [Å] and angles [°]	
Pt(1)-P(1)	2.203(2)
Pt(1)-P(2)	2.269(2)
Pt(1)-Br(2)	2.4859(8)
Pt(1)-Br(1)	2.4979(8)
F(3)-C(8)	1.330(9)
F(2)-C(8)	1.343(9)
C(6)-C(5)	1.384(11)
C(6)-C(1)	1.417(10)
C(6)-C(8)	1.518(10)
F(1)-C(8)	1.349(8)
C(1)-C(2)	1.412(10)
C(1)-P(1)	1.848(7)
C(2)-C(3)	1.384(11)
C(2)-C(7)	1.512(10)
P(2)-C(13)	1.808(9)
P(2)-C(9)	1.815(8)
P(2)-C(11)	1.839(9)
C(4)-C(3)	1.371(12)
C(4)-C(5)	1.380(12)
F(6)-C(7)	1.333(9)
F(5)-C(7)	1.361(9)
F(4)-C(7)	1.324(10)
C(13)-C(14)	1.492(13)
C(9)-C(10)	1.532(11)
C(12)-C(11)	1.498(14)
P(1)-O(2)	1.580(5)
P(1)-O(1)	1.589(5)
P(1)-Pt(1)-P(2)	94.79(7)
P(1)-Pt(1)-Br(2)	176.20(5)
P(2)-Pt(1)-Br(2)	87.55(5)
P(1)-Pt(1)-Br(1)	91.80(5)
P(2)-Pt(1)-Br(1)	172.16(6)
Br(2)-Pt(1)-Br(1)	86.11(3)
C(5)-C(6)-C(1)	121.3(7)
C(5)-C(6)-C(8)	114.9(7)
C(1)-C(6)-C(8)	123.7(7)
F(3)-C(8)-F(2)	108.3(6)
F(3)-C(8)-F(1)	105.6(6)
F(2)-C(8)-F(1)	105.4(6)
F(3)-C(8)-C(6)	115.2(6)
F(2)-C(8)-C(6)	112.1(6)
F(1)-C(8)-C(6)	109.6(6)
C(2)-C(1)-C(6)	116.0(6)
C(2)-C(1)-P(1)	121.4(5)
C(6)-C(1)-P(1)	122.2(5)
C(3)-C(2)-C(1)	120.9(7)
C(3)-C(2)-C(7)	115.8(7)
C(1)-C(2)-C(7)	123.2(7)
C(13)-P(2)-C(9)	104.6(4)
C(13)-P(2)-C(11)	106.4(4)
C(9)-P(2)-C(11)	105.0(4)
C(13)-P(2)-Pt(1)	113.1(3)
C(9)-P(2)-Pt(1)	118.4(3)
C(11)-P(2)-Pt(1)	108.4(3)

Bond lengths [Å] and angles [°]	
C(3)-C(4)-C(5)	118.9(8)
F(4)-C(7)-F(6)	107.9(6)
F(4)-C(7)-F(5)	105.7(6)
F(6)-C(7)-F(5)	104.4(6)
F(4)-C(7)-C(2)	114.6(7)
F(6)-C(7)-C(2)	114.3(6)
F(5)-C(7)-C(2)	109.1(6)
C(4)-C(3)-C(2)	121.5(8)
C(14)-C(13)-P(2)	112.7(7)
C(10)-C(9)-P(2)	115.2(6)
C(12)-C(11)-P(2)	113.8(7)
C(6)-C(5)-C(4)	120.8(7)
O(2)-P(1)-O(1)	104.7(3)
O(2)-P(1)-C(1)	103.2(3)
O(1)-P(1)-C(1)	103.1(3)
O(2)-P(1)-Pt(1)	114.3(2)
O(1)-P(1)-Pt(1)	113.5(2)
C(1)-P(1)-Pt(1)	116.5(2)

Table 8 - Bond lengths [Å] and angles [°] for $C_{14}H_{20}Br_2F_6O_2P_2Pt$

	U11	U22	U33	U23	U13	U12
Pt(1)	27(1)	19(1)	16(1)	0(1)	0(1)	1(1)
Br(2)	37(1)	33(1)	22(1)	-5(1)	-5(1)	-2(1)
Br(1)	33(1)	25(1)	22(1)	4(1)	0(1)	4(1)
F(3)	33(2)	40(3)	26(2)	-2(2)	6(2)	6(2)
F(2)	18(2)	55(3)	41(3)	2(2)	-2(2)	7(2)
C(6)	23(4)	28(4)	23(3)	6(3)	2(3)	-5(3)
F(1)	42(3)	55(3)	36(3)	16(2)	19(2)	-2(2)
C(8)	23(3)	41(4)	22(4)	5(3)	5(3)	3(3)
C(1)	24(4)	17(3)	18(3)	-1(3)	0(3)	-4(3)
C(2)	21(4)	25(4)	32(4)	-5(3)	5(3)	2(3)
P(2)	42(1)	20(1)	22(1)	0(1)	-3(1)	-1(1)
C(4)	45(5)	17(4)	56(6)	-2(4)	14(5)	-6(4)
F(6)	25(2)	30(2)	38(3)	-5(2)	3(2)	-3(2)
F(5)	26(3)	40(3)	86(4)	-5(3)	19(3)	6(2)
F(4)	46(3)	52(3)	34(3)	-15(2)	22(2)	-18(2)
C(7)	18(4)	31(4)	46(5)	-5(3)	11(3)	-3(3)
C(3)	30(4)	24(4)	59(6)	-8(4)	16(4)	0(3)
C(13)	66(6)	34(4)	30(4)	0(4)	-6(5)	12(4)
C(9)	59(6)	27(4)	22(4)	3(3)	-9(4)	-6(4)
C(14)	63(6)	58(6)	51(5)	-1(6)	6(6)	19(5)
C(12)	46(6)	58(6)	53(6)	16(5)	-3(5)	6(5)
C(11)	52(6)	32(5)	49(5)	12(4)	-11(4)	-12(4)
C(10)	108(10)	29(5)	36(5)	14(4)	-17(6)	-11(5)
C(5)	30(4)	30(4)	43(5)	13(4)	9(4)	-3(3)
P(1)	23(1)	18(1)	17(1)	1(1)	2(1)	2(1)
O(1)	28(3)	32(3)	18(2)	3(2)	1(2)	2(2)
O(2)	35(3)	23(3)	20(2)	0(2)	5(2)	-1(2)

Table 9 Anisotropic displacement parameters ($Å^2 \times 10^3$) for $C_{14}H_{20}Br_2F_6O_2P_2Pt$. The anisotropic displacement factor exponent takes the form: $-2\pi^2 [h^2 a^2 U11 + 2 h k a^* b^* U12]$

	x	y	z	U(eq)
H(4)	2310(5)	-390(4)	3456(8)	51
H(3)	3305(4)	140(4)	2884(7)	45
H(13A)	2641(5)	4716(4)	5658(8)	52
H(13B)	2523(5)	5168(4)	4662(8)	52
H(9A)	2879(5)	3877(4)	2430(6)	44
H(9B)	2136(5)	3945(4)	2909(6)	44
H(14A)	1518(9)	4600(36)	4297(16)	86
H(14B)	1481(8)	4837(26)	5462(43)	86
H(14C)	1653(5)	4065(12)	5190(56)	86
H(12A)	4729(16)	4306(18)	3279(47)	78
H(12B)	4084(17)	3986(34)	2718(22)	78
H(12C)	4402(32)	3618(16)	3695(28)	78
H(11A)	3798(5)	4933(5)	3801(8)	53
H(11B)	4041(5)	4495(5)	4758(8)	53
H(10A)	2214(33)	5147(14)	2860(39)	87
H(10B)	2371(41)	4859(5)	1745(22)	87
H(10C)	2980(11)	5104(16)	2463(59)	87
H(5)	1501(4)	252(4)	4364(7)	41
H(1)	1571(11)	2670(45)	4015(12)	39
H(2)	3145(40)	2254(17)	2398(35)	39

Table 2.10 Hydrogen coordinates (x 10^4) and isotropic displacement parameters ($Å^2$ x 10^3) for $C_{14}H_{20}Br_2F_6O_2P_2Pt$

A.2.3 1,1-dihydroxy-2,6-bis(trifluoromethyl)phenylphosphane

This crystal structure represents the product formed by the slow air oxidation of $Ar'PH_2$. It is interesting to note that the hydrogen atoms on the OH groups attached to phosphorus, are both directed towards the electron rich CF_3 groups. This factor may explain the stability of the compound. Hydrolysis of a P(III) compound normally results in the formation of a P(V) compound via the rearrangement of a P-OH bond into a P=O bond and a P-H bond.

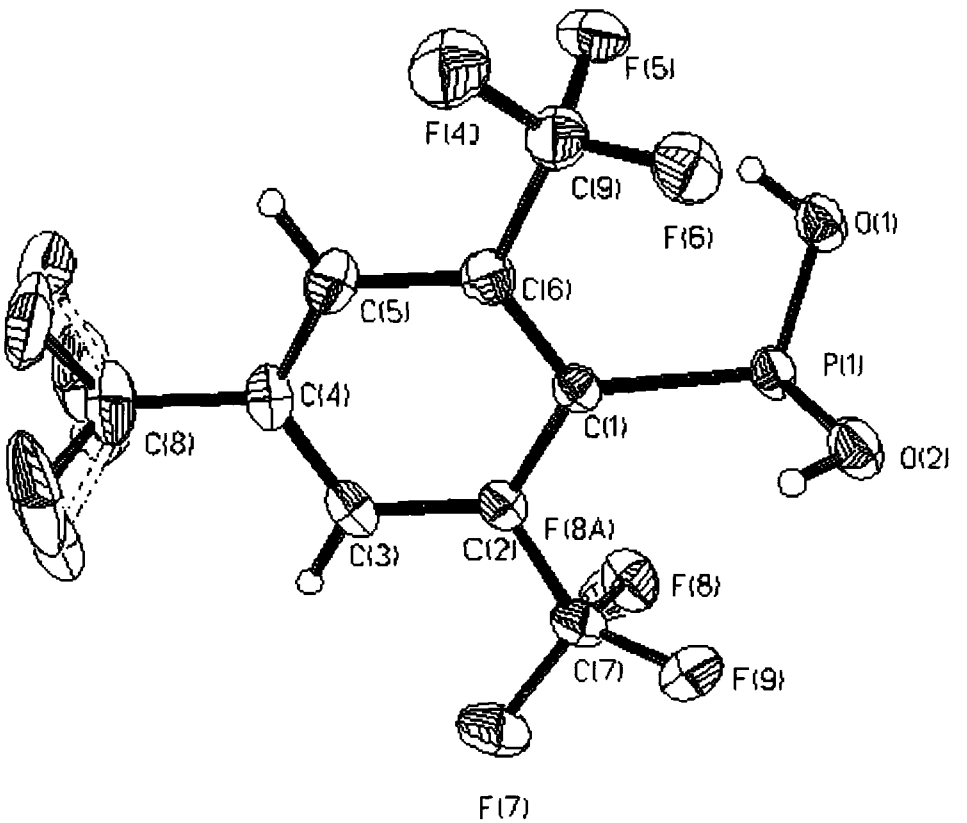

Figure A2.3 – Thermal ellipsoid diagram at 150K (50% Probability) for $ArP(OH_2)$

Crystal data and structure refinement	
Identification code	Ar'P(OH)$_2$
Empirical formula	$C_9 H_4 F_6 O_2 P$
Formula weight	346.09
Temperature	293(2) K
Wavelength	0.71073 Å
Crystal system	Monoclinic
Space group	$P2_1/c$
Unit cell dimensions	a = 8.397(2) Å α = 90 ° b = 6.4175(13) Å β = 96.08(3) ° c = 11.150(2) Å χ = 90 °.
Volume	597.4(2) Å^3
Z	2
Number of reflexions used	4286
Crystal description	cube
Crystal colour	colourless
Density (calculated)	1.924 g/cm^3
Absorption coefficient	3.50 cm^{-1}
F(000)	340
Crystal size	0.2 x 0.2 x 0.2 mm
Theta range for data collection	1.84 to 30.07 °.
Index ranges	-11<=h<=11, -8<=k<=7, -14<=l<=15
Experiment device	Siemens SMART
Experiment methods	ω scans
Reflections collected	4286
Independent reflections	2528 [R(int) = 0.0187]
Refinement method	Full-matrix least-squares on F^2
Data / restraints / parameters	2528 / 1 / 236
Goodness-of-fit on F^2	1.018
Final R indices [I>2σ(I)]	R_1 = 0.0349, wR_2 = 0.0866
R indices (all data)	R_1 = 0.0442, wR_2 = 0.0901
Absolute structure parameter	.43(13)
Largest diff. peak and hole	0.502 and -0.354 e.Å^{-3}

Table 11 Crystal data and structural refinement

	x	y	z	U(eq)
P(1)	-39(1)	1618(1)	1093(1)	23(1)
O(1)	220(2)	1554(2)	-208(1)	28(1)
O(2)	80(2)	-530(2)	1712(1)	30(1)
C(1)	1358(2)	3351(3)	1986(2)	20(1)
C(2)	840(2)	4585(3)	2932(2)	22(1)
C(3)	1810(2)	6116(3)	3505(2)	28(1)
C(4)	3333(2)	6446(3)	3161(2)	27(1)
C(5)	3914(2)	5216(3)	2256(2)	26(1)
C(6)	2940(2)	3661(3)	1718(2)	23(1)
C(7)	-818(2)	4354(3)	3340(2)	31(1)
F(4)	5322(1)	2346(2)	1038(1)	50(1)
F(5)	3392(2)	3048(2)	-329(1)	43(1)
F(6)	3254(1)	343(2)	812(1)	37(1)
C(8)	4324(3)	8197(4)	3772(2)	42(1)
F(1)	5642(4)	8631(6)	3105(4)	73(1)
F(1A)	5836(4)	7983(6)	3706(4)	75(1)
F(2)	4238(3)	8064(5)	5043(2)	50(1)
F(2A)	4807(5)	7949(6)	4824(3)	79(1)
F(3)	3646(4)	10035(6)	3531(3)	22(1)
F(3A)	3385(6)	9974(9)	3733(5)	43(1)
F(3B)	3975(8)	10008(10)	3401(6)	67(2)
C(9)	3705(2)	2346(4)	795(2)	33(1)
F(7)	-906(2)	5238(2)	4421(1)	50(1)
F(8)	-1933(3)	5365(5)	2642(3)	44(1)
F(8A)	-1958(3)	5222(6)	2519(3)	36(1)
F(9)	-1246(1)	2361(2)	3441(1)	40(1)

Table 12 Atomic coordinates (x 10^4) and equivalent isotropic displacement parameters ($Å^2$ x 10^3) for Ar'$P(OH)_2$. U(eq) is defined as one third of the trace of the *ortho*gonalized Uij tensor

Bond lengths [Å] and angles [°]	
P(1)-O(1)	1.4901(12)
P(1)-O(2)	1.5399(14)
P(1)-C(1)	1.832(2)
C(1)-C(6)	1.406(2)
C(1)-C(2)	1.423(2)
C(2)-C(3)	1.389(3)
C(2)-C(7)	1.517(3)
C(3)-C(4)	1.389(3)
C(4)-C(5)	1.375(3)
C(4)-C(8)	1.516(3)
C(5)-C(6)	1.403(3)
C(6)-C(9)	1.525(3)
C(7)-F(8)	1.322(4)
C(7)-F(9)	1.337(3)
C(7)-F(7)	1.342(2)
C(7)-F(8A)	1.370(4)
F(4)-C(9)	1.356(2)
F(5)-C(9)	1.331(2)
F(6)-C(9)	1.341(3)
C(8)-F(2A)	1.211(4)
C(8)-F(3B)	1.258(7)
C(8)-F(1A)	1.287(4)
C(8)-F(3)	1.324(5)
C(8)-F(3A)	1.384(6)
C(8)-F(1)	1.424(4)
C(8)-F(2)	1.429(4)
F(1)-F(1A)	.791(5)
F(1)-F(3B)	1.716(6)
F(1A)-F(2A)	1.591(6)
F(2)-F(2A)	.564(6)
F(3A)-F(3B)	.649(9)
O(1)-P(1)-O(2)	113.74(8)
O(1)-P(1)-C(1)	113.25(8)
O(2)-P(1)-C(1)	106.98(8)
C(6)-C(1)-C(2)	116.6(2)
C(6)-C(1)-P(1)	122.39(13)
C(2)-C(1)-P(1)	120.79(13)
C(3)-C(2)-C(1)	121.7(2)
C(3)-C(2)-C(7)	116.3(2)
C(1)-C(2)-C(7)	122.0(2)
C(2)-C(3)-C(4)	119.5(2)
C(5)-C(4)-C(3)	120.8(2)
C(5)-C(4)-C(8)	121.4(2)
C(3)-C(4)-C(8)	117.8(2)
C(4)-C(5)-C(6)	119.8(2)
C(5)-C(6)-C(1)	121.4(2)
C(5)-C(6)-C(9)	115.9(2)
C(1)-C(6)-C(9)	122.7(2)
F(8)-C(7)-F(9)	109.9(2)
F(8)-C(7)-F(7)	102.6(2)
F(9)-C(7)-F(7)	106.7(2)
F(8)-C(7)-F(8A)	6.7(2)
F(9)-C(7)-F(8A)	105.7(2)
F(7)-C(7)-F(8A)	109.1(2)

Bond lengths [Å] and angles [°]	
F(8)-C(7)-C(2)	113.0(2)
F(9)-C(7)-C(2)	112.5(2)
F(7)-C(7)-C(2)	111.6(2)
F(8A)-C(7)-C(2)	111.0(2)
F(2A)-C(8)-F(3B)	118.9(4)
F(2A)-C(8)-F(1A)	79.0(3)
F(3B)-C(8)-F(1A)	106.1(4)
F(2A)-C(8)-F(3)	114.0(3)
F(3B)-C(8)-F(3)	14.2(4)
F(1A)-C(8)-F(3)	119.2(3)
F(2A)-C(8)-F(3A)	105.7(3)
F(3B)-C(8)-F(3A)	27.9(4)
F(1A)-C(8)-F(3A)	130.4(3)
F(3)-C(8)-F(3A)	13.9(3)
F(2A)-C(8)-F(1)	109.4(3)
F(3B)-C(8)-F(1)	79.3(4)
F(1A)-C(8)-F(1)	33.4(2)
F(3)-C(8)-F(1)	93.5(3)
F(3A)-C(8)-F(1)	107.1(3)
F(2A)-C(8)-F(2)	22.8(3)
F(3B)-C(8)-F(2)	110.3(4)
F(1A)-C(8)-F(2)	101.8(3)
F(3)-C(8)-F(2)	100.9(3)
F(3A)-C(8)-F(2)	89.5(3)
F(1)-C(8)-F(2)	130.7(2)
F(2A)-C(8)-C(4)	116.7(3)
F(3B)-C(8)-C(4)	116.1(3)
F(1A)-C(8)-C(4)	113.2(2)
F(3)-C(8)-C(4)	111.4(2)
F(3A)-C(8)-C(4)	108.2(3)
F(1)-C(8)-C(4)	109.3(2)
F(2)-C(8)-C(4)	108.5(2)
F(1A)-F(1)-C(8)	63.7(4)
F(1A)-F(1)-F(3B)	102.0(5)
C(8)-F(1)-F(3B)	46.1(2)
F(1)-F(1A)-C(8)	82.9(4)
F(1)-F(1A)-F(2A)	126.2(5)
C(8)-F(1A)-F(2A)	48.4(2)
F(2A)-F(2)-C(8)	56.3(5)
F(2)-F(2A)-C(8)	100.9(6)
F(2)-F(2A)-F(1A)	153.2(6)
C(8)-F(2A)-F(1A)	52.6(2)
F(3B)-F(3A)-C(8)	65.1(8)
F(3A)-F(3B)-C(8)	87.0(9)
F(3A)-F(3B)-F(1)	141.2(10)
C(8)-F(3B)-F(1)	54.6(3)
F(5)-C(9)-F(6)	108.0(2)
F(5)-C(9)-F(4)	106.4(2)
F(6)-C(9)-F(4)	106.0(2)
F(5)-C(9)-C(6)	113.1(2)
F(6)-C(9)-C(6)	112.4(2)
F(4)-C(9)-C(6)	110.5(2)

Table 13 - Bond lengths [Å] and angles [°] for Ar'P(OH)$_2$

	U11	U22	U33	U23	U13	U12
P(1)	27(1)	20(1)	20(1)	-2(1)	-1(1)	-2(1)
O(1)	42(1)	20(1)	21(1)	0(1)	1(1)	-3(1)
O(2)	45(1)	24(1)	20(1)	0(1)	-2(1)	-4(1)
C(1)	23(1)	19(1)	18(1)	1(1)	1(1)	2(1)
C(2)	26(1)	20(1)	20(1)	0(1)	1(1)	2(1)
C(3)	34(1)	26(1)	22(1)	-6(1)	-2(1)	4(1)
C(4)	27(1)	22(1)	31(1)	-2(1)	-6(1)	-1(1)
C(5)	23(1)	25(1)	37(1)	1(1)	0(1)	-1(1)
C(6)	25(1)	20(1)	25(1)	-2(1)	2(1)	1(1)
C(7)	34(1)	37(1)	25(1)	-7(1)	9(1)	-1(1)
F(4)	26(1)	55(1)	71(1)	-21(1)	14(1)	3(1)
F(5)	53(1)	47(1)	30(1)	-4(1)	18(1)	-6(1)
F(6)	38(1)	28(1)	45(1)	-9(1)	9(1)	7(1)
C(8)	37(1)	29(1)	56(1)	-12(1)	-8(1)	-2(1)
F(1)	46(2)	67(2)	108(3)	-37(2)	20(2)	-29(2)
F(1A)	29(1)	91(2)	106(3)	-65(2)	17(2)	-28(2)
F(2)	50(2)	62(2)	34(1)	-16(1)	-8(1)	-11(2)
F(2A)	123(3)	41(2)	59(2)	16(2)	-65(2)	-25(2)
F(3)	24(2)	19(2)	21(2)	1(2)	-2(1)	0(1)
F(3A)	49(3)	25(2)	57(3)	-6(2)	12(2)	-10(2)
F(3B)	94(5)	32(3)	69(4)	9(3)	-25(3)	-27(3)
C(9)	27(1)	33(1)	40(1)	-7(1)	7(1)	1(1)
F(7)	51(1)	66(1)	35(1)	-19(1)	21(1)	-7(1)
F(8)	29(1)	50(2)	56(2)	11(2)	18(1)	9(1)
F(8A)	21(1)	49(2)	37(2)	-9(2)	-3(1)	6(1)
F(9)	43(1)	40(1)	38(1)	3(1)	13(1)	-11(1)

Table 14 Anisotropic displacement parameters ($Å^2$ x 10^3) for Ar'P(OH)$_2$. The anisotropic displacement factor exponent takes the form: $-2\pi^2$ [$h^2 a^2$ U11 + 2 h k a* b* U12]

Appendix 3

Courses attended

A.3 Courses Attended

A.3.1 First Year Induction Courses : October 1993

The course consists of a series of one hour lecture on the services available in the department.

1. Departmental Safety
2. Safety Matters
3. Electrical Appliances and Infrared Spectroscopy
4. Chromatography and Elemental Analysis
5. Atomic Absorption and Inorganic Analysis
6. Library Facilities
7. Mass Spectroscopy
8. Nuclear Magnetic Resonance
9. Glassblowing Techniques

A.3.2 Examined Lecture Courses : October 1993 – April 1994

Three courses were attended consisting of 6 one hour lectures followed by a written examination in each.

"Diffraction and Scattering Methods" 6 lectures by Prof. Judith Howard

"Synthetic Methodology in Organometallic Chemistry and Coordination Chemistry", 3 lectures by Prof. V. C. Gibson and 3 lectures by Prof. D. Parker.

"Practical NMR" 6 lectures by Alan Kenwright

Appendix 4

Colloquia, Lectures and Seminars organised by the Department of Chemistry 1994-1997

A.4 COLLOQUIA, LECTURES AND SEMINARS FROM INVITED SPEAKERS

A.4.1 1994 - 1995 (August 1 - July 31)

1994

October 5 Prof. N. L. Owen, Brigham Young University, Utah, USA
Determining Molecular Structure - the INADEQUATE NMR way

October 19 Prof. N. Bartlett, University of California
Some Aspects of Ag(II) and Ag(III) Chemistry

November 2 Dr P. G. Edwards, University of Wales, Cardiff
The Manipulation of Electronic and Structural Diversity in Metal Complexes - New Ligands

November 3 Prof. B. F. G. Johnson, Edinburgh University
Arene-metal Clusters

November 9 Dr G. Hogarth, University College, London
New Vistas in Metal-imido Chemistry

November 10 Dr M. Block, Zeneca Pharmaceuticals, Macclesfield
Large-scale Manufacture of ZD 1542, a Thromboxane Antagonist Synthase Inhibitor

November 16 Prof. M. Page, University of Huddersfield
Four-membered Rings and β-Lactamase

November 23 Dr J. M. J. Williams, University of Loughborough
New Approaches to Asymmetric Catalysis

December 7 Prof. D. Briggs, ICI and University of Durham
Surface Mass Spectrometry

1995

January 11 Prof. P. Parsons, University of Reading
Applications of Tandem Reactions in Organic Synthesis

January 18 Dr G. Rumbles, Imperial College, London
Real or Imaginary Third Order Non-linear Optical Materials

January 25 Dr D. A. Roberts, Zeneca Pharmaceuticals
The Design and Synthesis of Inhibitors of the Renin-angiotensin System

February 1 Dr T. Cosgrove, Bristol University
Polymers do it at Interfaces

February 8 Dr D. O'Hare, Oxford University
Synthesis and Solid-state Properties of Poly-, Oligo- and Multidecker Metallocenes

February 22 Prof. E. Schaumann, University of Clausthal
Silicon- and Sulphur-mediated Ring-opening Reactions of Epoxide

March 1 Dr M. Rosseinsky, Oxford University
Fullerene Intercalation Chemistry

March 22 Dr M. Taylor, University of Auckland, New Zealand
Structural Methods in Main-group Chemistry

April 26 Dr M. Schroder, University of Edinburgh
Redox-active Macrocyclic Complexes : Rings, Stacks and Liquid Crystals

May 4 Prof. A. J. Kresge, University of Toronto
The Ingold Lecture Reactive Intermediates : Carboxylic-acid Enols and Other Unstable Species

A.4.2 1995 - 1996 (August 1 - July 31)

1995

October 11 Prof. P. Lugar, Frei Univ Berlin, FRG
Low Temperature Crystallography

October 13 Prof. R. Schmutzler, Univ Braunschweig, FRG.
Calixarene-Phosphorus Chemistry: A New Dimension in Phosphorus Chemistry

October 18 Prof. A. Alexakis, Univ. Pierre et Marie Curie, Paris,
Synthetic and Analytical Uses of Chiral Diamines

October 25 Dr. D.M Davies, University of Northumbria
Chemical reactions in organised systems.

November 1 Prof. W. Motherwell, UCL London
New Reactions for Organic Synthesis

November 3 Dr B. Langlois, University Claude Bernard-Lyon
Radical Anionic and Psuedo Cationic Trifluoromethylation

November 8 Dr. D. Craig, Imperial College, London
New Stategies for the Assembly of Heterocyclic Systems

November 15 Dr A. Sella, UCL, London
Chemistry of Lanthanides with Polypyrazoylborate Ligands

November 17 Prof. D. Bergbreiter, Texas A&M, USA
Design of Smart Catalysts, Substrates and Surfaces from Simple Polymers

November 22 Prof. I Soutar, Lancaster University
A Water of Glass? Luminescence Studies of Water-Soluble Polymers.

November 29 Prof. D. Tuck, University of Windsor, Ontario, Canada
New Indium Coordination Chemistry

December 8 Professor M.T. Reetz, Max Planck Institut, Mulheim
Perkin Regional Meeting

1996

January 10 Dr B. Henderson, Waikato University, NZ
Electrospray Mass Spectrometry - a new sporting technique

January 17 Prof. J. W. Emsley , Southampton University
Liquid Crystals: More than Meets the Eye

January 24 Dr A. Armstrong, Nottingham Univesity
Alkene Oxidation and Natural Product Synthesis

January 31 Dr J. Penfold, Rutherford Appleton Laboratory,
Soft Soap and Surfaces

February 7 Dr R.B. Moody, Exeter University
Nitrosations, Nitrations and Oxidations with Nitrous Acid

February 12 Dr P. Pringle, University of Bristol
Catalytic Self-Replication of Phosphines on Platinum(O)

February 14 Dr J. Rohr, Univ Gottingen, FRG
Goals and Aspects of Biosynthetic Studies on Low Molecular Weight Natural Products

February 21 Dr C R Pulham , University. Edinburgh
Heavy Metal Hydrides - an exploration of the chemistry of stannanes and plumbanes

February 28 Prof. E. W. Randall, Queen Mary & Westfield College
New Perspectives in NMR Imaging

March 6 — Dr R. Whitby, University of Southampton
New approaches to chiral catalysts: Induction of planar and metal centred asymmetry

March 7 — Dr D. S. Wright, University of Cambridge
Synthetic Applications of Me_2N-p-Block Metal Reagents

March 12 — RSC Endowed Lecture - Prof. V. Balzani, Univ of Bologna
Supramolecular Photochemistry

March 13 — Prof. D. Garner, Manchester University
Mushrooming in Chemistry

April 30 — Dr L. D.Pettit, Chairman, IUPAC Commission of Equilibrium Data
pH-metric studies using very small quantities of uncertain purity

A.4.3 1996 - 1997 (August 1 - July 31)

1996

October 9 — Professor G. Bowmaker, University Aukland, NZ
Coordination and Materials Chemistry of the Group 11 and Group 12 Metals : Some Recent Vibrational and Solid State NMR Studies

October 14 — Professor A. R. Katritzky, University of Gainesville,University of Florida, USA
Recent Advances in Benzotriazole Mediated Synthetic Methodology

October 16 — Professor Ojima, Guggenheim Fellow, State University of New York at Stony Brook
Silylformylation and Silylcarbocyclisations in Organic Synthesis

October 22 — Professor L. Gade, University Wurzburg, Germany
Organic transformations with Early-Late Heterobimetallics: Synergism and Selectivity

October 22 — Professor B. J. Tighe, Department of Molecular Sciences and Chemistry, University of Aston
Making Polymers for Biomedical Application - can we meet Nature's Challenge?
Joint lecture with the Institute of Materials

October 23 — Professor H. Ringsdorf (Perkin Centenary Lecture), Johannes Gutenberg-Universitat, Mainz,
Germany
Function Based on Organisation

October 29 Professor D. M. Knight, Department of Philosophy, University of Durham.
The Purpose of Experiment - A Look at Davy and Faraday

October 30 Dr P. Mountford, Nottingham University
Recent Developments in Group IV Imido Chemistry

November 6 Dr M. Duer, Chemistry Department, Cambridge
Solid-state NMR Studies of Organic Solid to Liquid-crystalline Phase Transitions

November 12 Professor R. J. Young, Manchester Materials Centre, UMIST
New Materials - Fact or Fantasy?
Joint Lecture with Zeneca & RSC

November 13 Dr G. Resnati, Milan
Perfluorinated Oxaziridines: Mild Yet Powerful Oxidising Agents

November 18 Professor G. A. Olah, University of Southern California, USA
Crossing Conventional Lines in my Chemistry of the Elements

November 19 Professor R. E. Grigg, University of Leeds
Assembly of Complex Molecules by Palladium-Catalysed Queueing Processes

November 20 Professor J. Earnshaw, Deptartment of Physics, Belfast
Surface Light Scattering: Ripples and Relaxation

November 27 Dr R. Templer, Imperial College, London
Molecular Tubes and Sponges

December 3 Professor D. Phillips, Imperial College, London
"A Little Light Relief" -

December 4 Professor K. Muller-Dethlefs, York University
Chemical Applications of Very High Resolution ZEKE Photoelectron Spectroscopy

December 11 Dr C. Richards, Cardiff University
Sterochemical Games with Metallocenes

1997

January 15 Dr V. K. Aggarwal, University of Sheffield
Sulfur Mediated Asymmetric Synthesis

January 16 Dr S. Brooker, University of Otago, NZ
Macrocycles: Exciting yet Controlled Thiolate Coordination Chemistry

January 21	Mr D. Rudge, Zeneca Pharmaceuticals High Speed Automation of Chemical Reactions
January 22	Dr N. Cooley, BP Chemicals, Sunbury Synthesis and Properties of Alternating Polyketones
January 29	Dr J. Clarke, UMIST What can we learn about polymers and biopolymers from computer-generated nanosecond movie-clips?
February 4	Dr A. J. Banister, University of Durham From Runways to Non-metallic Metals - A New Chemistry Based on Sulphur
February 5	Dr A. Haynes, University of Sheffield Mechanism in Homogeneous Catalytic Carbonylation
February 12	Dr G.-Jan Boons, University of Birmingham New Developments in Carbohydrate Chemistry
February 18	Professor Sir James Black, Foundation/King's College London My Dialogues with Medicinal Chemists
February 19	Professor B. Hayden, University of Southampton The Dynamics of Dissociation at Surfaces and Fuel Cell Catalysts
February 25	Professor A. G. Sykes, University of Newcastle The Synthesis, Structures and Properties of Blue Copper Proteins
February 26	Dr T. Ryan, UMIST Making Hairpins from Rings and Chains
March 4	Professor C. W. Rees, Imperial College Some Very Heterocyclic Chemistry
March 5	Dr J. Staunton FRS, Cambridge University Tinkering with biosynthesis: towards a new generation of antibiotics
March 11	Dr A. D. Taylor, ISIS Facility, Rutherford Appleton Laboratory Expanding the Frontiers of Neutron Scattering
March 19	Dr K. Reid, University of Nottingham Probing Dynamical Processes with Photoelectrons